Publication No. 05-042-142

HOW DOES PHOSPHOGYPSUM STORAGE AFFECT GROUNDWATERS?

Prepared by
Florida State University

under a grant sponsored by

FIPR
Florida Institute of Phosphate Research

March 1998

The Florida Institute of Phosphate Research was created in 1978 by the Florida Legislature (Chapter 378.101, Florida Statutes) and empowered to conduct research supportive to the responsible development of the state's phosphate resources. The Institute has targeted areas of research responsibility. These are: reclamation alternatives in mining and processing, including wetlands reclamation, phosphogypsum storage areas and phosphatic clay containment areas; methods for more efficient, economical and environmentally balanced phosphate recovery and processing; disposal and utilization of phosphatic clay; and environmental effects involving the health and welfare of the people, including those effects related to radiation and water consumption.

FIPR is located in Polk County, in the heart of the central Florida phosphate district. The Institute seeks to serve as an information center on phosphate-related topics and welcomes information requests made in person, by mail, or by telephone.

Research Staff

Executive Director
Paul R. Clifford

Research Directors

G. Michael Lloyd Jr.	**-Chemical Processing**
Jinrong P. Zhang	**-Mining & Beneficiation**
Steven G. Richardson	**-Reclamation**
Gordon D. Nifong	**-Environmental Services**

Florida Institute of Phosphate Research
1855 West Main Street
Bartow, Florida 33830
(863) 534-7 160
Fax:(863) 534-7 165
http://www.fipr.state.fl.us

HOW DOES PHOSPHOGYPSUM STORAGE AFFECT GROUNDWATERS?

FIPR Project # 94-05-042

FINAL REPORT

Environmental Radioactivity Measurement Facility
Department of Oceanography
Florida State University
Tallahassee, Florida 32306-4320

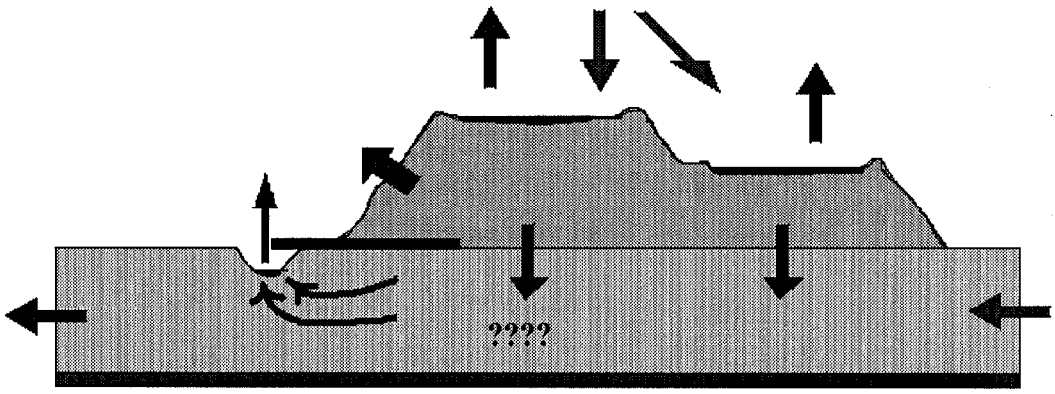

Prepared for

FLORIDA INSTITUTE OF PHOSPHATE RESEARCH
1855 West Main Street
Bartow, Florida 33830

Contract Manager: Gordon D. Nifong

March 1998

DISCLAIMER

The contents of this report are reproduced herein as received from the contractor.

The opinions, findings and conclusions expressed herein are not necessarily those of the Florida Institute of Phosphate Research, nor does mention of company names or products constitute endorsement by the Florida Institute of Phosphate Research.

PERSPECTIVE

Gordon D. Nifong, Ph. D.

Florida Institute of Phosphate Research

The Florida Institute of Phosphate Research, through its "Strategic Research Priorities," currently is stressing six program areas, three that are technology oriented and three that are more environmental in nature. A major focus is on phosphogypsum because the issue is of high priority from both technical and environmental standpoints. While one question is what could be done with the material, another question is what are the consequences of doing nothing with it and simply leaving it stockpiled on the ground? A major concern about phosphogypsum storage is the potential for contamination of groundwater under and near the stacks. Data from previous studies have shown there is some influence on the aquifers from the presence of the gypsum stack in terms of several chemical parameters, but evidence for radionuclide contamination is much less clear. This study addresses the specific question of whether or not a phosphogypsum stack contributes any significant amount of radionuclides to underlying aquifers. The approach taken was production of a flow model for an inactive stack, followed by a characterization of stack solutions and groundwaters, and solid phase gypsum core samples.

Phosphogypsum is composed mostly of calcium sulfate and is a by-product of the reaction between sulfuric acid and phosphate rock in the manufacture of phosphoric acid. Currently almost one billion tons of the material are stockpiled, or stacked, on the ground in central and north Florida, and more than thirty million tons are being added each year. Phosphogypsum, its uses and its environmental impacts, has been a priority of the Institute since virtually its inception twenty years ago. Large-scale uses, such as in road construction or in agriculture, have been mostly banned by the Environmental Protection Agency due to elevated levels of radionuclides. Material from central Florida typically contains about twenty-five picoCuries per gram of radium-226, although north Florida gypsum is much lower. Thus most material continues to be stored on the ground.

This study suggests that most radionuclides present in groundwater under and near phosphogypsum stacks are there because of the natural geology of the region, and not because of the presence of the stack. Model results indicate that at most one per cent of infiltrating water ever reaches the aquifer, most of the rest being intercepted by ditch drains around the stack. Radium-226 levels in stack fluids are only slightly elevated above background groundwater values, and are less than those found in most area monitor wells. It appears that various removal mechanisms, including adsorption within the stack, precipitation just below the stack, and especially interception by drainage ditches, prevent large-scale migration of radionuclides to the underlying aquifers.

ABSTRACT

This study was initiated to investigate the processes responsible for controlling the interaction and release of radionuclides from phosphogypsum from a phosphogypsum stack at Piney Point Phosphates. Our approach consisted of: (i) flow modeling of the stack-aquifer system; (ii) chemical/radiochemical characterization of fluid samples from monitor wells placed around and directly into the stack, and (iii) geochemical modeling. The flux analysis showed that only a small amount (-1%) of the infiltrating stack fluids escapes capture by the drainage ditches. Analyses of the stack solutions showed them to be acidic with high ionic strength, containing high total dissolved solids (18,700±2300 ppm) with a pH of 2.43±0.10. The stack wells are exceptionally high in activities of uranium (generally 600-1000 dpm/L ^{238}U) and ^{210}Pb (generally 400-4000 dpm/L). Concentrations of ^{226}Ra in the stack fluids, however, are only slightly elevated (range about 5-10 dpm/L) above normal groundwater values and are actually less than most of the monitor well concentrations measured around the Piney Point gypsum stack. Our observations suggest that various removal mechanisms including adsorption within the stack, precipitation within the soil horizons just below the stack, and interception of stack fluids by drainage ditches, prevent large-scale migration of radionuclides to the underlying aquifer.

ACKNOWLEDGMENTS

The vast majority of the fieldwork performed on this project could not have taken place without the cooperation of the personnel at Piney Point Phosphates, Inc. We wish to thank Dr. Ivan Nance and his crew for providing the facilities as well as considerable assistance in the form of manpower, equipment, and professional services. Mr. Alan Baker of Florida State University was extremely helpful in conducting the fieldwork and in the radiochemistry laboratory. We also wish to acknowledge the helpful reviews of an earlier version of this report by Dr. Sam Upchurch of Environmental Resources Management and Dr. Ivan Nance of the Mulberry Corporation. Finally, we express our thanks to the Florida Institute of Phosphate Research for their continued support.

W. Burnett
Florida State University

TABLE OF CONTENTS

HOW DOES PHOSPHOGYPSUM STORAGE AFFECT GROUNDWATERS?

EXECUTIVE SUMMARY

Phosphogypsum, a waste by-product derived from the wet process production of phosphoric acid, represents one of the most serious problems facing the phosphate industry today. This by-product gypsum precipitates during the reaction of sulfuric acid with phosphate rock and is stored at a rate of about 40 million tons per year on several stacks in central and northern Florida The main problem associated with this material concerns the relatively high levels of natural uranium-series radionuclides and other impurities which could impact the environment and which currently makes its commercial use impossible.

One of the prime concerns often expressed about phosphogypsum storage is the potential for contamination of fresh water aquifers underlying the stacks. Data from previous studies have shown that there is often influence from the gypsum stacks for some chemical parameters. The data for radionuclides is less clear. Past studies have usually relied on monitor wells which are historically situated more on a regulatory rather than a scientific basis, i.e., wells are often placed on the property lines rather than where they would provide the best information. In addition, since most gypsum stacks are located on mineralized land, there are likely going to be elevated levels of some radionuclides (as ^{226}Ra) associated with the natural uranium-enriched phosphate rock. Thus, the finding of elevated levels of radionuclides in a monitor well near a gypsum stack does not necessarily imply contamination.

Because of these problems in interpretation, we specifically designed this study to address the question of whether or not a gypsum stack contributes significant amounts of radionuclides to the underlying aquifer. We focused primarily on one inactive stack at Piney Point Phosphates, Inc. and established monitor wells both around and directly into the stack. Cores of phosphogypsum were also obtained through the entire stack. We thus had the opportunity to investigate migration of radionuclides by looking at both fluid and solid phase components. Both geochemical and flow modeling were performed for the Piney Point hydrological system to place the radionuclide results in perspective.

During the course of this investigation a total of 28 new monitor wells were constructed into and around the Piney Point stack (11 wells were drilled into the stack and 17 new monitor wells were placed around its perimeter). We conducted 9 fieldtrips over an approximately eighteen-month period (Feb., 1995 - Sept., 1996). A total of 77 samples was collected from these wells for chemical analyses of 53 parameters (a total of 4081 analyses). During the same period, we collected 84 samples for radiochemical analyses of 5 parameters (a total of 420 analyses). Two cores were drilled into the Piney Point stack from which 31 samples of phosphogypsum and soil were radiochemically

analyzed. An additional 24 soil/sediment samples were analyzed from cuttings collected during the construction of the new monitor wells around the stack. Twenty-four phosphogypsum samples, collected from near the surface of the Piney Point stack and a stratigraphic section from the CF Bartow stack were also analyzed.

The overall approach used in this study may be summarized as follows:

1) Production of a flow model and water budget for the Piney Point stack;
2) A chemical/radiochemical characterization of stack solutions, adjacent groundwaters, and solid phase phosphogypsum from cores; and
3) Geochemical modeling of the stack fluids and associated groundwaters.

This report is laid out in the same manner as described above, with one chapter for each of these main points. **Chapter 1,** prepared by Manford Koch and Takashi Shinkawa of Temple University, describes a hydrological modeling approach to characterize flow processes in the Piney Point stack. Aquifer tests included pressure transducer tests, pump and recovery tests such as the Cooper-Jacob straight-line method, the Kirkham auger hole test, the Bouwer Rice test for partially screened and partially penetrating wells, and in situ flowmeter tests which allowed the determination of the vertical stratification of the hydraulic conductivity. A steady-state numerical mounding model was constructed using the MODFLOW code to simulate the hydraulic effect of the stack on the regional flow and to quantify flux rates from the phosphogypsum stack into the surficial aquifer. The flux analysis estimates the actual volumetric impact of the stack to the surficial aquifer and illustrates the effectiveness of the ditch drains in intercepting fluids that otherwise may have infiltrated from the gypsum stack into the surficial aquifer. In fact, the model results indicate that only a small amount (~1%) of the infiltrating stack fluid is not captured by the ditches and is thus transported into the surficial aquifer. However, because of the lack of estimates for stack water losses due to flank evaporation, spray losses, and dewatering pipes, the real rate of infiltration may be even less than the value indicated by the water budget analysis.

Chapter 2 presents a detailed description of the radiochemistry and chemistry of the stack and monitor well fluids at Piney Point Phosphates. We also describe the results for the phosphogypsum and soil samples at Piney Point and CF Bartow. Results showed that the stack solutions are acidic with high ionic strength, containing high total dissolved solids (TDS) of 18,700±2300 ppm and a pH of 2.43±0.10. The waters from the monitor wells surrounding the stack have a much lower average TDS of 3,300±3200 ppm and a pH of 6.33±0.65. Qualitative relationships between dissolved PO_4^{3-} and F^- and SiO_2 with F^- are thought to imply solution controls by the solid phases carbonate fluorapatite and alkali fluorsilicates. Radiochemically, the stack wells are exceptionally high in activities of uranium (generally 600-1000 dpm/L ^{238}U) and ^{210}Pb (generally 400-4000 dprn/L). One very significant finding is that the activities of ^{226}Ra in the stack fluids

are only slightly elevated (range about 5-10 dpm/L) above normal (unmineralized) groundwater values and are, in fact, less than most of the monitor well concentrations measured around the Piney Point gypsum stack. The consistently low specific activities of ^{226}Ra in the gypsum stack fluids argues strongly against the stack as a source of radium to the aquifer. Observations in solid phase materials, both from the stratigraphic section at the CF plant and the two cores in the Piney Point stack, are consistent with the results from the fluid analyses. Our observations suggest that substantial amounts of radionuclides are sequestered within or just below the stack before entering the underlying aquifer.

The geochemical modeling aspects of this project reported **in Chapter 3** were handled by Prof. Alan W. Elzerman of Clemson University. The chemical and radionuclide data were modeled using the computer code MINTEQA2. Results showed that increased concentrations of many ligands resulted in significant changes in predicted equilibrium speciation. Most pronounced were the increases in metal and radionuclide complexes with sulfate and phosphate, resulting in uncharged or negatively charged solution species which would likely be more mobile in the aquifer than positively charged metal or radionuclide ions. Fluoride from the stack solutions can significantly affect the speciation of aluminum, silicon, iron and possibly uranium. The second major effect of the phosphogypsum stack solution inputs is to cause oversaturation of a variety of solids. Contaminated solutions with such low pH values would normally be associated with small amounts of solid phase precipitation out of fresh waters. However, the dissolved solids content and some specific ion concentrations in these solutions are sufficiently high to cause oversaturation. Although the model results should not be considered comprehensive in terms of the potential solid phases that could form, the general trend of predicted precipitation reactions does indicate that such reactions are likely for certain components. Silicon containing solids are particularly likely since it is oversaturated in the uncontaminated solutions and much more so in the stack fluids. Other predicted solids formed included the components iron, aluminum, phosphate, calcium, manganese, barium, fluorine and uranium. Precipitation of various and probably multicomponent solids are thus expected to occur both in and below the phosphogypsum stacks. These solids could well scavenge reactive radionuclides, preventing their transport into the aquifer.

The common theme in all of our results is that while the phosphogypsum stack solutions do contain significant quantities of dissolved radionuclides, various removal mechanisms including adsorption within the stack, precipitation within the soil horizons just below the stack, and interception of stack fluids by drainage ditches, prevent large-scale migration to the underlying aquifer.

CHAPTER 1

HYDROLOGICAL FLOW MODEL AND WATER BUDGET

Manford Koch
Takashi Thomas Shinkawa
Temple University

INTRODUCTION

Phosphate mining in Florida is currently one of the state's largest industries, and produces approximately 40 million tons of material per year (Miller and Sutcliffe, 1984). Estimates from previous studies indicate that over 600 million tons of phosphatic waste have been stockpiled in above-ground formations called "Phosphogypsum Stacks" (defined as such by the source and product of their existence). Gypsum and silicon hexafluoride make up the slurry waste that is pumped out to large evaporite ponds, where the former is allowed to precipitate. Over time, accumulation at the bottom of the pond is dug out and piled on the embankments of the pond. This practice is intended to strengthen the walls of the pond, as it grows in size and elevation. Approximately eighteen such industrial facilities are located in the Tampa area, with an average area of 227 acres and a range of heights between 30 and 140 feet.

As the stockpile of gypsum stacks grow to a projected billion-plus tons by the year 2000 (May and Sweeney, 1983), the high concentrations of radionuclides, acid, fluoride, phosphate, and sulfate become an increasingly problematic characteristic of this resource, with a potential for groundwater pollution.

The primary focus of this study was to investigate the hydrologic controls of the phosphogypsum stack, and to provide a model of groundwater flux upon which a future transport and geochemical model can determine the migration and fate of possible contaminant leachate plumes and to delineate the physical and chemical processes involved. As to the more particular objectives of the hydrological part of the research,

they amount to a quantification of the vertical and horizontal flow rates in the phosphogypsum stack and the surficial aquifer, respectively, as well as to a determination of the hydraulic impact of the phosphogypsum stack on the surficial aquifer.

ENVIRONMENTAL SETTING

Geography

The Piney Point Phosphates facility, located along the coast of western Florida, lies approximately 30 kilometers south of downtown Tampa in Manatee County, along U.S. Route 41 **(Fig. 1-1).** The study area is a rural setting with cattle ranches, citrus groves, and vegetable farms making up a majority of the businesses close by. Topographically, the area is relatively flat with drainage flowing either to the Manatee River in the north, McMullen Creek in the south, or to Tampa Bay in the west **(Fig. 1-2).** The Piney Point Phosphates complex is at an elevation of 3 - 8 m above mean sea level, and is about two kilometers from the shoreline of Tampa Bay.

The climate of the research area is subtropical. Convective thunderstorms dominate the rainy weather of the summer months, while winter and spring are fairly dry. Consequently, irrigation demands on the groundwater reach a peak from March through May.

This particular site, although presently inactive, is an ideal location for studying fluid migration from phosphogypsum stacks, owing to the fact that local groundwater movement is toward Tampa Bay and away from any large population in the area.

There are three aquifers which potable water may be drawn from in this region: (1) a surficial aquifer system within surficial sands and clays; (2) an intermediate aquifer system and confining unit within the Hawthorn Group (Peace River and Arcadia Formations); and (3) the Floridan aquifer.

Major lithologies of stratigraphic units in the area have been defined by Scott (1988) **(Fig. 1-3).** The base of the stratigraphic column in this area is made up of the Avon Park Limestone. Together with the Suwanee and Ocala Limestones, these formations comprise the 150 - 250 m thick unit referred to as the Floridian Aquifer. The boundaries of this aquifer are defined beneath by a carbonate unit within the Avon Park containing intergranular evaporites, and above by another carbonate unit with higher percentages of clays (Miller and Sutcliffe, 1984; Scott, 1988).

Overlying the Floridian Aquifer are alternating sandy limestone and clay layers. This alternation of layers is classified as a second lithological group, the Hawthorn Group. Although this intermediate group can be used as a source of water, it is primarily

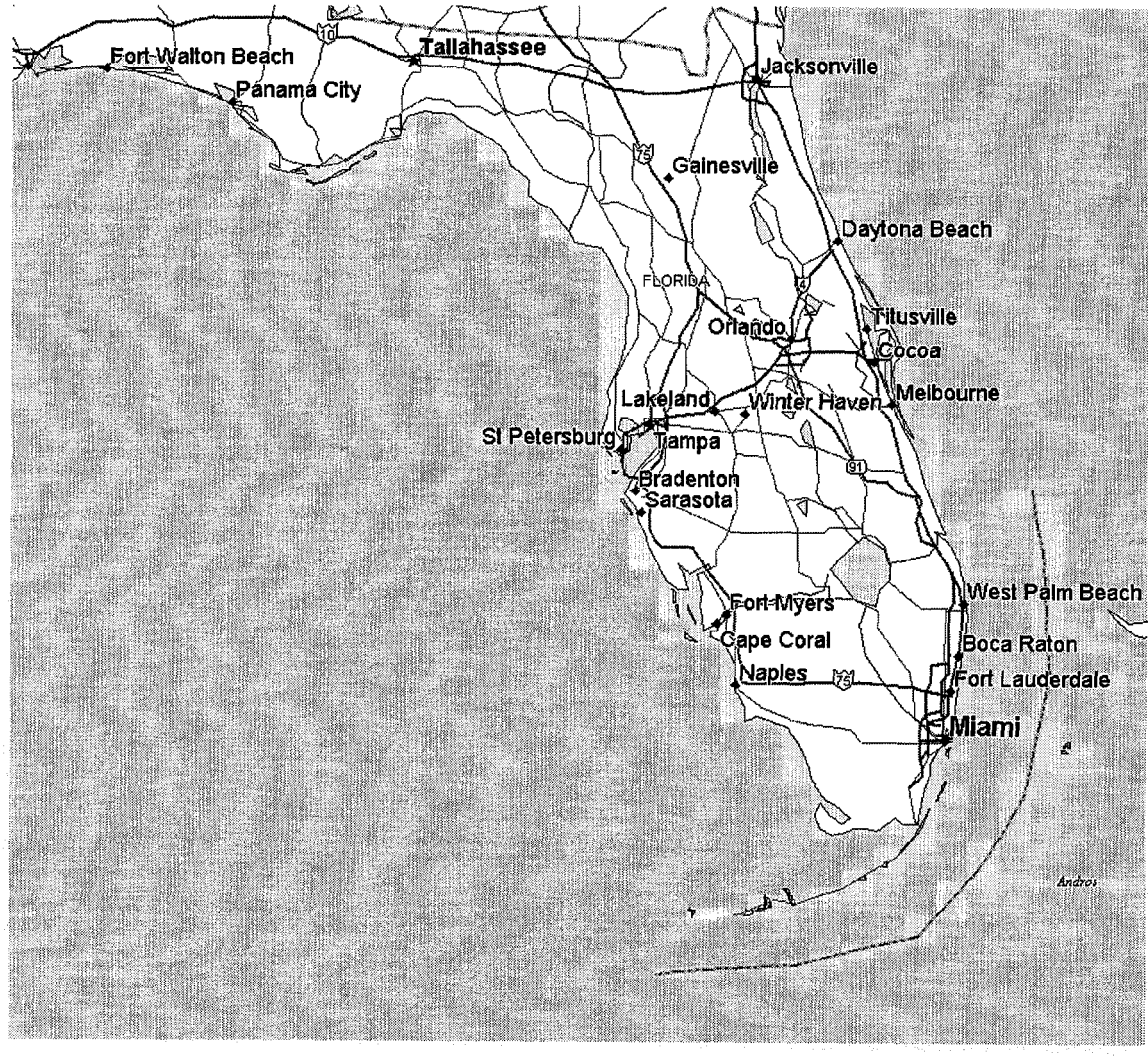

Figure 1-1 Index map of the State of Florida. The study area is just south of the Tampa Bay region.

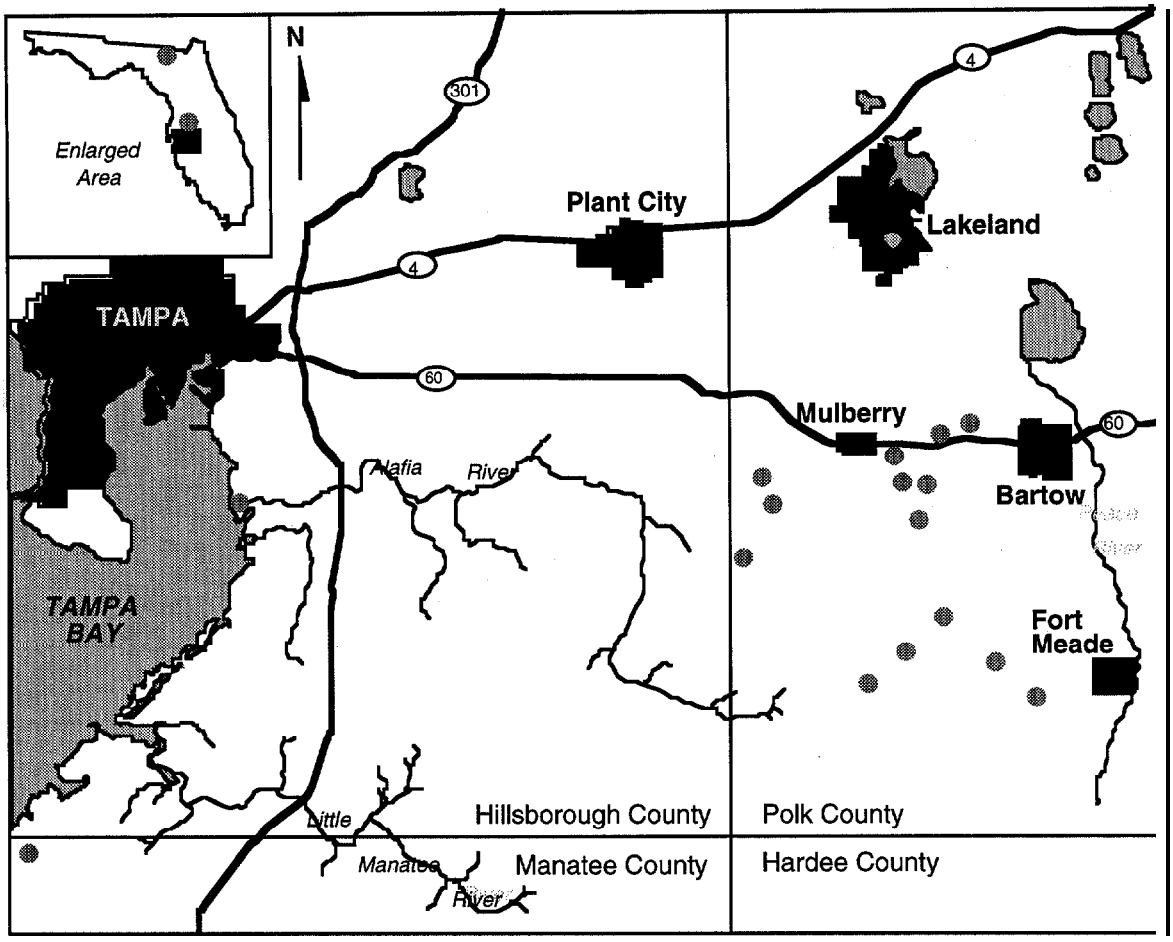

Figure 1-2. Location of phosphogypsum stacks within the Central Florida Mining District. The Piney Point Phosphates gypsum stack is located in the extreme western side of Manatee County, near Tampa Bay. Analyses of phosphogypsum samples from most of these stacks have been reported in Burnett et al. (1995).

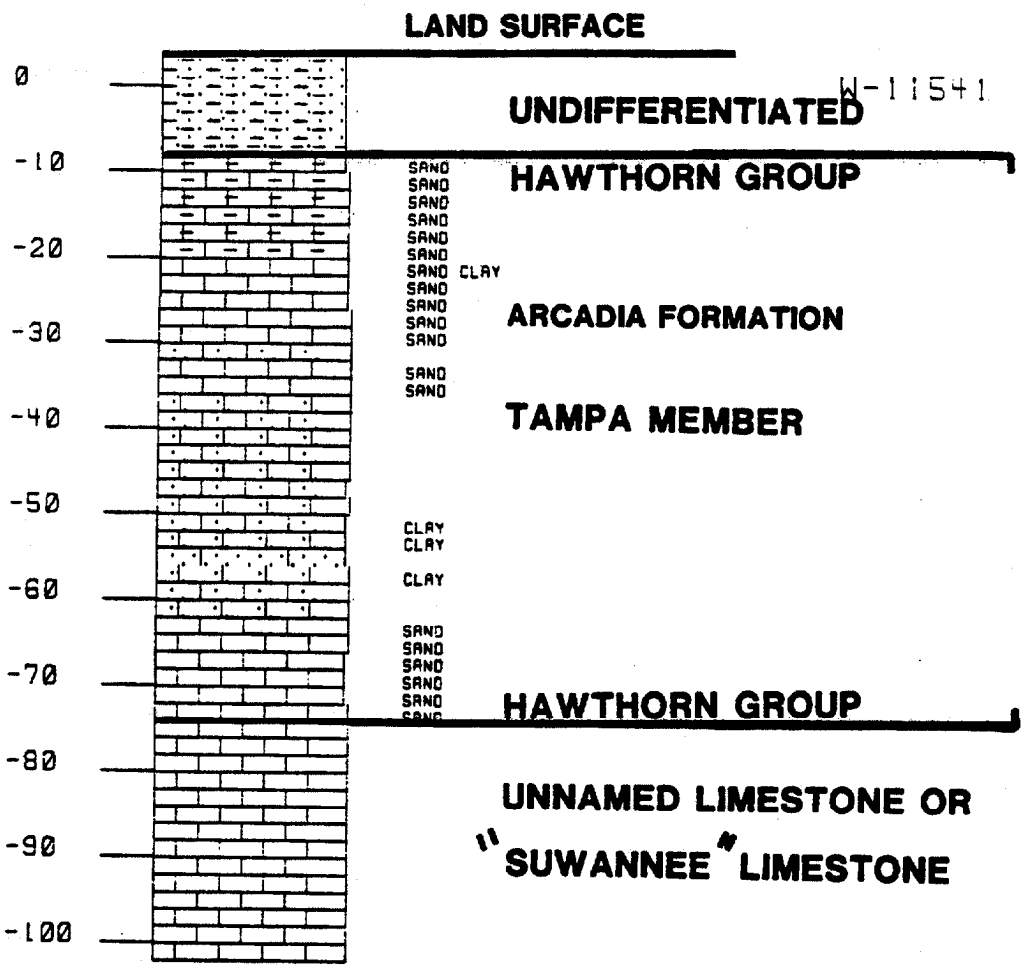

Figure 1-3 Reference core for the Tampa member of the Arcadia Formation, Ballast Point #1, W-11541, Hillsborough County (reproduced from Scott, 1988).

made of various clays. The upper confining unit is delineated by a phosphatic clay, known as the Bone Valley Member. Much of the ore for the phosphate industry in the area is mined from the Bone Valley and it has been called "one of the world's most important sources of phosphate" (Miller and Sutcliffe, 1984). Thickness of the intermediate unit is from 75 - 125 m , with the phosphatic clay composing the upper 10 - 20 m.

At the surface, a 10-20 m thick unit of undifferentiated sands and clays is lithologically distinct from the units below.

Hydrogeology

Groundwater in the area is commonly drawn from one of the three available water producing units described above. Flow within these aquifers is, for the most part, in the horizontal direction with little leakage between layers. The water table in the unconfined unit varies with precipitation and evaporation, while underlying units modulate their potentiometric yields according to changing lateral flow from inland areas of recharge and local points of discharge. Seasonal highs and lows of the potentiometric surfaces for the Floridan aquifer have been recognized by the U.S. Geological Survey (Johnson et. al., 1981) as September and May, respectively, and are mainly associated with groundwater pumpage for agricultural irrigation.

Comparison of the potentiometric surfaces in the southeastern United States by Johnston et al. (1980, 1981) before and after development has shown a regional trend in the vertical flow between aquifer units. Following extensive development of the area in the late 1970's, Polk County to the east had become an area of recharge whereas the coastal area along Tampa Bay had become a zone of discharge to the Gulf of Mexico. This trend dictates a downward flow to the Floridan Aquifer in the area of recharge, and an upward flow in the area of discharge. Because the Piney Point facility is in the area of discharge, there exists an upward flow gradient in the water-bearing units through their confining beds.

Locally, groundwater is drawn primarily from the Floridan Aquifer, although the surficial and intermediate aquifers are equally important to some. The surficial unit is used for domestic lawn irrigation, while the intermediate aquifer system is tapped for use as a rural domestic source of water and for agricultural irrigation. Additionally, the Floridan aquifer quite a bit to the south of the Piney Point facility contains mineralized water, and promotes the intermediate aquifer as the primary source for municipal water.

In the studies of Miller and Sutcliffe (1982) and Miller and Sutcliffe (1984) the aquifer system around the Piney Point complex was probed for the first time in more detail. About forty test holes (wells) whose depths extended from the surficial, unconfined aquifer to the intermediate, confined (artesian) aquifer were drilled around the

ponds and the gypsum stack during this study. A few older, mostly abandoned irrigation wells that extend further down into the confined Floridan aquifer were also monitored. Various geophysical well-logging techniques were applied in some of the boreholes to determine the lithology of the aquifer substratum. Groundwater table elevations were taken during the time and three wells were monitored continuously by means of recorders. The hydrographs for the three continuously monitored wells show sporadic evidence of an upward hydraulic head gradient between the intermediate and the surficial aquifer. This has been taken as evidence that potential surface contamination cannot leak into the lower intermediate aquifer. However, during the dry season (April to June), when the intermediate aquifer is heavily pumped for agricultural irrigation, the situation may be reversed and a downward gradient is observed. The water elevation data also shows a topographic mounding effect of the gypsum stack on the groundwater-level in the surficial aquifer.

The Piney Point Phosphate Inc.'s quarterly reports of the groundwater monitoring survey around the phosphogypsum stack to the Florida Department of Environmental Protection (FDEP) provide some evidence of the direction of the regional groundwater flow in the vicinity of the stack. As part of the proposed extension of the phosphogypsum stack to its present-day size, Gerathy & Miller Inc. was retained by Piney Point Inc. to install 7 monitor wells extending into the surficial aquifer on the premises of the company, Most of these monitor wells are still in use today and are being sampled on a regular basis. **Figures 1-4** and **1-5** show the piezometric isolines for two particular dates and **Figure 1-6** illustrates the hydraulic head surface for one of these dates in 3D form. One can observe from these figures that the groundwater flow is mainly in the northwestern direction. Moreover, the flow system in the surficial aquifer appears to be very much in steady-state, as witnessed by the similarity of the isoline contours taken over a period of two years.

As for the hydrogeology in the phosphogypsum stack itself, only the geotechnical study of the slope stability carried out by Oaks Geotechnical Inc. (1980) as part of the proposed extension of the gypsum stack to its present-day size provides some rudimentary clues about the water flow in the stack. During this study several boreholes were drilled into the flanks of the stack and water-table levels were monitored over a period of several months. Because the exact well construction data has not been reported, precise inferences on the stack-flow cannot be made.

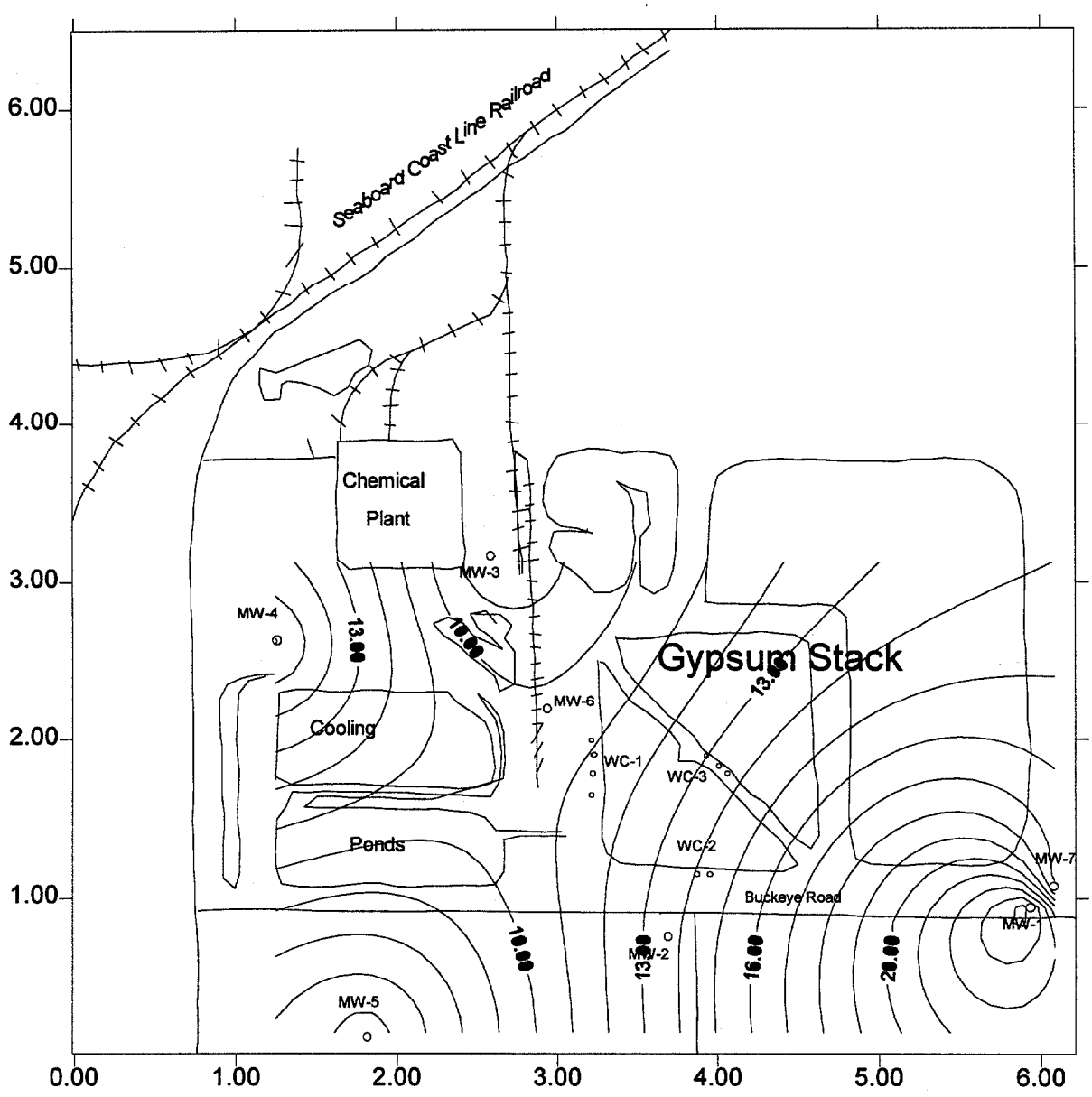

Figure 1-4. Contour plot of the piezometric heads in the surficial aquifer on November 4, 1991 (contour levels are in ft).

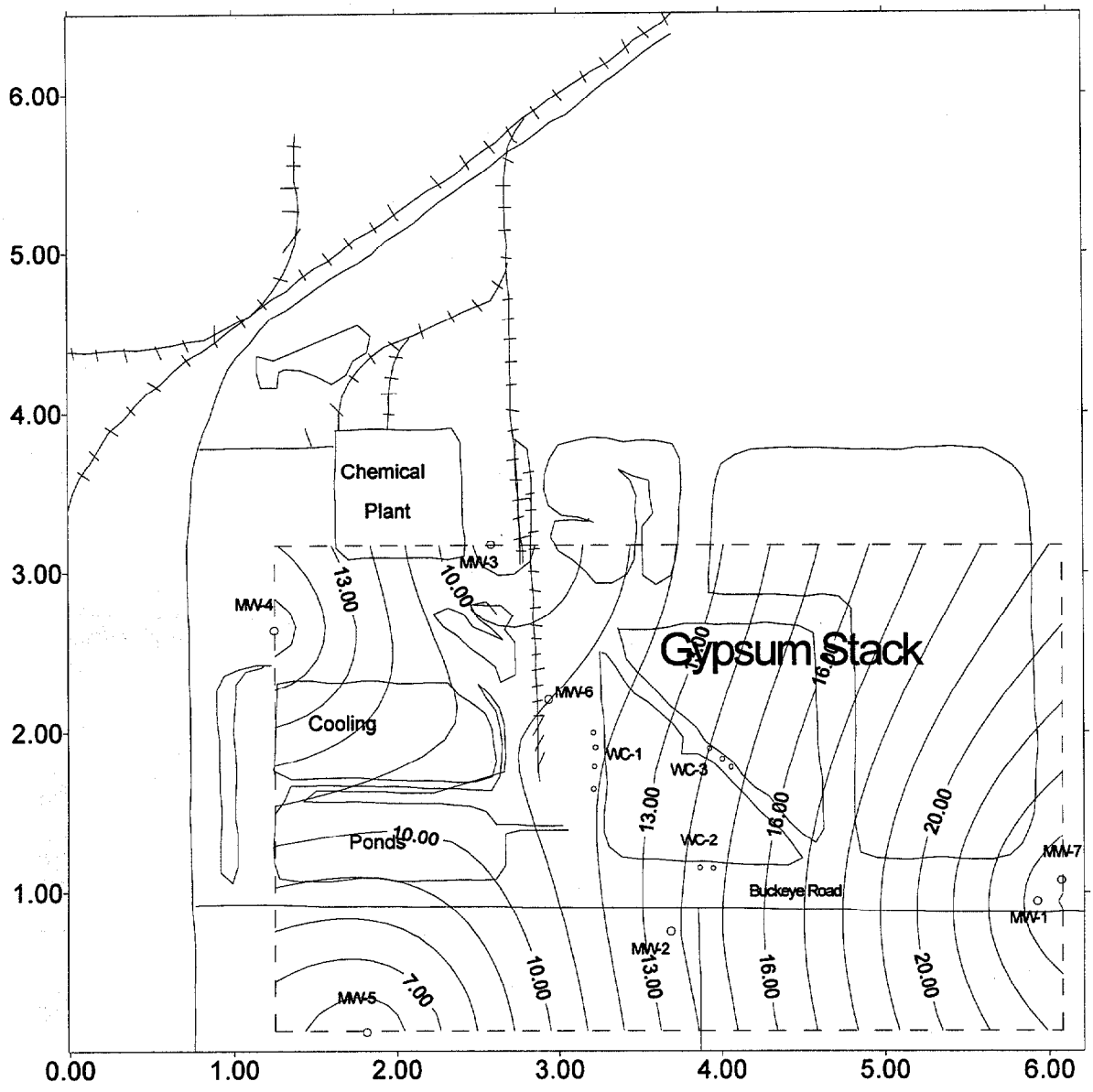

Figure 1-5. Contour plot of the piezometric heads in the surficial aquifer on September 23, 1993 (contour levels are in ft).

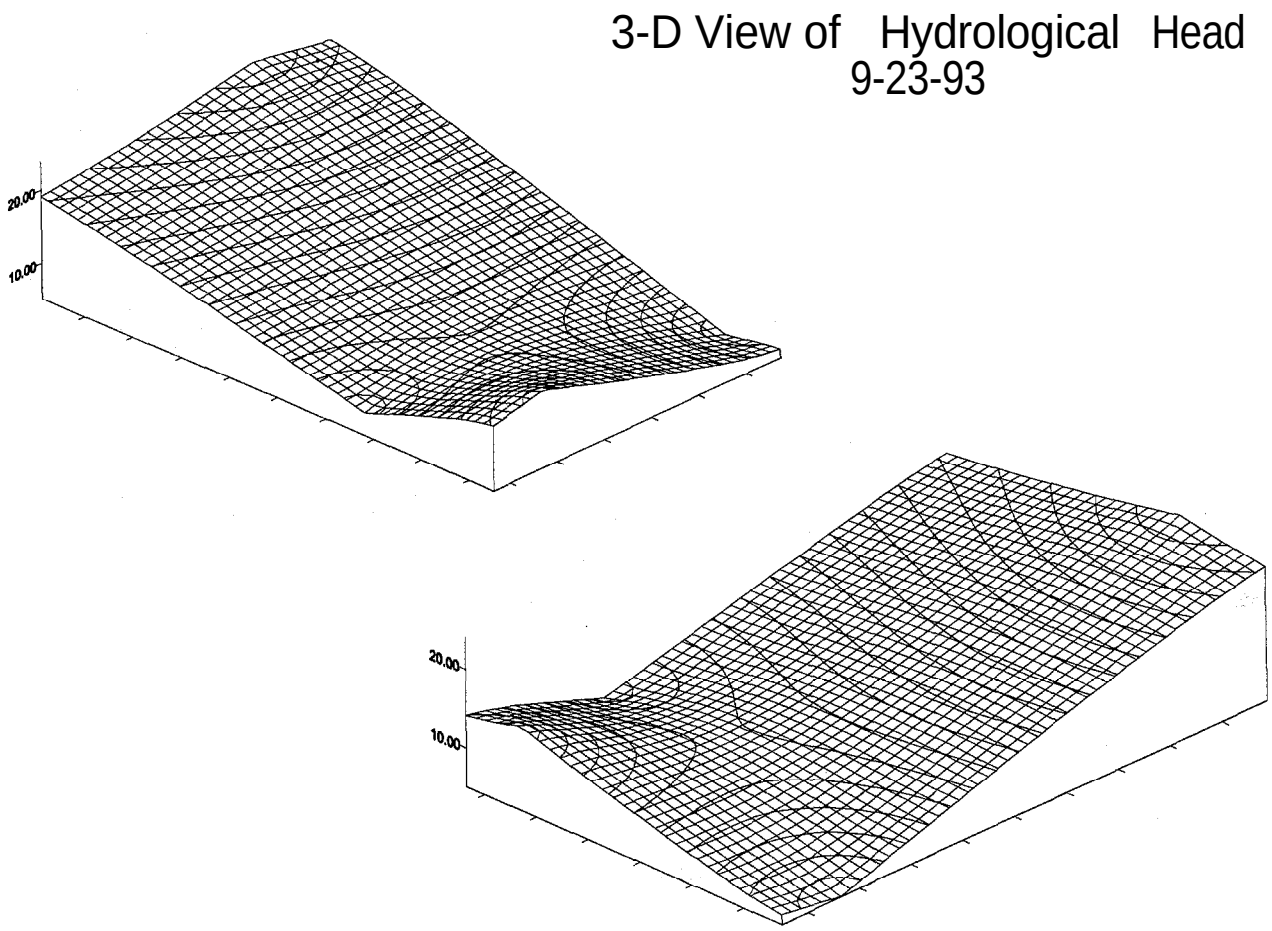

Figure 1-6. 3D plot of the piezometric heads in the surficial aquifer on September 23, 1993.

METHODS OF DATA ANALYSIS

Compilation of the data as well as computation for the analyses was conducted in spreadsheet format using Microsoft Excel. Representation of these data as graphs, in addition to a regression for the topographical analysis, were done in Axum 5.0. Modification of some figures was accomplished through use of Microsoft Paint, and Hijaak Pro.

Phosphogypsum Stack

Identification of hydrologic flow within the phosphogypsum pile itself was carried out through a series of investigations centered around quantifying the hydrologic parameters of the stack material, and identifying vertical gradients between stratigraphic layers. Ten partially screened wells and one fully screened well were drilled into the oldest portion of the stack. The wells were set at various depths **(Table 1-1)** in two clusters of four wells and one cluster of three. Cluster one (PPl) in the west wall and cluster three (PP3) in the center of the stack along an old working road wall had four wells, while cluster two (PP2) in the south wall only had three wells **(Fig. 1-7).** The gypsum-aquifer interface (base of the stack) is at a depth of 20.8 m from the surface, so there is only one well (PP2-0) which taps the surficial aquifer through the gypsum stack.

Table 1-1 Depths of sampling wells drilled into the stack.

Cluster # - Well #	Total Well Depth (in m. from top of riser)	Cased Section (m. depth)	Screened Section (m. depth)
1 - 1	18.0	0 - 14.8	14.8 - 18
1 - 2	14.8	0 - 12.5	12.5 - 14.8
1 - 3	12.5	0 - 9.5	9.5 - 12.5
1 - 4	9.5	0 - 6.6	6.6 - 9.5
2 - 0	23.6	0 - 22.0	22.0 - 23.6
2 - 1	18.0	0 - 14.8	14.8 - 18.0
2 - 2	14.8	0 - 12.5	12.5 - 14.8
2 - 3	11.5	0 - 8.2	8.2 - 11.5
3 - 1	18.0	none	0 - 18.0
3 - 2	14.8	0 - 12.5	12.5 - 14.8
3 - 3	11.5	0 - 8.2	8.2 - 11.5

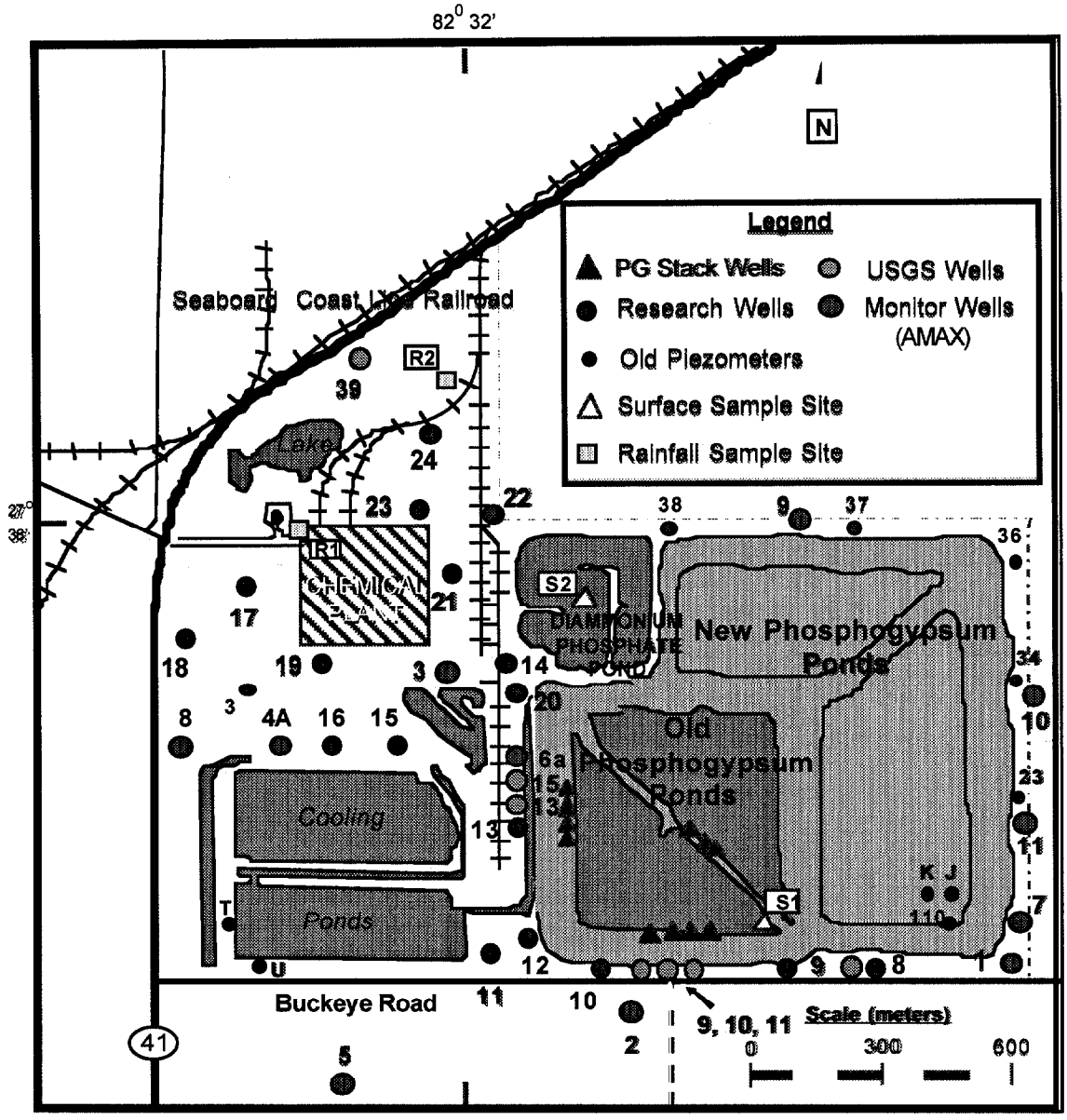

Figure 1-7 Locations of monitoring wells at the Piney Point Phosphates, Inc. at Palmetto, Florida.

All wells were constructed with a 10-cm. diameter PVC pipe. Screens were packed in 20-30 mesh sand with approximately 50 cm of bentonite hole plug overlying the sand pack except for the PP 2-0 well which has a 2-m thick bentonite plug over the sand pack. The risers were grouted to the surface with a bentonite-cement mixed grout compound. For the fully screened well (PP 3-0) grout-plugs were set at intervals of 1.5m, in order to reduce the possibility of vertical outer-borehole flow which could corrupt the borehole flowmeter tests.

Quantification of hydrologic parameters within the stack was determined by one of the most commonly used non-equilibrium aquifer tests, the Cooper-Jacob (straight-line) method. This method was used over the more popular Theis-curve match for its asymptotic approximation of the well function for a small radius and long times, because it is important to rule out the bias of values representative of the region directly around the well. A Grundfos 1.2-amp pump was used to pump water out of the well at an approximate rate of 6 L/min., and head measurements were taken with an electrical head level indicator.

Hydraulic gradients within the stack were determined by using a pressure transducer, a new electromagnetic borehole flowmeter (Molz et al., 1994), and through a comparison of hydraulic head values. Due to the significance of a hydrologic gradient for the understanding of the flow system in the stack, the use of these different methods should increase the reliability of the results obtained.

In situ vertical head measurements were made using a set of infIatable packers and a 20 psi pressure transducer. Inflation of the packers above and below the pressure transducer allowed a section of the well to be isolated, and a reading to be taken. Measurements of the in situ pressure were taken at all screened intervals possible, along with 3 - 5 cased intervals (to provide a standard hydrostatic gradient upon which to compare the screened readings). Variations of anomalous readings in the screened sections were correlated with the presence of a pressure perturbation (i.e., a flow gradient).

Borehole flowmeter tests were conducted by Quantum Engineering Corporation using the deepest well of each stack cluster. Ambient flow, induced flow, and aquifer test measurements were conducted at all wells; however, a complete analysis was only done for well 1-1. Results for wells 2-1 and 3-1 were incomplete, owing to the onset of a thunderstorm the day that the measurements were taken. Results from this testing have provided data for ambient flow direction and magnitude, as well as response of various vertical sections of the stack to induced flow conditions. Utilization of these induced flow rates with the measurements for net flow can also be used.

Hydraulic head measurements for the monitoring wells on the stack were taken approximately every three months. Because wells in the same cluster were within a few meters of each other, comparison of the head measurements were used to indicate

possible variations of head gradients in the vertical direction within the stack. Organization of the data as a cross-sectional view provided information on internal stack-stratification.

Surficial Aquifer

Analysis of the hydrology in the surficial aquifer includes calculations of hydraulic conductivities and transmissivities, a contour analysis of monitoring well head levels, and regional flow gradients in the surficial aquifer. Primary interest of this research was to quantify horizontal flow rates in the surficial aquifer, as well as to establish. the direction of flow in an attempt to determine the hydraulic impact of the phosphogypsum stack on the surficial aquifer.

Hydraulic conductivity analyses were conducted by two different analytical methods, allowing for respective well geometries that were available. The USGS well #9 **(Fig. 1-7)** was treated as an auger hole, while all other research wells were drilled to be partially screened for their lowest 10 feet.

The hydraulic conductivity for the auger hole was calculated according to a method prescribed by Boast and Kirkham (1971). The well was pumped out by a Grunfos machine, and the water table (i.e., head) allowed to rebound over the next hour. Measurements of the rebounding head elevation were taken with a conductive measuring tape, and entered into in a spreadsheet calculation program.

The analysis for the partially penetrating monitor wells was conducted on proprietary wells 1 and 8, and research wells 11, 18, 21, 22, and 24, using a method described by Bouwer and Rice (1976). A volume of approximately 200 liters was pumped out of each well using a Grunfos machine, and then the well was allowed to recharge. As the hydraulic head rebounded, elevation measurements were taken and imported into a spreadsheet program.

The contours of the water table on site were compiled every three months using hydraulic head elevations taken from the following wells: proprietary wells 1 - 5, 8-11, research wells 8 - 24, U.S.G.S. wells 8, 9, 34, 36, 37, 39, and stack well 2-0. Data files were entered into a PC program called Surfer, and contours generated using the kriging method. Because of the importance of the head measurement at well 2-0 (which wasn't drilled until March 1996), only contours for months that include measurements at this well are presented.

The regional flow of the surficial aquifer is partly controlled by the confining unit beneath it, and the direction and gradient of the surficial aquifer was estimated through an assumption of a consistent surficial aquifer thickness. Because of a lack of monitor wells further away from the phosphogypsum stack that would have allowed to properly define

the groundwater gradient the standard assumption was made that the regional flow in the surficial aquifer is primarily determined by the topographic slope of the land surface. To determine the latter a three-dimensional regression of the drainage basin using an equidistant node grid of elevations was made, leading to a first-order representation of the regional flow without the mounding effect of the phosphogypsum stack. Calculations of the topographic plane were made in the AXUM graphing program using a collection of data points taken from topographical maps of the area. The transects for the data point collection were made at a one unit interval (representing 200 m.) of plotted data in an AutoCAD drawing.

The precipitation for the area was measured daily at stations on site, and at the U.S.G.S. stations in Ruskin (10 miles to the north), and Bradenton (5 miles to the south). These data were compared to monitoring well heads and stack pond levels in hydrograph format. In addition, these hydrographs were analyzed for temporal and spatial relevance to the possible recharge of the aquifer and the phosphogypsum stack.

CHARACTERIZATION OF THE HYDROLOGICAL ENVIRONMENT

This section presents the results of the hydrologic characterization of the gypsum stack and the underlying surficial aquifer, including an analysis of the regional precipitation data. These characterizations are necessary for the parameter adjustments of the groundwater model presented in the following chapter. Complete data plots are presented in the appendices (I, II, III) to this chapter.

Stack Analysis

Analysis of Hydraulic Heads. Hydraulic head measurements for all three well clusters demonstrate a downward flow in all instances. Specific gradients between stratigraphic layers of the gypsum stack can be made for each of the well regions, as well as a determination of the flow gradient to the surficial aquifer. Patterns of relative head do not change over time, but can be correlated to the precipitation record (presented at the end of this section).

Well cluster 1 **(Fig. 1-8)** shows a typical illustration of a gradual downward flow. The occurrence of a slight plateau between wells 1-2 and 1-3 points to a region of slower flow when compared to the neighboring head gradients to wells 1-1 and 1-4.

Well cluster 3 **(Fig. 1-9)** illustrates flow toward the screening depth of well 3-2, which is conceptually consistent with well cluster 1, because even though well 3-1 is the deepest of the three wells, it is fully screened. Thus, head measurements are responding according to their highest screened elevations and force downward flow gradients between all wells.

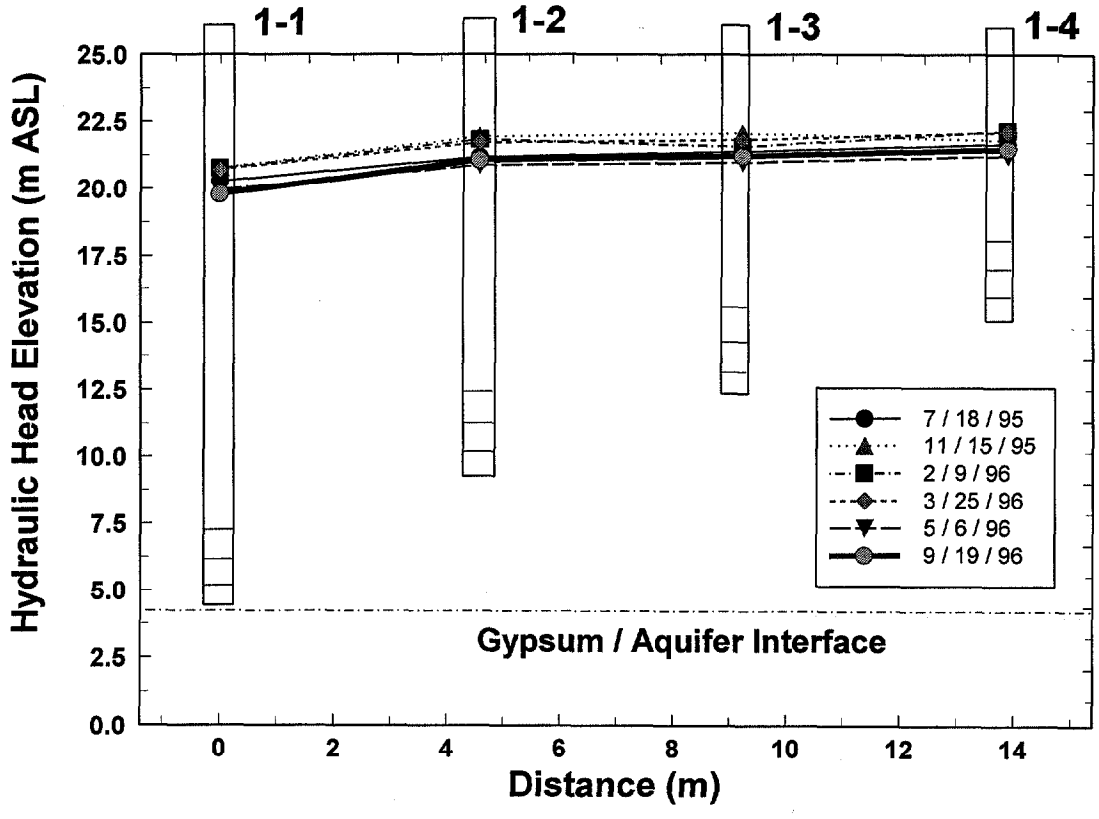

Figure 1-8. Hydraulic head comparison for well cluster 1. A general downward gradient is found in consecutively deeper wells.

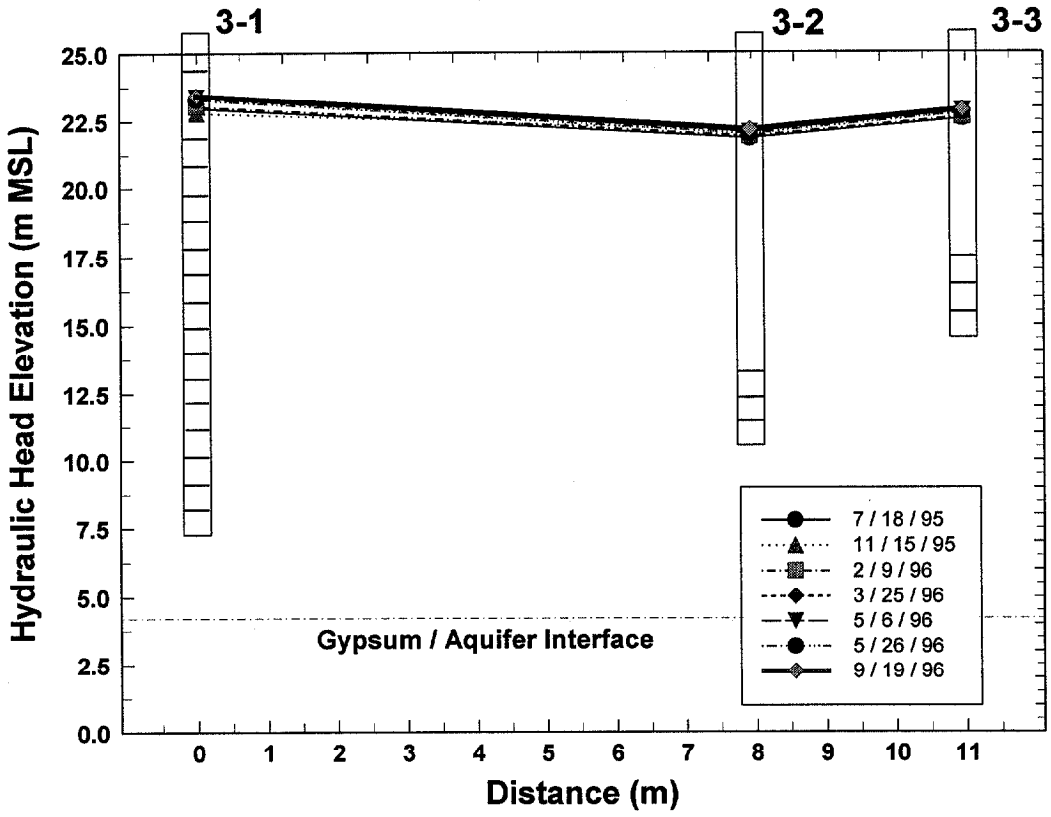

Figure 1-9. Hydraulic head comparison for well cluster 3. A downward gradient is found toward well 3-2 which represents a head level for the deepest section of screening in the gypsum stack.

Well cluster 2 **(Fig. 1-10)** is of particular significance due to well 2-0, which is drilled into the surficial aquifer. Gradients between all wells are still downward, which also includes down into the surficial aquifer. The presence of a gradient toward well 2-0 provides one of the most critical factors needed for a distinction of flow into the surficial aquifer. However, the relative magnitude of the actual gradient and of the hydraulic conductivity will determine the flow velocity and the fluxes of stack water that can seep into the surficial aquifer. A comparison to surficial aquifer head levels, as well as quantitative modeling of flow rates, will provide a clearer picture of the factors controlling the hydrological environment here.

Cooper-Jacob Straight-line Method. Transmissivity and storativity values were determined through a modification of the Cooper-Jacob equation. The latter represents an asymptotic solution for large times t of the Theis equation which describes the radially symmetric, non-equilibrium head-drawdown *s(r,t)* in a confined aquifer as a function of the radius (distance) r and time t under the influence of pumping. The Cooper-Jacob equation is then (Driscoll, 1986):

$$s(r,t) = \frac{Q}{4\pi T} \cdot (-0.57772 - \ln u) \qquad (1.1a)$$

By substituting for the expression $u = \frac{r^2 S}{4Tt}$, and converting to log base-10 format one gets the following equation:

$$s(r,t) = \frac{23Q}{4\pi T} \cdot Log(2.25\frac{Tt}{r^2 S}) \qquad (1.1b)$$

By obtaining the drawdown *s(r,t)* observed in one log unit **(Figs. 1-11, 1-12),** and a known value for the pumping rate Q, a value for the transmissivity can be calculated for the wells that were pumped (i.e., PP1-2, PP2-2, and PP3-1).

The storativity S is determined from the intercept time t_0 which corresponds to a zero drawdown s=0 (i.e., is obtained by setting the log-term equal to one). The intercept time t_0 is depicted graphically from the intercept of the straight line tangent to the drawdown curve with the horizontal axis. Values for the storativity S cannot be determined for the wells that were pumped, since there is a singularity in the solution for r =0.

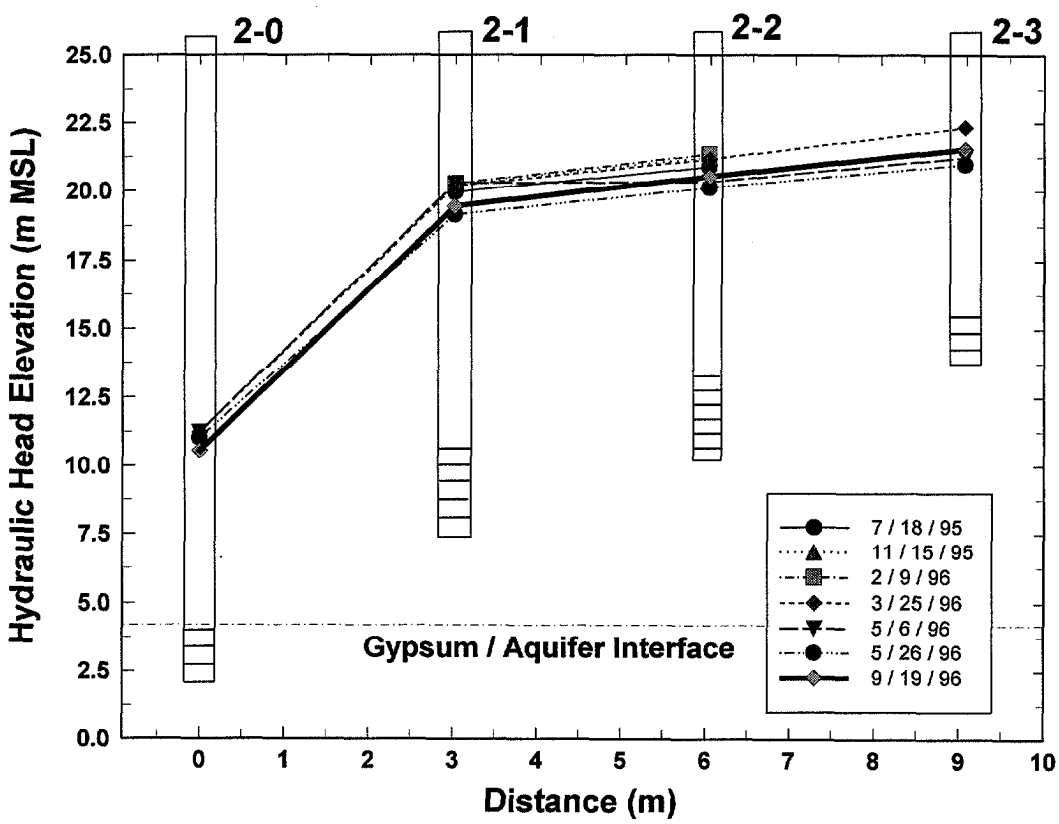

Figure 1-10. Hydraulic head comparison for well cluster 2. A downward gradient is found into the surficial aquifer represented by well 2-0.

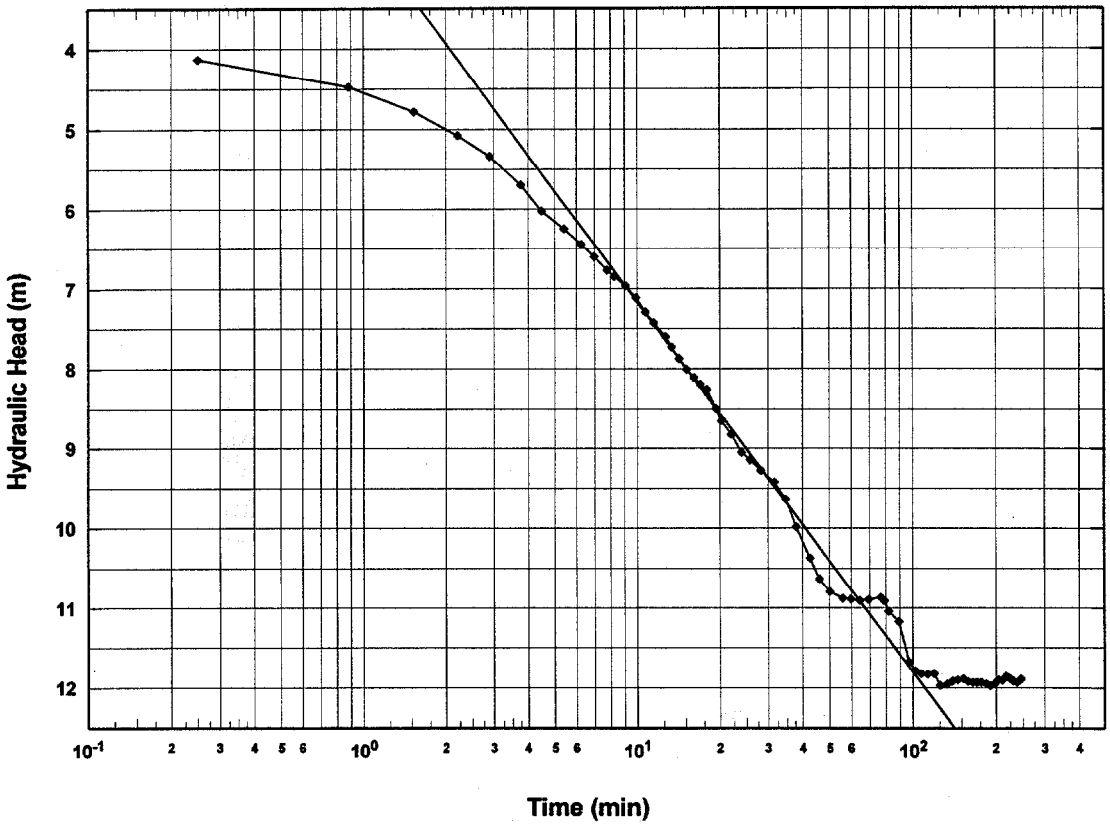

Figure 1-11. Pump drawdown versus time in stack well 2-1. Of particular note is the recharge indicated by the data between 50 and 80 minutes of pumping.

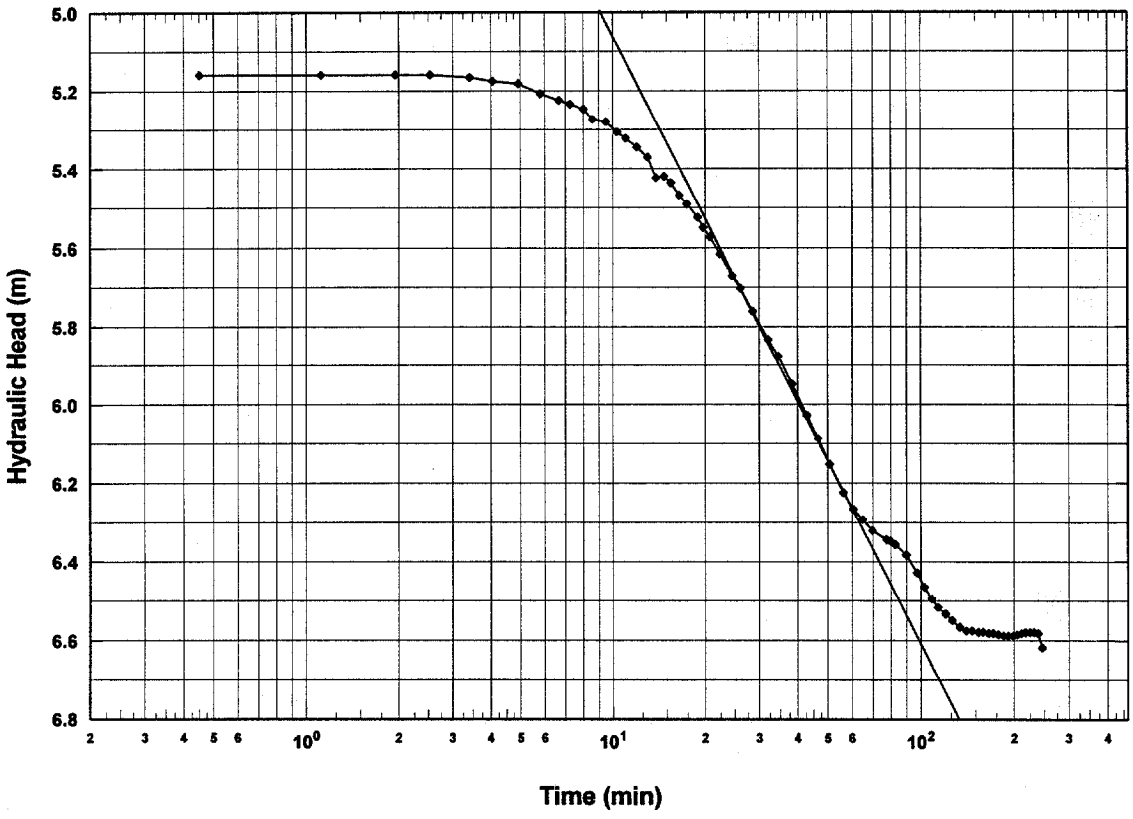

Figure 1-12. Pump drawdown versus time in stack well 2-2. Of particular note is the recharge indicated by the data between 65 and 90 minutes of pumping.

Even though transmissivity values for only three of the stack wells were obtained **(Table 1-2),** the wide range found indicates a variation of the transmissivity throughout the stack. This variation may be caused by modification of the stack structure during structural maintenance of the stack, whereby gypsum material from the pond is dug out to strengthen the confining walls. The transmissivity value for well 3-1 is the best representation of conductivity for the stack as an entire unit (owing to the well's representative screened length), while the values for wells 1-2 and 2-2 are more indicative of particular horizons within the stack.

Storativity values are well constrained, with all values falling within one log unit. An average of 4.8 x 10^{-5} denotes a value comparable to that of natural gypsum, indicating that the waste material maintains storage properties similar to that of its chemically related compound.

Table 1-2. Transmissivity and storativity values for stack wells.

Well Designation	Transmissivity (m^2/day)	Storativity
1 - 1	16.163	0.00009143
1 - 2	6.883	-
1 - 3	47.638	0.00001568
1 - 4	90.512	0.00008784
2 - 1	2.526	0.00006698
2 - 2	0.846	-
3 - 1	0.445	-
3 - 2	10.842	0.00001706
3 - 3	32.526	0.000008922

Although drawdown curves for most of the analyses are typical of a normal aquifer response, wells 2-1 **(Fig. 1-11)** and 2-2 **(Fig. 1-12)** demonstrate a plateau in their data close to the equilibrium stage of pumping. This occurrence has been classified as an influence of recharge, resulting from a proximity to the stack pond. Additionally, the delay observed between the wells is attributed to the recharge occurring closer to the pump source. On the other hand, the plateau at well 2-2 is less dramatic because it is on the perimeter of the drawdown influence.

Pressure Transducer Tests. Investigation with the pressure transducer was intended to provide an identification of horizontal flow within the stack interior. Complete analysis of the pressure at every depth in all three cluster areas was not possible because of the limited range provided in the screened sections. Regardless of this restriction, anomalous horizontal flow was identified in three of the wells. Wells 1-3 **(Fig. 1-13)** and 3-1 **(Fig. 1-14)** illustrate sections of decreased ambient pressure, while

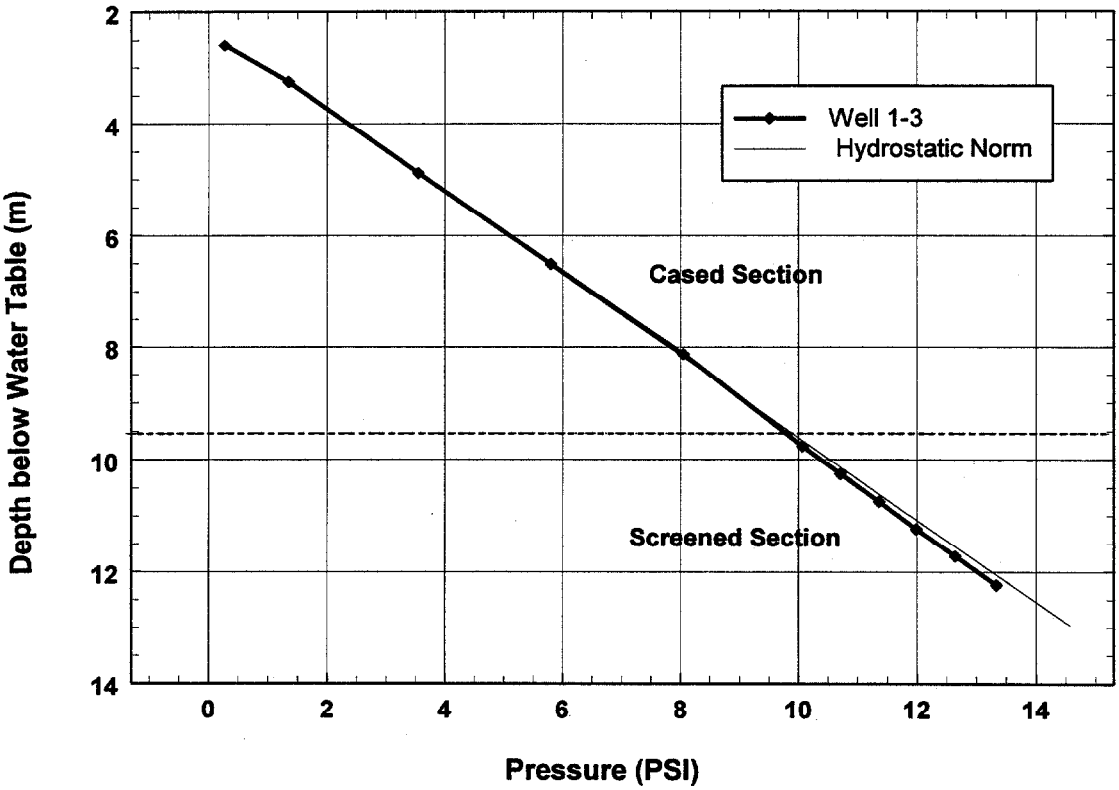

Figure 1-13. Pressure transducer measurements for well 1-3. Deviation of readings in the screened section (9.5 - 12.5 m.) below the hydrostatic norm show a regional decrease in ambient pressure.

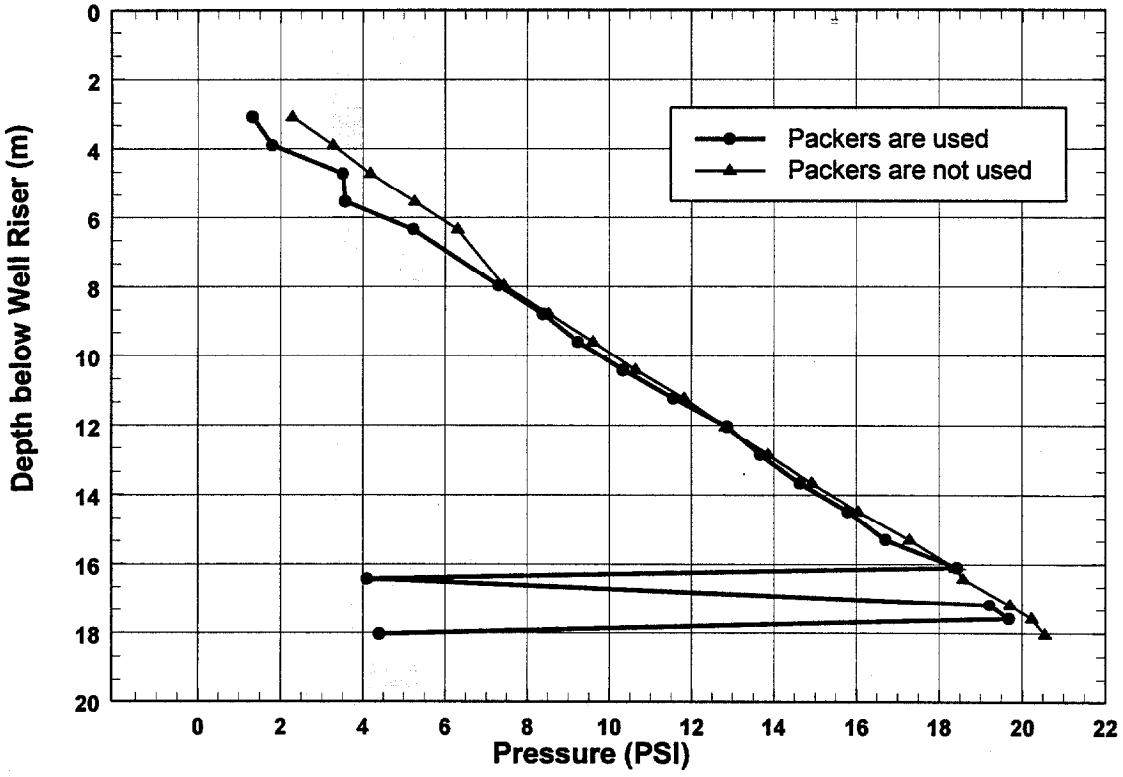

Figure 1-14. Pressure transducer measurements for well 3-1. Deviation of readings in two sections below the hydrostatic norm (no packers used) show a regional decrease in ambient pressure.

well 3-2 **(Fig. 1-15)** demonstrates a single section of increased pressure. All other wells showed no deviation from the hydrostatic reference pressure, as computed from the density of the gypsum stack-water solution, indicating no significant vertical variations of the pressure and the hydraulic heads in those depths. This means that either there is no significant amount of vertical flow in that depth-section of the stack that would lead to a detectable amount of vertical pressure head gradient, or the pressure transducer is just not sensitive enough to pick it up.

The low pressure zone found at well 1-3 is on the west wall indicating the presence of a vertical flow gradient at depths approximately 10 m below the surface. Analysis of well 2-1 examines the same interval on the south wall, but does not indicate flow different from the expected hydrostatic reference. Thus, no support for a conclusive statement on the stack edges can be made, but the possibility for flow still exists.

Measurements made at well 3-1 were conducted in a different manner, owing to the fully screened section of the well. Comparison to unpacked pressure readings instead of a hydrostatic line allows a broader interpretation of the readings; however, two areas of pressure anomalies are still apparent. Lower pressures found in the "packed" measurements from 2 - 8 m are most likely an influx of fluid flow from the nearby pond, whereas spikes found at depths of 16.5 and 18.0 m are more of a mystery. This development is either evidence of poor field methods, or an indication of a flow conduit. The latter would suggest cracks at the intervals of the spikes, although the large contrast in pressure would suggest that this explanation is unlikely. Therefore, the spikes are interpreted as evidence of poor grouting of the well, whereby flow can seep vertically between the outer side of the borehole casing and the back-fill formation.

The high pressure zone of well 3-2, at an approximate depth of 13 - 15 m is quite important since it is located in the center of the stack between the north and south ponds. This reading is an indication of an increase in overburden pressure and is evidence for the conceptualized flow of a typical groundwater mounding model. Because of the fact that this anomaly is located close to the low pressure anomaly found in well 3-1, the measurements do not support a regional characterization of downward flow. Thus, conflicting evidence from both wells indicates heterogeneity of the gypsum stack at depth. However, because well cluster PP3 is located essentially at an old pond construction road, there is also the possibility that some of the observed anomalies do not reflect the phosphogypsum formation alone, but also the compacted back-fill material of the road.

Borehole Flowmeter Tests. The Borehole Flowmeter Tests (cf. Burnett et. al., 1995 for details) yield the following three major pieces of information:

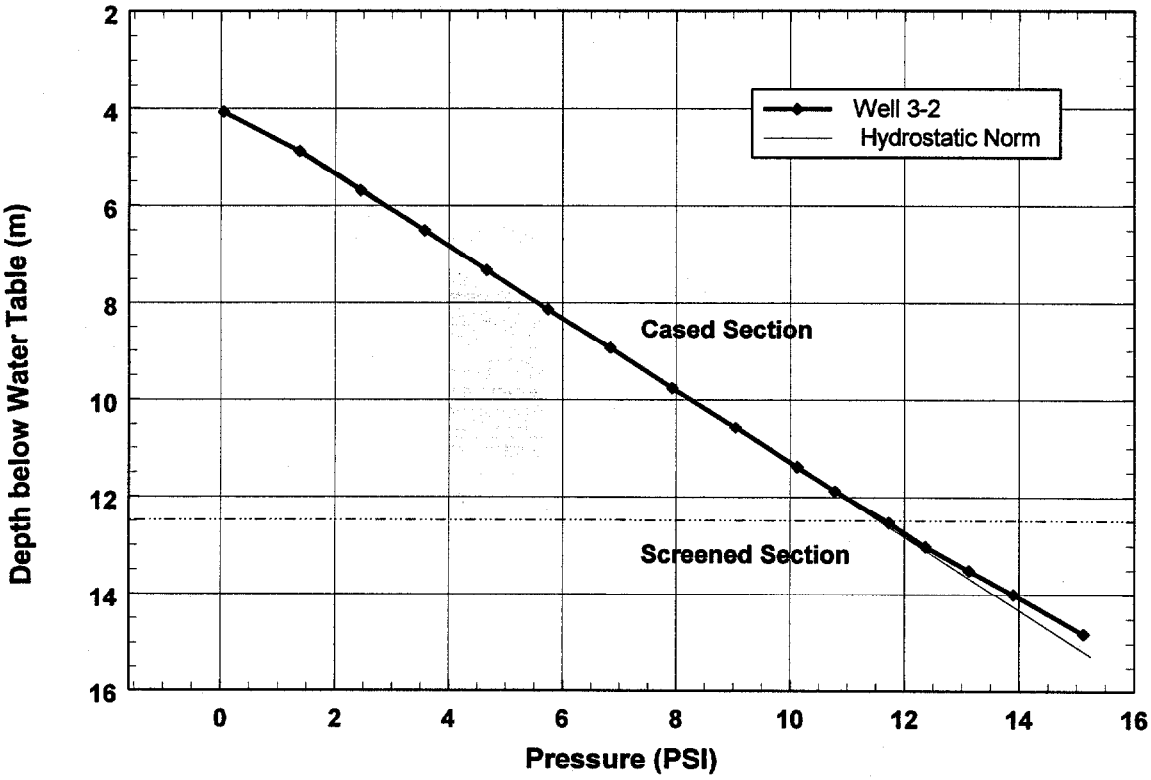

Figure 1-15. Pressure transducer measurements for well 3-2. Deviation of readings in the screened section (12.5 - 15.0 m.) above the hydrostatic norm show a regional increase in ambient pressure.

1) Ambient flow in the well under natural conditions. The nature of the ambient flow, especially its direction, provides clues on anomalous fracture and fault zones and vertical variations of the hydraulic heads.

2) Flow rates for each vertical section under steady-state pumping conditions.

3) Using the results from 1) and 2) vertical variations of the net flow rate in each of the probed intervals that are directly proportional to the hydraulic conductivity K in that vertical aquifer section.

Ambient flow measurements for both well 1-1 **(Fig. 1-16)** and well 3-1 **(Fig. 1-17)** provide strong support for a natural, downward flow of fluid in the stack. This evidence enhances the theory for topographical mounding of stack waters on the surficial aquifer, and clarifies specific internal heterogeneities at particular depths. The ambient differential readings of well 3-1 illustrate this point; readings fluctuate throughout the stack. These flow inconsistencies indicate that localized fracturing and/or bedding planes control flow.

A gradual decrease in the ambient flow is noted for both wells near the stack base, and is important to qualifying the significance of any topographical mounding. Although this trend is typical of unconfined units, its utilization in clarifying the permeability of the surficial aquifer interface is critical. Understanding of flow beneath the interface will determine whether this decrease is a product of an impermeable boundary or the result of an unconfined situation.

Induced pumping of the wells was undertaken in an attempt to investigate the response of the aquifer to such conditions and to quantify possible vertical stratifications of the hydraulic conductivity within the stack, as might be indicated by the presence of bedding planes that are clearly visible at the stack. As depicted in well 3-1, changes in increase of the net flow (or 2x net flow) denote a region of varied hydraulic conductivity. This finding gives strength to a theory of the stack as a layered hydraulic structure, with varying conductivities in different layers. Absolute values for these conductivities could be calculated from a more complete set of values determined by the Cooper-Jacob Test, along with the specific thicknesses of various identifying layers. However, this task has not been carried out here since layered stack conductivities will not be required as an input parameter in numerical mounding model to be presented in the next section.

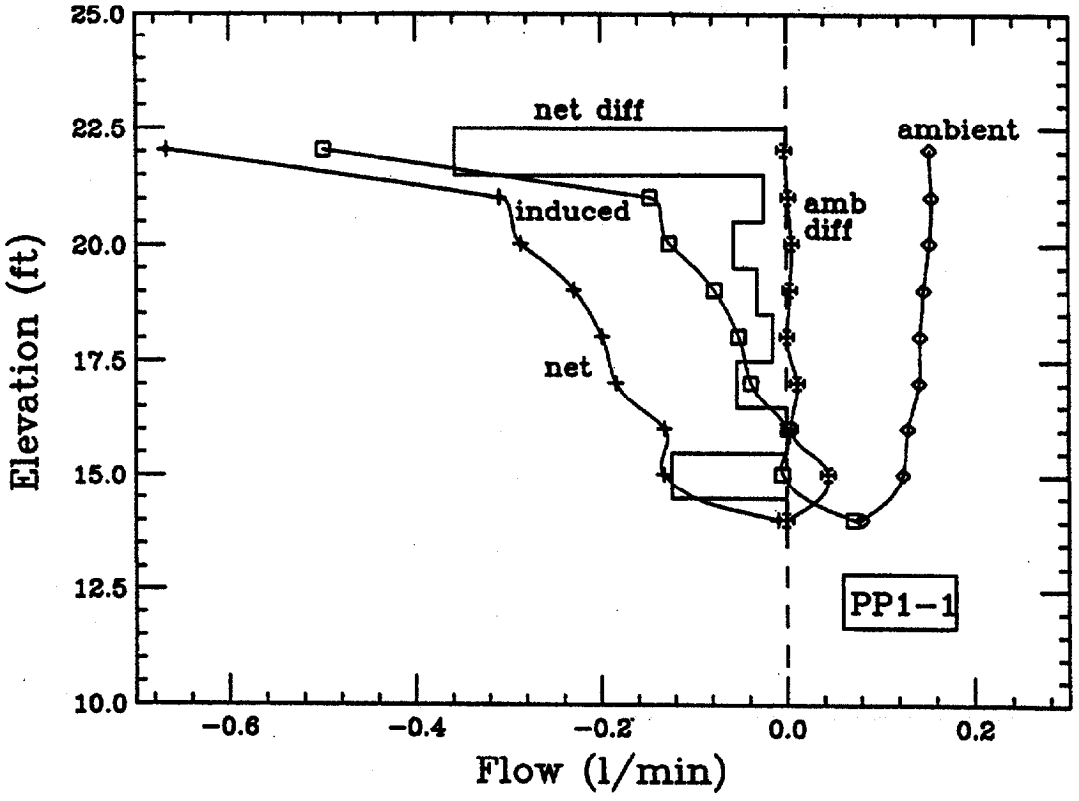

Figure 1-16. Borehole flowmeter results for stack well 1-1. Positive values denote downward flow and negative values upward flow.

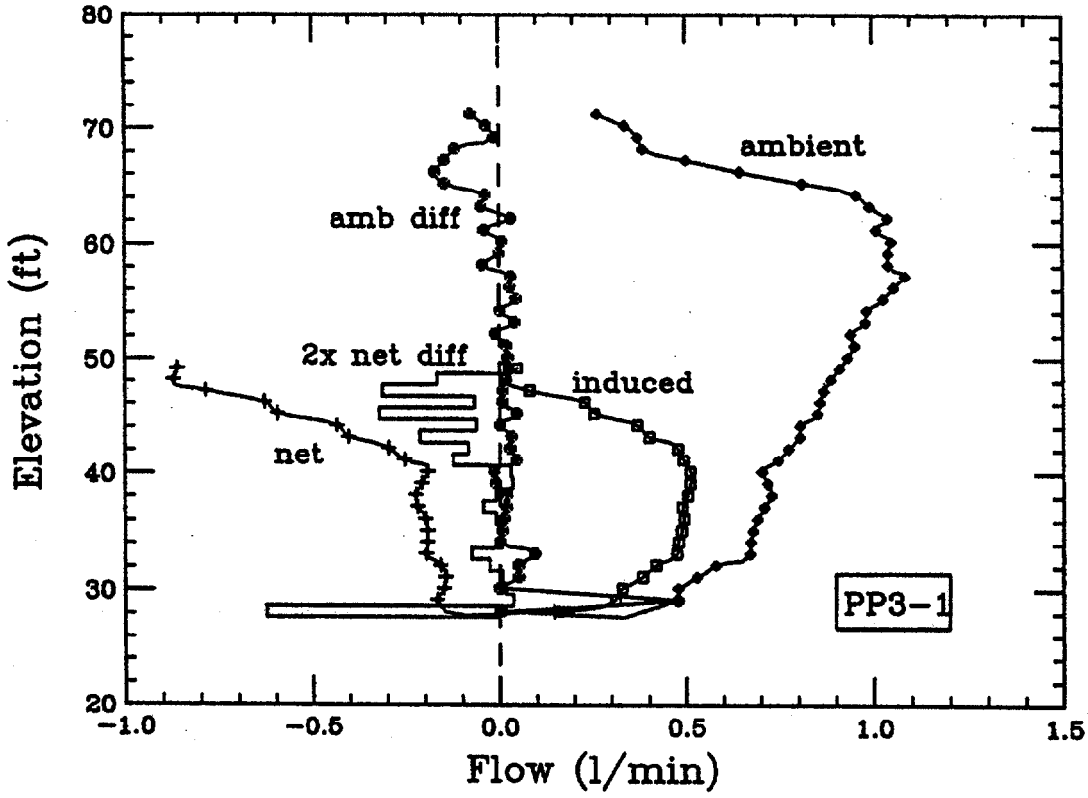

Figure 1-17. Borehole flowmeter results for stack well 3-1. Positive values denote downward flow and negative values upward flow.

Surficial Aquifer

Regional Flow Trend. The regression plot of topographical data **(Fig. 1-18)** denotes a flow gradient of 1.977 x 10^{-3} at an azimuthal direction of 303.19°. This gradient is at such a low angle that localized influence of the water table will be a large factor on the direction and speed of flow. Thus, these results may not represent small-scale flow patterns and gradients for the area, but they do give the best approximation for a generalized regional flow pattern. In addition, topography around the gypsum stack complex is relatively flat, so that the resulting gradient from this calculation is still a good representation of ambient conditions.

Water Table Contours. Contours of hydraulic heads for surficial aquifer monitoring wells are greatly impacted with the addition of well 2-0 which penetrates through the bottom of the stack. Thus, accurate representation of the water table in the unconfined zone cannot be made without inclusion of a measurement taken at this well. Contours for measurements taken on May 6, 1996 **(Fig. 1-19)** and September 19, 1996 **(Fig. 1-20)** arc typical of other data sets analyzed, and represent the extent of values found in the calculation of the water table for the surficial aquifer. Additional contours drawn from measurements at other sampling dates are depicted in Appendix III for this chapter.

Most significant of the contouring plots is the influence of the head-reading taken at well 2-0. The gradient between its location and other monitoring wells, namely, wells MW 1, RW 8, 11, 18,21,22, & 24 is indicative of a flow in the vertical direction, as well as a flow away from the gypsum stack in almost all horizontal directions. Flow to the southeast, however, is hindered due to the opposing force of regional flow. A water table low in the southwest quadrant may be the result of the cooling pond and the ditch system in that area. Presence of the ditches draws water flowing toward them to be evaporated and essentially taken out of aquifer system. Thus, the existence of the evaporating system leads to a lowering of the local water table.

Conductivity Analysis

Kirkham Auger Hole Test. Hydraulic conductivity of the well designated as USGS 9 was determined following the so-called auger hole method described by Boast and Kirkham (1971) and Amoozegar and Warrick (1986). This calculation dictates a relationship between the drawdown (y), time (t), and hydraulic conductivity (K) in the following equation:

$$K = \{\pi r^2 / [C(t_{i+1} - t_i)]\} \ln(y_i / y_{i+1}) \qquad (1.2)$$

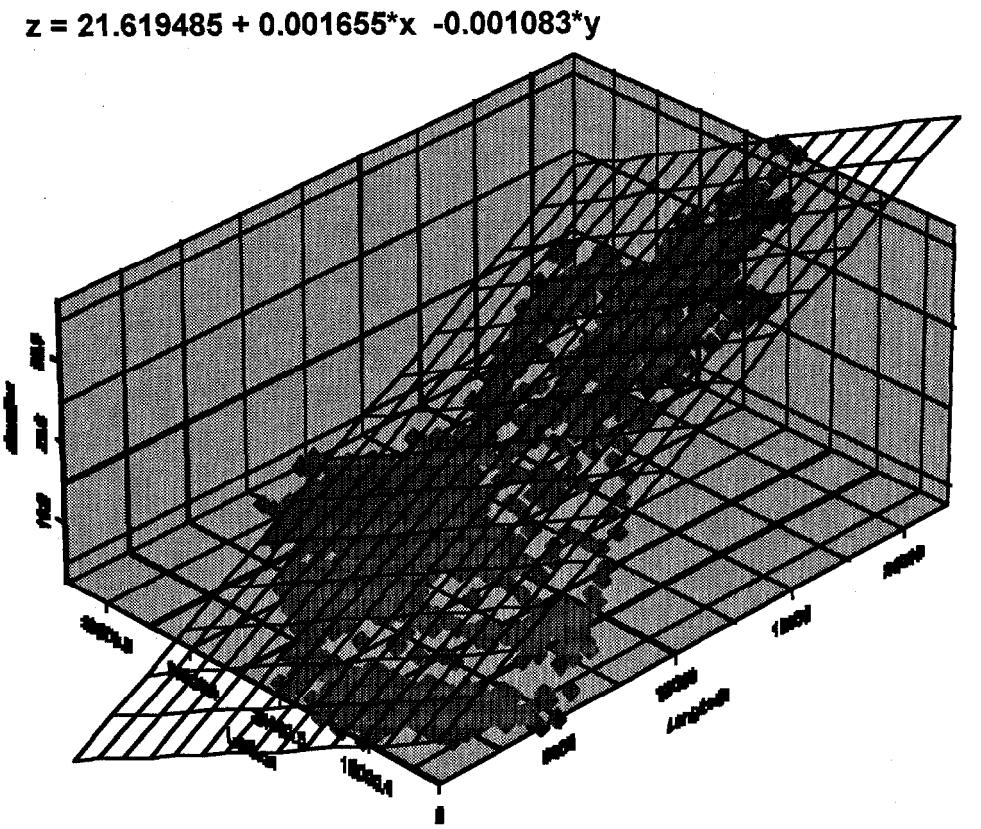

Figure 1-18. A 3-dimensional regression plot of topographic data. The above equation represents the trending plane in units of meters, although the slope and direction of the plane is determined by the x and y coefficients, which do not change. Resulting slope and direction of the regression plane are approximated as regional flow characteristics of the surficial aquifer due to a consistent thickness of the unconfined layer.

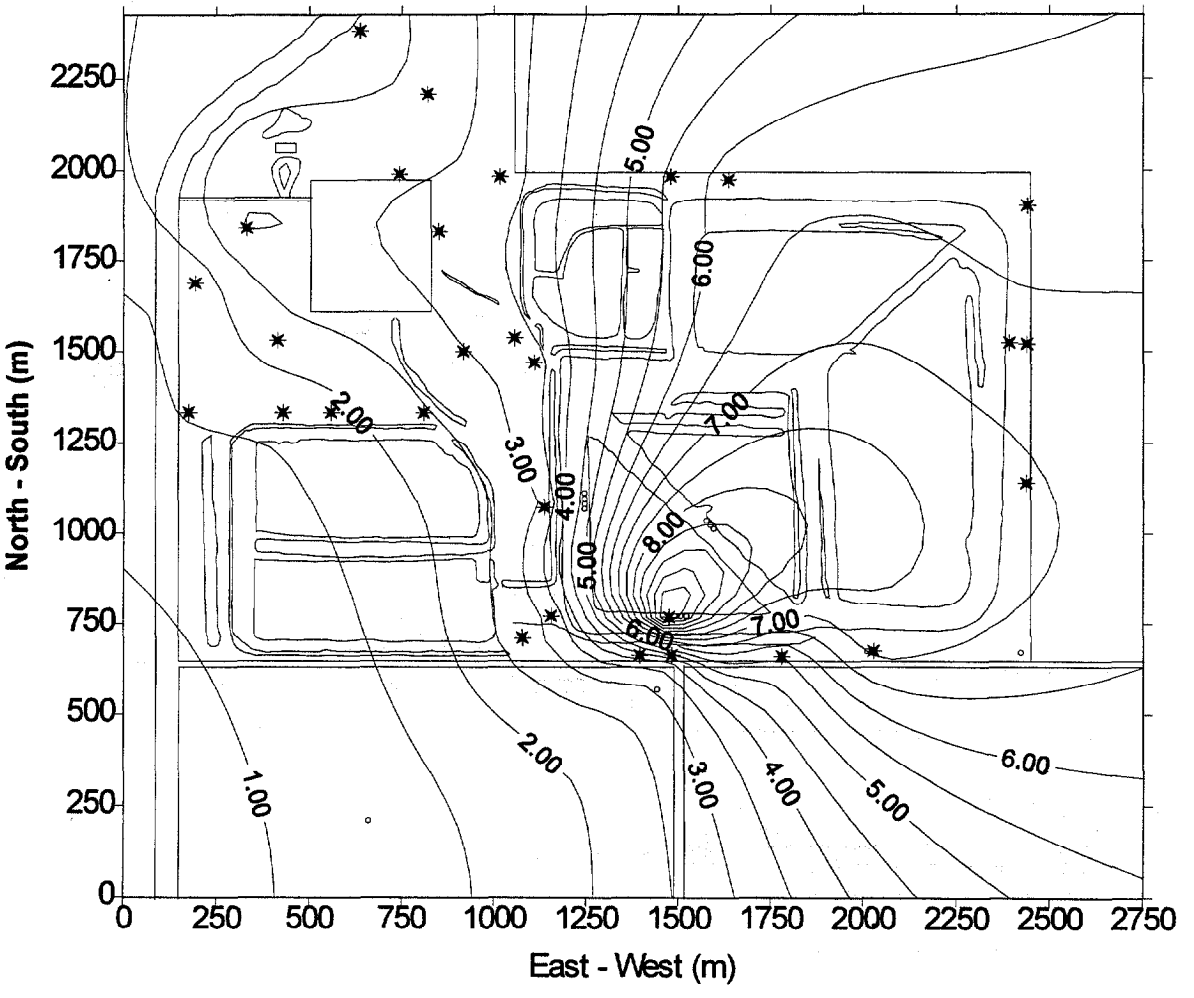

Figure 1-19. Contour plot of water levels in the surficial aquifer on May 6, 1996. Asterisks represent well measurements upon which the contours are based. Noteworthy characteristics of the map include a large head value at well 2-0 and regional low in the southwest quadrant.

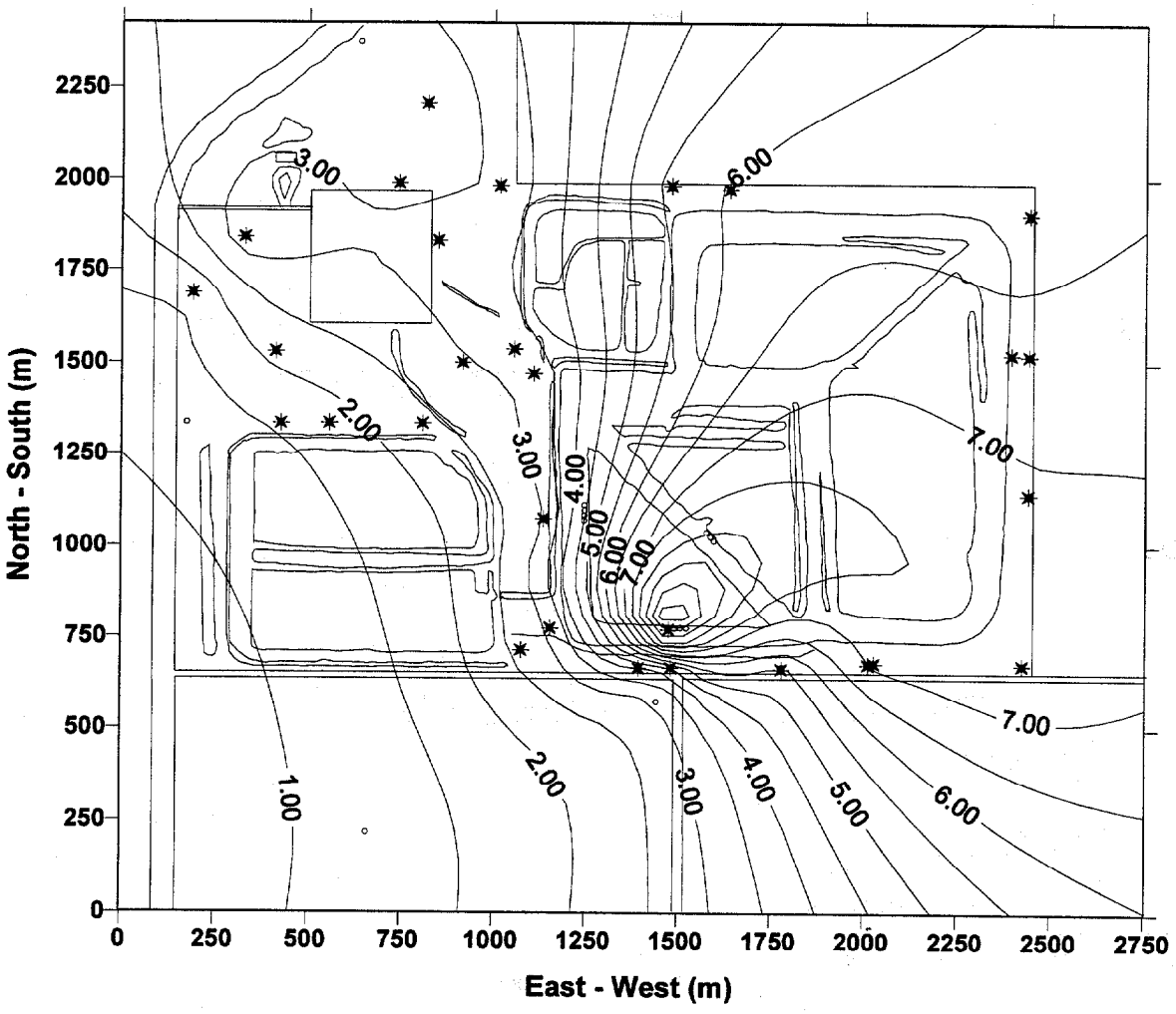

Figure 1-20. Contour plot of water level in the surficial aquifer for September 19, 1996. Asterisks represent well measurements upon which the contour is based. Noteworthy characteristics of the map include a large head value at well 2-0 and a regional low in the southwest quadrant.

The hydraulic conductivity is in units of cm/sec, and is compared to known ranges of unconsolidated material (Bear, 1979). C is a shape factor that is commonly referred to as a constant of the equation. Three variables are used to calculate the value of C/r in equation 1.2 :

(1) the ratio of the cavity height to the well radius;
(2) the ratio of the cased well section to the well radius; and
(3) the ratio of the impermeable layer depth beneath the cavity to the well radius.

Although the geometry of USGS 9 does not allow the determination of a constant from known values (Youngs, 1968), a log base E curve-fit of these values **(Fig. 1-21)** was able to obtain a viable solution for many ratios of the cavity height to the well radius hc/r. Based on the most likely geometry of the well, the "hc/r=0" curve was selected as the most reliable one. Using this type-curve a hydraulic conductivity in the range of 0.00075 - 0.00190 cm/sec was determined,-which is in the range of two geomorphic classifications: clean sand ($1 - 10^{-4}$) and silty sand ($10^{-1} - 10^{-5}$).

Bouwer Rice Test. The procedure for the aquifer analysis of wells 2-0, MW 1, RW 8, 11, 18,21,22, & 24 followed a "slug" recovery method, developed by H. Bouwer and R.C. Rice (1976). This procedure takes into account the partially screened nature of many monitoring wells **(Fig. 1-22)** in the calculation of hydraulic conductivity, and allows a spatial analysis of conductivities around the site.

The Bouwer / Rice theory is based upon a modification of the Thiem equation to:

$$Q = 2\pi K L \frac{y}{\ln(R_e / R_w)} \qquad (1.3)$$

where Q is the volume of water flowing into a well at a specific depth y, K is the hydraulic conductivity, L is the length of the screened section, and R_e/R_w is a ratio of the effective radius of the pumping influence over the effective radius of the well (including the grouted radius). The rate of water level rise (dy/dt) can be represented as:

$$dy/dt = -Q/\pi r_c^2 \qquad (1.4)$$

where r_c is the radius of the cased well section. Insertion of equation 1.4 into 1.3, followed by integration will produce:

$$\ln y = -\frac{2KLt}{r_c^2 \ln(R_e/R_w)} + \text{constant} \qquad (1.5)$$

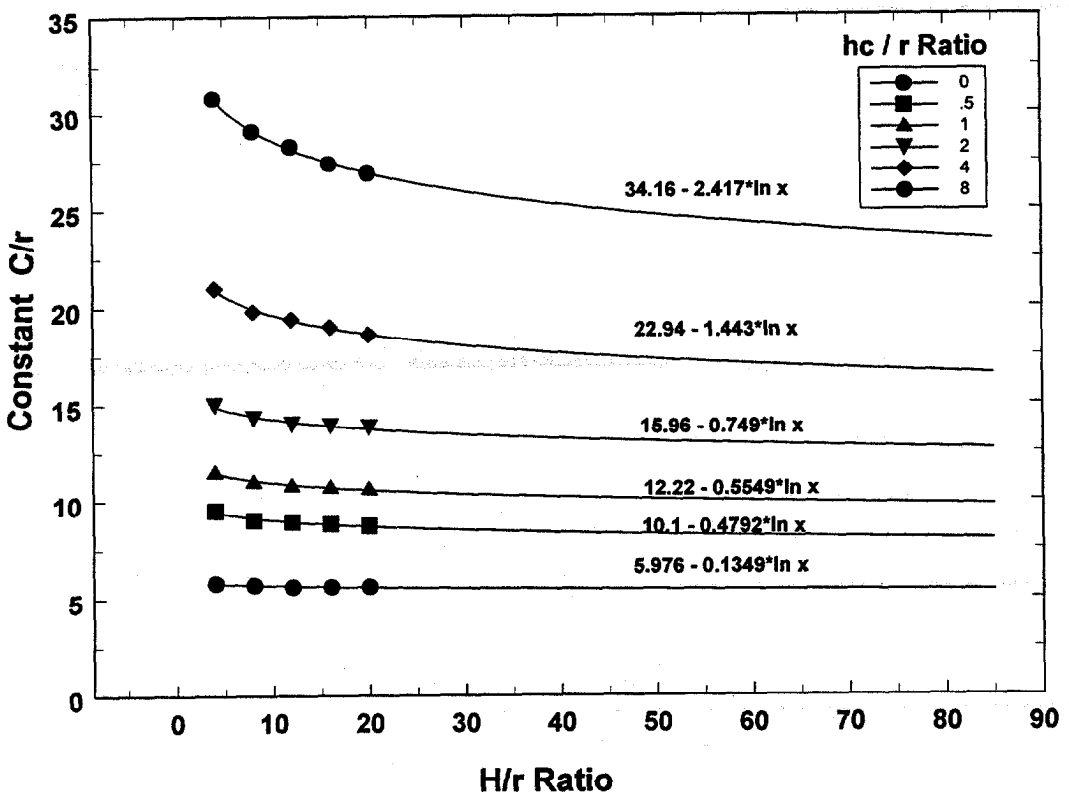

Figure 1-21. Determination of the shape factor C/r by a natural log curve-fit. Approximation of the shape factor for large H/r values was needed in calculating the conductivity for USGS well #9.

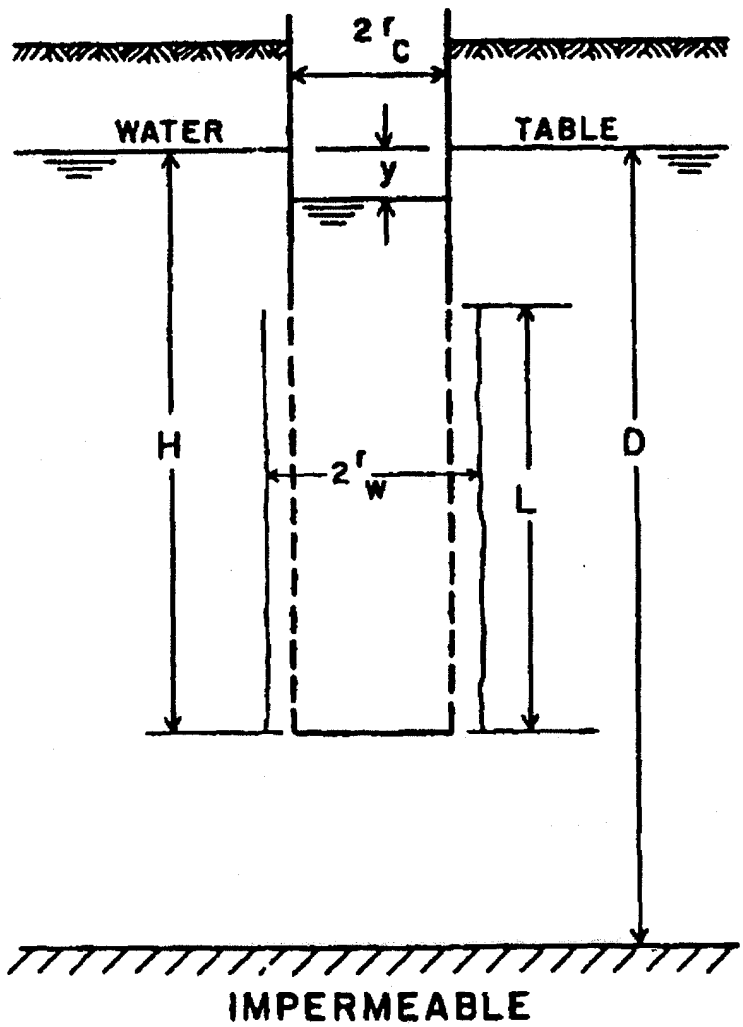

Figure 1-22. Generalized well geometry of a partially screened well. Note values for H, L, and D.

Applying this solution for limits y_0 and y_t where t = 0 to t while solving for K yield the final equation that was used:

$$K = \frac{r_c^{\,2} \ln(R_e/R_w) \ln(y_0/y_t)}{2Lt} \qquad (1.6)$$

Although most parameters are easily determined in the calculation, ln (R_e/R_w) is somewhat variable within various geologic environments. More specifically, the effective radius of influence will vary in relation to the depth of the underlying confining unit below the bottom of the well. Bouwer and Rice (1976) determined that ln (R_e/R_w) varies inversely with ln [H / R_w] and linearly with ln [(D-H)/ R_w]. Results enabled derivation of the following two equations: eq (1.7) for partially penetrating wells and eq (1.8) for completely penetrating wells (where D-H = 0):

$$\ln R_e/R_w = \left[\frac{1.1}{\ln H/R_w} + \frac{A + B\ln[(D-H)/R_w]}{L/R_w} \right]^{-1} \qquad (1.7)$$

$$\ln R_e/R_w = \left[\frac{1.1}{\ln H/R_w} + \frac{C}{L/R_w} \right]^{-1} \qquad (1.8)$$

Coefficients A, B, and C from equations 1.7 and 1.8 are resolved by a relationship that has been determined through an electrical node analysis **(Fig. 1-23)** presented in Bouwer and Rice (1976).

In addition to the determination of the value for ln (R_e/R_w), hydraulic head values were graphed against time in a log plot **(Fig. 1-24)** (additional graphs are depicted in the appendix IV). The resulting slope of the line determined an average value for $ln(y_o/y_t)/t$ to be used in the calculation of the hydraulic conductivity.

Results for the hydraulic conductivities determined by this method **(Table 1-3)** characterize three zones of regional conductivity. Well 2-0 represents an area of a low conductivity (1.3 x 10^{-5} cm/sec) for the region beneath the stacks, while higher conductivities (mean ~ 3.9 x 10^{-5} cm/sec) are found in wells to the northwest (RW 18, 21, 22, 24). Southward of the stack (MW 1, USGS 9, RW 8 & 11) moderate values for conductivities are found (mean ~1.3 x 10^{-4} cm/sec). A comparison of the conductivities for the wells in the south to those in the northwest shows that the highest conductivities are determined for RW 18 and 24, where values are 3 - 4 times higher than the mean for the more southern wells. This is peculiar in relation to the wells' proximity to the

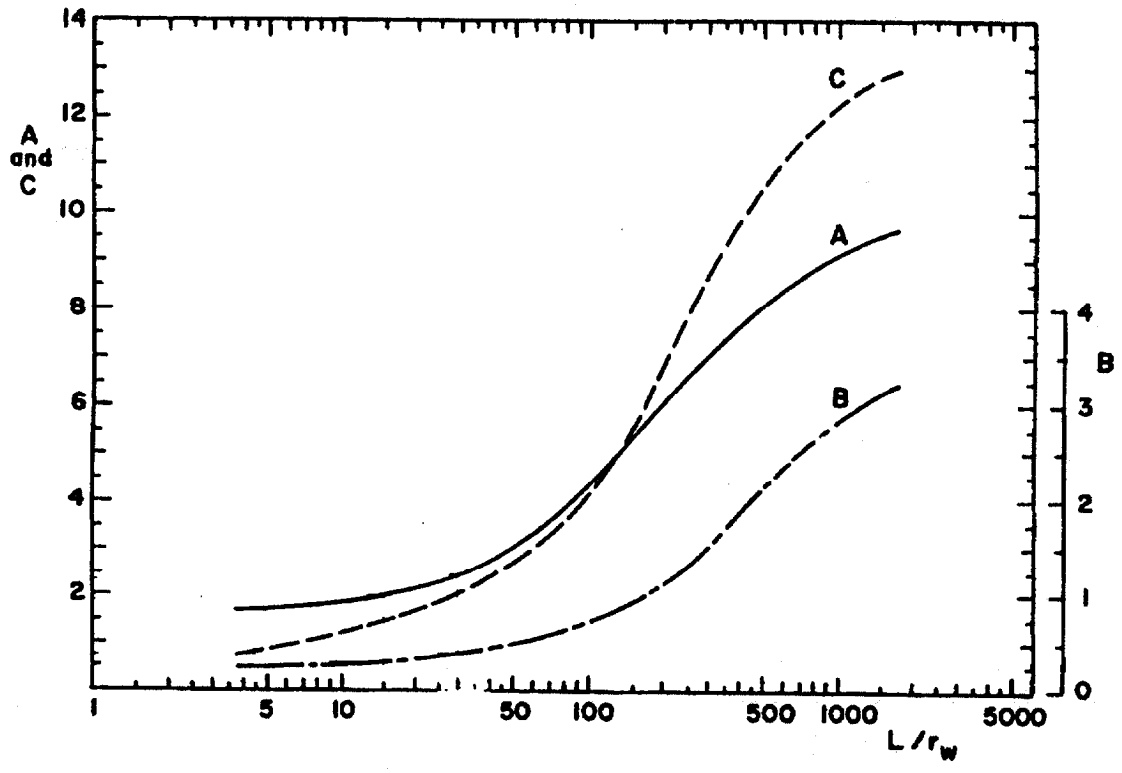

Figure 1-23. Relationships of A, B, and C for the calculation of R_e/R_w.. Using the formulas from the Bouwer/ Rice method, a range of possible conductivities were determined for the pump analyses.

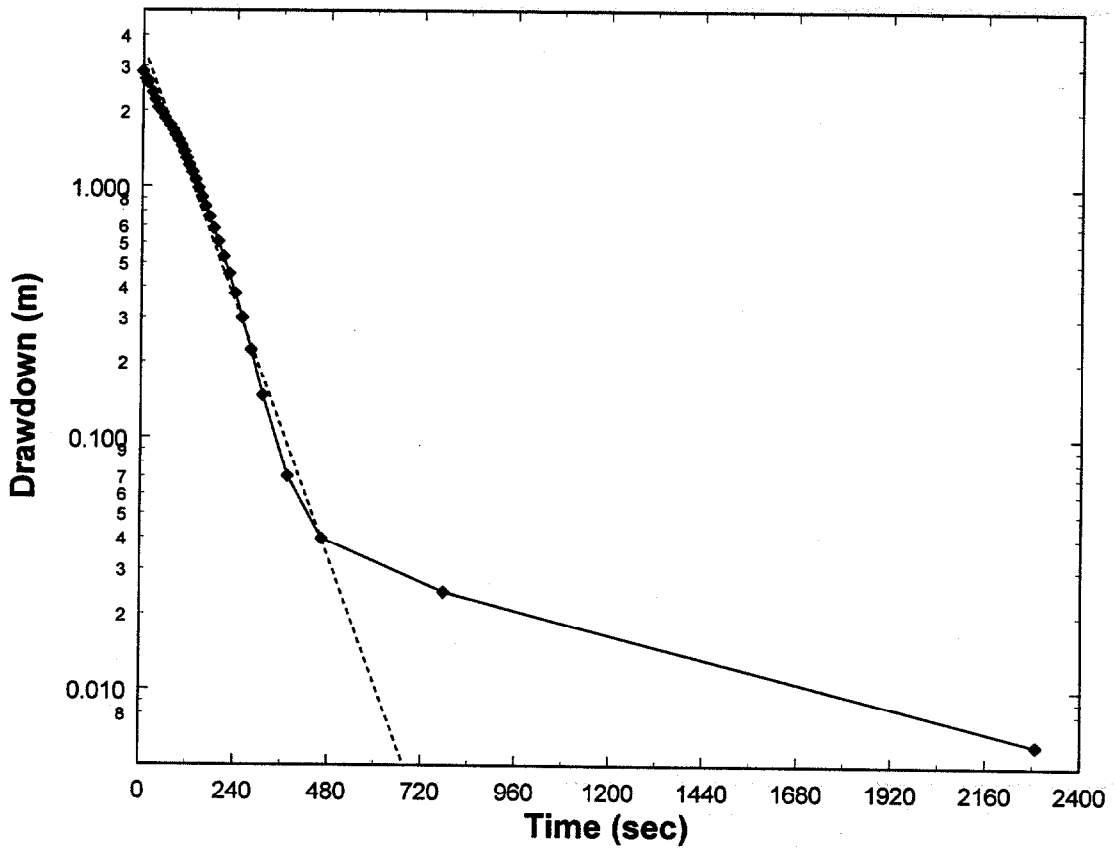

Figure 1-24. Drawdown versus time plot for well 18. The slope of the dashed line above is used in the calculation of conductivity as the value for *log (yo/yt)/t.*

influence of the stack, but the difference can be attributed to variations in the local geologic composition of the surficial aquifer.

Table 1-3. Conductivity ranges for surficial aquifer wells. Units for all values are in cm./sec, with maximum and minimum values approximated from individual slopes between head values in the drawdown plots.

Well	Mean	Minimum	Maximum
PP 2- 0	0.0000131	0.0000093	0.0000136
MW 1	0.0001290	0.0000900	0.0001620
MW 8	0.0000710	0.0000360	0.0001690
USGS 9	0.0001480	0.0001330	0.0002290
MW 11	0.0001700	0.0001100	0.0003480
MW 18	0.0006130	0.0002100	0.0007690
MW 21	0.0002440	0.0001700	0.0003090
MW 22	0.0002590	0.0001130	0.0003180
MW 24	0.0004370	0.0002770	0.0006960

Precipitation

Precipitation records from all three available sources indicated that each was unique in its measurements, and that not all of the sources could be relied upon in correlation with the hydrologic system in the stack area. Thus, records from on-site measurements for 1995-1996 were relied upon in the correlation to precipitation, while readings from Bradenton and Ruskin were not considered.

Precipitation measurements showed a high degree of correlation to stack pond levels **(Fig. 1-25)** and monitor well levels **(Fig. 1-26).** Therefore, hydrologic controls of these water bodies were considered to be at relative equilibrium with their environment. Water-table levels of the stack pond were shown to be very small on a monthly scale and found to impact ambient levels only during large precipitation events, as depicted in the records for October of 1994. Water-table elevations in monitoring wells are seen to recover within weeks, owing to the high conductivity of the sandy composition in the surficial aquifer.

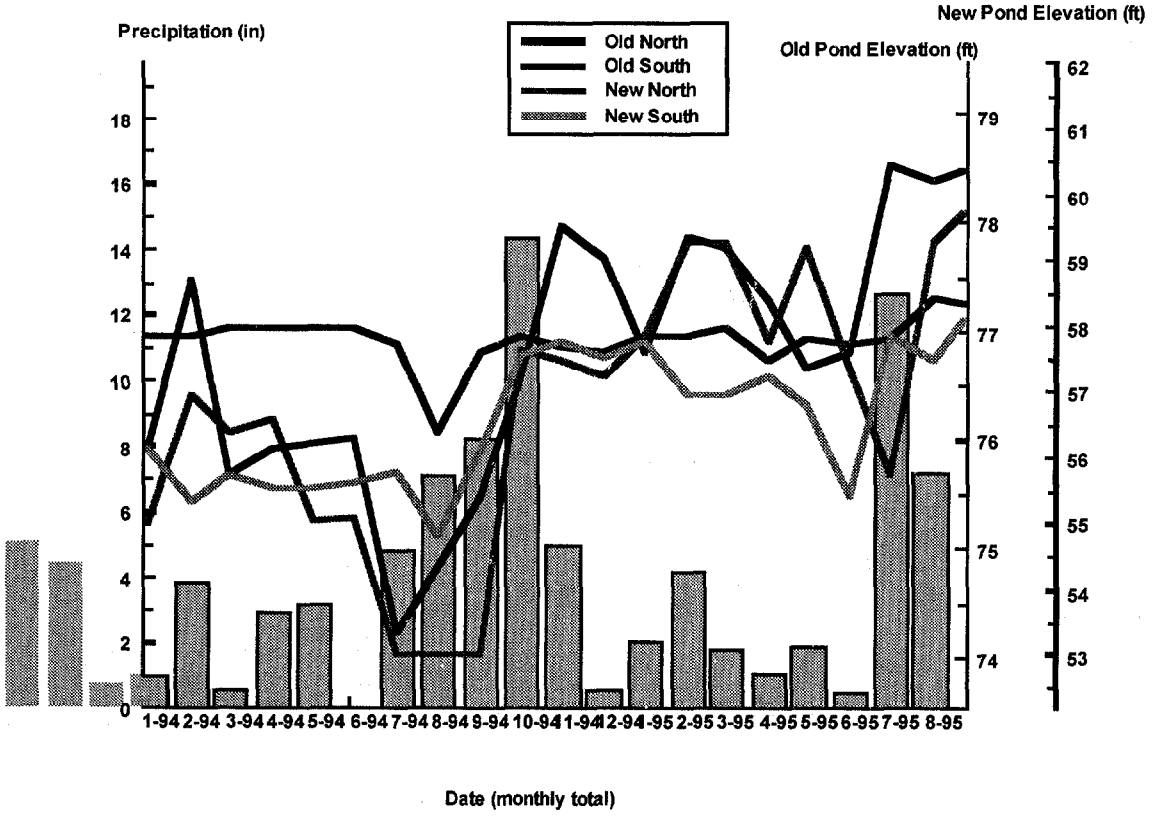

Figure 1-25. Comparison of precipitation records to stack pond elevations. Correlation between the records is most evident during October, 1994.

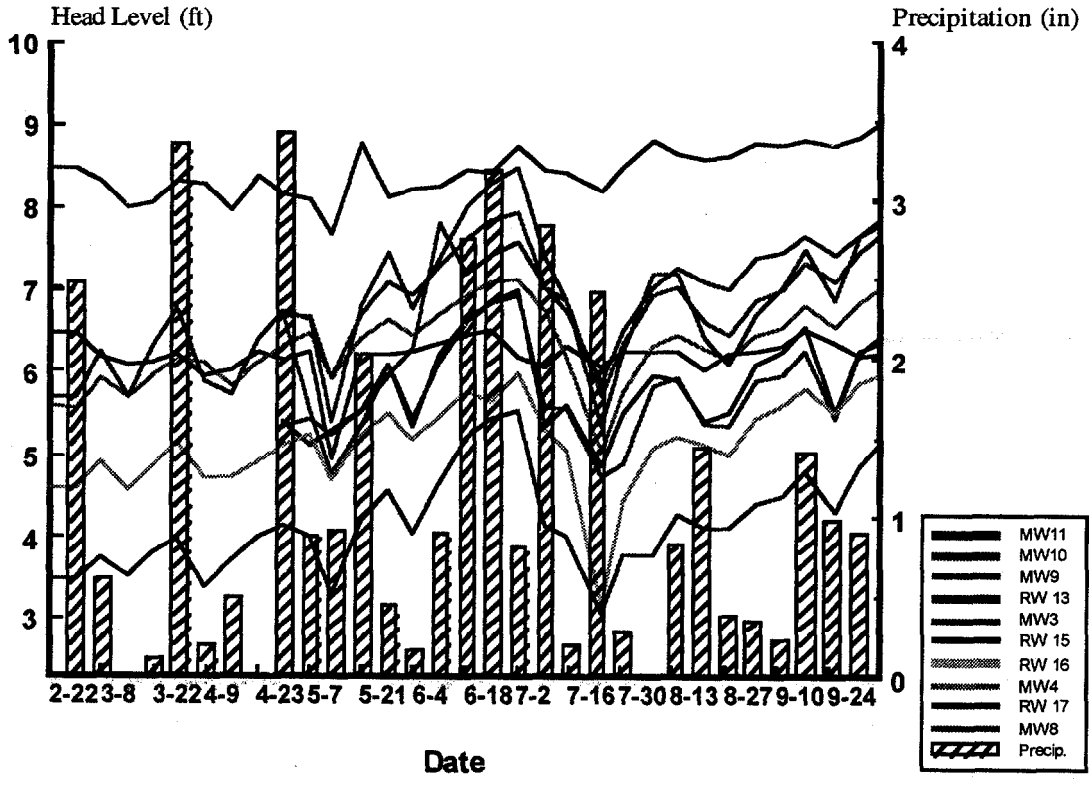

Figure 1-26. Comparison of precipitation records to monitor well levels. Correlation between the records is most evident during mid-June.

Annual precipitation for 1995 was 159.2 cm with the highest monthly records in July and August, and the lowest in the months of December and January. Precipitation highs and lows are attributable to seasonal variations, with large annual numbers due to the area's latitude and proximity to the Gulf of Mexico. Annual totals are minimally variable from year to year, and consistent in their pattern of distribution each month.

In summary, precipitation has been highly variable spatially over the area but similar in annual totals. This will, of course, lead to localized variations of the recharge flux into the hydrologic environment (i.e., the gypsum stack and the surficial aquifer) from day to day, but should even out when considered on a regional scale over longer periods of time. Large precipitation events will impact hydraulic head levels in the stack ponds for months, while influences on the surficial aquifer are found to only last weeks.

GROUNDWATER FLOW MODEL

Description of the MODFLOW model

Groundwater flow at the Piney Point facility was simulated using *Processing Modflow for Windows* (1994), a computer-simulation software package (hereinafter referred to as MODFLOW) that utilizes a three-dimensional, modular finite difference method, first developed by McDonald and Harbaugh (1988) for the U.S. Geological Survey. This modeling practice makes use of a nodal network, whereby each node represents a hydraulic head and is modified through adherence to aquifer parameters (i.e., hydraulic conductivity and transmissivity) and environmental constraints (i.e., ditches and ponds, recharge from precipitation and evaporation). These simulations may be run under transient or steady-state conditions; however, only steady-state solutions are considered here.

Mathematical Theory

Modflow simulates groundwater flow under the assumption of constant fluid density, and generates head values for each node within its environment by solving the following partial differential equation (groundwater flow equation) for the hydraulic head h as a function of space (x,y,z) and time t (cf., Anderson and Woessner, 1992):

$$\frac{\partial}{\partial x}(K_x\frac{\partial x}{\partial h}) + \frac{\partial}{\partial y}(K_y\frac{\partial y}{\partial h}) + \frac{\partial}{\partial z}(K_z\frac{\partial z}{\partial h}) = S_s\frac{\partial h}{\partial t} - R \qquad (1.9)$$

where K_x, K_y, and K_z are hydraulic conductivity values in the x, y, and z coordinate directions, S_s is the specific storage of the geologic unit, h is the hydraulic head, and R is a

generalized sink/source term of external nature to the system (Anderson and Woessner, 1992).

Eq (1.9) is used in its steady-state form by setting the dh/dt-term on the right side to 0. The resulting steady-state groundwater flow equation changes then to the Poisson equation which is then integrated by a finite-difference method whereby discrete head values at each node, by using information from neighboring nodes, are iterated through the equation until the head change between two consecutive iterations is less than a chosen value. The numerical procedure used for the iteration process was the Preconditioned Conjugate Gradient method.

Design of the Flow Model

The Conceptual Model. Primary consideration for the design of the conceptual model was to isolate the stack-surficial aquifer boundary in the environment, so that a determination of the hydrologic flux between these two units could be made from the simulated hydraulic conditions.

The model is comprised of two layers that represent the two aquifer units being studied, the stack and the surficial aquifer **(Fig. 1-27).** The overlying stack layer consists of two regions of 8 and 15m thicknesses, representing new and old stack accumulations, respectively **(Fig. 1-28),** while the surficial aquifer layer is constructed as a flat-lying bed of a constant 10 m thickness. Regions of the top layer not representing a gypsum unit are designed to be insignificant through construction as a very thin unit (1 mm) with high hydraulic conductivity; thus, any water contained within each unit is drained immediately into the underlying layer and is of no consequence to any other head values.

Topography of the land surface will vary at the site, but it will have no influence upon the hydrologic head because this value in an unconfined unit will be impacted more by the elevation of the water table. Thus, the effect of stack control on head levels in the surficial aquifer are just as easily modeled impacting a topographically flat geologic unit as a varied one.

Grid Geometry, The simulation of the stack environment encompasses an area of 1183.36 hectares and is organized into 6400 cells on an 80 x 80 unit grid **(Fig. 1-28).** Each of the unit cells is in a square configuration with dimensions of 43 m x 43 m, and models an actual land surface of 1849 m^2. Although the gypsum stack represents only 6.1% of the total grid, a large modeling area was intended so that boundary conditions of the modeled environment would not have any major effect on head values in the stack region.

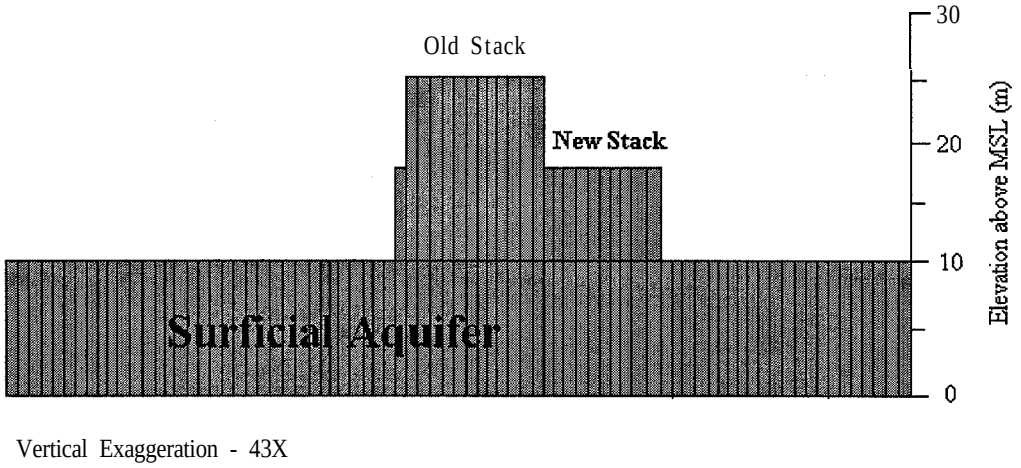

Figure 1-27. Vertical cross-section of the modeled environment. Actual representation of the environment is made with each rectangle representing a unit cell.

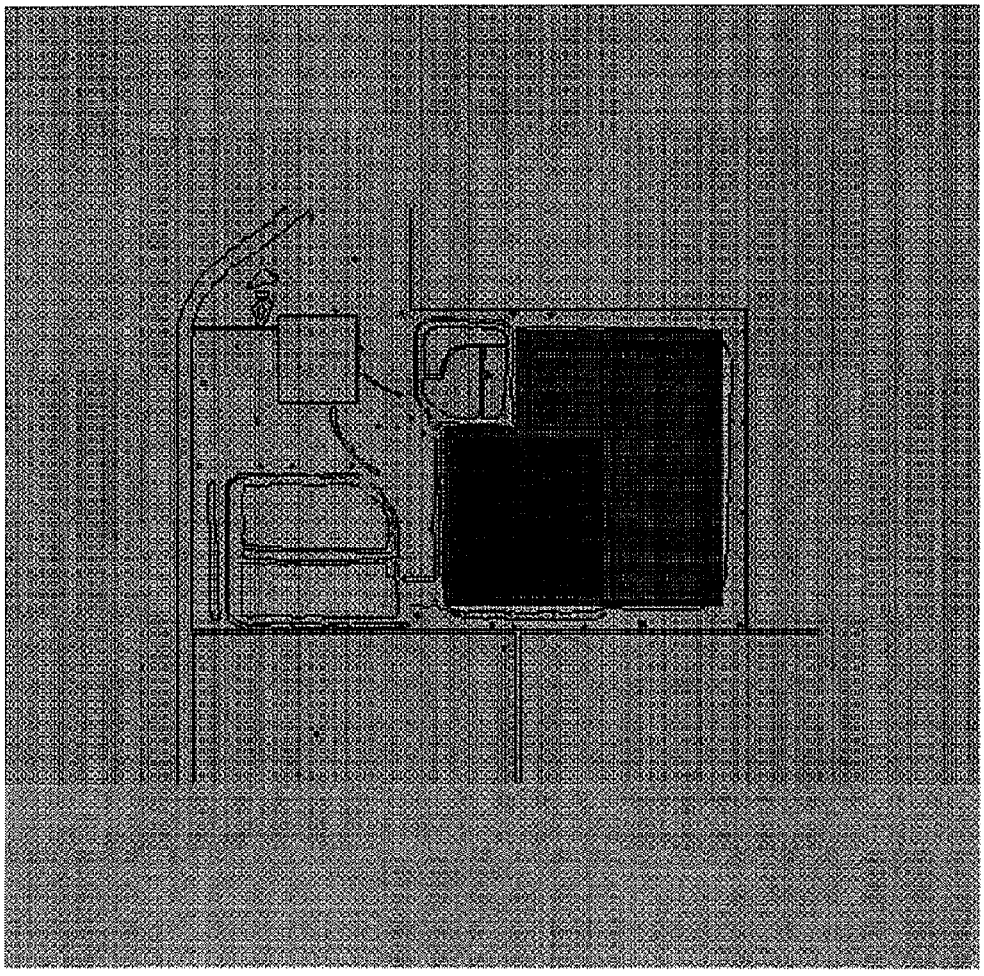

Figure 1-28. Specification of layer 1 regions. The darkest cells are representative of values in the old stack, the medium grey cells represent values in the new stack, and the light grey cells are the designation of insignificance in the top layer.

Hydrologic Parameters. Values for the hydraulic conductivities in both layers are adjusted so that the horizontal component is calculated from the horizontal conductivity and thickness values specified, while the vertical component is modeled in the model over the leakance values between the stack and the surficial aquifer. The leakance value for the stack is varied in the range of $1.0x10^{-2}$ - $1.0x10^{-3}$ day^{-1}, while the value at the bottom of the surficial aquifer is specified to be five orders of magnitude lower, owing to the presence of the confining Hawthorn Croup clays. The horizontal conductivities in both units were defined from the results of the aquifer pump tests. These estimations include the transmissivity found for well 3-1 (0.443 m^2/day) and the average of the conductivities measured at the north and south monitoring wells (1.3 x 10^{-6} m/s and 3.9 x 10^{-6} m/s).

Regions of horizontal conductivity are specified in the surficial aquifer **(Fig. 1-29)** as three different sections: a sub-stack area (7.0 x 10^{-7} m/s), a northwest high conductivity zone (3.9 x10^{-6} m/s), and a generalized hydraulic conductivity for the remainder of the modeled cells ($1.3x10^{-6}$ m/s). This modification was made to allow for a good match of the modeled to the observed contoured head data.

Boundary Conditions. Constant head cells are specified in the top layer with initial head measurements of 18 m and 25 m for the new and old stack regions, respectively **(Fig. 1-27).** The implication of the constant head acting as a consistent source of water from stack ponds is intended, as the ponds are kept at relatively constant levels from precipitation recharge.

Constant head cells are also specified at the east and west grid boundaries in order to simulate regional groundwater flow driven by a constant gradient between these boundaries. The angle and the slope of the regional head trend (determined from topographical regression discussed earlier) is generated through an offset of northward decreasing initial head values of the constant head cells. Initial head values for variable cells of the surficial aquifer are set to 5 m.

Sources and Sinks. Sources of water in the system were generated from the constant head designation discussed above, while sinks for the system were modeled through use of the drain package in the MODFLOW program.

Drainage cells have been included in the top layer to simulate evaporation from stack flanks, and in the bottom layer to model the influence of engineered ditches around the perimeter of the stack as well as an influential pond south of the stack **(Fig. 1-30).** The insertion of drainage cells involves a specification of the drain conductance and the elevation of the drain bottom. Drains in the top layer are specified with an elevation of 10 m and a conductance of 43 m^2/day. The latter has been determined as the product of the area, the hydraulic conductivity of the ditch fill, and the assumed thickness of the ditch bottom.

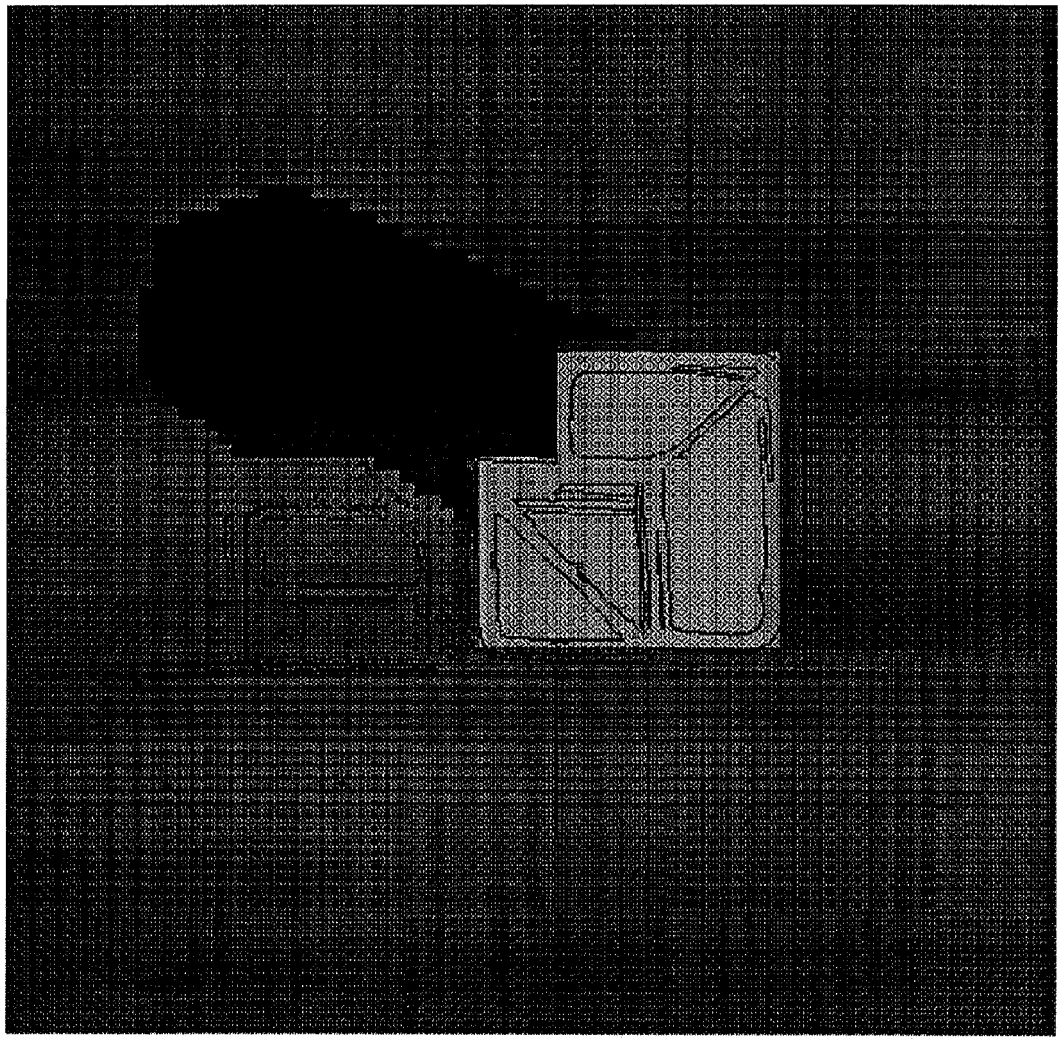

Figure 1-29. Zones of hydraulic conductivity in the surficial aquifer. Consecutively darker colors signify a relatively faster conductivity; the darkest grey denotes a conductivity of $4.0x10^{-5}$ m/s, medium a conductivity of $1.3x10^{-5}$, and the lightest shading a conductivity of $7.0x10^{-6}$.

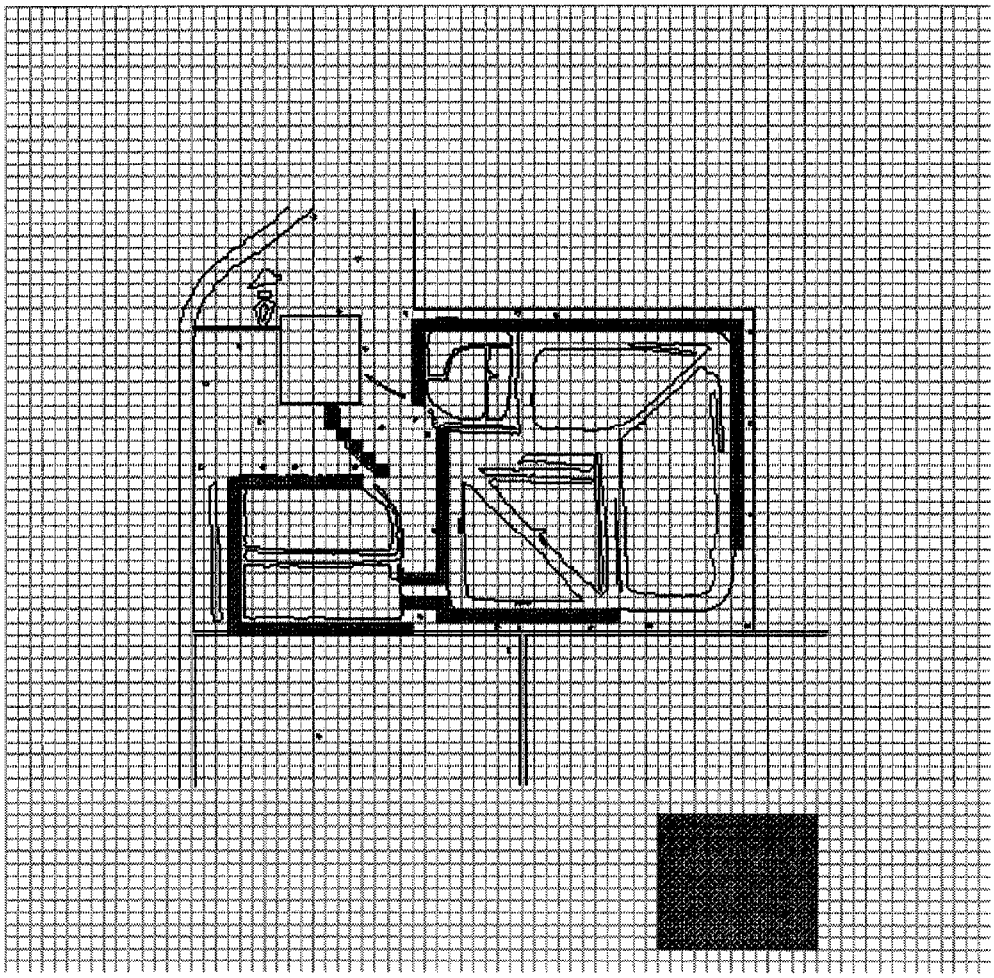

Figure 1-30. Designation of drainage cells in the surficial aquifer. Darkened cells of the grid are specified as sinks conducting water out of the system. Representation as ditches and a pond is intended.

Drains in the surficial aquifer are generally located at elevations of 3.0 and 6.0 m with respective conductances of 43 and 21 m^2/day. Drainage for the pond south of the stack was specified at an elevation of 3.0 m, with a conductance of 43 m^2/day.

Calibration. The water table in the surficial aquifer did not vary enough to demand a complete calibration of the model to each of the set of monitoring well head levels. Thus, a calibration to within 10% of the average deviation for any particular head data set was accepted as satisfactory for the steady state solution. Heterogeneities that could not be determined or modeled within the aquifer environment were believed to be responsible for most of the large deviations between modeled and actual head values.

Calibration of the head values in the model to their present form **(Fig. 1-31)** was initiated as a large scale match to a set of contrived constant head cells which represented values for a data set of actually measured head observations. Model parameters were then adjusted until aberrations caused by the constant head cells disappeared and the contours seemed adequately fit. After this was accomplished, the constant head values for monitoring wells were taken out, and fine tuning of the parameter values was attempted. All parameter values were kept as uniform as possible, so as to bring out inconsistencies that would clarify local heterogeneities. Actual calibration of the model was done conceptually in four steps:

1) balancing of stack leakance values with sub-stack conductivity to produce a head match to well 2-0 located in the surficial aquifer;
2) adjustment of stack leakance values to generate vertical fluxes that are consistent with the effective recharge of the gypsum stack from precipitation (minus evaporation);
3) adjustment of horizontal conductivity values in the surficial aquifer to produce head values close to those of nearby monitoring wells; and
4) modification of drain conductance and elevation to constrain large anomalies in head contours.

The first two steps in the calibration involved a determination of the leakance value attempting to match both the observed hydraulic head in the surficial aquifer well 2-0 and the estimated effective recharge of the gypsum stack as calculated from the difference between precipitation and evaporation as measured in the region over the last few years (see earlier section on precipitation). Results of this calibration effort show the strong dependency of the vertical stack-aquifer flux upon the leakance value chosen **(Fig. 1-32).** With an estimated effective recharge of about 1600 m^3/day over the total area of both the new and the old stack, an optimal leakance value of 3 $\mathbf{x10^{-3}/day}$ is obtained,

In the second step, values for horizontal conductivity zones outside of the stack region were found to be accurately quantified from the aquifer pump tests, and did not need to be adjusted.

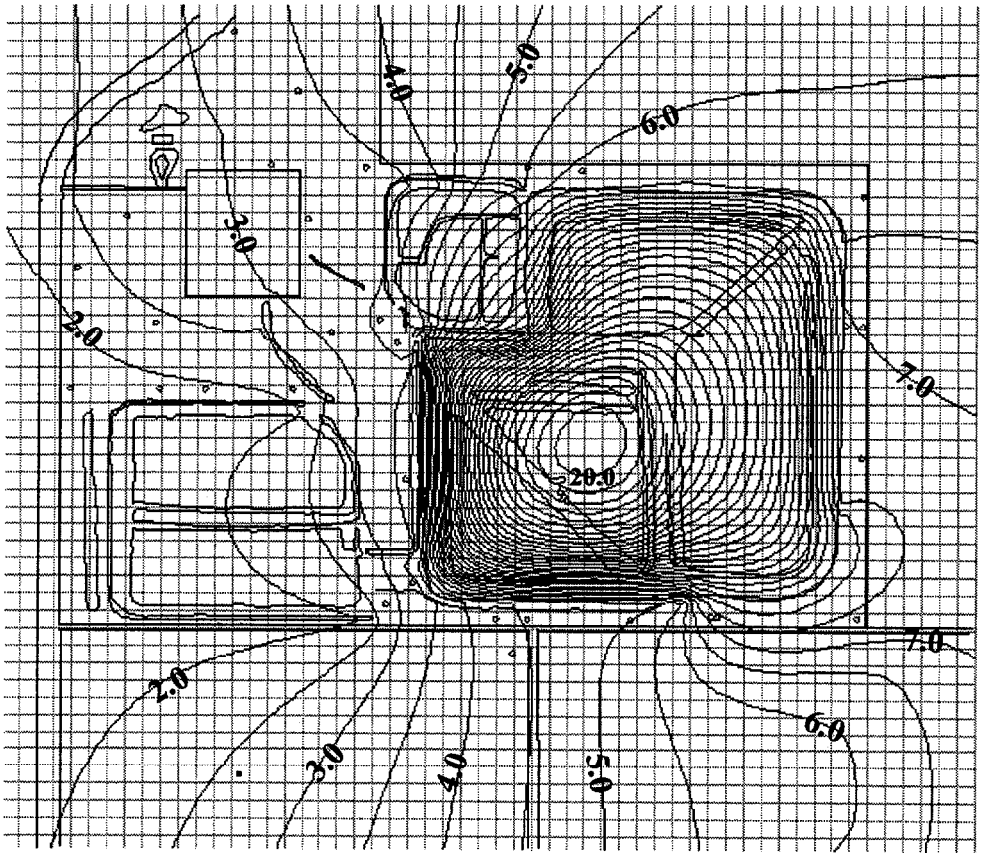

Figure 1-31. Contours of the modeled heads in the surficial aquifer. Contours are in m intervals. Note the large influence of the cooling pond ditches on the water table in the northeast section of the model.

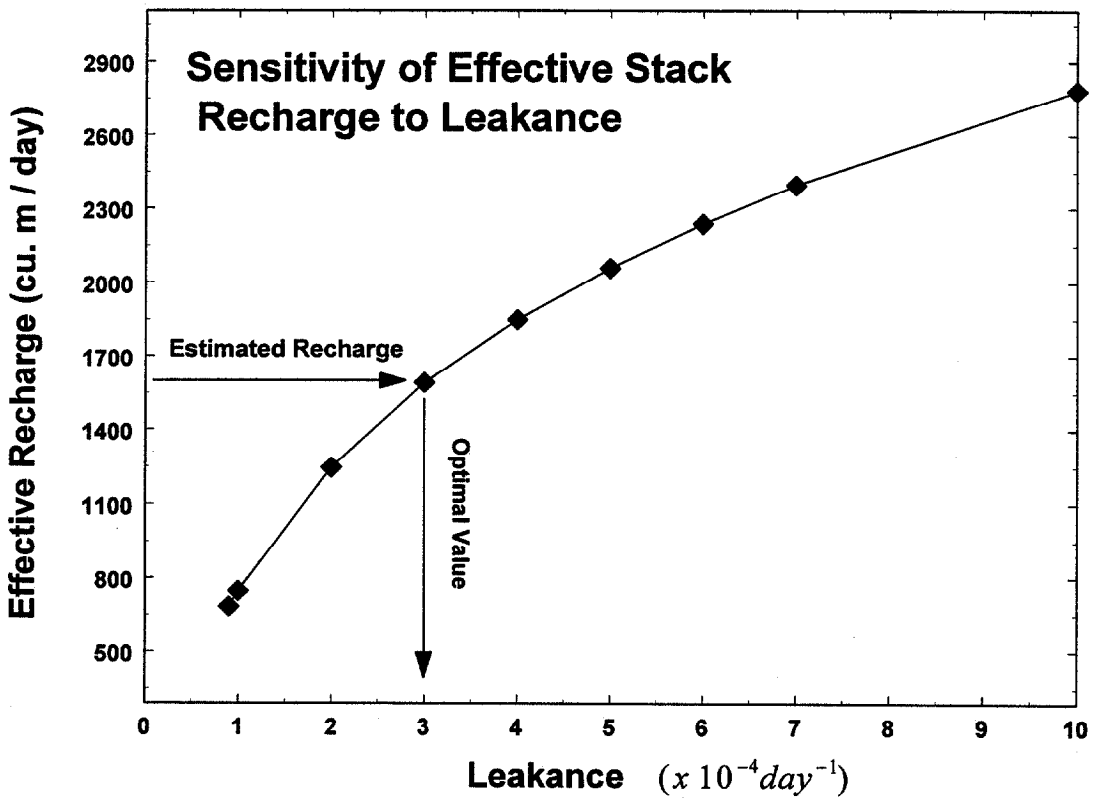

Figure 1-32. Relationship of stack recharge to leakance value. Estimated recharge values are compared to leakance values so that an optimal leakance value can be inferred.

The final part of the calibration was made through changes in ditch elevations and ditch conductances. Within this step was the addition of drainage cells to represent a pond to the southeast of the stack. It was thought that impact of this pond contributed to some of the head drop from the stack in that region. The incorporation of the drainage cells modeled partly also illustrate the effective evaporation of groundwater from the pond and from the stack flanks, the exact value of which was not explicitly known in this study.

Comparison of modeled head values to observed values for September 19, 1996 **(Fig. 1-20)** was made to ensure a model fit **(Table 1-4** and **Fig. 1-33).** The average deviation of modeled values from well measurements was found to be 24 centimeters, which approximated an 8.7% variance from actual values. The largest deviation of modeled head was found to be at MW 5, which is isolated in an agricultural field south of the research area, and could possibly be under influence of additional hydrologic factors not considered (i.e., irrigation pumping). Another significant deviation is exhibited at well RW 17, which by itself is an anomaly. Contour plots of observed data **(Fig. 1-19** and **Fig. 1-20)** show that RW 17 forces a loop in the 3 m equipotential contour around the complex area. This pattern is not quite understood, but may be the influence of a high conductivity region or additional recharge to the groundwater in that area.

Sensitivity Analysis

Values of significance to the calibration of the model were also prime candidates for a sensitivity analysis of the hydrologic control parameters in both the gypsum stack and the surficial aquifer. Modeled parameters for leakance, hydraulic conductivity, and ditch specifications were modified over a range of one order of magnitude in either direction to investigate their relative effect on the contoured modeled heads.

Leakance

Uniform leakance volumes from beneath the stack were the most critical value in reference to overall head values for the entire grid. Conceptually, the leakance was important in supplying the general volume of water available for flow into the stack and the surficial aquifer. The sensitivity of the effective recharge from the stack ponds and, owing to a lack of information, neglecting the flank water losses, ergo the flux into the surficial aquifer to the leakance value chosen can be clearly observed from **Figure 1-32.** Thus a variation of a unit change in the leakance was found to increase head levels beneath the stack on the meter-scale, with a modification by one order of magnitude leaving too much of an impact on volume fluxes of water into the surficial aquifer. Thus, the physical flux through the confining layer between the gypsum stack and the surficial aquifer surface has the most significant impact on the modeled environment.

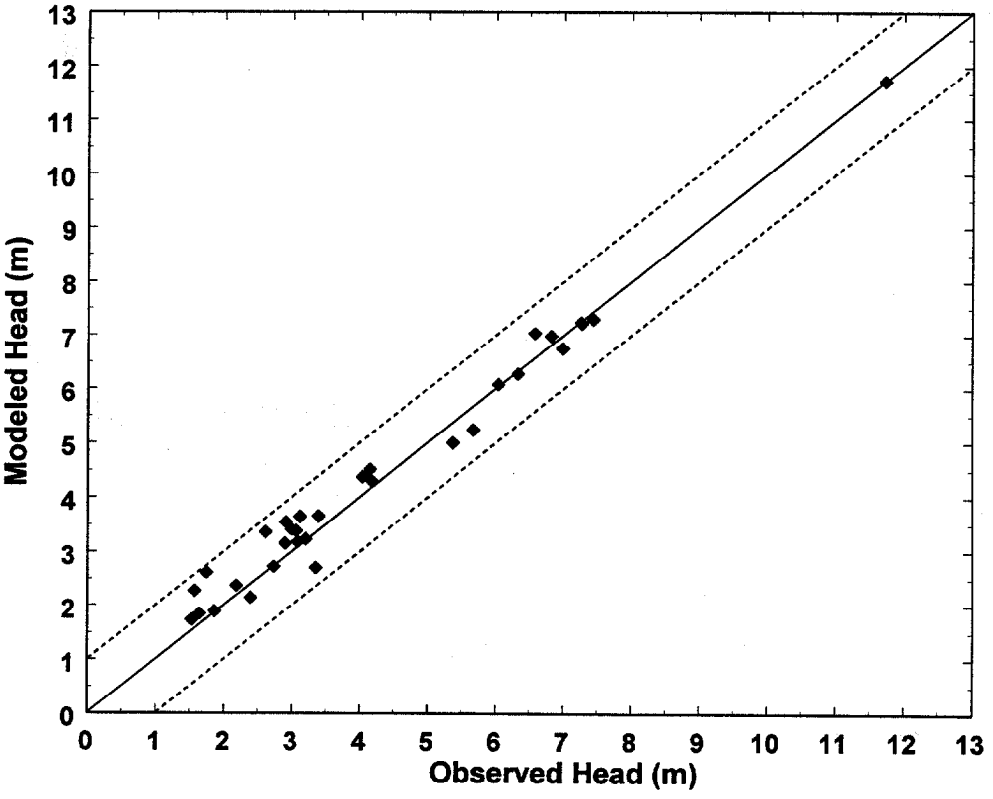

Figure 1-33. Modeled versus observed head values. Shown are the listed values of table 5 with the +/- 1m error band between modeled and observed heads.

Table 1-4. Model output comparison to actual head values. Comparison is expressed as both an absolute depth value (in meters above MSL) and as a percentage.

Well number	9/19/96 Value	Modeled Value	Difference	Percentage
MW 1	7.59	7.3	-0.29	-3.82
MW 2	4.17	4.3	0.13	3.12
MW 3	3.08	3.18	0.10	3.25
MW 4a	1.64	1.84	0.20	12.20
MW 5	1.74	2.61	0.87	50.00
MW 8	1.53	1.73	0.20	13.07
MW 9	6.39	5.24	-1.15	-18.00
MW 10	6.82	6.99	0.17	2.49
MW 11	7.26	7.24	-0.02	-0.28
RW 8	7.27	7.22	-0.05	-0.69
RW 9	5.55	5	-0.55	-9.91
RW 10	4.04	4.37	0.33	8.17
RW 11	2.73	2.72	-0.01	-0.37
RW 12	2.97	3.41	0.44	14.81
RW 13	2.91	3.54	0.63	21.65
RW 14	3.39	3.65	0.26	7.67
RW 15	2.44	2.14	-0.30	-12.30
RW 16	1.86	1.89	0.03	1.61
RW 17	3.43	2.7	-0.73	-21.28
RW 18	1.57	2.27	0.70	44.59
RW 19	2.18	2.36	0.18	8.26
RW 20	3.12	3.64	0.52	16.67
RW 21	3.20	3.23	0.03	0.94
RW 22	3.06	3.38	0.32	10.46
RW 23	2.90	3.15	0.25	8.62
RW 24	2.61	3.36	0.75	28.74
USGS 8	6.99	6.76	-0.23	-3.29
USGS 9	4.15	4.51	0.36	8.67
PZ 34	6.58	7.04	0.46	6.99
PZ 36	6.33	6.28	-0.05	-0.79
PZ 37	6.04	6.08	0.04	0.66
Stack 2 - 0	11.73	11.73	0.00	0.00
Average			0.24	8.70

Conductivities

Modeled conductivity values in the surficial aquifer zones were found to be definitely within at least one order of magnitude of their actual, measured "group" quantity. Modification of these values by single units allowed for better model fits to some data sets, but not to others. Since a generalized, rather homogenous hydraulic conductivity was intended, the best fit for a generic head representation of observed values yielded the best solution (as indicated by the differences between modeled and observed heads of **Table 1-4)** in the steady state mode. Thus, the modeled values for the hydraulic conductivities are probably within a range of 5 units from the actual values determined from the aquifer pump tests (cf. **Fig. 1-29).** It is thought that internal heterogeneities of the hydraulic conductivity are responsible for localized head anomalies.

Ditch Specifications

Ditch elevation and conductance was determined to be of the most importance to sinks within the hydrologic environment. Although conductance signified the degree of impact each ditch had, the elevation of the ditches was a limiting factor on whether or not any impact would be made to the flow system. The presence of ditches within the system therefore, were a crucial part of the flow barrier surrounding the stack. Actual values of the ditch elevations were critical to head values nearer to the stack, and although these numbers were not directly specified from engineered specifications, slight modifications of the elevation could be made up with additional conductance (which was also not quantified to specifications but rather to the model fit). Regardless, ditch presence was absolutely necessary and its parameters could not be altered very much.

As an example of the sensitivity of the model to the conductance of the ditches, **Figure 1-34** illustrates a case whereby a conductance of 0.43 m^2/day, instead of the 43 m^2/day **in Figure 1-31,** was used for the cooling pond ditches. With such a low conductance the inclination of the head contours toward the cooling pond in the western part of the model, as indicated by the actual heads **(Fig. 1-20),** has nearly disappeared.

Predictions for alteration of the hydrologic system are somewhat restricted to a change in ditch presence, owing to the fact that hydraulic conductivities and water recharge from the stack will most likely not change. Filling in of ditches will allow a larger transfer of groundwater from the stack into the surficial aquifer, and will create a larger impact (mounding effect) of the stack on the surficial aquifer. Quantification of this influence will be dependent upon how much of the ditch is actually filled in. Greatest influence of such a change would be made to the west and southwest perimeters, as the head gradients in those ditches support the largest volume of water conducted out of the system. As a recommendation for future studies of the problem, ditch elevations should be monitored more precisely than has been undertaken during the course of this investigation.

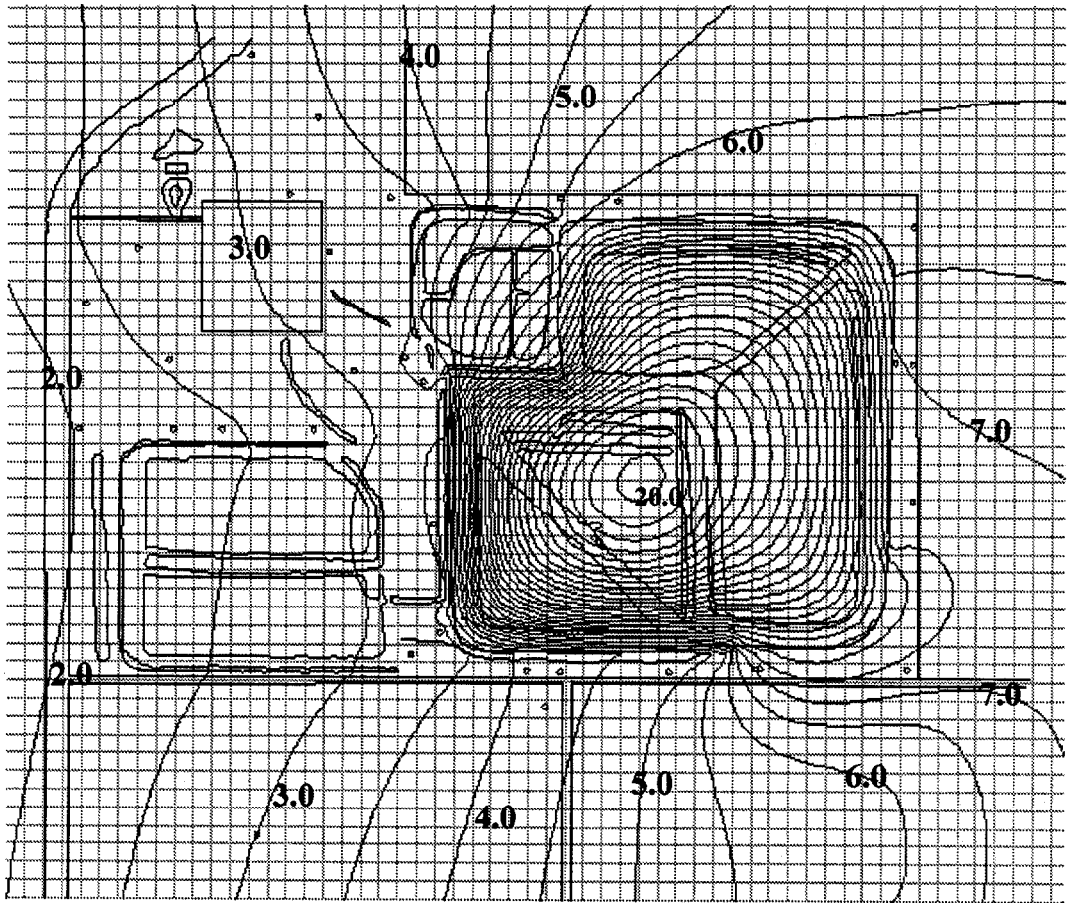

Figure 1-34. Sensitivity of the modeled heads in the surficial aquifer to the conductance of the cooling pond ditches. In comparison with **Figure 1-31** where a conductance of 43 m^2/day was used, this model uses only only 0.43 m^2/day.

Water Budget Analysis

A volumetric flux analysis of the surficial aquifer **(Fig. 1-35)** shows the actual impact of the stack on the surficial aquifer. Values for fluxes of the hydraulic system as obtained from the MODFLOW program and from measured hydrological input parameters made possible such an analysis of the total water budget of the aquifer system (stack plus surficial aquifer).

The volumetric calculation of the budgets were made in terms of m^3/day and followed the generalized form of the continuity equation:

Input - Output = Change in Storage

Although there is a short term (weekly and seasonal) change in storage which is indicated by water level changes in the stack ponds, it can be assumed that there is no change in storage over longer periods that are of the order of the residence times of water in the gypsum stack and the surficial aquifer (i.e., several seasons to years). Thus, input will equal output, as required in the steady-state model.

The volumetric input flux of the stack is described completely upon the precipitation, with large contributors of output flux being pond evaporation and stack leakance to the surficial aquifer, Pond evaporation was calculated as 50 % of the input flux, with the leakance taken from a water budget file in MODFLOW. Actual fluxes were only modeled after pathways that were known, so that smaller pathways of output fluxes such as flank evaporation, dewatering pipes, and sprayers on top of the stack were not considered. Upon determination of larger contributions of these smaller fluxes to the total net output, a smaller vertical flux to the surficial aquifer could be calculated in the future. The value determined here **(Fig. 1-35)** is, therefore, most likely overestimated by an unspecified amount and would thus represent a worst-case scenario for the infiltration of possibly toxic leachates from the phosphogypsum tailings into the surficial aquifer. With these reservations, the inputs for the surficial aquifer unit include an (overestimated) leakance from the gypsum stack and transport of regional flow from the southeast. Outputs include the ditch system, as well as regional losses of groundwater to the northwest. Most important of to this flux analysis is the comparison of regional flow input and output to the relative inputs and outputs of the stack and ditches. For the most part, volumes of water transferred from the stack are taken up entirely by the ditch system. Any volume of water not taken up by the ditches is added into the regional flow and seen as a hydrologic impact from primarily the stack, i.e., the mounding effect.

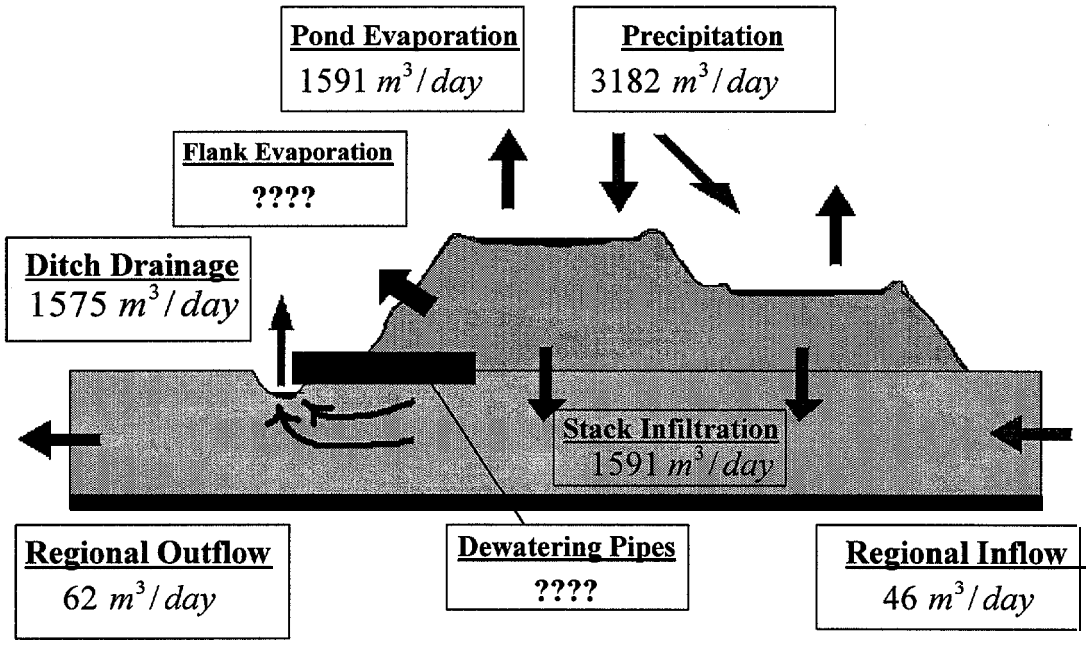

Figure 1-35. Water budget analysis. Input and output of volumetric fluxes to the gypsum stack and the surficial aquifer are represented as arrows.

The conceptualization of the flux budget given above is important for the understanding of the hydraulic control of water in the system. A relatively complete consumption of water to the ditches indicates that engineering of the hydraulic balances used to minimize impact on the groundwater are fairly adequate and even if toxic leachate from the gypsum's stack infiltrates into the surficial aquifer, it will, to a large extent, be intercepted by the ditch drainage system. **Figure 1-35** illustrates that only about 16 m^3/day of water is bypassing the ditch structure and being swept along with the regional flow. Although such an amount of non-captured diluted leachate may seem large at first glance, the value must be taken to be relative to total fluxes in the system. When compared to the input of the surficial aquifer, it is ~38% of that value, however, in comparison to the stack leakance, this value is ~1% of the infiltrating flux. Thus, the addition of water to the system is quite small in comparison to the amount of water that could be impacting the aquifer were there no ditches. However, the quantity of flux to the system is quite large when considering the regional flow and must be taken as somewhat of a considerable impact to the groundwater environment in the vicinity of the phosphogypsum stack.

CONCLUSIONS

This study investigated one particular phosphogypsum stack and its environment in an attempt to characterize flow processes that would be typical for many of the other stacks in west central Florida. In an effort to assess flow and transport in a specific phosphogypsum stack and the possible interaction of the low pH stack solutions with groundwater in the adjacent surficial aquifer, a comprehensive investigation that included hydrological testing and flow modeling has been carried out.

Several wells were drilled into the stack and the adjacent aquifer and various experimental aquifer tests were performed and head measurements over a period of about 18 months taken. The aquifers tests include pressure transducer tests, pump and recovery tests such as the Cooper-Jacob straight-line method, the Kirkham auger hole test and the Bouwer Rice test for partially screened and partially penetrating wells, and in situ flowmeter tests which allow the determination of the vertical stratification of the hydraulic conductivity.

The pressure transducer tests provide evidence for small vertical gradients that are reflecting the mounding effect of the stack, accentuated by the presence of a standing water pond on its top. Although the pump tests result in only average values of the transmissivity and storativity of the phosphogypsum stack, together with the vertical head gradients, it hints of some vertical recharge into the gypsum formation and, because of a significant head gradient between the gypsum stack and the underlying surficial aquifer, there is the possibility of vertical leakage of gypsum water into the surficial aquifer.

The Bouwer Rice pump tests resulted in an anomalously low hydraulic conductivity beneath the gypsum stack but indicated a high conductivity zone in the northwest section of the model area. The results of the flowmeter tests for the hydraulic conductivity support the notion that flow may be partly only along horizontal bedding planes that were formed during the "sedimentation" process of the phosphogypsum slurry.

The hydrological data was used in a steady-state numerical mounding model using the MODFLOW model to simulate the hydraulic effect of the stack on the regional flow and to quantify flux rates from the phosphogypsum stack into the surficial aquifer. The model was calibrated to within 10% of the average deviation for any particular observed head data set by adjusting various hydrological input parameters, namely the horizontal conductivity values in the surficial aquifer; the stack leakance values, and the drain conductances and elevation of the dewatering ditches.

The sensitivity analysis of the hydrologic control parameters in both the gypsum stack and the surficial aquifer illustrates that the model is the most sensitive to the leakance rate and the ditch specifications. By adjusting the vertical stack leakance values in the model, such as to generate vertical fluxes that are consistent with the effective recharge of the gypsum stack from precipitation, an optimal value of 3 $\mathbf{x10^{-4}\ day^{-1}}$ was found for the leakance.

The volumetric flux analysis of the surficial aquifer shows the actual impact of the stack on the surficial aquifer and illustrates furthermore the effectiveness of the ditch drains in intercepting possible toxic leachate that may have infiltrated from the gypsum stack into the surficial aquifer. In fact, only a small amount (~1%) of the infiltrating flux of gypsum stack water is not captured by the ditches and is carried further horizontally through the surficial aquifer. However, because of the neglect of water losses due to flank evaporation, spray losses, and dewatering pipes, the real rate of infiltration may even be less than the value indicated by the budget analysis presented here. Unfortunately, a more precise evaluation of the true flux-impact of the phosphogypsum stack onto the surficial aquifer will be possible only after a more precise quantification of these stack water losses will have become available.

CHAPTER 2

CHEMICAL AND RADIOCHEMICAL CHARACTERIZATION OF THE PINEY POINT STACK

INTRODUCTION AND SIGNIFICANCE

Project Description

Compositional and limited radiochemical data are routinely produced for samples of groundwaters collected from monitor wells located near phosphogypsum stacks in Florida. Several studies have been published which address either the radiochemical and compositional leaching of phosphogypsum or various aspects of groundwater interactions near phosphate ore bodies, phosphogypsum stacks, and gypsum ponds (May and Sweeney, 1982, 1983, Miller and Sutcliffe, 1982, 1984; PEI Associates, Inc., 1986; Nifong, 1988, 1993; Oural et al., 1986, 1988a, 1988b; Berish, 1990; Burnett, 1988; Kennedy et al., 1991; Upchurch et al, 1991; Carter et al, 1993a, 1993b; and Carter and Schneider, 1992). As informative and useful as these past studies have been, detailed compositional and radiochemical analyses of solutions actually circulating within Florida phosphogypsum stacks are extremely limited and these data are fundamental for documenting and describing stack solution - surficial groundwater interactions. This lack of integrated compositional, radiochemical, and hydrogeological data, which are required to fully evaluate the degree that phosphogypsum storage may impact adjacent groundwater aquifers, is emphasized by the seemingly contradictory conclusions of some of these studies. Some studies have concluded that there has been significant input of radionuclides from the stacks while other studies suggest there has not. These apparent contradictions may be the result of naturally-elevated levels of radionuclides associated with the uranium-enriched phosphate rocks in the same areas as phosphogypsum stacks. In addition, the number and distribution of monitor wells near stacks are generally not adequate for describing the hydrological conditions and compositional fluxes in

groundwaters. Monitor wells tend to be sited to satisfy regulatory, rather than technical issues.

The study by Miller and Sutcliffe (1984) provided some excellent information and some of the most complete data on potential contaminants which could migrate from Florida phosphogypsum stacks. However, the radionuclide portion of their study was limited to ^{226}Ra and gross alpha and beta measurements. The research reported here expands the work of Miller and Sutcliffe (1984) at the same site - the Piney Point Phosphates facility (formerly AMAX) near Palmetto, Florida. Their evaluation of radionuclides in solution was improved by assessment of additional uranium-series isotopes sampled from several wells drilled directly into the stack. In addition, the investigations reported here were done in concert with studies of the flow dynamics within the stack (Chapter l), and geochemical modeling of these fluids (Chapter 3).

This research at Piney Point represents the first known attempt to quantify the fluxes of radionuclides and chemical components within a phosphogypsum stack and in the adjacent surficial aquifer systems. The Piney Point site was ideal for this research. The area occupied by the stack is mineralized but has not been mined, the chemical facility has been temporarily off-line, the regional hydrology is fairly well understood, and the management of Piney Point/Mulberry Phosphates was extremely helpful in providing logistical support and access to proprietary data.

Supplemental research on the re-distribution of radionuclides within a phosphogypsum stack was also carried out in the excavated cut through the phosphogypsum stack at the CF Phosphate Operations at Bartow. This site offered the advantage of being able to study the internal structure of a phosphogypsum stack and how these structures may affect the hydrogeology of stacks and the adjacent groundwater aquifer systems. An additional benefit of working at CF Bartow was the opportunity to collect phosphogypsum samples along a well-defined stratigraphic section. This ability to relate samples spatially as well as temporally is invaluable in determining how radionuclides in phosphogypsum stacks are re-distributed during storage.

This project addresses the radiochemistry and composition of phosphogypsum, soil samples, groundwaters, and stack solutions in the unlined phosphogypsum storage stack and the aquifers adjacent to the stack. The study is an integrated approach for evaluating actual phosphogypsum - groundwater interactions using radiochemical, geochemical, hydrological, and numerical modeling techniques. This is a far more sensitive approach for characterizing potential radionuclide fluxes from stacks than earlier studies that relied solely on solid phase analyses (e.g., May and Sweeney, 1982, 1983).

Specific research questions addressed in this research include:

1) How are radionuclides and chemical components distributed between solid and liquid phases within the stacks?
2) Are radionuclides, especially ^{226}Ra, retained or released from phosphogypsum stacks?
3) What processes and conditions control retention or release of radionuclides from phosphogypsum?
4) To what extent do phosphogypsum stacks influence the hydrology of aquifer systems adjacent to the storage areas?
5) If chemical components and radionuclides are entering solution and being transported away from stacks, what processes control the solubilities of these aqueous species?

Although many of the questions which were addressed by this research are to an extent site specific, the multidisciplinary approach helped identify the most feasible and cost-effective techniques to investigate additional sites prior and subsequent to the implementation of mandated stack closures in Florida. The resources involved in implementing the stack closures that are required by the year 2001 may range into hundreds of millions of dollars. Therefore, it seemed logical to expend a very small fraction of that amount to ascertain to what extent radionuclides infiltrate the shallow aquifer around the stack. Later studies may then address an evaluation of the degree of success that is attained by isolating the phosphogypsum from the surrounding environment under the presently planned site closure methodology.

MATERIALS AND METHODS

Monitor and Stack Wells

The pre-existing monitor wells at Piney Point have 5.0-foot long screens. The majority of these wells were drilled in 1979 and 1980 for the studies of Miller and Sutcliffe (1982). These pre-existing surficial aquifer monitor wells were not sand packed in the filter screen. Sediments removed during augering the bore were used rather than a sand pack. The well depths and screened intervals for all monitor wells are provided in the appendix to this report.

Seventeen new monitor wells (MW) were drilled into the surficial aquifer around the gypsum stack and eleven wells were drilled directly into the older phosphogypsum stack at Piney Point. The locations of all new and pre-existing surficial aquifer monitor wells are shown in **Figure 2-1.** The locations of stack wells are shown in more detail in **Figure 2-2**. All new monitor wells were constructed with filter screens (0.010 inch slotted liner) in the deepest 10.0 feet of the total depth of the well. Screens were packed in 20-30 mesh sand with an approximately 1.5-ft bentonite hole plug overlying the sand pack. The 4-

inch diameter risers were grouted to the surface with a bentonite-cement mixed grout compound. Potentiometric surface data were collected prior to pumping the wells or otherwise perturbing the hydrological system. All coring and well drilling, completion,

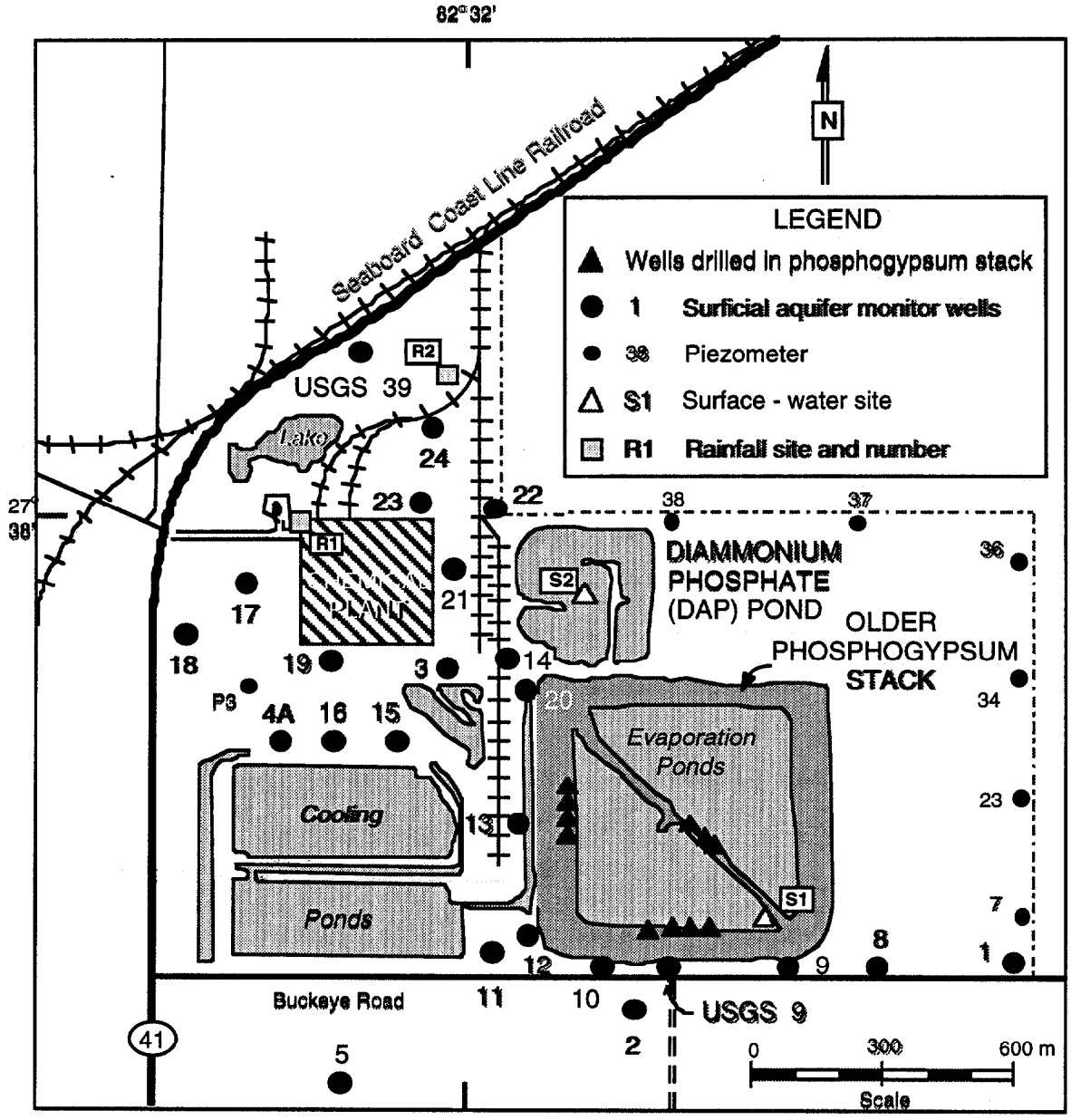

Figure 2-1 Map of the Piney Point Phosphates site showing the locations of surficial aquifer monitor wells, piezometers, wells drilled into the older phosphogypsum stack, and surface sampling locations.

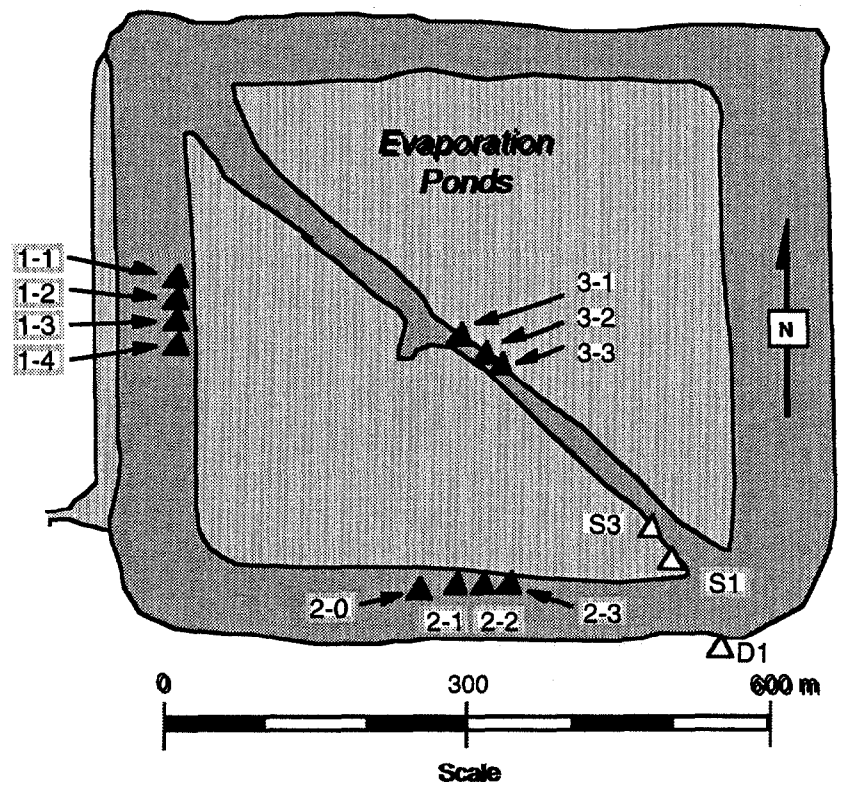

Figure 2-2 Detailed map of the older stack showing the locations of the "PP" stack wells and surface sampling sites.

and development was performed by Huss Drilling, Inc. of Dade City, Florida. Absolute elevations of risers, relative to sea level, of the new monitor wells and stack wells were measured by Clements Surveying, Inc. of Palmetto, Florida.

All well drilled on the stack except PP3-1 were also constructed with filter screen in the deepest 10.0 feet of the well. Well PP3-1 was screened throughout for hydrological measurements (see chapter 1). In addition, two continuous cores of phosphogypsum were recovered at sites PP1-1 (March 1995) and PP2-0 (March 1996). The PP2-0 well in the stack had a 5.0-foot screen set at a well depth of 66.8 - 71.8 feet (top of the screen is 3.3 feet beneath the base of the stack) and is completely within the surficial aquifer with no direct connection to the stack. That well has a 6-7 foot thick bentonite plug over the sand pack. The 4-inch diameter risers for all wells were grouted to the surface with a bentonite-cement mixed grout compound.

Construction parameters for the wells drilled into the stack are identical with those of the monitor wells with the exception that the stack wells were rotary drilled and bentonite drilling mud was used rather than the wells being auger drilled. The PP2-0 well was cored prior to opening up the bore and setting a 4-inch diameter casing with a 5-foot filter screen. The well was designed so the 5-foot screen would be entirely within the surficial aquifer, well below and physically segregated from the stack and not in direct contact with stack solutions. The filter screen was set just above, but isolated from, a phosphate-ore bearing clay horizon which is likely a thin clay seam near the bottom of the surficial aquifer or the top-most member of the intermediate aquifer complex in this region.

Sample Collection

Fluids. All monitor wells were pumped using a submersible pump system for a period adequate to replace at least three well volumes and reach stable in situ measurements of pH, electrical conductivity, and temperature prior to collecting samples. Samples for radiochemical analyses were collected first followed by the chemical compositional samples. Liquid samples (3 liters for analysis of dissolved ^{238}U, ^{226}Ra, ^{210}Pb and ^{210}Po) were filtered using a 0.45 µm filter, acidified with ultrapure HNO_3 to a pH <1, and appropriate isotopic spikes and carrier solutions added in the field immediately after collection. Separate samples for ^{222}Rn were collected in triplicate by drawing l0-mL aliquots with a syringe and placing each directly into 20-mL glass liquid scintillation vial with premeasured cocktail. Filtered and unfiltered non-acidified aliquots of well solutions were also collected for analyses of anions and cations, laboratory pH, and other parameters. Samples of solutions that were pumped from wells drilled into the stack at Piney Point required longer pumping times prior to collection in order for the electrical conductivity and pH of the solutions to stabilize.

Solid Samples. The cores were the only intact solids that could be collected during drilling operations. Well cuttings from the rotary drilled wells could not be retrieved since the phosphogypsum was disaggregated and dissolved while being lifted up the bore in the bentonite mud slurry. The fine-grained quartz sand and resistant minerals were all that could be separated from the drilling mud by use of stacked sieves. Distinct beds (planar structures that appear to be sedimentary in origin) with a variety of thicknesses were often separated by <0.08 to ~0.15 in. thick lamellae of very fine-grained, black material. This apparently organic material appears to be identical with the dark material being deposited in discharge channels on active gypsum stacks and the material which commonly defines bedding plane horizons and the thick, black bed in stratigraphic section measured at the excavated cut through CF stack in Bartow (see description below). The phosphogypsum in cores appeared to be fairly well lithified, and seemed to be more consolidated with lower permeabilities near the base of the stack.

Grab samples of phosphogypsum were also collected at several elevations along sections up the western and southern flanks of the old stack at Piney Point. An east-west section line was defined on the western flank that terminates to the east with the Cluster 1 wells (PP1-1 through PP1-4). A north-south section line was similarly defined that terminates to the north with the Cluster 2 wells (PP2-0 to PP2-3). Phosphogypsum samples on the southern flank were collected primarily from different structural features on the stack. The lowest sample in this section was a soil from the Quaternary alluvium that was collected from beneath the base of the stack in the perimeter ditch. Five samples of phosphogypsum were also collected at different elevations up the north-south oriented section line. The weathered surface layer on the stack was removed prior to collecting phosphogypsum samples on the flanks of the stack.

Phosphogypsum from Stratigraphic Sections at CF Phosphate Operations. An excavated cut through the CF Industries phosphogypsum stack in Bartow provided an excellent exposure of what appear to be sedimentary structures within a large phosphogypsum stack. The most pronounced features of the internal structure of the stack were the continuous, sub-horizontal layers of phosphogypsum. The layers resemble sedimentary depositional beds that are clearly bounded above and below by sharp contacts very much like the structures observed in the cores from Piney Point. These layers are usually coated with extremely fine-grained, black material that may be the residue of the organic components of de-foaming agents used during phosphate ore acidulation. These beds are continuous for hundreds of feet and range in thickness from less than 0.4 in. to about 8 in., with an average thickness of about 3 in., and the individual beds are generally uniform in thickness. The most notable feature in the excavated cut at the CF phosphogypsum stack is the horizontally continuous layer of black colored phosphogypsum eight to ten inches thick at the 189 foot level in the southern face of the cut. This horizontally continuous layer is also apparent in the northern exposure of the excavation, which is capped with clay and soil.

About 190 beds were counted in the first stratigraphic section from the base of the temporary road at 157 feet to the top of the stack, which has an elevation of 215 feet at this location on the southern face of the cut. Eight samples were collected on 15 July 1994 from discrete layers of phosphogypsum in this section. A diagrammatic cross section together with sampling locations along this stratigraphic section are shown in **Figure 2-3.**

Radioanalytical Techniques

Fluid Samples. With a few exceptions, stack and monitor well samples were analyzed for radionuclides by methods described in Burnett et al. (1995). U isotopes were analyzed by a combination of alpha spectrometry and PERALS spectrometry (see below). Ra-226 was determined by radon emanation following the procedures adapted from Key et al. (1979) and Mathieu et al. (1988). Po-210 activities were determined by

spontaneous deposition onto pure Ag plates following by low-level alpha-particle spectrometry. A calibrated ^{209}Po solution was used as an isotopic tracer for the ^{210}Po measurements. Pb-210 was scavenged using a known amount of a stable Pb carrier, precipitated as a sulfate, filtered, weighed, and counted on a low-level gas flow proportional counter. Rn-222 was assayed by standard liquid scintillation counting techniques. The short-lived radionuclides (^{222}Rn and ^{210}Po) have been corrected for ingrowth and/or decay to the time of sampling.

Uranium Isotopic Analyses. During the course of this research, it was discovered that the high ionic strength fluids from the stack wells presented a problem with the normal chemical separations for uranium isotopes. It was decided therefore, to investigate an alternative procedure to the standard alpha spectrometric analysis. The procedure investigated was PERALS (Photon/Electron Rejecting Alpha Liquid Scintillation) spectrometry with two new preparatory procedures (designated Method "A" and "B") designed by personnel at Ordela, Inc.

In method "A" uranium and other alpha-emitters are concentrated by co-precipitation on ferric hydroxide ($Fe(OH)_3$) after boiling an acidified water sample to remove carbonate. The supernatant is decanted and discarded, and the precipitate is dissolved in a mixture of nitric acid (HNO_3) and hydrochloric acid (HCl). Polonium, which can interfere with the U spectrum on PERALS, is extracted with an extractive scintillator which is selective for polonium. Ferric hydroxide is then reprecipitated from the remaining aqueous solution and separated by centrifugation. The precipitate is washed with dilute ammonium hydroxide (NH_4OH), and redissolved in approximately 10 mL of a sulfuric acid (H_2SO_4)/sodium sulfate (Na_2SO_4) solution at a pH between 1.0 and 1.5. Ascorbic acid is added to reduce Fe(III) to Fe(II) and uranium is extracted from this solution with an extractive scintillator which is selective for uranium. The sample is then counted on a high-resolution PERALS spectrometer.

Method "B" starts by boiling an acidified water sample until the volume is less than 50 milliliters. The solution is then made 0.01M in diethlenetriamine pentaacetic acid (DTPA), and the pH is adjusted with 6M NaOH to between 2.5 and 3.0. The sample is transferred to a Teflon separatory funnel and equilibrated with 1.50 mL of an extractive scintillator containing a dialkyl phosphoric acid extracting agent. Under these conditions only uranium is transferred to the organic phase while other alpha-emitters (as ^{210}Po), as well as most metal ions, remain in the aqueous phase. The counting is done in exactly the same manner as in method "A".

Initially, method "A" was used for a group of test samples provided for an ASTM intercomparison. This sample set consisted of 3 samples (3 replicates each) and 3 blanks. The samples were run blind by 8 laboratories, including FSU. Our results are shown together with the mean values from the other labs in **Table 2-1.**

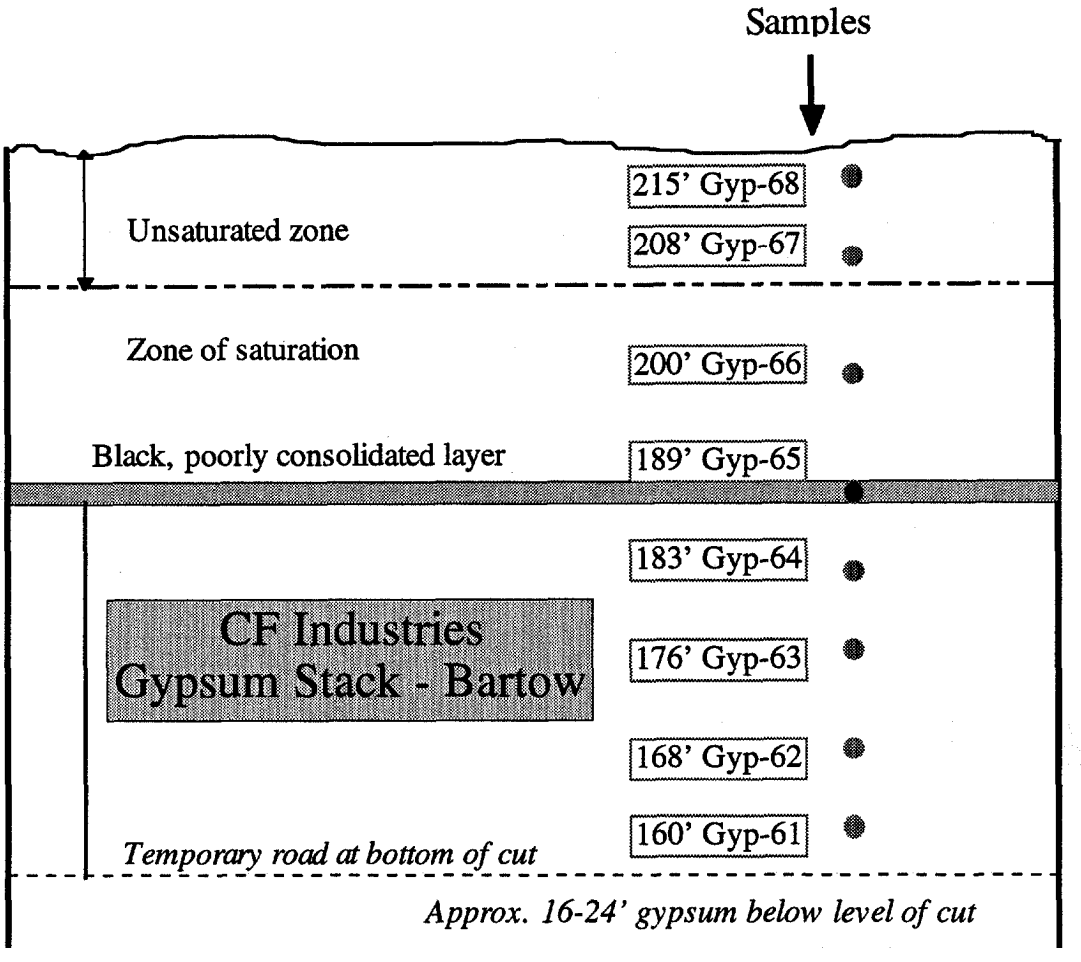

Figure 2-3. Diagrammatic geologic cross-section of the south face of the excavated cut through the CF Industries (Bartow) phosphogypsum stack west of Bonnie Mine Road. Line of stratigraphic section and sampling locations are shown.

Table 2-1. Intercomparison of results for total uranium in drinking water as determined by method "A" and PERALS spectrometry in our laboratory and the mean as determined by 8 laboratories in an ASTM intercomparison exercise.

Sample Number	Total U (pCi/L) FSU	ASTM
1	5.4±0.3	5.9±0.3
2	68±2	73±2
3	272±7	276±8

The comparison of our results to the ASTM mean is clearly excellent. Further testing showed that equally good results could be obtained by method "B" which is significantly shorter because there are no precipitation steps and only one extraction. To further validate this new approach, we analyzed a representative number of stack and monitor well samples by both PERALS method "B" and standard alpha spectrometry. In addition, duplicate samples of an EPA intercomparison water sample (April 16, 1996) were run by both techniques. Both analyses used the same calibrated ^{232}U tracer. The results of this internal intercomparison are shown in **Figure 2-4** and the individual results are tabulated in **Appendix 2-1.** When all samples are plotted together, the regression of the PERALS results for ^{238}U versus the ^{238}U via alpha spectrometry is excellent (slope = 1.001; r^2 = 1.000). When just the monitor wells are examined (concentrations below 4 dpm/L; inset in **Fig. 2-4),** the results are still very good (slope = 0.916; r^2 = 0.946) in spite of the low concentrations. The "total natural uranium" result reported by the EPA for the intercomparison sample was 58.4 pCi/L (129.6 dpm/L) which is equivalent to 63.3 dpm/L for ^{238}U and ^{234}U assuming secular equilibrium. All of our results for that sample are within 1% of that value.

Chemical Analyses. Analyses for major and minor components of selected well waters and stack solutions were determined using analytical techniques that could provide the precision and detection limits required for the geochemical modeling (see Chapter 3). Samples for compositional analyses of cations were analyzed by Inductively Coupled Plasma (ICP) spectrometry. Analyses of selected cations, anions, complex anions, laboratory pH, and F^- were performed using turbidimetric, ion-specific electrode, Atomic Absorption Spectrometry (AAS), calorimetric, and temperature-correcting pH probe techniques. All of these analyses were performed by Western Analysis, Inc. (Salt Lake City, Utah).

Phosphogypsum Analyses. Since water exists in the crystalline lattice of both dihydrate (DH) and hemihydrate (HH) forms of phosphogypsum and there exists a potential difference of about 15.7% between the formula weights of the two crystal forms, it is important not to use high temperatures when drying these types of samples. All phosphogypsum samples for this study were thus prepared by drying the sample under atmospheric conditions until moisture was sufficiently reduced to allow a preliminary grinding of 400 - 600 grams of sample to a grain size of less than 500 µm (30 mesh). After drying to constant mass in a vacuum desiccator at room temperature, samples were ground to a grain size of less than 250 µm (60 mesh), split with a powder sample splitter, and stored in sealed containers.

We used a closed-end coaxial intrinsic germanium (IG) detector to determine activities of ^{238}U, ^{226}Ra, and ^{210}Pb in phosphogypsum samples. Samples and standards for measurement on the coaxial IG detector were thoroughly homogenized prior to packing the sample powders in 100 cm^3 aluminum cans that were then sealed with an aluminum lid lined with a gas impermeable compound. The detector was calibrated using

natural matrix soil, sediment, and rock standards having radionuclide activities certified by the National Institute of Standards and Technology (NIST) and the International Atomic Energy Agency (IAEA).

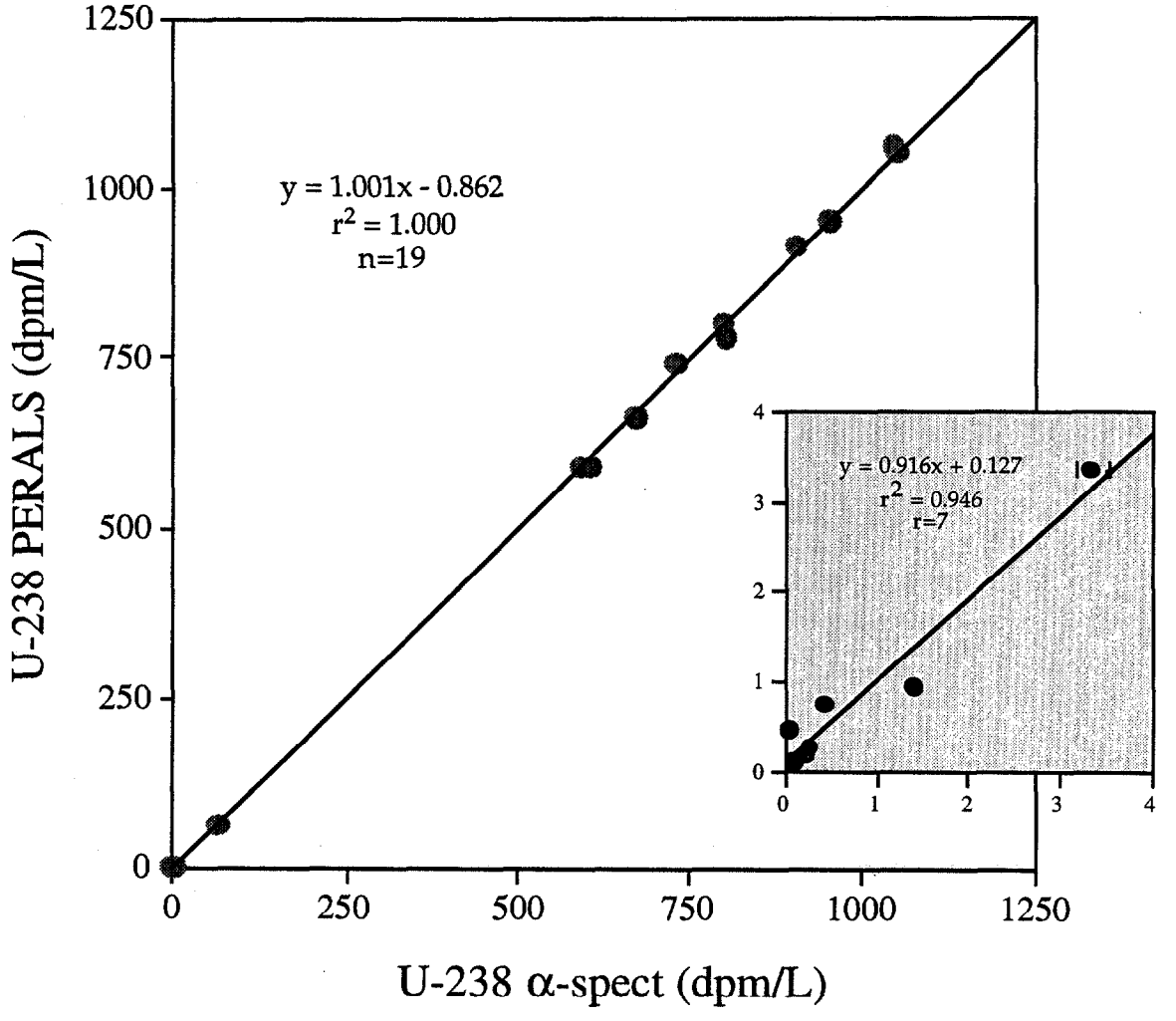

Figure 2-4 Plot of ^{238}U as determined by method "B" and PERALS spectrometry versus ^{238}U in the same samples as determined by alpha-particle spectrometry. The large plot is for all 19 samples (mixture of stack solutions, monitor wells, and EPA intercomparison samples). The small inset represents only the low activity monitor wells.

The ^{226}Ra activities were determined by taking the mean activity of three separate photopeaks of the daughter nuclides ^{214}Pb at 295.2 keV and 351.9 keV, and ^{214}Bi at 609.3 keV. Photopeaks of ^{214}Bi at 1120.2 keV and 1764.5 keV were also observed for comparative purposes, but not used in calculating the mean activity of ^{226}Ra. Because

phosphogypsum does not retain ^{222}Rn well, it was necessary to wait for about three weeks after sealing the aluminum sample cans to ensure that ^{222}Rn had reached equilibrium with ^{226}Ra before counting (Burnett et al., 1995).

Self-absorption corrections for the low-energy ^{210}Pb and ^{234}Th photopeaks were calculated using an approach modified from that suggested by Cutshall et al. (1983). A mixed, sealed transmission source was produced so photon transmission measurements for ^{210}Pb and ^{234}Th could be quickly and simultaneously measured through individual samples and directly related to a relative absorption factor over a broad range of density (Burnett et al., 1993). Good agreement with the "recommended" values was obtained when this method was applied to IAEA-306, a deep-sea sediment used by the IAEA as an international intercomparison sample for natural decay-series nuclides (Ballestra et al., 1989).

RESULTS AND DISCUSSION

Chemical Characteristics of Fluids

A compilation of all the major and minor element data is presented as **Appendix 2-2** and the trace element results are given as **Appendix 2-3**. We present here a summary of the major features of these data to show some of the more important qualitative trends in the results. A summary of the monitor well parameters (well depth, screened interval, etc.) as well as field data (pH, electrical conductivity, and measured total dissolved solids) is given in **Appendix 2-4**. A summary of these results, presented as a mean and standard deviation of the stack fluids and the shallow aquifer waters, is given in **Table 2-2.** In general, the stack solutions are high in Na, K, Ca, Mg, Al, Si, Sr, Mn, NH_4, Cl, F, SO_4, and PO_4 in comparison to the monitor well samples. Both the stack and the monitor wells have comparable amounts of Fe and very low Ba in all wells. Only the monitor wells, which have pH values above 6.0, have detectable HCO_3^-.

It is clear from Table 2-2 that one cannot produce the composition of these fluids by simple mechanical mixing between the stack fluids and the shallow aquifer. Note that while the TDS and several major components (e.g., Na^+, Ca^{2+}, NH^{4+}, and SO_4^{2-}) range between 3-6 times more concentrated in the stack solutions, other components (e.g., SiO_2, PO_4^{3-}, and F^-) are many more times enriched in the stack solutions. Fluoride, for example, is almost 1900 times more enriched in the average stack solution than in the aquifer. The extreme range in the stack/aquifer ratios indicates that a considerable amount of non-conservative behavior (precipitation, adsorption, etc.) must be occurring in the stack in addition to mixing of the stack solutions with underlying groundwaters.

In general, our results showed good agreement between parameters that were measured in the field and measured or calculated again in the laboratory **(Fig. 2-5).** The

laboratory and field pH measurements were all within expected variations with the exception of samples from one well, MW-2. That well is located on the south side of Buckeye Road and it is very unlikely that it has been influenced by the stack. One possibility for the consistently lower (more acidic) lab readings is that an organic acid present in this sample (the well is located in a tomato patch) dissociated during the time interval between sample collection and measurement in the laboratory. The field-laboratory agreement for the electrical conductivities was excellent as was the agreement between the calculated (from the chemical analyses) and measured total dissolved solids.

Table 2-2 Average and standard deviation of major cations and anions, total dissolved solids, and pH of stack solutions and shallow aquifer surrounding the Piney Point stack.

Parameter	Stack ppm	Aquifer ppm
Na^+	1,540±220	500±580
Ca^{2+}	660±60	290±230
SiO_2	740±200	57±65
NH_4^+	1,060±250	300±350
PO_4^{3-}	8,900±1300	420±1000
SO_4^{2-}	5,190±340	1,300±1500
F^-	1,120±380	0.6±0.5
TDS	18,700±2300	3,300±3200
pH	2.43±0.10	6.33±0.65

An interesting aspect of the chemical results concerns the apparently strong interdependence of phosphate, fluoride, and silica in the stack solutions **(Fig. 2-6).** We did not observe any obvious trends in these parameters in the monitor well samples. At least some of the control on PO_4^{3-} and F^- is probably associated with the main mineral phase of the phosphate ore, carbonate fluorapatite $[Ca_5(PO_4,CO_3)_3(F,OH)_2]$, which may reprecipitate under these conditions. We suspect that the relationship of F^- to SiO_2 is related to control by the solid phase known in the phosphate industry as "alkali fluorsilicates." This material, often seen growing as large crystals in seeps of discharge fluids on the stacks and known to clog filter screens in the chemical plants, is actually an alkali silica hexafluoride, $(Na,K)_2SiF_6$, since it has no structural oxygen. Note that the mole ratio of F:Si from our regression is about 5.1:1, close to the theoretical ratio of 6.0. It is also possible that some F^- may be associated with pachnolite $(NaCaAlF_6 \cdot H_2O)$ which Upchurch (1982) documented as occurring in Tampa Bay, apparently as a result of precipitation from fluoride-rich effluent from a phosphate chemical plant.

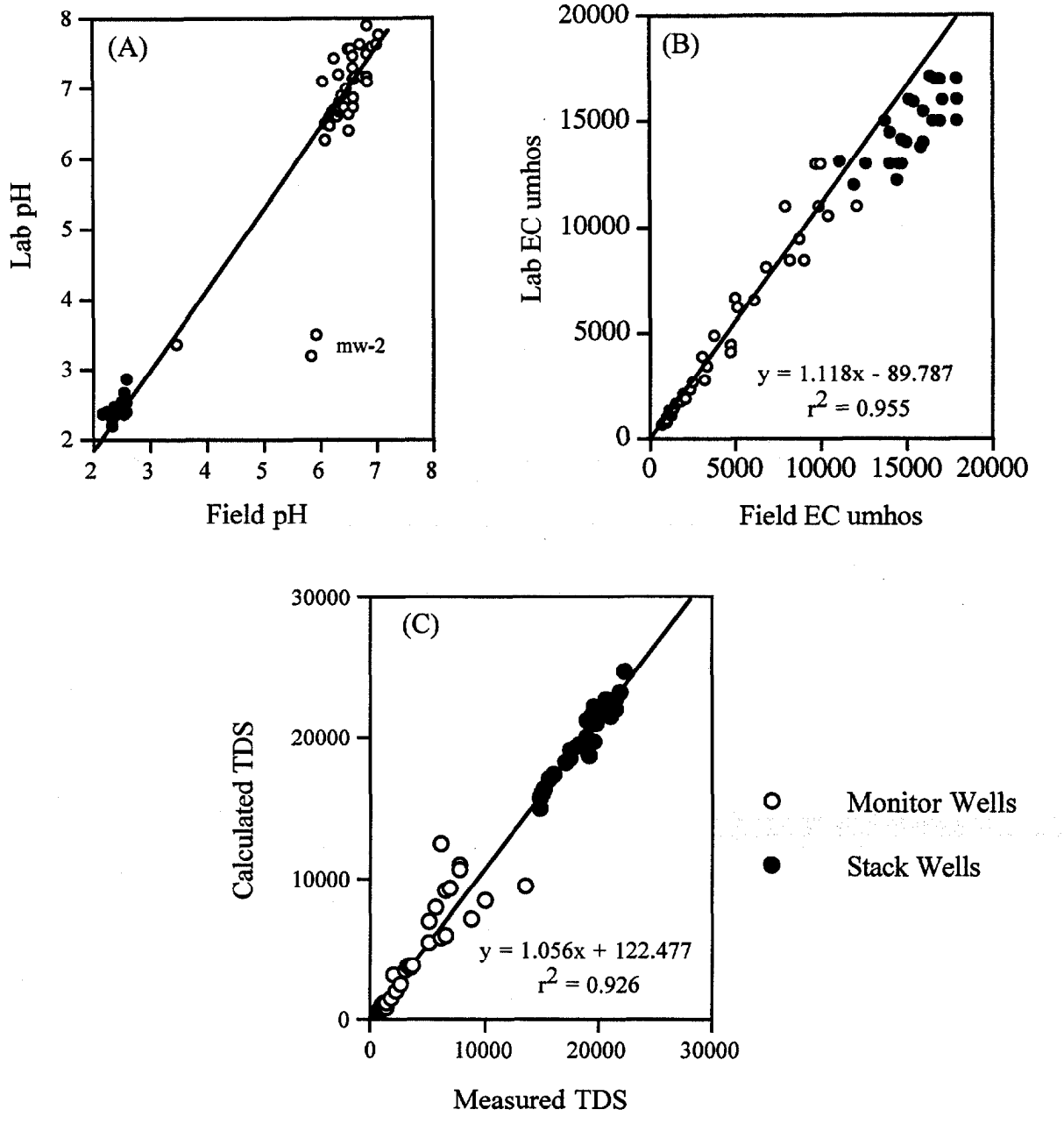

Figure 2-5 Plots of (A) laboratory pH versus field pH; (B) laboratory electrical conductivity versus field conductivity; and (C) calculated total dissolved solids (TDS) versus measured TDS. The trend line in (A) is not a regression but a 1:1 reference line. Open circles refer to monitor well samples while closed circles represent samples collected from the stack wells.

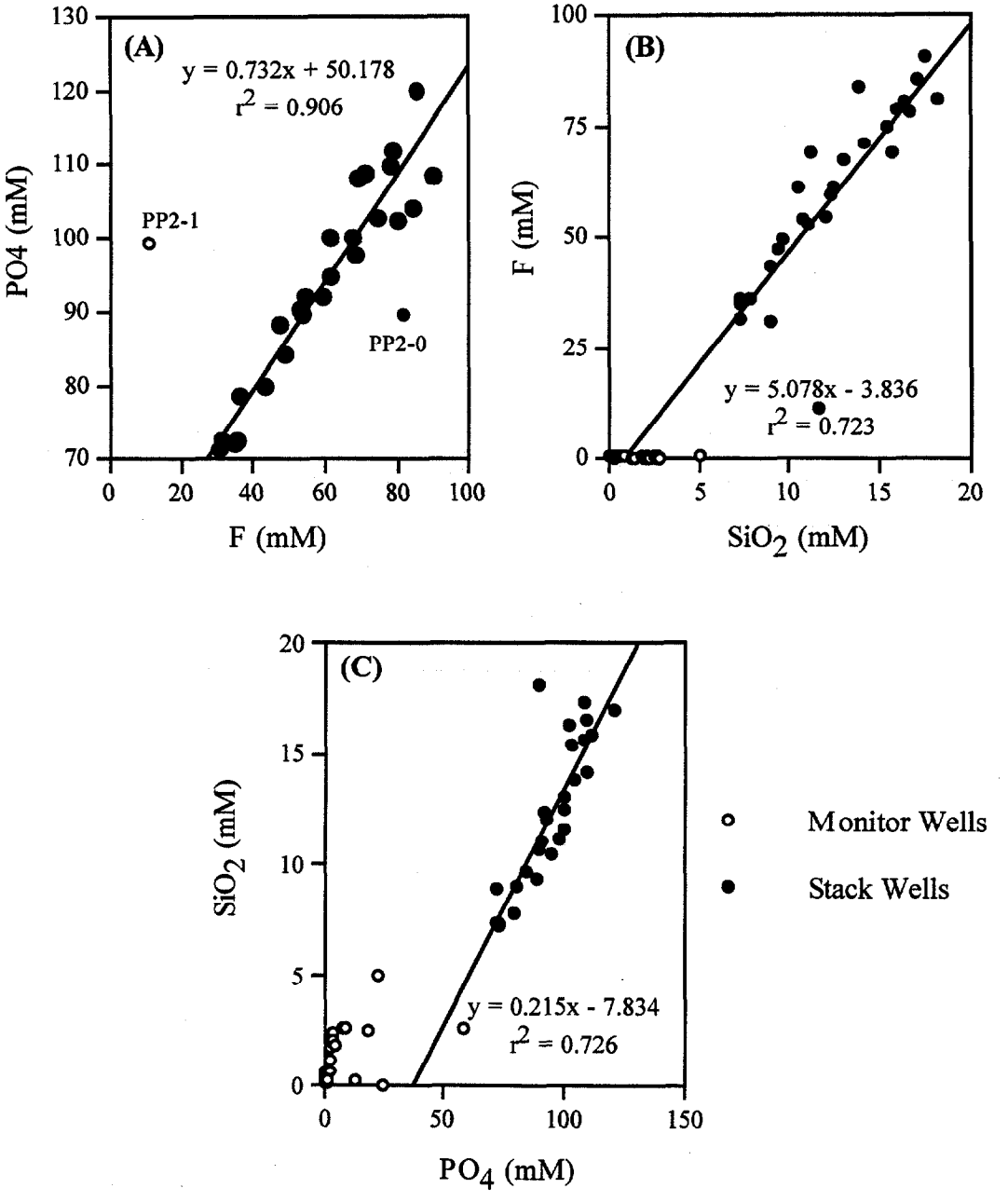

Figure 2-6 Plots showing relationships in the PO_4-SiO_2-F system in the monitor and stack wells. Regressions have been drawn just through samples from the stack wells.

A very graphic way to illustrate the difference and relationship between the stack fluids and the shallow groundwater is on a SO_4^{2-} versus pH plot **(Fig. 2-7)**. As discussed in more detail in Chapter 3 of this report, such a plot resembles a classic acid-base titration curve as performed in freshman chemistry laboratories. In fact, this is a very good analogy to what is actually happening in this situation. High sulfate, low pH fluids in the stack are titrating the relatively low sulfate groundwaters with near neutral pH. Note from the figure that the sulfate occurs over the entire concentration range while pH changes very abruptly as the acidity from the stack solutions is buffered by the shallow groundwater, i.e., there is a titration "end point,"

The near-conservative behavior of sulfate may also be seen when one plots Na, normally considered a very conservative element, against SO_4^{2-} **(Fig. 2-8).** In this case, we see an almost continuous transition between the high concentrations in the stack fluids and the low concentrations typical of the shallow groundwaters distant from the stack. The only exceptions are for the high-sodium, low sulfate samples collected from MW-23, directly next to the chemical plant. We also show the case for Ca plotted against SO_4^{2-} in an accompanying diagram in the same figure. Here there is evidence for non-conservative behavior at intermediate concentrations of SO_4^{2-}, perhaps due to precipitation of a calcium sulfate phase at the higher pH characteristic of the aquifer waters.

Radiochemical Characteristics of Fluids

A complete data compilation including analyses for U isotopes, ^{226}Ra, ^{222}Rn, ^{210}Pb, and ^{210}Po is given as **Appendix 2-5**. The results show that the stack wells (designated "PP" in the appendix) are very high in activities of uranium (generally 600-1000 dpm/L ^{238}U) and ^{222}Rn (range from about 20,000-70,000 dpmL) and fairly high in ^{210}Pb (generally 400-4000 dpmL). Somewhat surprisingly, the activities of ^{226}Ra are only slightly elevated (range about 5-10 dpm/L) above groundwater values for mineralized areas and are, in fact, less concentrated than most of the monitor well concentrations measured around the Piney Point stack. The ^{210}Po concentrations in most stack fluids are high (most values between 3-50 dpm/L) yet significantly less than the corresponding ^{210}Pb activities.

The monitor well samples are much lower in U isotopes than the stack solutions. The concentration of ^{238}U is generally less than 1 dpm/L with the notable exception of MW 12 (265 and 304 dpm/L for two samplings) and MW 22 (18 and 15 dpm/L for two samplings). Although high, these two monitor wells still display U concentrations much lower than the stack solutions. The low pH in MW 12 (pH=3.48 and 3.19 on the two occasions it was sampled) indicates that there is some effect from the stack solutions in this well (located very close to the stack on the southwest side). MW 22, on the other hand, shows pH values (6.60 and 6.51) comparable to the normal groundwater in the area. The pH of the stack fluids is generally very low (generally pH ranges from 2.2-2.6). A

summary which compares the radiochemical character of both the stack fluids and the monitor wells is given in **Table 2-3.**

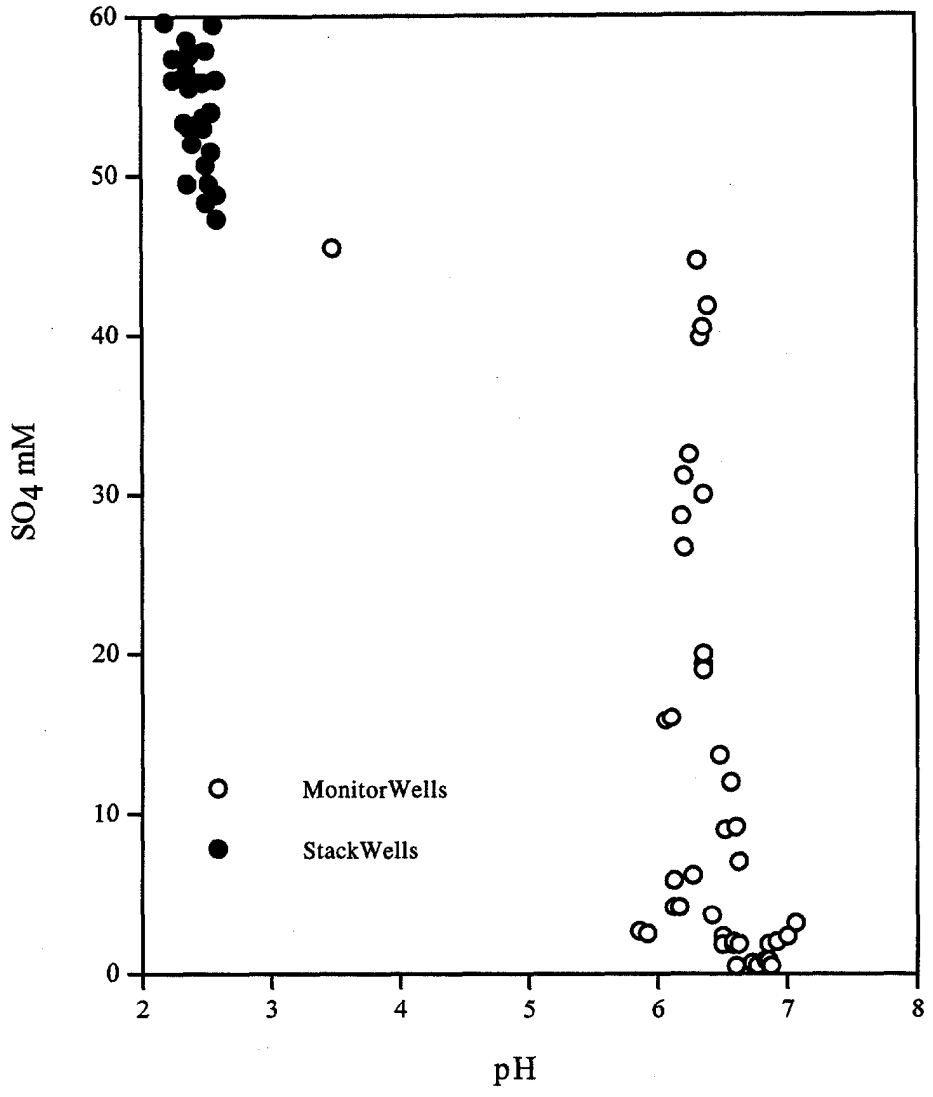

Figure 2-7 Concentrations of dissolved SO_4^{2-} versus field pH for both stack and monitor wells. The shape of this curve mimics a classic acid-base titration curve.

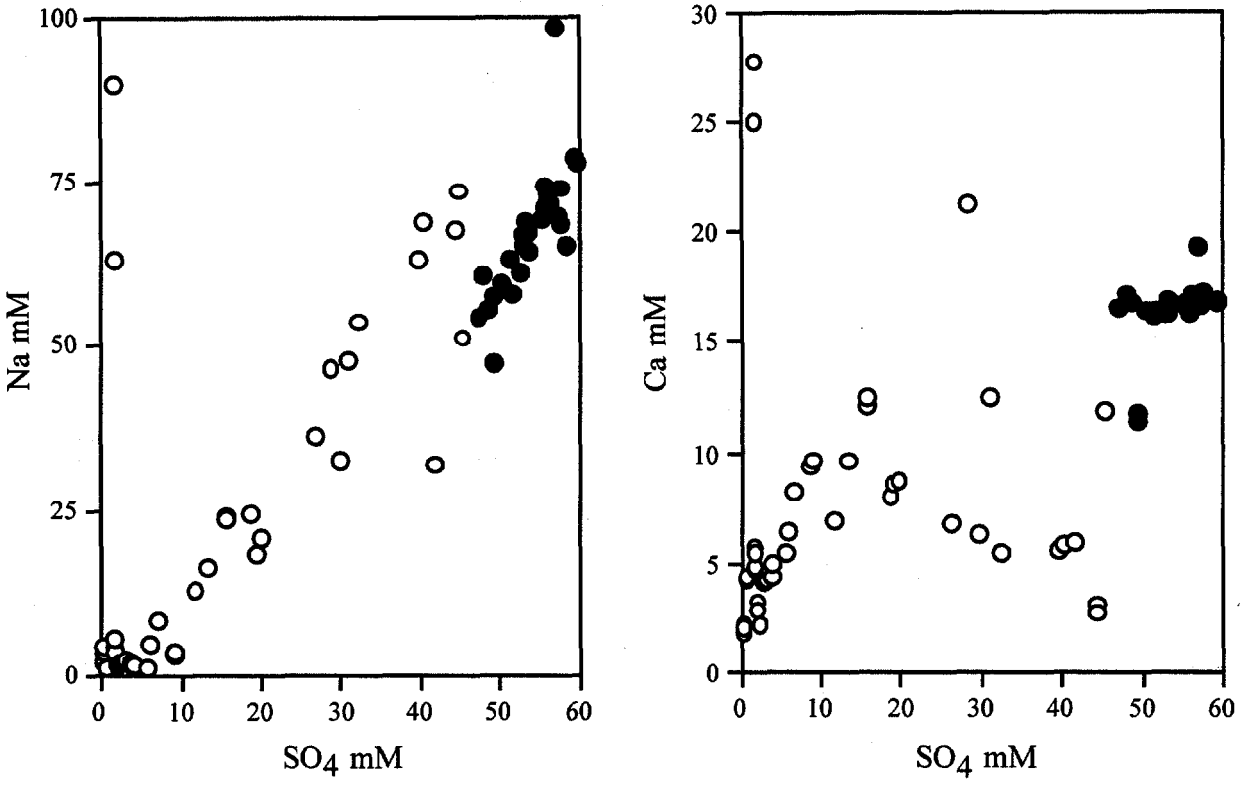

Figure 2-8 Plots of sodium versus sulfate and calcium versus sulfate for both monitor wells (open circles) and stack wells (closed circles). The sodium plot displays near conservative behavior while Ca shows evidence of non-conservative behavior at higher sulfate concentrations.

Table 2-3 Geometric mean concentrations and average deviations of radionuclides in the stack solutions and shallow aquifer surrounding the Piney Point stack.

Parameter	Stack dpm/L	Aquifer dpm/L
^{238}U	970±350	0.3±1.6
^{226}Ra	7±3	6.0±16
^{222}Rn	20,200±19,200	4,600±4,400
^{210}Pb	1100±900	1.0±0.9
^{210}Po	21±69	0.9±2.0

We report the geometric mean values for the radiochemical results because they tend to have a log-normal distribution. We did not include the ^{238}U and ^{210}Pb values for MW-12 because that well is obviously impacted by stack fluids as discussed above. No matter how one presents these results, however, the general character of these analyses is reflected in the table, i.e., there are extreme radiochemical differences between the stack and monitor wells with ^{210}Pb and U isotopes showing the greatest enrichment in the stack solutions. Although ^{222}Rn has the highest absolute activity in the stack fluids, its ratio to the aquifer waters is not nearly as high as that for ^{210}Pb and ^{238}U. Significantly, the stack fluids actually contain less ^{226}Ra than the surrounding monitor well waters.

When we examined inter-element relationships of uranium to stable elements in the stack and monitor wells, we found the strongest correlations to SiO_2, PO_4^{3-}, and F^- **(Fig.** 2-9). It was shown earlier (see Fig. 2-6) that there are strong relationships between all three of these chemical components themselves, so a link between U isotopes and one of these parameters would give the appearance of a link to all three. Thus, it is not possible to predict which of these parameters may control the speciation of U isotopes in the stack fluids based on these observations alone. Uranium may be complexed by both PO_4^{3-} and F^- so either of these is likely to play an important role in migration of U within the stack. This question will be addressed further in the geochemical modeling section of this report (Chapter 3).

The most striking feature of the gypsum stack well radiochemistries besides the extremely elevated ^{238}U and ^{210}Pb values are the consistently low specific activities of ^{226}Ra. The low ^{226}Ra is reflected in $^{210}Pb/^{226}Ra$ activity ratios of about 20 to 600 in the stack wells. We predicted low specific activities of ^{226}Ra in gypsum stack solutions in our laboratory experiments involving selective extractions of phosphogypsum (Burnett et al., 1995) that demonstrated that Ra is not significantly mobile when gypsum is present. The relationships of ^{226}Ra to Ca and SO_4^{2-} in both stack and monitor well waters **(Fig. 2-10)** show that, while the stack fluids may supply dissolved Ca and SO_4^{2-} to the surrounding aquifer, there is no way that the stack can be a source of Ra. Some of the monitor wells are somewhat enriched in ^{226}Ra compared to typical groundwater values with activities of 10-50 dpm/L, and, in the case of MW-23, extremely high values of 150-170 dpm/L That particular monitor well is located several hundred meters to the northwest of the stack, immediately adjacent to the old chemical plant. Phosphogypsum was apparently used for the base of a parking lot built next to the plant although it seems doubtful this has any bearing on the enriched ^{226}Ra. MW-23 water is not enriched in any other of the measured radionuclides but is also very high in Na, Ca, and Cl - higher, in fact, than most of the stack solutions. The origin of the contamination in MW-23 is unclear, but it is certainly not derived from the gypsum stack. We have checked the elemental ratios to see if seawater intrusion could be responsible for the elevated salt levels. Both the Na/Cl and Cl/SO_4 ratios in MW-23 water suggest that these waters are enriched in Cl relative to normal seawater.

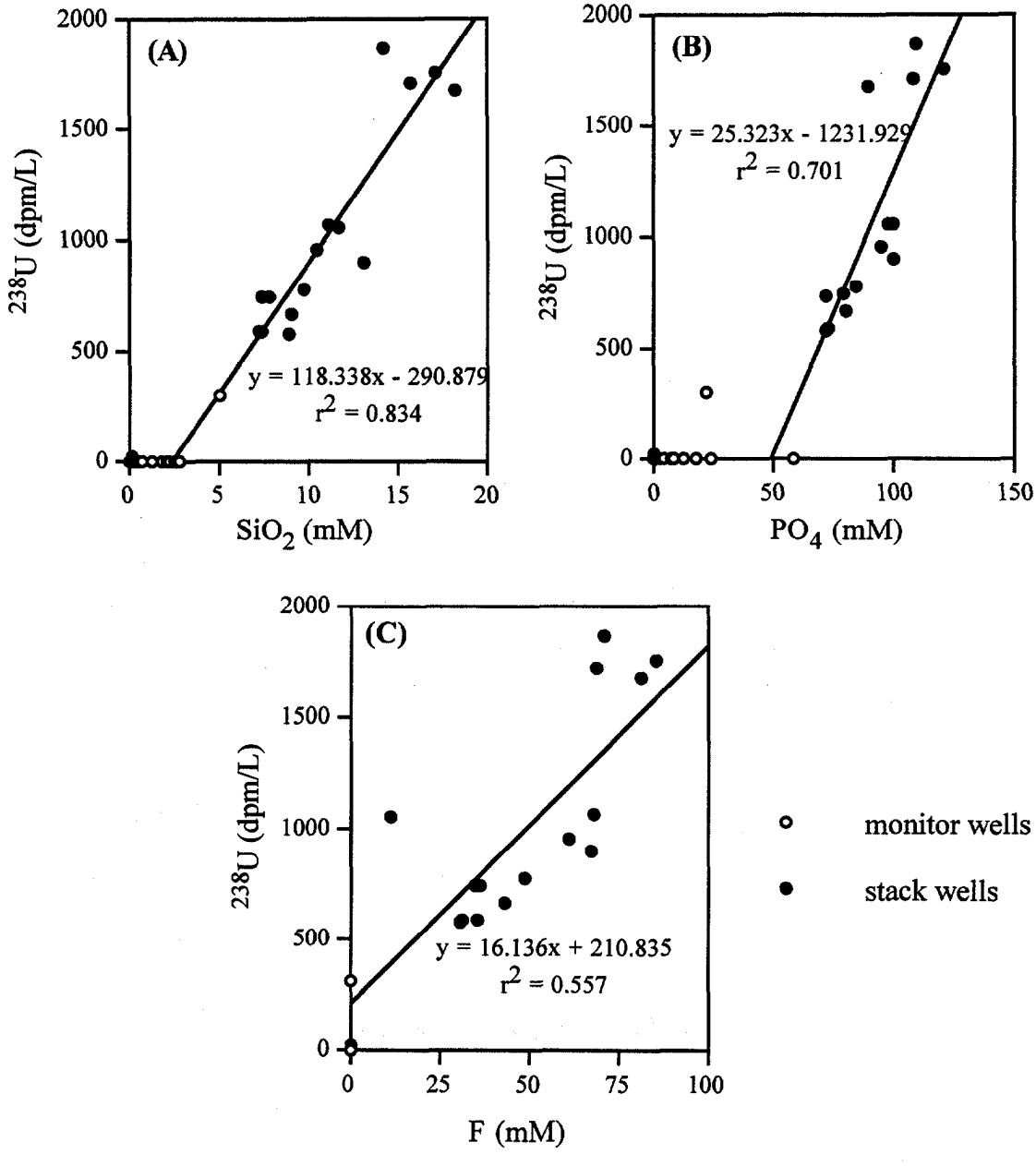

Figure 2-9 Plots of ^{238}U activity versus SiO_2 (A); PO_4 (B), and F (C) for both monitor wells (open circles) and stack wells (closed circles). The regression lines are drawn through the stack well samples.

The fact that the stack fluids are relatively low in ^{226}Ra is an important finding. Radium is one of the most important environmental radionuclides from a biokinetic point of view. Its presence in monitor wells near gypsum stacks is often cited as evidence of contamination from the stack. Yet the data presented in this report indicate that the stack

cannot possibly be a source of ^{226}Ra to the shallow aquifer around the Piney Point stack. Although gypsum contains substantial amounts of ^{226}Ra and the ^{226}Ra can be mobilized when the $CaSO_4$ phase is totally dissolved, radium from recirculating fluids is apparently strongly sorbed by phosphogypsum surfaces. The gypsum stack thus apparently acts as a sink, rather than a source, for dissolved radium.

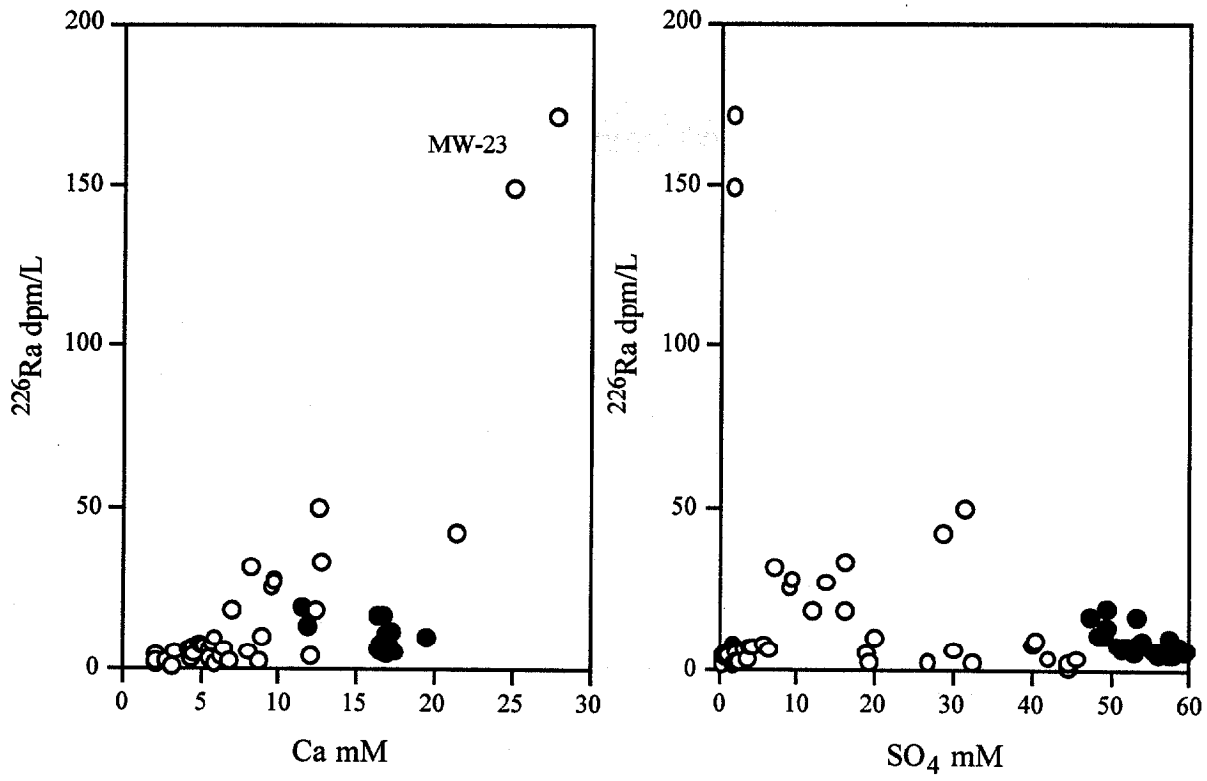

Figure 2-10 Plots of ^{226}Ra activity versus Ca (A) and SO_4 (B) for both monitor wells (open circles) and stack wells (closed circles). The MW-23 samples (collected next to the old chemical plant) are high in ^{226}Ra and Ca^{2+}, yet low in SO_4^{2-}.

What then, is the source for the somewhat elevated ^{226}Ra activities in some of the monitoring wells surrounding the gypsum stack? With the exception of MW-23, the only reasonable answer appears to be from the phosphate ore itself. The Piney Point Complex is built on mineralized land (Miller and Sutcliffe, 1982) which has not, as yet, been mined. Release of ^{226}Ra into groundwaters from phosphate rock has been observed before (Burnett, 1988) and is the most logical explanation in this case.

The activities of ^{210}Pb in the stack solutions are extremely high with a range from 320 to 3900 dpm/L, somewhat higher than the activities of ^{238}U found in the same solutions. The monitor well water activities are much lower, most often less than 1.0

dpm/L, with the exception of MW-12 which has activities near 30 dpmL This monitor well is directly next to the stack, on the southwest side, and shows chemical evidence for being impacted by the stack. The waters of MW-12 contain high concentrations of all the components characteristic of the stack fluids (Ca, SO_4, PO_4, etc.) and is the only monitor well studied with a significantly reduced pH. The only qualitative trend we noticed when plotting the ^{210}Pb activities against other parameters was a rough trend with SiO_2, i.e., the ^{210}Pb concentrations tend to be higher in the stack solutions with the greatest SiO_2 concentrations **(Fig. 2-11).** At the low pH characteristic of the stack solutions, more than one half the Pb may be in the form on an uncharged (aqueous) sulfate complex (see Chapter 3). When the fluids flow into the shallow aquifer and the pH is buffered, the Pb probably hydrolyzes very quickly and precipitates out of solution. Further observational evidence of this process will be shown in the following section where we discuss the radiochemistries of the core materials.

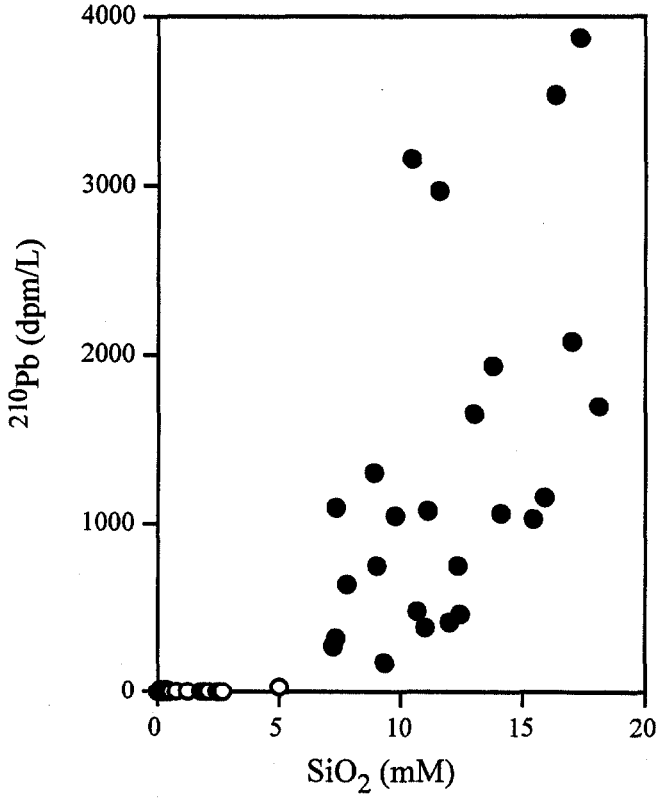

Figure 2-11 Plot of ^{210}Pb activity versus SiO_2 for both monitor wells (open circles) and stack wells (closed circles).

We also examined the radiochemical data for the stack solutions to evaluate whether there was any relationship between concentrations and depth in the stack, i.e., depths to the screened intervals of the monitor wells. The activities of ^{226}Ra and ^{210}Po do not show

any trend but stay at comparable levels throughout the stack. The concentrations of ^{238}U and ^{210}Pb, however, do increase more-or-less systematically with depth in the stack **(Fig. 2-12).** This is what one would expect if these components were acting as soluble species being added to the fluids as they pass through the stack. Note that the PP 2 cluster of wells shows an increased concentration of ^{210}Pb with depth until the very deepest section is encountered (PP 2-0) where the ^{210}Pb concentration drops nearly in half. This is the well that is screened below the bottom of the stack.

Radiochemistry of Phosphogypsum

CF Bartow Stack. All eight phosphogypsum samples collected from the stratigraphic section in the excavated cut at CF Bartow have been radiochemically analyzed and the results are presented in **Table 2-4**. The radiochemistries of these samples are unlike most of the analyses of the phosphogypsum samples collected from the unsaturated portions of gyp-stacks during our earlier phosphogypsum study (Burnett et al., 1995). The ($^{210}Pb/^{226}Ra$) in the four samples collected from strata below Gyp-65 in the section are all >1.3. These high activity ratios could conceivably be due to fractionation during the acidulation process since it takes ^{210}Pb about 110 years to come into secular equilibrium with ^{226}Ra. However, this is not considered to be likely since most "fresh" phosphogypsum samples we have analyzed have activity ratios much closer to unity.

Our previous work on the radiochemistry of Florida phosphogypsum has shown that radionuclide mobilization is possible in the stack environment, with ^{210}Pb being more subject to leaching and remobilization than ^{226}Ra. If this is the case at CF Bartow, ^{210}Pb in solution has migrated downwards through the stack and has been incorporated in layers of phosphogypsum near the base. All of the phosphogypsum in the CF Bartow stack is older than 12 years and samples near the base of the stacks are greater than 25 years old so the ($^{210}Po/^{210}Pb$) activity ratio offers some insight into the fractionation and mobilization of radionuclides during storage.

The relatively low specific activities of ^{210}Po in the lower layers represented by Gyp-61 - Gyp-63 and the ($^{210}Po/^{210}Pb$) activity ratios are less than about 0.40 for these samples implying that ^{210}Po has been leached from solids at the base of the stack. Harada et al. (1989) have shown that ^{210}Po can be mobilized in acidic, reducing environments and solutions that are discharging from in the lower portion of the excavated cut are anoxic. The Gyp-64 sample appears to be enriched in ^{210}Pb and ^{210}Po that has been leached from the high activity organic horizon (Gyp-65) directly above it.

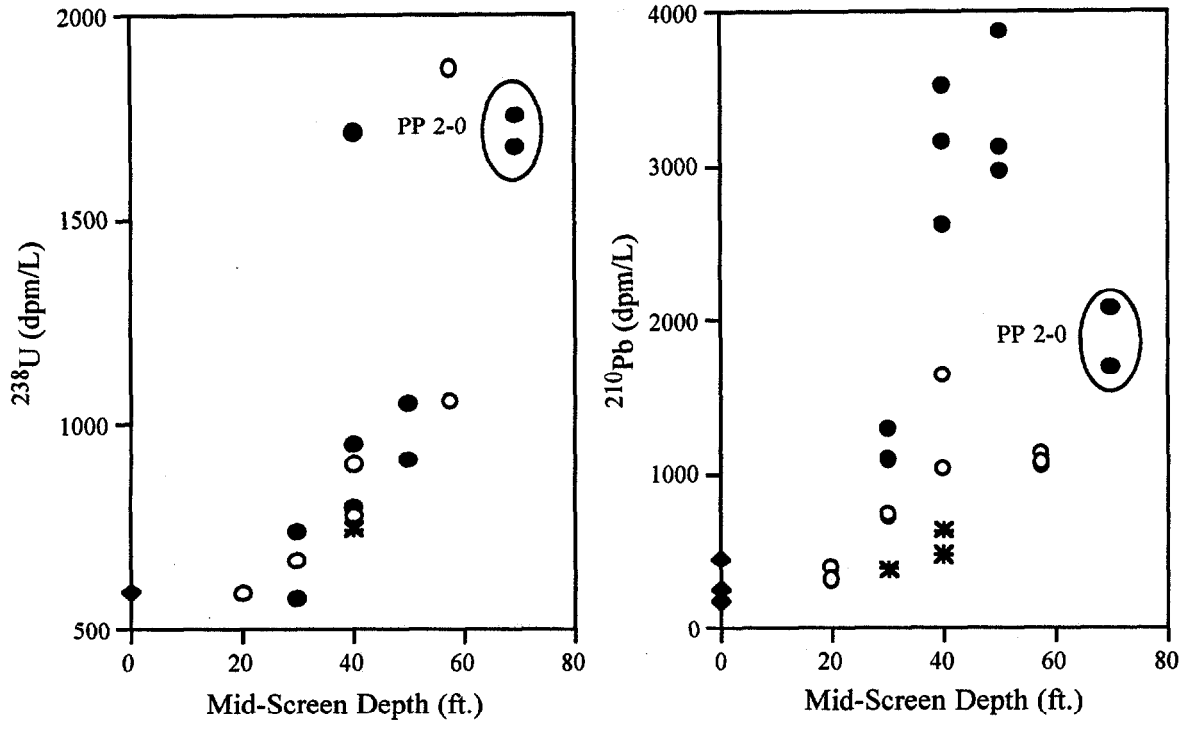

Figure 2-12 Plot of ^{238}U and ^{210}Pb activities (dpm/L) versus mid-screen well depth for all stack wells. Points at zero depth represent samples from the pond surface. The other symbols refer to the three well clusters: PP 1 (open circles); PP 2 (closed circles); and PP 3 (stars). The results from well PP 2-0, screened below the stack in the surficial aquifer, are circled. Note that the ^{210}Pb displays a significant drop in concentration in this well compared to overlying collection points in the stack.

The Gyp-65 horizon appears to be a boundary between samples that are appreciably "enriched" in ^{210}Pb below this stratum compared to the more "typical" (^{210}Pb/^{226}Ra) ratios in samples collected above the Gyp-65 layer. The Gyp-65 sample, a dark colored, poorly consolidated bed, has the highest activities of ^{210}Pb (976±3 dpm/g) and ^{226}Ra (1760±20 dpm/g) of any phosphogypsum sample we have analyzed or any analysis of phosphogypsum we are aware of in the scientific literature. These activities are about twelve times higher than average activities of ^{210}Pb and twenty times higher in ^{226}Ra than beneficiated ore rocks from the Central and Southern Phosphate District of Florida. Phosphogypsum samples from the same area have an average ^{210}Pb activity of 51.6 dpm/g and an average ^{226}Ra activity of 54.4 dpm/g. The (^{210}Pb/^{226}Ra) and (^{210}Po/^{210}Pb) activity ratios for Gyp-65 are also unique and are some the lowest we have measured in phosphogypsum. A preferential adsorption/desorption or exchange process followed by mobilization of both ^{210}Pb and ^{210}Po in stack solutions is the probable explanation of such activity ratios.

Table 2-4 Radiochemical analyses of bulk phosphogypsum samples collected along the southern face of the excavated cut through the phosphogypsum stack at CF Industries Bartow Phosphate Operations. The sampling locations are shown in Figure 2-3. All radionuclide activities are ingrowth/decay corrected to the date of sample collection. Uncertainties are given at the lo level based on counting statistics.

Elevation (ft) MSL	Sample ID	^{238}U dpm/g	^{226}Ra dpm/g	^{210}Pb dpm/g	^{210}Po dpm/g	$^{210}Pb/^{226}Ra$ Activity Ratios	$^{210}Po/^{210}Pb$ Activity Ratios
Top of Section							
215	Gyp-68	3.1±0.8	62.2±0.7	60.9±1.0	21.8±0.3	0.98±0.02	0.36±0.01
208	Gyp-67	4.6±0.5	67.5±0.2	57.9±0.8	36.3±0.5	0.86±0.01	0.63±0.01
200	Gyp-66	3.5±0.5	53.3±0.3	51.5±0.7	40.2±0.4	0.97±0.01	0.78±0.01
189	Gyp-65	66±2	1760±20	976±3	286±2	0.55±0.01	0.29±0.01
183	Gyp-64	5.3±0.6	42.0±0.3	54.4±0.8	68.8±0.9	1.30±0.02	1.26±0.01
176	Gyp-63	2.6±0.5	35.3±0.3	50.0±0.3	10.9±0.2	1.42±0.01	0.22±0.01
168	Gyp-62	2.3±0.6	36.9±0.3	48.0±0.8	8.9±0.1	1.30±0.02	0.19±0.01
160	Gyp-61	4.0±0.4	33.1±0.6	46.5±0.5	12.8±0.2	1.40±0.03	0.28±0.01
Base of Section							

The dark horizon from which Gyp-65 was collected also seems to define a transition in the activities of ^{226}Ra in phosphogypsum deposited above and below this zone. Phosphogypsum below the horizon has lower specific activities of ^{226}Ra. This may be due to a change in the radionuclide content of the phosphate ore rock being used with the organic horizon representing sedimentation in a gypsum pond and a hiatus in the deposition of phosphogypsum at this site. Phosphogypsum laid down subsequent to the break in discharge may have been produced from ores with higher contents of radionuclides. An alternative hypothesis which seems less likely in view of our investigations of the chemical behavior of ^{226}Ra in the presence of gypsum, is that ^{226}Ra has also been leached from phosphogypsum strata stratigraphically beneath Gyp-65.

It is not yet known why the deposit sampled as Gyp-65 is so radioactive. The dark color of the deposit indicates that the sample probably contains an appreciably higher concentration of organic material, perhaps from the defoaming agent used in the acidulation process or from the ore itself. This deposit is believed to have formed at the bottom of a gypsum pond on the top of the stack. If this is the case, the sediment may have adsorbed significant quantities of radionuclides, perhaps appreciably more ^{226}Ra than other nuclides, from gypsum pond solutions as well as sorbing nuclides from solutions percolating through the stack. This sample was also analyzed by sequential extraction techniques to evaluate which fraction was most important for hosting the extremely high ^{226}Ra. This evaluation showed that the organic fraction was the most important for radium (Burnett, in prep.).

Phosphogypsum samples above the organic layer and nearer the top of the stack, represented by the Gyp-66, 67, and 68, have ^{210}Pb and ^{226}Ra activities that are more like samples typical of Florida phosphogypsum collected from the unsaturated zones of stacks. The (^{210}Pb/^{226}Ra) activity ratios for Gyp-66 and Gyp-68 are near unity, but the activity ratio for Gyp-67 is about 0.85, lower than for most samples of Florida phosphogypsum collected near stack surfaces. There also appears to be a downward migration of ^{210}Po in the upper portion of the stack as well since the samples at the top of the section are old enough for secular equilibrium to be attained between ^{210}Po and ^{210}Pb. The phosphogypsum near the top of the CF Bartow stack at this section line was deposited prior to 1983 (secular equilibrium of ^{210}Po with ^{210}Pb requires less than three years) so (^{210}Po/^{210}Pb) activity ratios <0.50 for all seven samples and about 0.60 for Gyp-66 provides unambiguous evidence for active migration of ^{210}Po within this stack. Apparently ^{210}Po is more mobile within the interior of gypsum stacks than previously believed based on the surface reactive nature of this element.

Phosphogypsum from the Piney Point Stack. Core PP 1-1 was drilled on the west side of the old stack at Piney Point (Fig. 2-2) on March 20, 1995. The core was sectioned and described soon after recovery and has been completely analyzed for the radiochemical components of interest **(Appendix 2-6).** The core was found to contain substantial amounts of phosphatic pellets and cobbles, consistent with the observations of Miller and Sutcliffe (1984). Plots of the radiochemical distribution as a function of depth proved most interesting. The distributions of ^{238}U and ^{210}Pb with depth **(Fig. 2-13)** show relatively uniform concentrations down to about -60 feet below the surface where there is a huge ^{210}Pb spike. The concentration of ^{226}Ra (not shown on the diagram for clarity) is even higher at this level (sample gyp-107 has a ^{226}Ra activity = 1098 dpm/g). This layer is composed of a dark, laminated material which appears to be organic-rich and thus appears very similar to the material from the CF Bartow stack described above (gyp-65, Table 2-4). The ^{238}U is also higher at the -60 foot level but displays a stronger peak further downcore at about -63 feet depth below the surface of the stack. The fact that the uranium spike was a few feet further downcore may imply

that uranium is at least somewhat more mobile in the stack solutions than radium. Also note that there is a secondary ^{210}Pb peak just above the bottom of the core. That secondary peak corresponds to an analysis of soil at the base of the gypsum stack, i.e., the topmost soil is significantly enriched in ^{210}Pb. If the enrichment of these radionuclides is secondary, i.e., occurring as the solutions move through the stack, these observations suggest that substantial amounts of radionuclides are redistributed within the stack and sequestered within the soil at the base of the stack before entering the underlying aquifer.

The distribution of the activity ratio ^{210}Pb/^{226}Ra with depth in the core is also very interesting. The activity ratio varies within a relatively narrow range of about 0.5 - 2.0 through much of the core until near the bottom where it rises first to about 4.3 (Gyp-76, an organic sand soil horizon at the very base of the stack) and then to 14.1 in the lowest sample (Gyp-75 which consists of sediments from the surficial aquifer). Apparently the ^{210}Pb, which migrates preferentially to the ^{226}Ra in the stack solutions, precipitates very rapidly when the underlying soil horizon is encountered. The incorporation of ^{210}Pb from stack solutions into the soil may be by adsorption, coprecipitation with iron hydroxides, or other secondary process. This observation is very significant in terms of potential migration of radionuclides away from the stack into the shallow aquifer.

Core PP 2-0 was drilled in the central area of the old stack at Piney Point (Fig. 2-2) on March 18, 1996. The distribution of radionuclides within the core material shows patterns similar to those described for both core PP 1-1 and the CF Bartow stratigraphic section. There is a dark-colored, organic-rich, laminated layer at 56 feet below the stack surface which is greatly enriched in radionuclides (sample gyp-117 ^{226}Ra = 491 dpm/g). This layer shows clearly as a spike in a plot of ^{238}U and ^{210}Pb versus depth **(Fig. 2-14).** Again both nuclides show a secondary maximum lower in the core, just at the point where the gypsum is in contact with the underlying soils. Since core PP 2-0 was drilled completely through the stack (the well was actually screened in the underlying aquifer), we had the opportunity to collect more samples under the stack and get a more complete picture of the radionuclide distribution with depth. Since ^{210}Pb is apparently behaving much differently than ^{226}Ra in the stack fluids, the ^{210}Pb/^{226}Ra activity ratio shows a dramatic increase right at the base of the stack with a quick return to values near secular equilibrium. This is excellent evidence that ^{210}Pb, although very high in the stack solutions, precipitates quickly upon encountering the higher pH groundwaters and is incorporated into the shallow soils. The observational evidence suggests that there is little radionuclide transfer from the stack solutions to the aquifer.

Radiochemical analyses of phosphogypsum samples collected on the western and southern flanks of the older stack are given in **Appendix 2-7**. Samples collected on the western flank were taken at specific elevations for comparison of the radionuclide contents in the core of the PP 1-1 well. The same reasoning was the motivation for

collection and radioanalyses of the phosphogypsum samples on the southern flank of the older stack, i.e., for comparison with the PP 2-0 core.

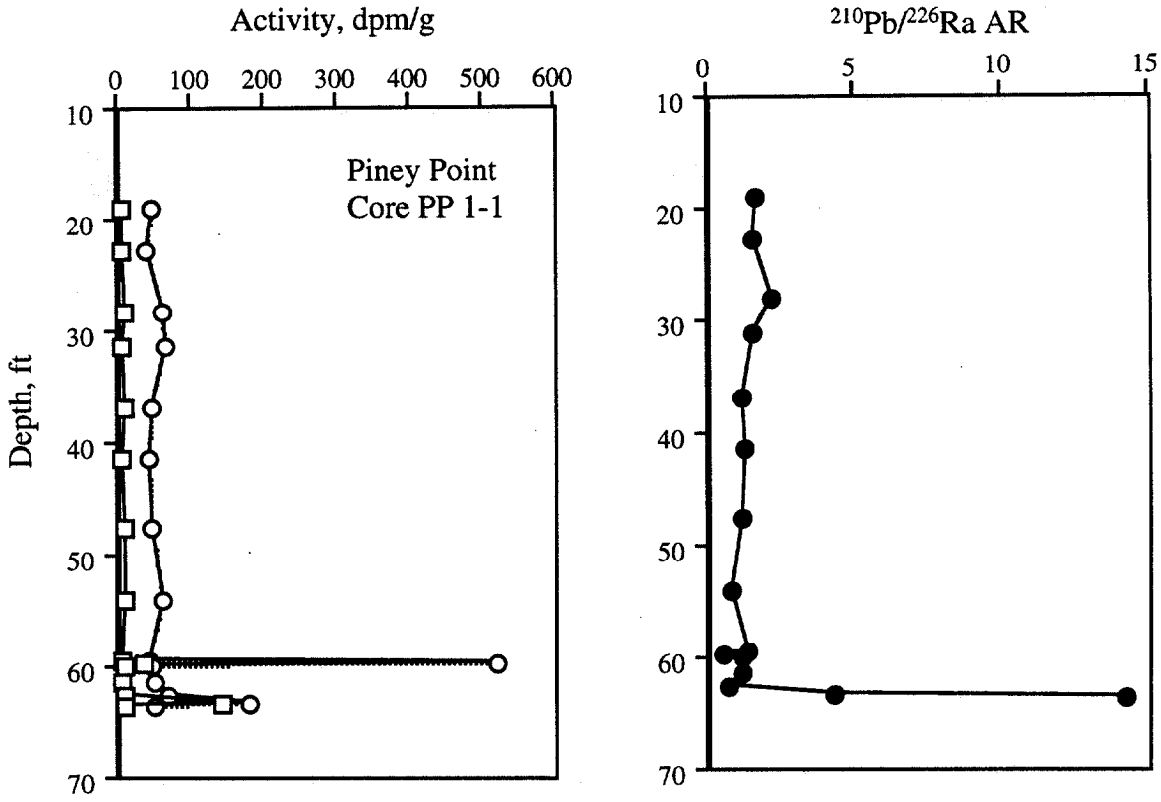

Figure 2-13 Plot of ^{238}U (open squares) and ^{210}Pb (circles) activities (dpm/g) versus depth in stack core PP 1-1. The right-hand drawing shows the activity ratio $^{210}Pb/^{226}Ra$ versus depth in the same core. The last two data points represent samples of soils underlying the gypsum stack.

The activities of ^{238}U and ^{226}Ra in the western flank samples do not vary appreciably, but the Gyp-71 sample that was collected near the base of the stack contains relatively higher activities of ^{210}Pb and ^{210}Po. These activity ratios are nearly identical at about 0.75 and it is likely that this re-distribution of ^{210}Pb and ^{210}Po is a semi-continual process rather than episodic. There has possibly been addition of ^{210}Pb to the Gyp-87 sample. Gyp-88 appears to be a re-worked sediment that was collected about 5 feet above Gyp-87 in the process water drainage ditch south of the stack.

We have also analyzed radiochemically sediment cuttings collected from all seventeen of the new monitor wells installed around the Piney Point stack. In most cases, samples were collected just from the lower portion of the well, i.e., the screened interval. These analyses **(Appendix 2-8)** are rather typical for radionuclides in phosphatic

sediments (approximately 10-40 dpm/g ^{238}U with comparable daughter activities). Note that virtually all the sediments are enriched in ^{210}Pb relative to ^{226}Ra, i.e., the $^{210}Pb/^{226}Ra$ activity ratios (AR) are all greater than 1.0 (most values in the 1.2 - 1.3 range with two samples much higher). The origin of this excess ^{210}Pb is probably a combination from stack fluids and by natural ^{222}Rn diffusion from underlying strata. The two well sediments with the greatest ^{210}Pb enrichment (MW-12 AR=1.9; and MW-20 AR=1.6) are both located directly next to the stack.

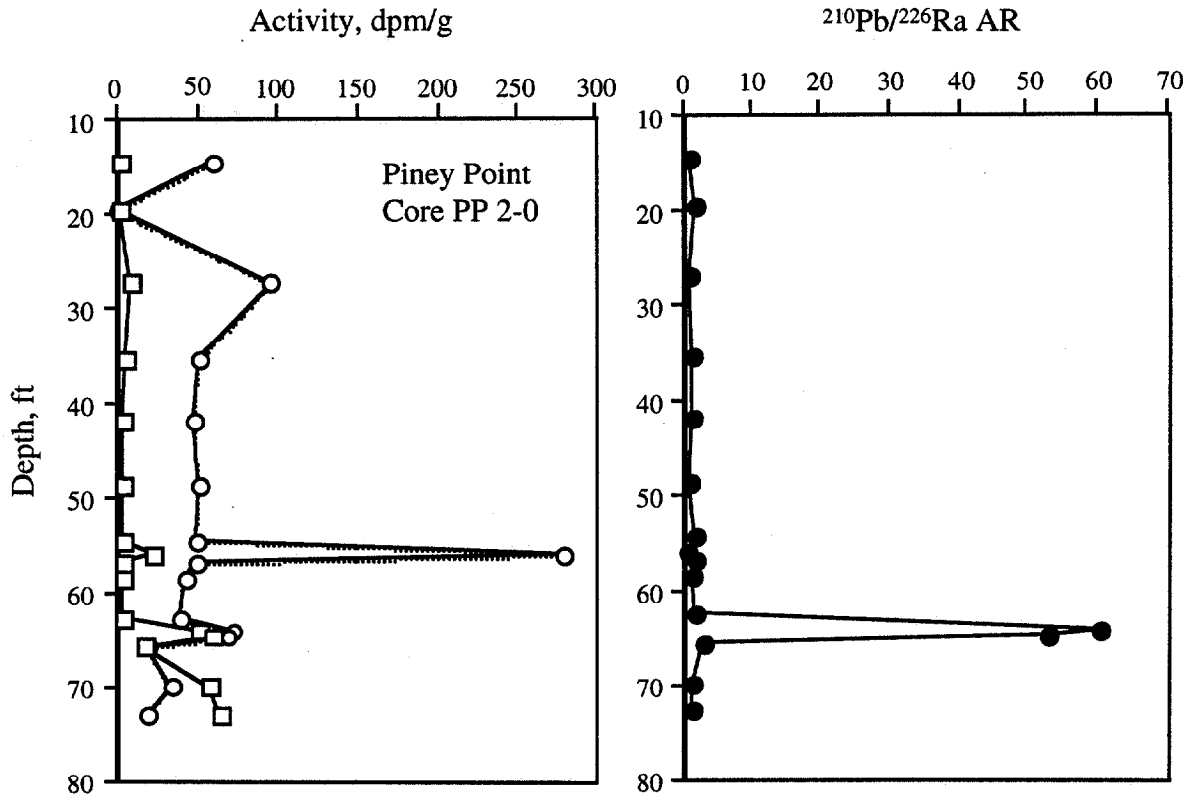

Figure 2-14 Plot of ^{238}U (open squares) and ^{210}Pb (circles) activities (dpm/g) versus depth in stack core PP 2-0. The right-hand drawing shows the activity ratio $^{210}Pb/^{226}Ra$ versus depth in the same core. This core penetrated the bottom of the stack - the lowest 5 samples are from the soils and sediments directly underlying the gypsum stack.

SUMMARY

This study was initiated to investigate the processes responsible for controlling the interaction and release of radionuclides from phosphogypsum from an actual phosphogypsum stack. Our approach used samples from monitor wells placed both around and directly into the Piney Point gypsum stack. Samples of fluids drawn from

these wells showed that in general, the stack solutions are acidic with high ionic strength, containing high total dissolved solids (TDS) of 18,700±2300 ppm and a pH of 2.43±0.10. The waters from the monitor wells surrounding the stack have a much lower average TDS of 3,300±3200 ppm and a pH of 6.33±0.65. Qualitative relationships between dissolved PO_4^{3-} and F^- and F^- with SiO_2 are thought to imply solution controls by the solid phases carbonate fluorapatite and alkali fluorsilicates. A plot of pH versus SO_4^{2-} ion concentration was shown to resemble a classic acid-base titration curve.

Radiochemically, the stack wells are exceptionally high in activities of uranium (generally 600-1000 dpm/L ^{238}U) and ^{210}Pb (generally 400-4000 dpm/L). Activities of ^{222}Rn are also elevated (range from about 20,000-70,000 dpm/L) although this is not surprising in view of the radium-rich nature of the surrounding phosphogypsum. One very significant result is that the activities of ^{226}Ra in the stack fluids are only slightly elevated (range about 5-10 dpm/L) above normal groundwater values and are, in fact, less than most of the monitor well concentrations measured around the Piney Point gypsum stack. These consistently low specific activities of ^{226}Ra in the gypsum stack fluids argues against the stack as a source of radium to the aquifer.

Observations in solid phase materials, both from the stratigraphic section at the CF plant and the two cores in the Piney Point stack, are consistent with the results from the fluid analyses. Our observations suggest that substantial amounts of radionuclides are sequestered within or just below the stack before entering the underlying aquifer. One of the strongest lines of evidence is the ^{210}Pb data in the cores. The $^{210}Pb/^{226}Ra$ activity ratios are near or below equilibrium throughout the entire stack until the underlying soils are encountered. At this point there is a large excess amount of ^{210}Pb observed (activity ratios of $^{210}Pb/^{226}Ra$ as high as 60) in the soils indicating precipitation of ^{210}Pb when the low pH stack solutions are buffered by the underlying soils and sediments. Although many of the sediments under the stack are enriched in U-series radionuclides, the contents below the upper surficial sands appear to be associated with the natural phosphatic minerals in those strata. The bulk of the observational evidence suggests that there is little radionuclide transfer from the stack solutions to the underlying aquifer.

CHAPTER 3

GEOCHEMICAL MODELING

Alan W. Elzerman
Environmental Systems Engineering
Clemson University

STATEMENT OF PROBLEM

Phosphogypsum is the $CaSO_4$-based leftover by-product of phosphoric acid production from combining sulfuric acid with the mined carbonate fluorapatite. Phosphogypsum is laden with other components as impurities, and is slightly radioactive (^{238}U, ^{226}Ra, ^{222}Rn, ^{210}Pb ^{210}Po). The heavy metals and radionuclides contained are of particular interest due to their potential environmental and health effects. Since phosphogypsum is also acidic from residual sulfuric acid, the conditions accompanying contaminants may allow significant mobility of the radionuclides and metals. Contributing to the concern is the tremendous quantities of PG produced (about 40 million metric tons per year) and the duration of the disposal (several decades), which has resulted in stockpiles (known as "stacks") over 100 feet high covering hundred's of acres. Contamination of local groundwater is an obvious concern. Consequently, it is imperative to understand which components might be transported to the groundwater and what factors control the mobility.

The objectives of this portion of the overall project are to produce chemical models of the solutions within the stack.

APPROACH

The overall project undertook field sampling of stack and adjacent soil solids and solutions, as well as groundwater from wells, geochemical and radiochemical characterization of stack solutions and adjacent groundwaters, water budget and flow models in and around stacks, and modeling of the system geochemistry. The results reported in this chapter consist of solution chemical speciation modeling and prediction of oversaturated solids for the groundwater solutions near stacks and away from immediate influence of stack contamination. Hydrological modeling was presented in chapter 1 while the geochemical and radiochemical characterization was covered in chapter 2. The specific approach adopted for this component of the study was as follows:

1. investigate trends and correlations in field data on solution concentrations for clues to sources of contaminants, transport, and processes;

2. evaluate groundwater equilibrium solution chemistry for dominant and controlling speciation that may then be related to relative mobility; and

3. predict equilibrium precipitation of solids from groundwater solutions.

METHODS

Field Data

All data used in this component of the project were obtained from the records of the overall project. Data for all 53 parameters determined for the 77 groundwater samples collected during 9 field trips over approximately 18 months were reviewed. These are the same results presented in chapter 2 and the relevant appendices to this report.

Geochemical Modeling

Computerized Geochemical Equilibrium Speciation and Precipitation Modeling. All geochemical modeling was accomplished with MINTEQA2, Version 3.11 (December 1991), available from the US Environmental Protection Agency, Office of Research and Development, College Station Road, Athens, GA 30613-0801 (phone: 706-546-3549). The program runs on PC computers in the DOS mode (any processor or speed).

This popular equilibrium speciation model has a thermodynamic database that is easily modified. In fact, the thermodynamic database used in this investigation has been updated over several years to include more species of radionuclides (a copy of this

database is available by request). However, these modifications would have affected only a few of the results reported here.

In all cases the pH was set as a fixed parameter. Although the program is capable of estimating resultant pH, known field data were available and were used for the solutions. Temperature was fixed at 25° C. Although temperature is a factor in equilibrium speciation, the deviations present from 25° C would not make a significant difference. The model was allowed to calculate ionic strength. Cation/anion ratios were usually within the range 0.9 to 1.1, except in those cases where a component was deliberately removed, consistent with (but not proving) accurate data for the major anions and cations. Since all solutions came from systems considered to be oxidizing, pe was not allowed to be a variable in the model calculations. All oversaturated solids were allowed to precipitate, but adsorption was not allowed. The carbonate concentration was input as total carbonate, not as alkalinity. A closed system was assumed for the groundwaters, and carbon dioxide excluded. This approach was considered most appropriate for the groundwater samples since they are isolated from the atmosphere and analytical values for HCO_3^- were reported. The number of allowed iterations was set at 200, since in some cases 40 was not sufficient.

Selection of Model Solutions for Calculations. Evaluation of the data quickly indicated the samples had fairly uniform characteristics within two distinct groups, those which had been significantly influenced by input of PG stack solutions versus those which had not (see analysis of trends and correlations below as well as those presented in chapter 2). Also, there was no significant variation, for purposes of geochemical modeling, in results from one sampling day to the next. Consequently, rather than produce numerous outputs for each sample varying only a little from each other, it was decided it would be more instructive to define an "uncontaminated" and a "contaminated" model solution to use in the geochemical modeling. Some MINTEQ runs were also made for solutions containing only the major components and for solutions with the dissolved silica removed to test the sensitivity of the outputs to these factors. The actual selections are discussed more fully in the section "Evaluation of Groundwater Solution Chemistry For Dominant and Controlling Speciation" below.

RESULTS

Investigation of Trends and Correlations in Field Data for Clues to Sources of Contaminants, Transport, and Processes

First Observations. Since the overall project had produced considerable field data on chemical components in the groundwater near and around the PG stacks, an obvious first step was to look for trends and correlations in the data. In fact, this proved very worthwhile. Several patterns were obvious in the data. For example, we observed that

contamination from the stacks was evident in samples collected to the west, down gradient in the groundwater flow from the area of the stacks. Contamination was evidenced by decreased pH values, and increases in TDS and correlated components such as sulfate and phosphate (see below). Similar evidence of stack contamination was not present in wells generally to the east, or upgradient. Since the signature of the stack contamination is so distinct (see below), the chemical composition becomes a reliable method of detecting contamination for all of the wells in the area.

Correlations of Data. Plots of the data were also very instructive, providing a way to evaluate correlations visually. For example, consider **Figure 3-1,** which shows concentrations of many ions vs. pH for all of the samples. While approximate concentrations for each ion can be read from this plot, that is not its purpose. What is very evident is that the data fall into two main groups, one with a higher pH (approximately 6.5) and one with a much lower pH (approximately 2.5). The lower pH group also has elevated levels of, at least, sulfate and phosphate. Correlations of other ions must be examined separately to clearly see relationships, as done below. Obviously, the lower pH group shows the most effects of contamination from the gypsum stacks (since the pH drop is not linear, as shown in Figure 3-3, samples receiving some contamination may still be in the higher pH range.). The tight grouping of data indicates initial modeling need only look at two solutions, one a model of "contaminated" samples and the other a model of "uncontaminated" samples. Figures 3-3 to 3-9 indicate there are "intermediate" samples, but the major factors should be evident by looking at the two "end members."

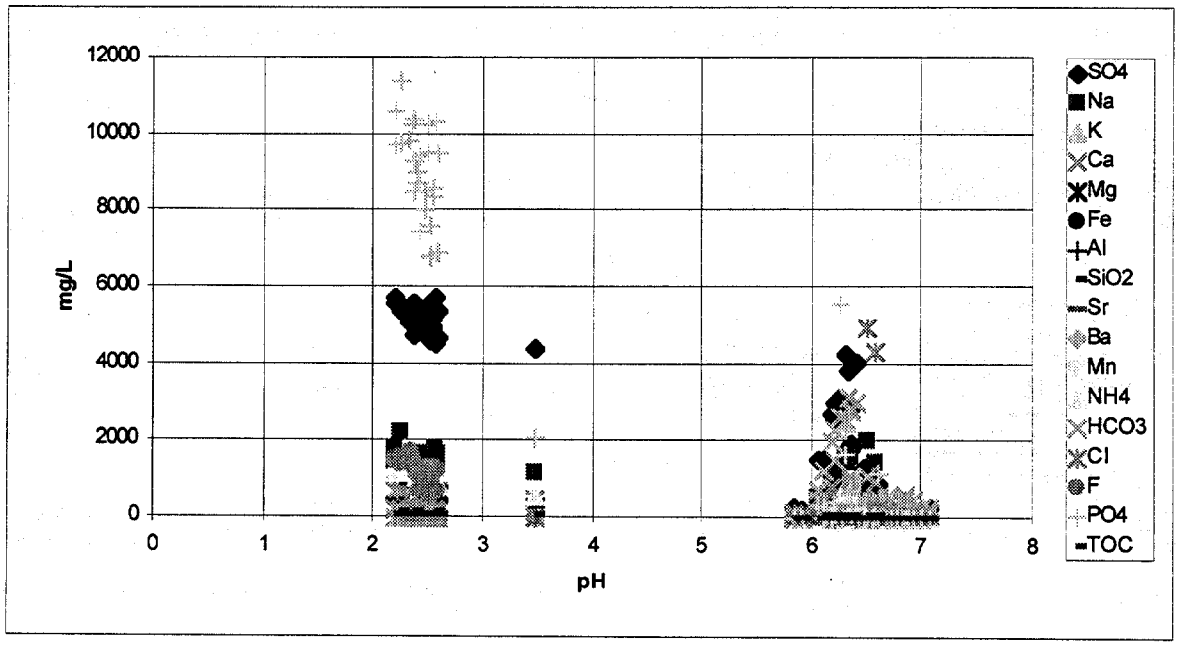

Figure 3-1 Ion concentrations versus pH for all samples analyzed in this study.

Note that there is one set of data in Figure 3-1, at approximately pH 3.5, which does not fit into either the contaminated or uncontaminated group. These data come from one well, MW-23, just north of the chemical plant. As will be shown below, this well produced water with characteristics that distinguished it from all of the others. Apparently, some local source, such as the chemical plant, resulted in inputs that caused this difference in chemical characteristics.

Since sulfate is an obvious potential tracer of the gypsum stack solution inputs, correlations of other ion concentrations with sulfate were considered. **Figure 3-2** plots various ion concentrations versus sulfate concentration for all of the samples. One indication from this plot is that there is a general trend of increasing ion concentrations with increasing sulfate concentrations, as would be expected from the input of a variety of ionic species from the PG stacks, as well as potentially from the increased solubilization of minerals that might occur from the lower pH values in the contaminated samples. In particular, the increasing phosphate values with increasing sulfate concentrations are apparent, indicating the contaminated samples are indeed being influenced by stack solutions.

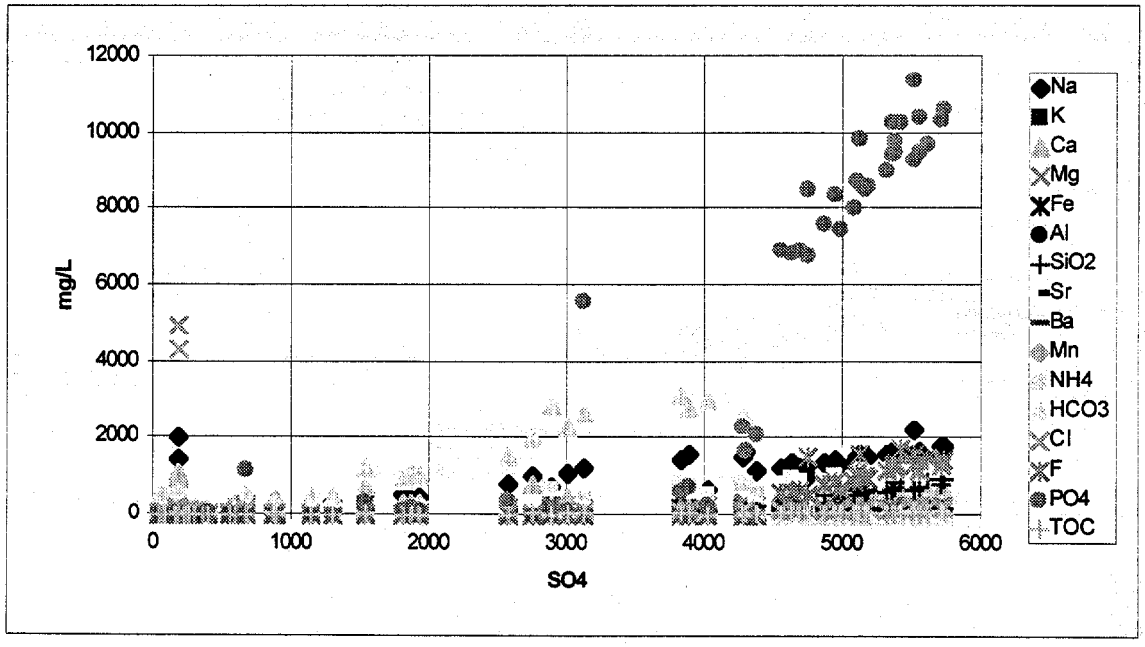

Figure 3-2: Concentrations of various ions versus SO_4^{2-} ion concentration for all samples.

A closer look at the relationship between pH and sulfate is also warranted since they should be integrally linked in contamination inputs. **Figure 3-3** shows a plot of pH versus sulfate concentration for all samples. As expected, the contaminated samples with

higher sulfate concentrations also exhibit lower pH values, a result of the input of sulfate as sulfuric acid and the residual acidity in the PG stacks. Also of note is the shape of the plot. Adding acid to soil is essentially a heterogeneous titration of a base with a strong acid. In keeping with typical neutralization reactions, as seen in titration curves, the basic shape of the plot is a "S" curve. The soil neutralizes the incoming acid until its neutralization capacity is exhausted, then there is a dramatic decrease in pH, followed by another plateau down near and approaching the pH of the input solution (analogous to the acid titrant). In Figure 3-3 there is an apparent analogous equivalence point at about pH 4, after an approximate input of 4300 mg/L of sulfate. Since the mass of soil contacted is not known, a soil neutralization capacity can not be estimated. However, the sulfate concentration is 45 mM, which, assuming all of it was input as sulfuric acid, would have brought in 90 mM H^+, most of which, as expected, was neutralized or the pH would have been about 1.

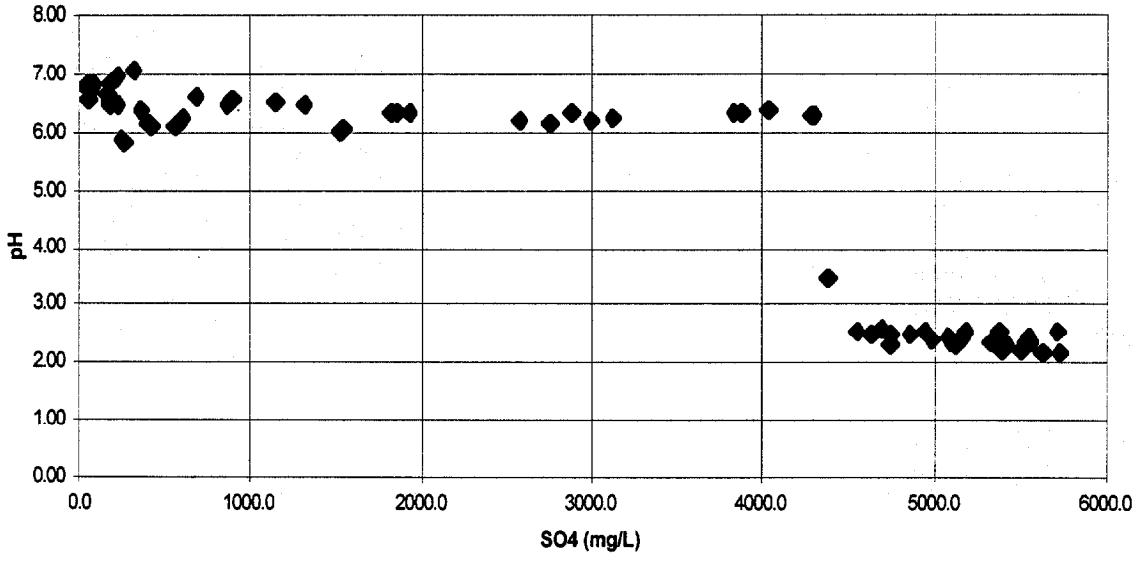

Figure 3-3: pH versus SO_4^{2-} ion concentration for all samples.

Given the common input from stack solutions and the observations of the field data above, a strong positive correlation between phosphate and sulfate would be expected. Indeed, **Figure 3-4** shows such a correlation exists for the higher sulfate concentrations.

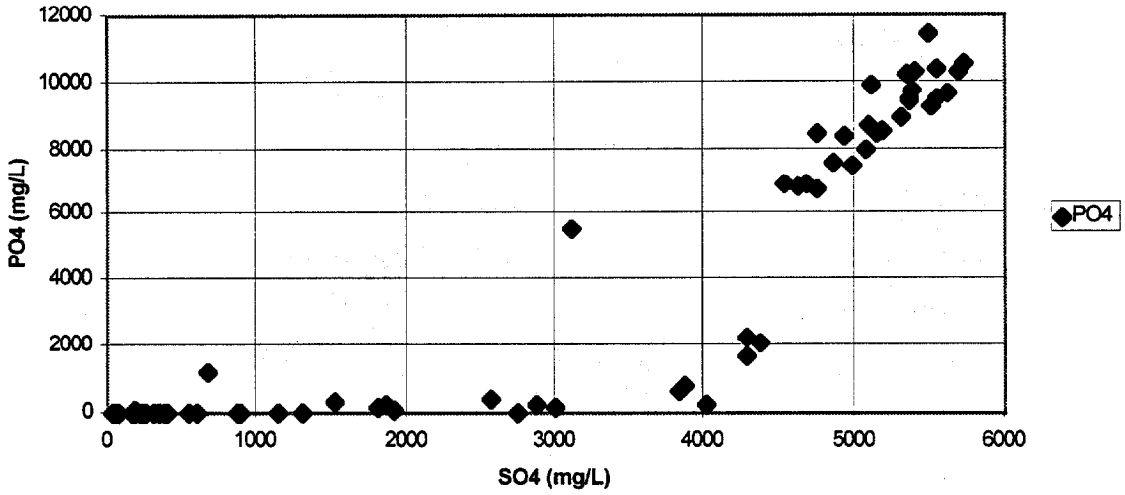

Figure 3-4: PO_4 versus SO_4 concentrations for all samples.

A strong positive correlation also exists between sodium concentrations and sulfate concentrations, as shown in **Figure 3-5.**

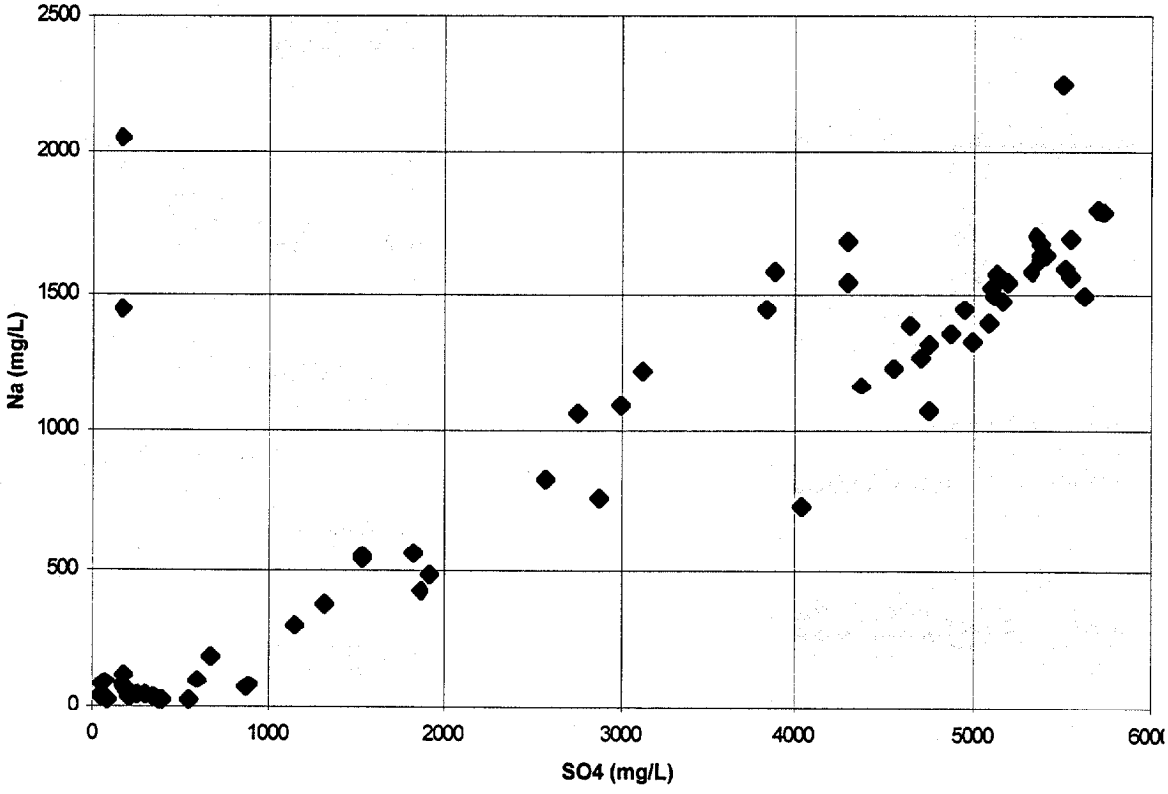

Figure 3-5 Na versus $S0_4$ concentrations for all samples.

However, there is a less strong correlation between calcium and sulfate concentrations compared to sodium, as shown in **Figure 3-6.**

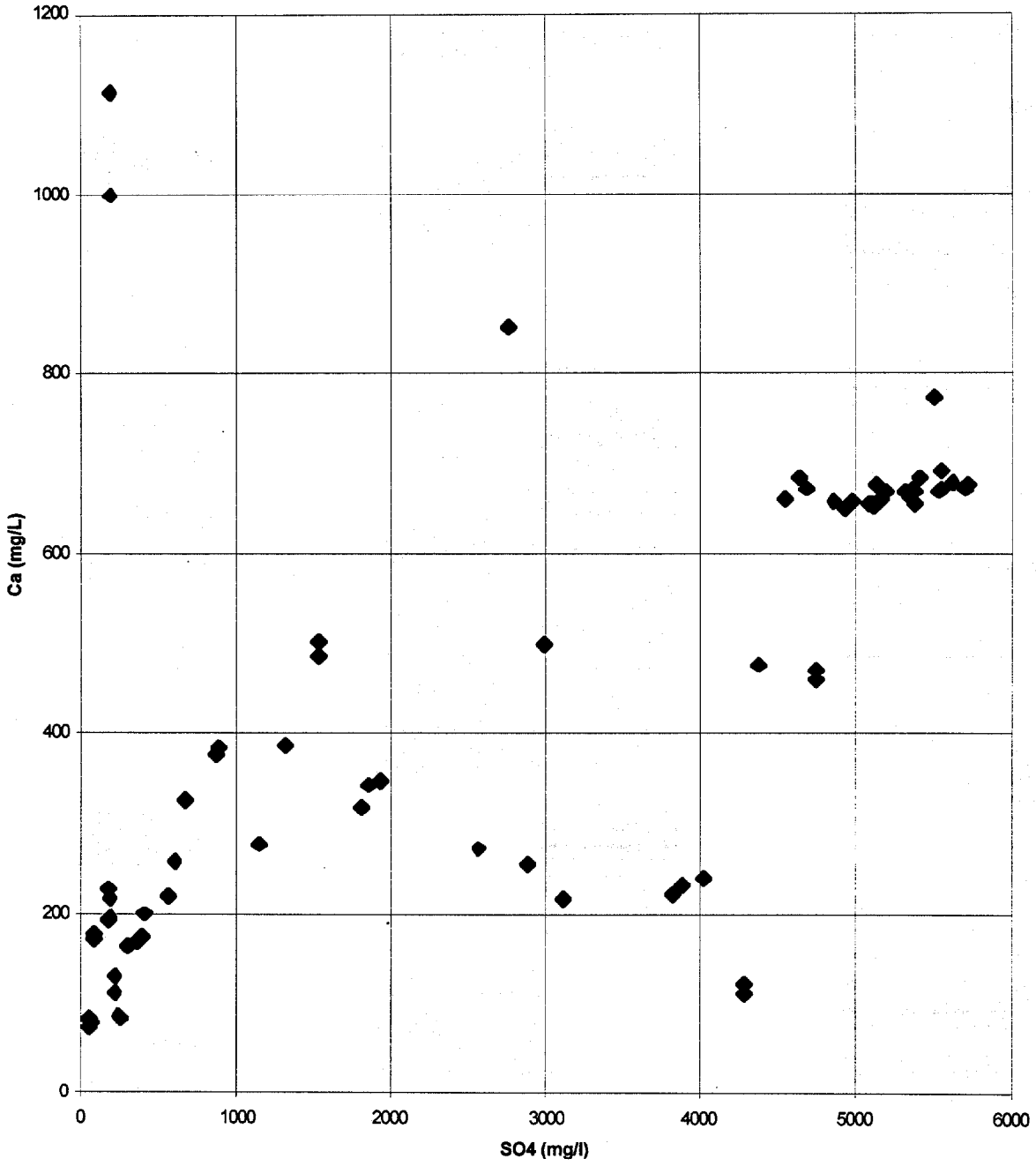

Figure 3-6 Ca versus SO_4 concentrations for all samples.

The difference between calcium and sodium in relation to sulfate may be related to their reactivity. Sodium would be essentially conservative in these systems. However, calcium will participate in a variety of complexation and precipitation reactions.

Evaluate Groundwater Solution Chemistry for Dominant and Controlling Speciation

Major Ions in Groundwater Samples. A necessary step prior to geochemical modeling is choosing the input chemical components and their total concentrations. As stated above, the samples in this investigation fell into either a contaminated or an uncontaminated group, with well MW-23 being the only exception. Consequently, there should be a distinguishable difference in the patterns of major cation and anion concentrations for these samples. **Figures** 3-7 to 3-9 show the patterns for major cations in MW-1 (fieldtrip #l), chosen as the model for uncontaminated samples, PPl-3 (fieldtrip #2), chosen as the model for contaminated samples, and MW-23 (fieldtrip #9). The anions (shown at the top of each plot) were given negative values in these figures to break them apart from the cations. Note the pH of MW-1 was 6.73 and PP 1-3 was 2.44, while the pH of MW 23 was 6.4.

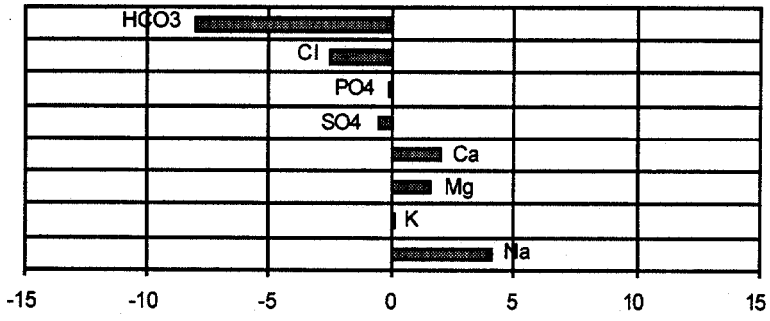

Figure 3-7 Cation and anion distributions for uncontaminated groundwater in MW-1 in mmole/L.

The cation/anion patterns exhibited for the three samples in the figures above are completely different, as expected. First, MW-1, the uncontaminated or “background” sample, has the characteristics typical of many freshwaters. The major cations are calcium and magnesium with some sodium and potassium. The difference here is that the sodium concentration is relatively high compared to the calcium and magnesium for a typical freshwater. This probably results from sodium chloride input from the marine sedimentary material in the aquifer or input from aerosols from the Gulf of Mexico, but other explanations are possible. The sodium chloride source is also indicated by the relatively high chloride concentration compared to bicarbonate. As is typical of fresh

waters, bicarbonate dominates the anions. The TDS for the sample is 672 mg/L, much lower than the contaminated sample, described below.

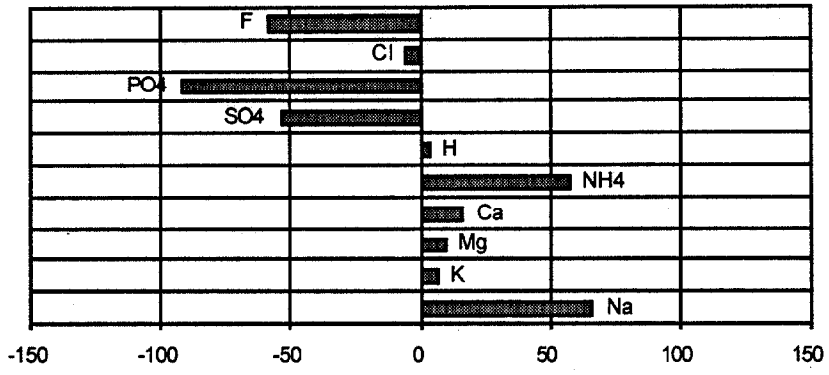

Figure 3-8 Cation and anion distributions for contaminated groundwater in PP 1-3 in mmole/L.

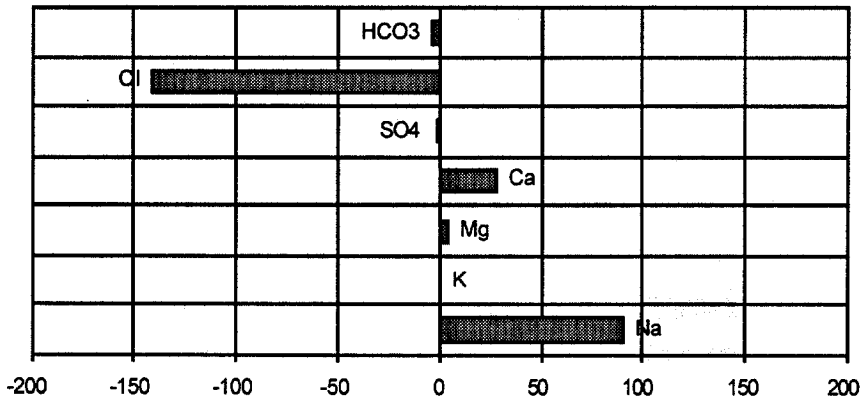

Figure 3-9 Cation and anion distributions for contaminated groundwater in MW-23 in mmole/L.

Looking next at the contaminated sample, PP1-3, as expected the ion concentrations are generally higher than in the uncontaminated sample (and the TDS is much higher, at 18,360 mg/L). Consistent with the assumed input of PG stack contamination, both the phosphate and sulfate concentrations are elevated. A significant concentration of fluoride, another marker of gypsum stack solutions, is also present, which could cause significant changes in chemical speciation since fluoride ion is a good ligand. Balancing the anions are a mixture of ammonia, calcium, magnesium and sodium cations.

The waters from MW-23 have a third pattern that distinguishes it from the others. From the chemical composition, it appears to be composed of the "background" fresh water with addition of significant amounts of sodium chloride, and possibly calcium chloride. Discharges from the chemical plant may be responsible, but no data on possible discharges were available.

Modeling of Uncontaminated and Contaminated Solutions

Components. To allow investigation of the solutions in steps, the components utilized as input to the MINTEQA2 model were broken into a group called the "Major Components" **(Table 3-1)** and another called the "Minor Components" **(Table 3-2)** as follows:

Table 3-1. Major components in model solutions.

CATIONS	ANIONS
H+	OH-
Na+	CO3-2
K+	Cl-
Ca+2	S04-2
Mg+2	

Table 3-2. Minor components added to major in model soluti

CATIONS	ANIONS
Fe+3	F-
Al+3	PO4-3
Sr+2	Br-
Ba+2	
Mn+2	
Pb+2	
NH4+	
Ra+2	
UO2+2 (or U+4, only at low pH)	

Notes to Tables:

1. *Water is implicit and hydrolysis products are allowed.*
2. *Dissolved silica (H_4SiO_4) is uncharged but a major contributor to TDS in these solutions, 53 mg/L in the uncontaminated solution and 1187 mg/L in the contaminated.*

Concentrations. As discussed, MW-1 was chosen as the model for the uncontaminated solutions and PP1-3 was chosen as the model for the contaminated solutions. The following total concentrations **(Table 3-3)** were used as input to MINTEQA2 (detection limits were used when no value was reported):

Table 3-3. Input components and total concentrations.

		Concentration (PPM)	
ID #	Name	Uncontaminated	Contaminated
500	Na+1	9.400E+01	1.529E+03
410	K+1	5.000E+00	2.460E+02
150	Ca+2	8.100E+01	6.570E+02
460	Mg+2	4.000E+01	2.290E+02
140	CO3-2	4.850E+02	6.000E-01
180	Cl-1	8.800E+01	1.680E+02
732	SO4-2	5.500E+01	5.091E+03
281	Fe+3	1.100E+00	2.000E+00
30	Al+3	5.000E-01	5.800E+00
800	Sr+2	5.200E-01	1.210E+01
100	Ba+2	2000E-02	2.000E-02
470	Mn+2	3.000E-02	5.000E+00
490	NH4+1	5.300E-01	1.053E+03
270	F-1	5.000E-01	1.120E+03
580	PO4-3	6.000E-01	8.720E+03
600	Pb+2	5.000E-02	5.000E-02
893	UO2+2	5.000E-01	5.000E-01
650	Ra+2	1.000E-06	1.000E-06
130	Br-1	5.000E-01	3.100E+00
770	H4SiO4	5.300E+01	
	1.187E+03		

Speciation of Selected Components. Summary tables listing the major species for each of the major components for each run are in **Appendix 3-1.** Printouts of the computer MINTEQA2 runs for each case are long (5-15 pages) and detailed, so are not included. However, they are on file with the author. Several general caveats need to be remembered when considering this type of information. The results are *estimations* (subject to the components and data entered and all of the assumptions and limitations of the MINTEQA2 model and the thermodynamic database utilized), and the predictions are for *equilibrium.* The results obtained are still very useful for identifying the probable speciation, but there is no guarantee all of the species are included or the quantitative results are exact. A summary is given below of some of the most important observations.

Calcium

Calcium is an important component since it is a major cation in the solutions, participates in many complexation and precipitation reactions, and may offer clues to the speciation of other important components, such as radium. **Table 3-4** summarizes the predicted speciation of calcium.

Table 3-4. Calcium distribution in solutions expressed as (%) major and minor components included in the solutions.

SPECIES	UNCONTAMINATED		CONTAMINATED	
Ca+2	93.2	(93.2)	48.1	(60.3)
CaSO4 AQ	3.3	(3.3)	28.5	(39.7)
CaHC03+	3.5	(3.5)	<1	(<1)
CaH2PO4+	<1	(<1)	23.2	(<1)

Notes:

1. *Values in parentheses represent solutions containing only major components.*
2. *Removing silica as a component made insignificant changes in the above results (< 0.5 %).*

Calcium results are consistent with the known characteristics of calcium. The pH of the uncontaminated solution is low enough (6.73) to keep most of the calcium as free ion, rather than hydroxide complexes, and as bicarbonate rather than carbonate complexes. Complexes formed are with the major anions, bicarbonate and sulfate. In the contaminated solution ligand concentrations are much higher, especially for sulfate and phosphate, so their complexes become more significant. Since all the interactions in Table 3-4 involve major components, removing the minor components from the solution did not affect the speciation (values in parentheses) for the uncontaminated solutions. Magnesium results, as expected, were similar to the calcium results above. The sulfate complex, being uncharged could contribute significantly to the mobility of the calcium, and other metals that experience similar complexation, such as barium and radium.

Sulfate and Phosphate

Since sulfate turned out to be one of the most important ligands in the system, it is useful to look in detail at the sulfate speciation, as shown in **Table 3-5.** Phosphate showed similar distributions, approximately 50% complexing with calcium and magnesium in the contaminated solution.

Table 3-5: Sulfate distribution in solution expressed as (%) major and minor components included in the solutions.

SPECIES	UNCONTAMINATED		CONTAMINATED	
SO4-2	79.2	(79.2)	65.0	(65.8)
NaSO4-	1.2	(<1)	6.2	(7.1)
CaSO4 AQ	11.5	(11.5)	<1	(6.4)
HSO4 -	<1	(<1)	10.5	(11.8)
MgSO4 AQ	8.2	(8.2)	4.3	(7.9)
NH4S04-	<1	(<1)	13.0	(<1)

Notes:

1. *Values in parentheses represent solutions containing only major components.*
2. *Removing silica as a component made insignificant changes in the above results (< 0.5 %).*

Sulfate remains primarily as the free sulfate ion, as shown in Table 3-5. However, significant fractions complex with calcium and magnesium (as also seen in Table 3-4), and in the contaminated sample also with sodium and ammonia. In addition, in the contaminated sample the pH is sufficiently low (2.44) to keep bisulfate a major component (pK_2 for sulfuric acid is 2.0), which is significant in calculations of total negative charge when doing a charge balance for these solutions. When only major components are considered, the ammonium ion complex drops out since ammonium ion would not be included as a cation.

Silica

Dissolved silica is a major component of the TDS of these samples (53 mg/L in the uncontaminated and 1187 in the contaminated sample, as H_4SiO_4), even though its presence as the uncharged species means it does not contribute to the ionic strength. However, there is an interesting aspect to the silicon speciation. It remains essentially all H_4SiO_4 except in the contaminated sample with the minor components included, when 97.6% is predicted to be SiF_6, and only 2.4% H_4SiO_4 . Obviously, one factor to consider in relation to the effect of the stack solutions is solubilization of silicon containing minerals by fluoride ion (the low pH is also important here). When these silicon fluoride complexes are transported to groundwater and the concentrations diluted, silicon would probably be supersaturated relative to one or a number of solid phases and precipitation reactions could ensue. Indeed, observations of precipitates formed in and below the stacks (see Chapter 2) are probably related to this mechanism.

Lead

Lead results are presented below as an example of the expected equilibrium speciation of a transition metal. Lead results are also of interest relative to the radionuclide ^{210}Pb. The major species predicted for lead are presented in **Table 3-6.**

Table 3-6: Pb distribution in solution expressed as (%) major and minor components included in the solutions.

SPECIES	UNCONTAMINATED	CONTAMINATED
Pb+2	5.6	33.2
PbCl-	<1	1.9
PbS04 AQ	<1	54.3
Pb(SO4)2-2	<1	10.5
PbC03 AQ	77.7	<1
PbHCO3+	14.9	<1

Note: Removing silica as component made insignificant changes in the above results (< 0.5 %).

Table 3-6 confirms what would be expected, speciation of transition metals in aqueous solutions is often more complicated than for alkaline or alkaline earth metals. First, a greater diversity of complexes formed for lead. Second, the complex formation is very pH dependent. Neither solution had a sufficiently high pH to produce the significant amounts of hydroxide complexes that occur in alkaline solutions. Also note that, despite the much higher ligand concentrations in the contaminated solution, there is a greater fraction of free lead ion than in the uncontaminated solution, a result of the much lower pH (2.44 vs. 6.73). The strength of the carbonate complex of lead is evident since even though bicarbonate would dominate over carbonate at pH 6.73 in the uncontaminated solution, there is a larger fraction of the carbonate complex. Chloride is a strong ligand with lead, so a chloride complex shows up in the major species in the contaminated solution. However, due to the relatively high sulfate concentrations, two sulfate complexes dominate the predicted complexation. Note that fully half of the lead is predicted to be in the uncharged sulfate complex, which could contribute significantly to its mobility (since it would be less prone to adsorb to charged aquifer solids). Other transition metals (radioactive and non-radioactive) would be expected to exhibit similar characteristics.

Uranium

Results for uranium added as uranyl ion (UO_2^{+2}, the expected stable form in oxygenated solutions) are presented in **Table 3-7.**

Table 3-7: U distribution in solution (%) (added as UO_2^{+2}) major and minor components included in solution.

SPECIES	UNCONTAMINATED	CONTAMINATED
UO2+2	<1	<1 (<1)
U02CO3 AQ	4.7	<1 (<1)
UO2(CO3)2-2	78.4	<1 (<1)
UO2(C03)3-4	16.5	<1 (<1)
UO2F2 AQ	<1	<1 (4.1)
U02F3-	<1	<1 (3.1)
U02H2P04+1	<1	2.4 (2.2)
U02H2(PO4)2-2	<1	93.0 (85.9)
UO2H2PH3P+1	<1	3.6 (<1)

Note: Removing silica as a component DID make signifcant changes in the above results for the contaminated sample only, as shown by the values in parentheses.

In the acidic environment of the contaminated solution (pH 2.44), U^{+4} may be stable, so MINTEQ runs were also made using U^{+4} as the input component **(Table 3-8).** Since redox reactions were not allowed, conversion between these different redox states of uranium was not allowed (the thermodynamic database is not yet reliable for such calculations).

Table 3-8: U distribution in solution expressed as (%) (added as U^{+4}) major and minor components included in the solutions.

SPECIES	UNCONTAMINATED	CONTAMINATED
UF3+	NOT	26.7 (4.8)
UF4 AQ	APPLICABLE	71.5 (76.7)
UF5-		1.6 (10.1)
UF6-2		<1 (8.5)

Note: Removing silica as a component DID make significant changes in the above results, as shown by the results in parentheses.

Obviously, uranium exhibits a complicated speciation behavior (made even more complicated when redox state transitions are considered). UO_2^{+2} speciation is dominated by a doubly charged phosphate anion. Such an anion would not be expected to adsorb to the normally negatively charged soil particles. However, specific (chemical) adsorption might still occur, and it is probable that positively charged soil particles would exist that

could attract the complex at the pH of the PG stack solutions (approximately 2.5). The U^{+4} speciation, on the other hand, is dominated by the fluoride complexes. In particular, the uncharged complex dominates, which could result in significant uranium mobility. Furthermore, for both forms of added uranium, including or not including dissolved silica did significantly affect the resultant speciation. In combination with information on predicted oversaturated solid phases (see below), a complicated set of interactions between Si, F and U emerges. Consequently, fundamental understanding of the speciation and fate of uranium in the PG stack system is multifaceted.

Radium

The MINTEQA2 outputs for radium indicated 100% would remain as the free ion, Ra^{+2}. One factor that tends to keep the radium in the free ion form is its low concentration compared to the major cations, which effectively out compete the radium for ligands. However, it should be noted the available thermodynamic database for radium complexes is not extensive. If any complexes were significant, it would probably be the sulfate complexes in the contaminated sample solution (although the monosulfate radium complex was included in the database, it did not account for > l% of the radium.). As discussed for calcium, above, the sulfate complexes could increase the mobility of the radium in the aquifer when present in the PG stack plume.

Other Factors Concerning Speciation. Other factors must also be considered in relation to geochemical modeling of the dissolved components of the groundwater and PG stack solutions. First, the contaminated field samples showed increased concentrations of organic carbon compared to the background samples, increasing to approximately 80 ppm TOC from approximately 9 ppm TOC. The nature of this organic carbon should be investigated. Should it be a strong ligand for any of the metals of interest, or should coat and thereby modify the surfaces of the aquifer solids, it may be a factor in metal and radionuclide mobility. Other processes that must be considered relative to mobility are adsorption, especially for transition metals, and coprecipitation, for example Ra may possibly coprecipitate with gypsum or barite.

Prediction of Precipitation of Solids from Groundwater Solutions

MINTEQA2 was utilized to predict oversaturated solids that would be predicted to precipitate. In fact, the gypsum stack solutions do appear to be oversaturated relative to a number of components, so observations of precipitates forming in the stacks, below the stacks, and in process solutions are no surprise. Even considering just the major components, the uncontaminated sample was predicted to be oversaturated with respect to quartz, and the contaminated sample oversaturated with respect to quartz and gypsum (precipitating up 57% of the calcium, 99.2% of the silicon, and 18% of the sulfate).

Adding the minor components results in a variety of predicted oversaturated solids. **Table 3-9** presents data on the solids predicted to precipitate in the uncontaminated and contaminated solutions.

Table 3-9. Predicted equilibrium solids precipitation including both major and minor components.

UNCONTAMINATED GROUNDWATER MODEL

HEMATITE (Fe203) (only when Si was not added)
UP207:20H20 (when UO_2^{+2} was added)
DIASPORE (AlHO2)
FCO3APATITE ([Ca]9.5[Na].36[Mg].14[PO4]4.8[CO3]1.2[F]2.5)
QUARTZ (SiO_2)
LEONHARDITE (Ca,Si,Al,H &O) or KAOLINITE (mostly Si,O and Al)

Percentages of Components in Precipitates:

U	85	
Ca		0.4
F	6.1	
Al		100
P	99	
Si		82

CONTAMINATED GROUNDWATER MODEL

FLUORITE (CaF2)
UP207:20H20 (when UO_2^{+2} was added)
MnHPO4
BARITE (BaSO4)
QUARTZ (SiO_2)
STRENGITE ($FePO_4.2H_2O$)

Percentages of Components in Precipitates:

U	100	
Ca		98
F	55	
P	99	
Si		70
Fe		88
Mn		99
Ba		77

Obviously, the oversaturated state of the uncontaminated solution and, especially, the contaminated solution, leads to a potentially complicated system relative to precipitation. The situation is further complicated by the fact that precipitation kinetics are notoriously slow and difficult to predict. Consequently, the equilibrium predictions of the model are limited not only by the solids contained in the database, but also by the fact that equilibrium relative to all solids is unlikely. Complexation reactions controlling the solution speciation that were discussed above are generally fast compared to the time scales of interest in and around gypsum stacks. However, that may not be true for precipitation reactions. Kinetic hindrances, for example, may lead to the formation of metastable solids, or solids which will later dissolve in favor of more stable ones. Hence

the reason for doing runs without Si added. If the Si precipitation is slow compared to another solid (e.g., hematite in Table 3-9), the faster precipitating solid may form and be metastable over long periods of time.

What can be said is that geochemical modeling indicates solids are likely to form in the gypsum stacks and in the groundwater receiving the stack solutions. It can also be concluded that the presence of the stack solutions will probably influence the actual solids formed (and probably their rate). Oversaturation relative to calcium, iron, manganese, silicon, uranium, sulfate, phosphate and fluoride are particularly noteworthy. Solids containing these materials are to be expected in the stack solutions and groundwater receiving such contamination.

SUMMARY

Field samples indicated dramatic alterations of the chemistry of groundwaters receiving gypsum stack solutions, making it easy to track the inputs. The major changes can be characterized as a shift in pH (from approximately 6.5 to 2.5), an increase in dissolved ions, especially sulfate and phosphate, but also including other ions such as chloride, fluoride, metals and radionuclides, and an increase in dissolved silica. The increased concentrations of many ligands results in significant changes in predicted equilibrium speciation. Most pronounced are increases in metal and radionuclide complexes with sulfate and phosphate, resulting in uncharged or negatively charged solution species which would likely be more mobile in the aquifer than positively charged metal or radionuclide ions. Fluoride from the stack solutions can significantly affect the speciation of aluminum silicon, iron and possibly uranium. The second major effect of stack solution inputs is to cause oversaturation of a variety of solids. The low pH of the contaminated solutions would generally indicate few solids would precipitate in most fresh waters. However, the dissolved solids content and some specific ion concentrations are sufficiently high to cause oversaturation. Although the model results should not be considered comprehensive in consideration of various potential solid phases that could form, the general trend of predicted precipitation reactions does indicate precipitation reactions are likely for certain components. Silicon containing solids are particularly likely since it is oversaturated in the uncontaminated solutions and much more so in the contaminated solutions. Precipitation of quartz was predicted in both contaminated and uncontaminated solutions, as well as other solids with silicon in the contaminated solutions. Other predicted solids formed included the components iron, aluminum, phosphate, calcium, manganese, barium, fluorine and uranium. Precipitation of various and probably multicomponent solids should be expected in and directly below the phosphogypsum stacks.

BIBLIOGRAPHY

Amoozegar A, and Warrick AW 1986. Hydraulic conductivity of saturated soils: field methods. Methods of Soil Analysis: Part 1 - Physical and Mineralogical Methods, Agronomy Monograph No. 9: 735-770.

Anderson MP, and Woessner, WW. 1992. Applied groundwater modeling: simulation of flow and advective transport. San Diego, California: Academic Press Inc., 381 p.

Ballestra SD, Lopez VJJ, Noshkin V. 1989. Intercomparison of radionuclide measurements in marine sediment sample IAEA-306. International Laboratory of Marine Radioactivity Report No. IAEA/AL/013, Monaco.

Bear J. 1979. Hydraulics of Groundwater, McGraw-Hill Inc., New York.

Berish, CW. 1990. Potential environmental hazards of phosphogypsum storage in central Florida. In: Proceedings of the Third International Symposium on Phosphogypsum, Bartow, Florida (ed. W. F. Chang), Florida Institute of Phosphate Research, 1-29.

Boast CW, Kirkham D. 1971. Auger hole Seepage theory. Soil Science Society of America Proceedings 35: 365-373.

Bouwer H, Rice RC, 1976. A slug test for determining hydraulic conductivity of unconfined aquifers with completely or partially penetrating wells. Water Resources Research 12: 423-428.

Burnett WC. 1988. Release of radium and other decay-series isotopes from Florida phosphate rock. Florida Institute of Phosphate Research Report No. 05-016-059, 164 p.

Burnett WC, Hull C, Young J, Cable P. 1993. A simple self-absorption correction for gamma-ray counting of soils and sediments (abs.). Proceedings: 39*th* Annual Conference on Bioassay, Analytical, and Environmental Radiochemistry, Colorado Springs, Colorado, Oct. 11-15, 1993.

Burnett WC, LaRock PA, Cowart JB, Hull CD, 1995. Microbiology and Radiochemistry of Phosphogypsum. Florida Institute of Phosphate Research Report No. 05-035-115.

Carter OC, Scheiner BJ. 1992. Investigation of metal and nonmetal migration through phosphogypsum. In: AIME Proc. on the Sym. on Emerging Process Technologies for a Cleaner Environment, Feb 24-27, 1992 Phoenix, AZ, (eds. PE Richardson and H El-Shall), 205-210.

Carter OC, Smith CW, Scheiner BJ. 1993a. Investigation of metal and nonmetal ion migration through an inactive phosphogypsum stack. In: The challenge of integrating diverse perpective in reclamation, Proc. of the 10*th* annual meeting of the American Soc. for Surface Mining and Reclam. (ed. BA Zamora and RE Connolly), Spokane, Wash., 175-184.

Carter OC, Smith CW, Scheiner BJ. 1993b. Environmental evaluation of soil and leaching characteristics of a Florida inactive phosphogypsum stack. In: Proc. of the Hazardous Materials Control Resources Institite Superfund XIV Conf., Wash. D.C., Nov 30 - Dec 2, 1993, l-6.

Chiang WH, Kinzelbach W. 1994. Processing Modflow for Windows: a simulation system for modeling groundwater flow and pollution. Instructional manual, 196 p.

Driscoll FG. 1986. Groundwater and Wells. Johnson Division, St. Paul, MN.

Gerathy and Miller, Inc. 1983. Groundwater monitoring plan, Amax chemical corporation, piney point plant. Final Report, prepared for Amax chemical corporation (Ground Water Consultants, Tampa, Florida), 82 p.

Gerathy & Miller, Inc. 1986. Revised groundwater monitoring plan at the AMAX Phosphate Inc. Complex, Technical Report, Gerathy & Miller Inc., Tampa, FL.

Harada K, Burnett WC, Cowart JB, LaRock PA. 1989. Polonium in Florida groundwater and its possible relationship to the sulfur cycle and bacteria. Geochim. Cosmochim. Acta 53: 143-150.

Johnston RH, Healy HG, Hayes LR. 1981. Potentiometric surfaces of the Tertiary limestone aquifer system, southeastern United States: May, 1980. U.S. Geological Survey Open File Report 81-486.

Johnston RH, Krause RE, Meyer RW, Ryder PD, Tibbals CH, Hunn JD. 1981. Estimated potentiometric surface for the tertiary limestone aquifer system, southeastern United States, prior to development. U.S. Geological Survey Open File Report 80-406.

Kennedy GA, Soroczak MM, Meischen SJ, Clayton JD, Driver JL. 1991. Chemistry of Gypsum Pond Systems. Florida Institute of Phosphate Research Project 05-025-l00, Final Report, 85 p.

Key RM, Brewer RL, Stockwell JH, Guinasso NL, Schink, DR. 1979. Some improved techniques for measuring radon and radium in marine sediments and in seawater. Marine Chemistry 7: 251-264.

Lardinoye MH, Weterings K, van der berg WB. 1982. Unexpected Ra-226 buildup in wet phosphoric acid plants. Health Phys. 42: 503-514.

Lindeken CL, Coles DG. 1978. The radium-226 content of agricultural gypsums. In: Radioactivity in Consumer Products (eds. A Moghissi, P Paras, M Carter, and R Barker), U.S. Regulatory Commission Report No. NUREG/CP-0001, 369-375.

Lewelling BR, Wylie RW. 1993. Hydrology and water quality of unmined and reclaimed basins in phosphate mining areas, west-central Florida. U.S. Geological Survey, Water Resources Investigations Report 93-4002, 93 p.

May A, Sweeney JW. 1982. Assessment of environmental impacts associated with phosphogypsum in Florida. U.S. Bureau of Mines. Report No. 8639, 1-19.

May A, Sweeney JW. 1983. Evaluation of radium and toxic element leaching characteristics of Florida phosphogypsum stockpiles. U.S. Bureau of Mines. Report No. 8776, 1-19.

Mathieu GG, Biscaye PE, Lupton RA, Hammond DE. 1988. System for measurement of Rn-222 at low levels in natural waters. Health Physics 55: 989-992.

Mcdonald MC, Harbaugh AW. 1988. MODFLOW: a modular three-dimensional finite difference ground-water flow model. U.S. Geological Survey Open File Report 83-875, 528 pp.

Miller RL, Sutcliffe H. 1984. Effects of three phosphate industrial sites on ground-water quality in central Florida, 1979 to 1980. U.S. Geological Survey Water Resources Investigations Report 83-4256, 184 p.

Molz FJ, Boman GK, Young SC, Waltrop WR. 1994. Borehole flowmeters: field applications and data analysis. J. Hydrology 163: 347-371.

Nifong GD. 1988. Environmental aspects of phosphogypsum. Florida Institute of Phosphate Research, unpublished manuscript, 13 p.

Nifong GD. 1993. Environmental monitoring of Polk and Columbia counties experimental phosphogypsum roads. Florida Institute of Phosphate Research Publication No. 05-033-101, 120 p.

Oaks Geotechnical Inc. 1980. Geotechnical investigation of the gypsum stack complex of AMAX Phosphate Inc., Report, Oaks Geotechnical Inc.

Oural CR, Brooker HR. 1986. Source of gross-alpha radiochemistry anomalies in recharge wells, Central Florida Phosphate District. Florida Institute of Phosphate Research Final Report # 82-05-014.

Oural CR, Upchurch SB, Brooker HR. 1988a. Radon progeny as sources of gross-a radioactivity anomalies in ground water. Health Phys. 55: 889-894.

Oural CR, Upchurch SB, Brooker HR. 1988b. Sampling interaquifer connector wells for polonium-210: implications for gross-alpha analysis. In: Field Methods for Ground Water Contamination Studies and their Standardization, (eds. AG Collins and AI Johnson), American Society for Testing Materials; ASTM STP 963: 290-303.

PEI Associates, Inc. 1986. Evaluation of waste management for the Florida phosphate processing industry. Prepared for the Florida Institute of Phosphate Research.

Rutherford PM, Dudas MJ, Arocena JM. 1995. Radium in phosphogypsum leachates. Jour. Envir. Qual. 24: 307-314.

Scott, TM. 1988. The Lithostratigraphy of the Hawthorn Group (Miocene) of Florida. Dept. Natural Resources, Florida Geological Survet Bulletin No. 59: 148 p.

Upchurch SB, Rea RA, Stevenson RG. 1982. Sedimentary pachnolite and fluorite from Tampa Bay, Florida. Am. Mineralogist 67: 1258-1264.

Upchurch SB, Oural CR, Foss DW, Brooker HR. 1991. Radiochemistry of uranium-series isotopes in groundwater (Chemical fate of uranium-daughter radionuclides in recharge wells, central Florida Phosphate District). Florida Institute of Phosphate Research Pub. No. 05-022-092, 131 p.

Youngs EG. 1968. Shape factors for kirkham's piezometer method for determining the hydraulic conductivity of soil in situ for soils overlying an impermeable floor or infinitely permeable stratum. Soil Science: 106: 235-237.

APPENDICES

CHAPTER 1

Cooper Jacob Straight-line Analyses

Pressure Transducer Tests

· Hydraulic Head Contour Plots

Bouwer Rice Conductivity Tests

Appendix I: Cooper Jacob Straight-line Analyses

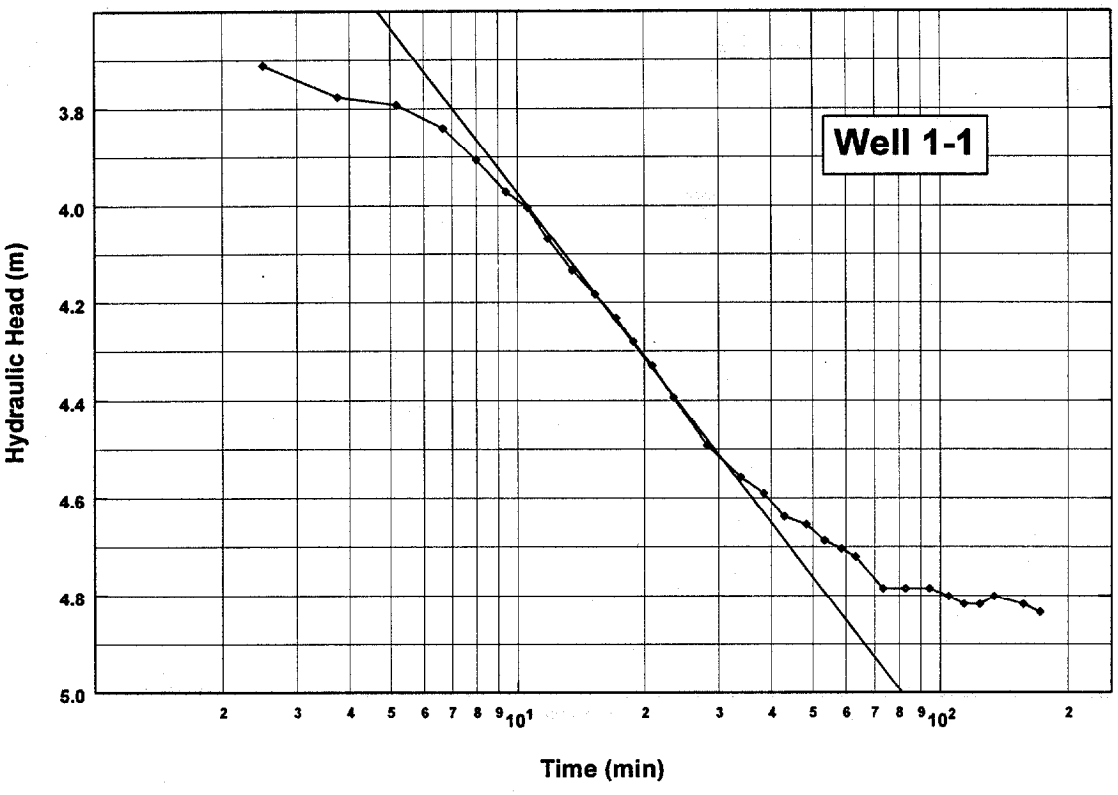

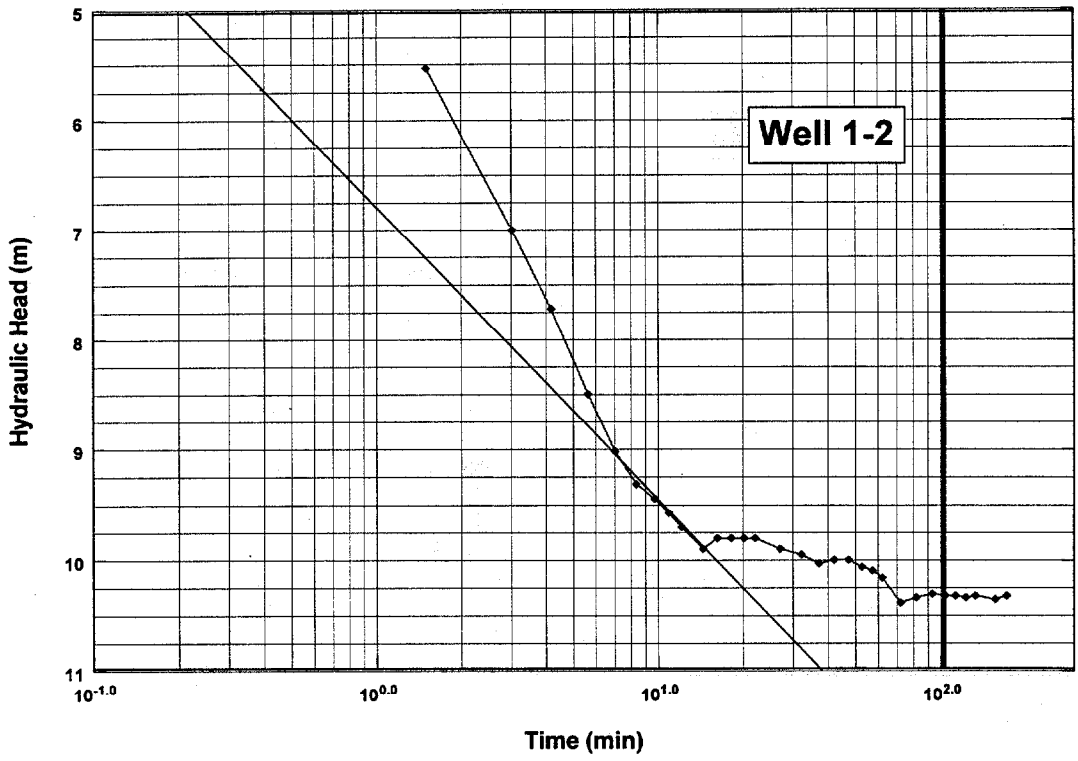
Well 1-2
Hydraulic Head (m)
5
6
7
8
9
10
11
$10^{-1.0}$
$10^{0.0}$
$10^{1.0}$
$10^{2.0}$
Time (min)

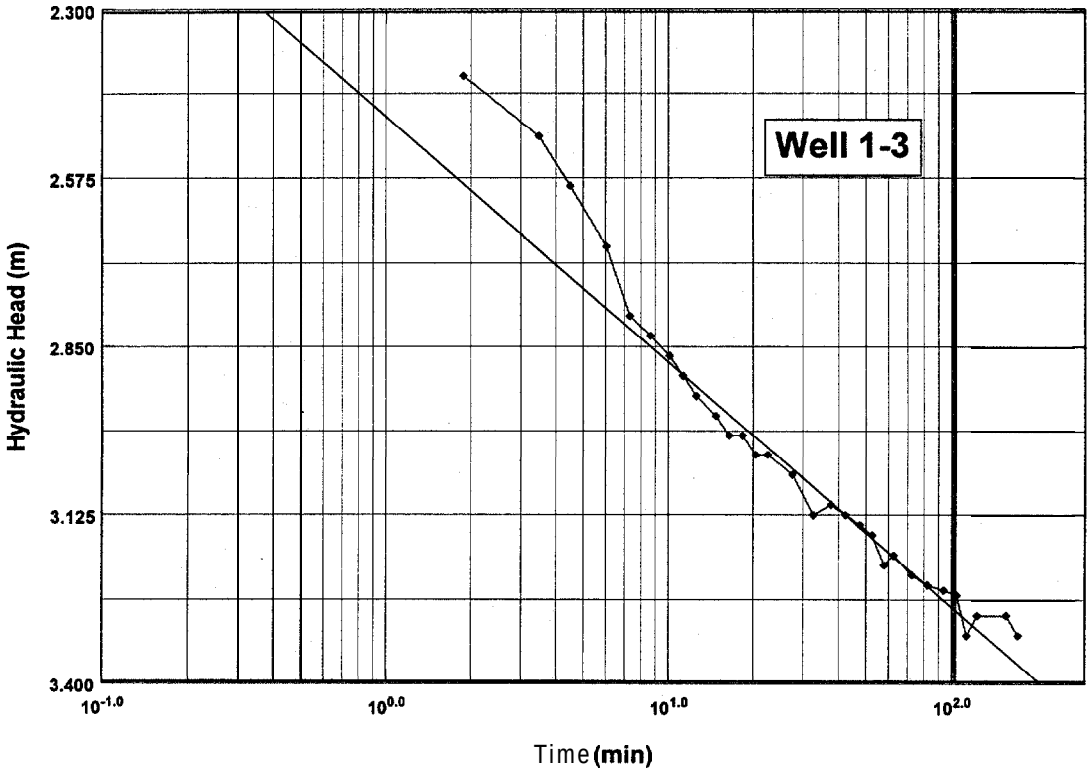
Well 1-3
Hydraulic Head (m)
2.300
2.575
2.850
3.125
3.400
$10^{-1.0}$
$10^{0.0}$
$10^{1.0}$
$10^{2.0}$
Time (min)

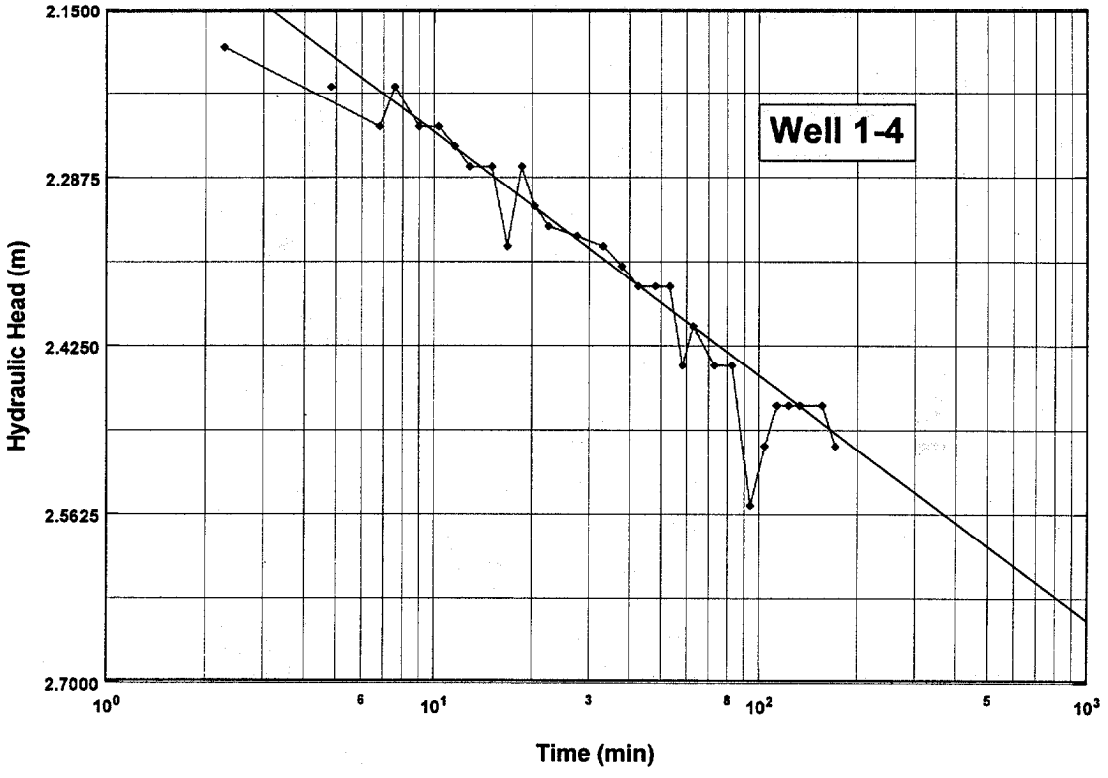
Well 1-4
Hydraulic Head (m)
2.1500
2.2875
2.4250
2.5625
2.7000
Time (min)
10^0
6
10^1
3
8
10^2
5
10^3

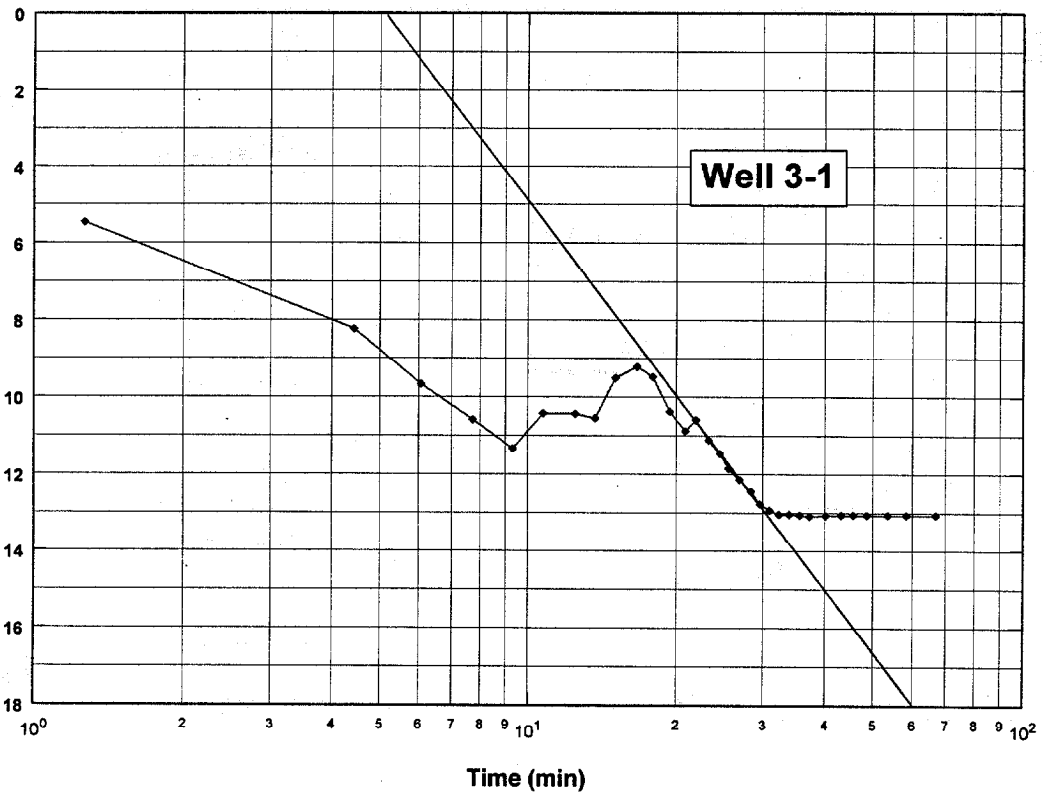
Well 3-1
0
2
4
6
8
10
12
14
16
18
10^0
2
3
4
5
6
7
8
9
10^1
2
3
4
5
6
7
8
9
10^2
Time (min)

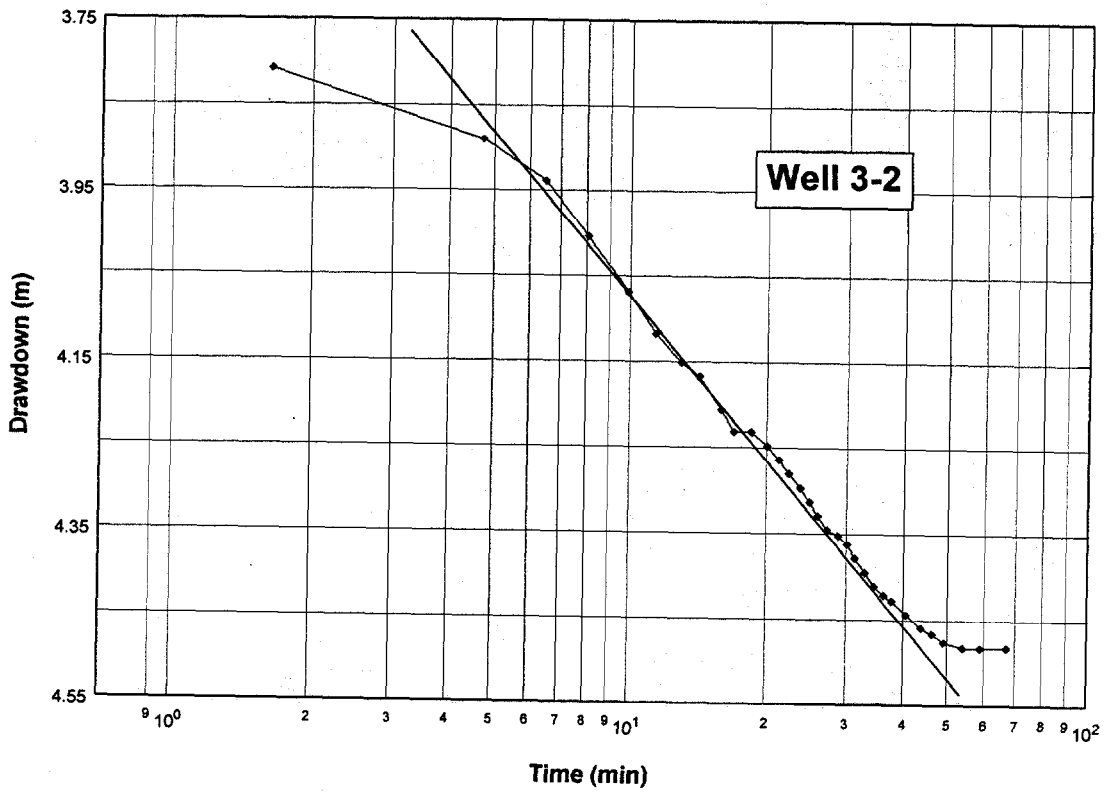
Well 3-2
Drawdown (m)
3.75
3.95
4.15
4.35
4.55
9 10^0 2 3 4 5 6 7 8 9 10^1 2 3 4 5 6 7 8 9 10^2
Time (min)

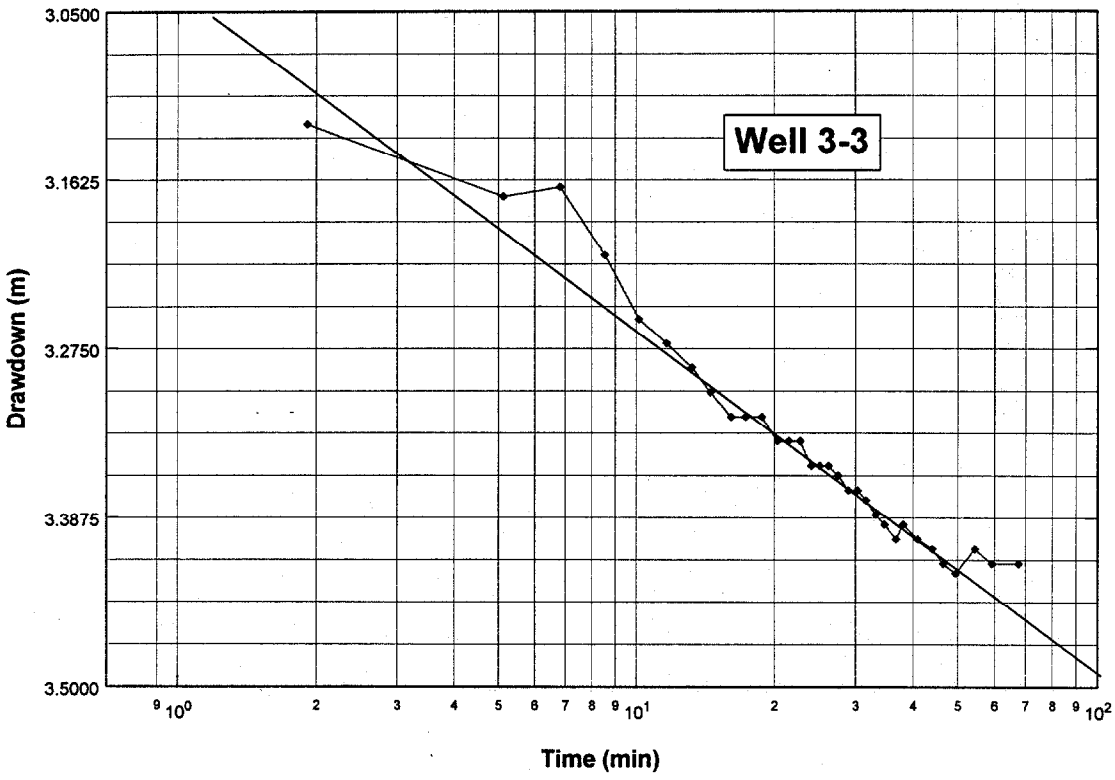
Well 3-3
3.0500
3.1625
3.2750
3.3875
3.5000
Drawdown (m)
9 10^0 2 3 4 5 6 7 8 9 10^1 2 3 4 5 6 7 8 9 10^2
Time (min)

Appendix II : Pressure Transducer Tests

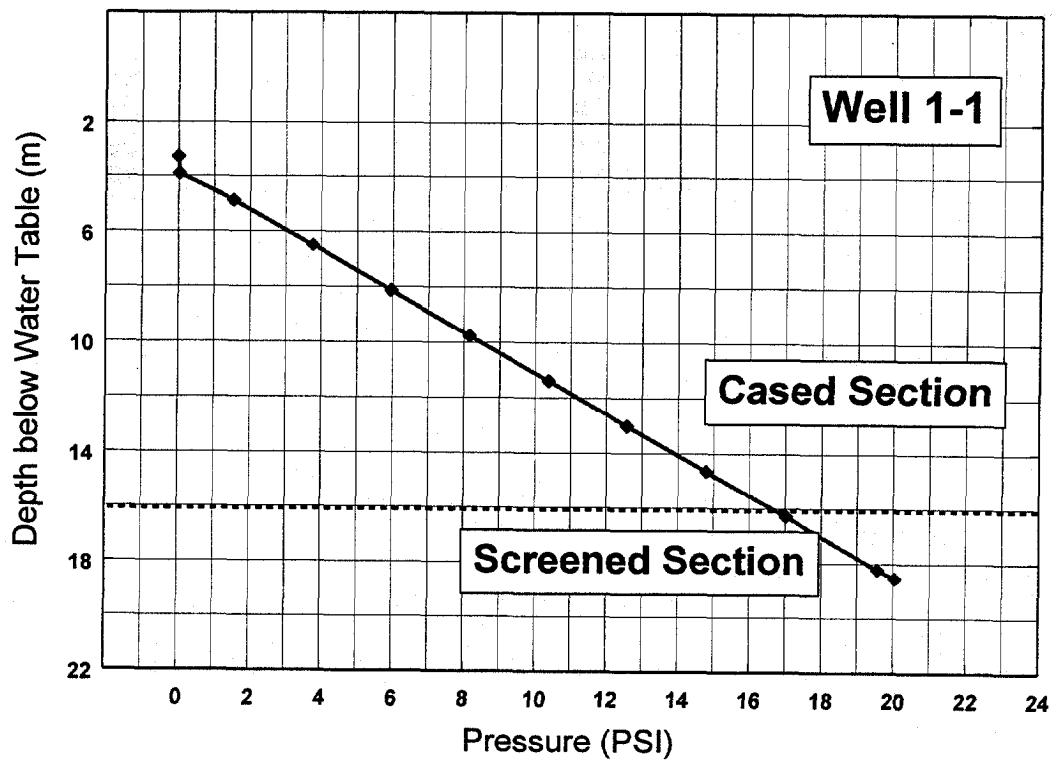

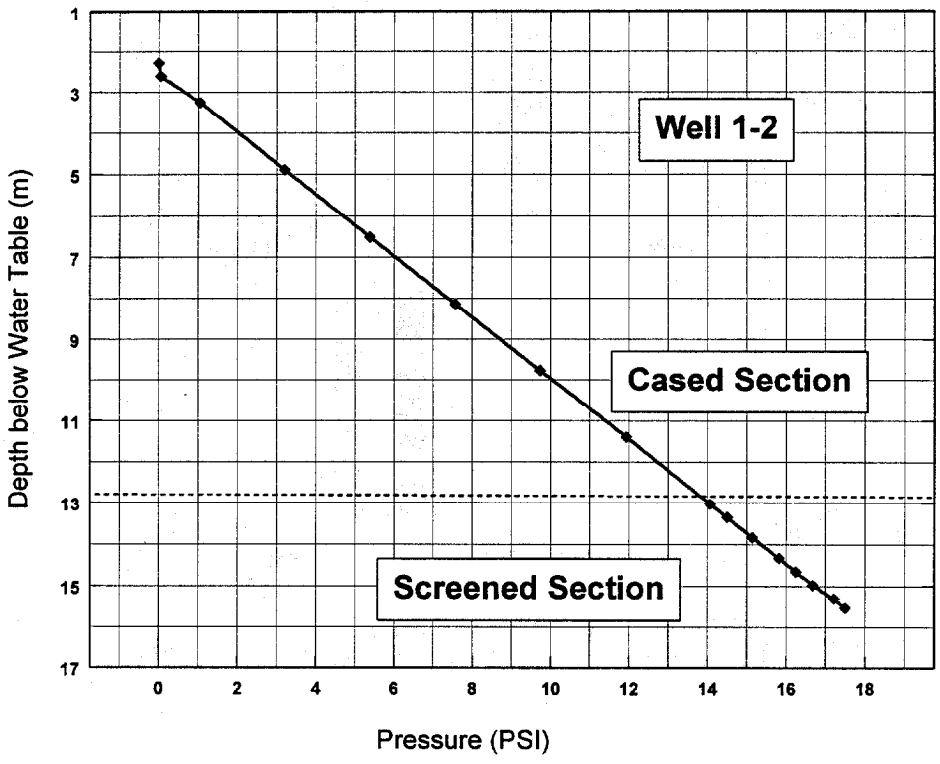
Depth below Water Table (m)
1
3
5
7
9
11
13
15
17
0
2
4
6
8
10
12
14
16
18
Pressure (PSI)
Well 1-2
Cased Section
Screened Section

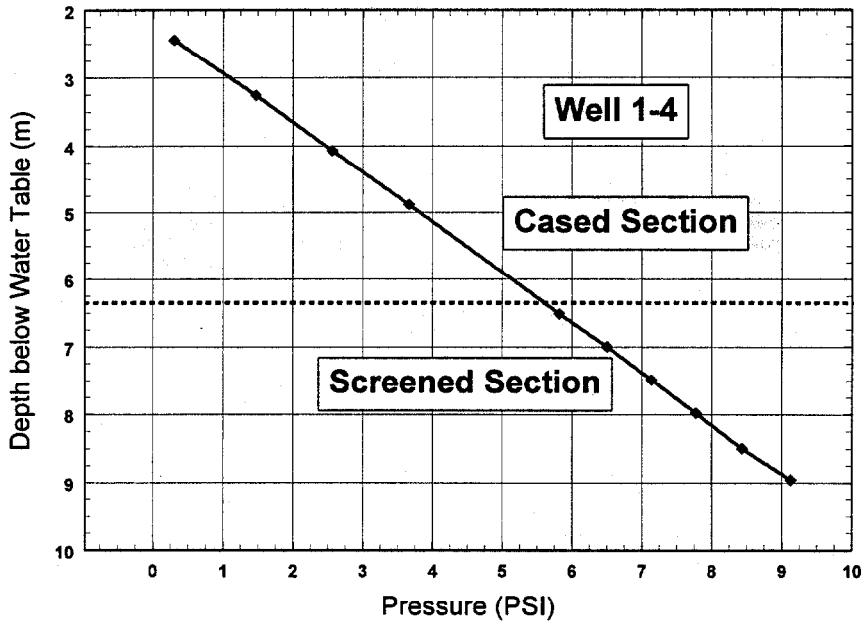
Depth below Water Table (m)
2
3
4
5
6
7
8
9
10
0
1
2
3
4
5
6
7
8
9
10
Pressure (PSI)
Well 1-4
Cased Section
Screened Section

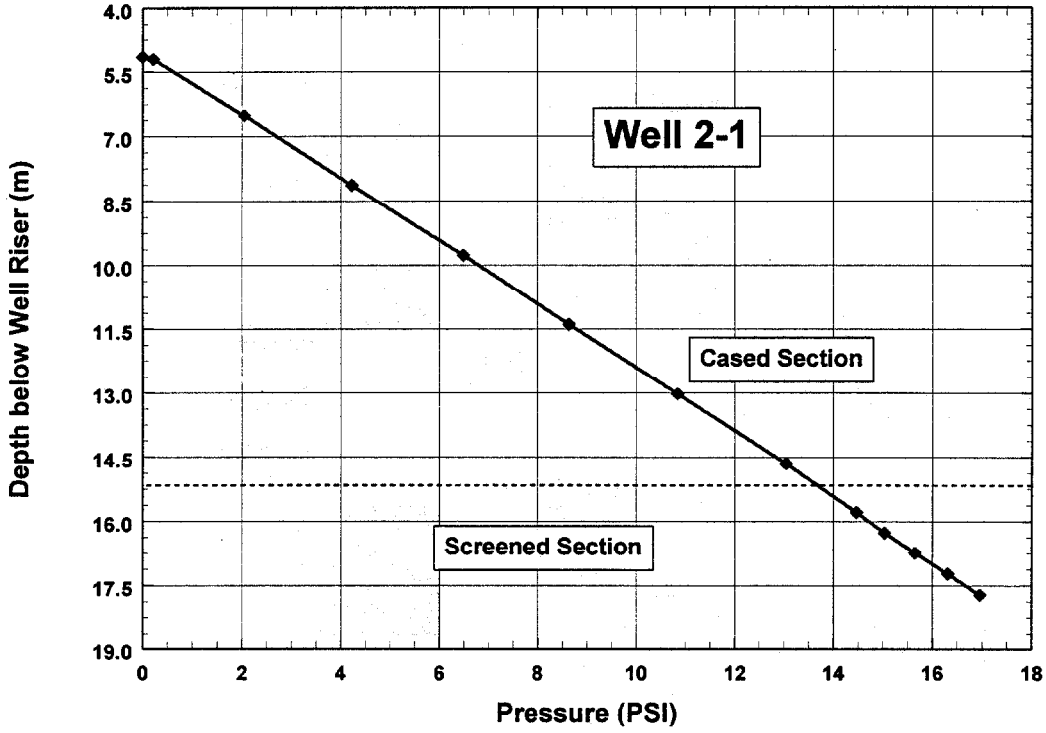
Well 2-1
Cased Section
Screened Section
Depth below Well Riser (m)
Pressure (PSI)
4.0
5.5
7.0
8.5
10.0
11.5
13.0
14.5
16.0
17.5
19.0
0
2
4
6
8
10
12
14
16
18

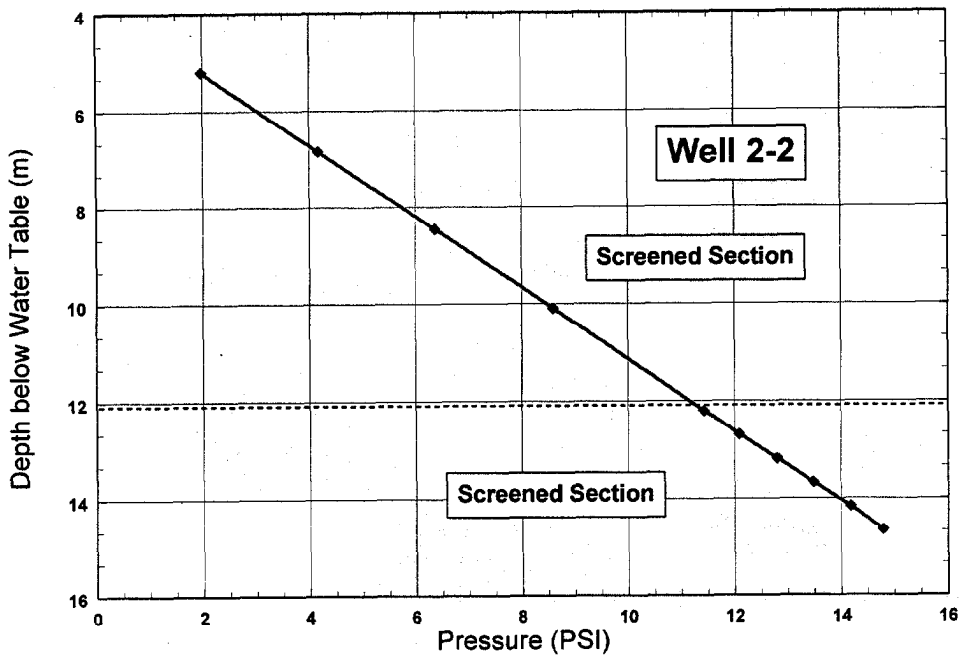
Well 2-2
Screened Section
Screened Section
Depth below Water Table (m)
Pressure (PSI)
4
6
8
10
12
14
16
0
2
4
6
8
10
12
14
16

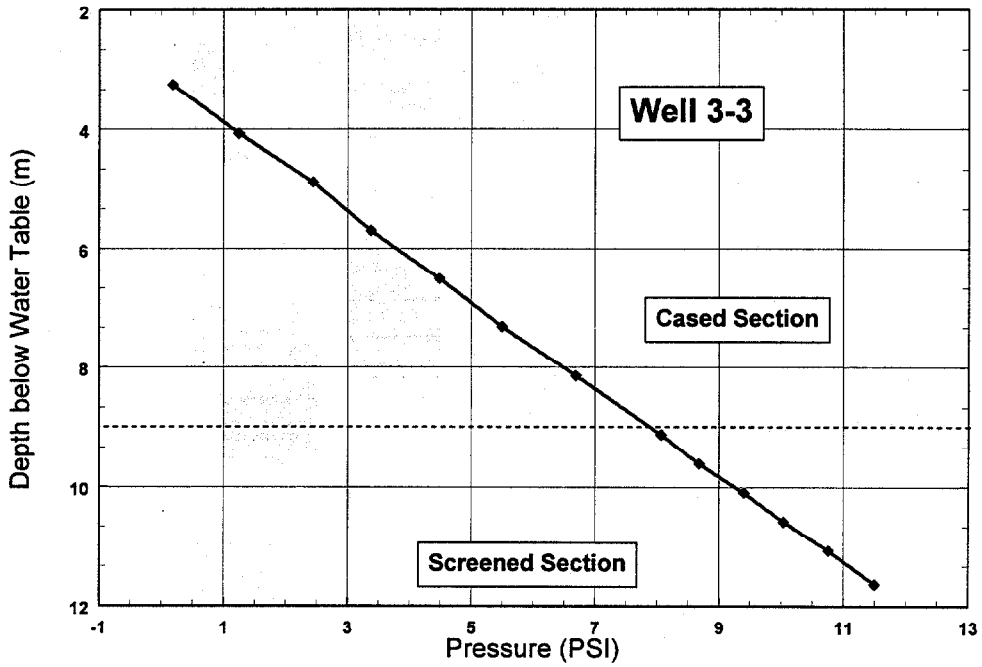
Well 3-3
Cased Section
Screened Section
Depth below Water Table (m)
Pressure (PSI)
2
4
6
8
10
12
-1
1
3
5
7
9
11
13

Appendix III : Hydraulic Head Contour Plots

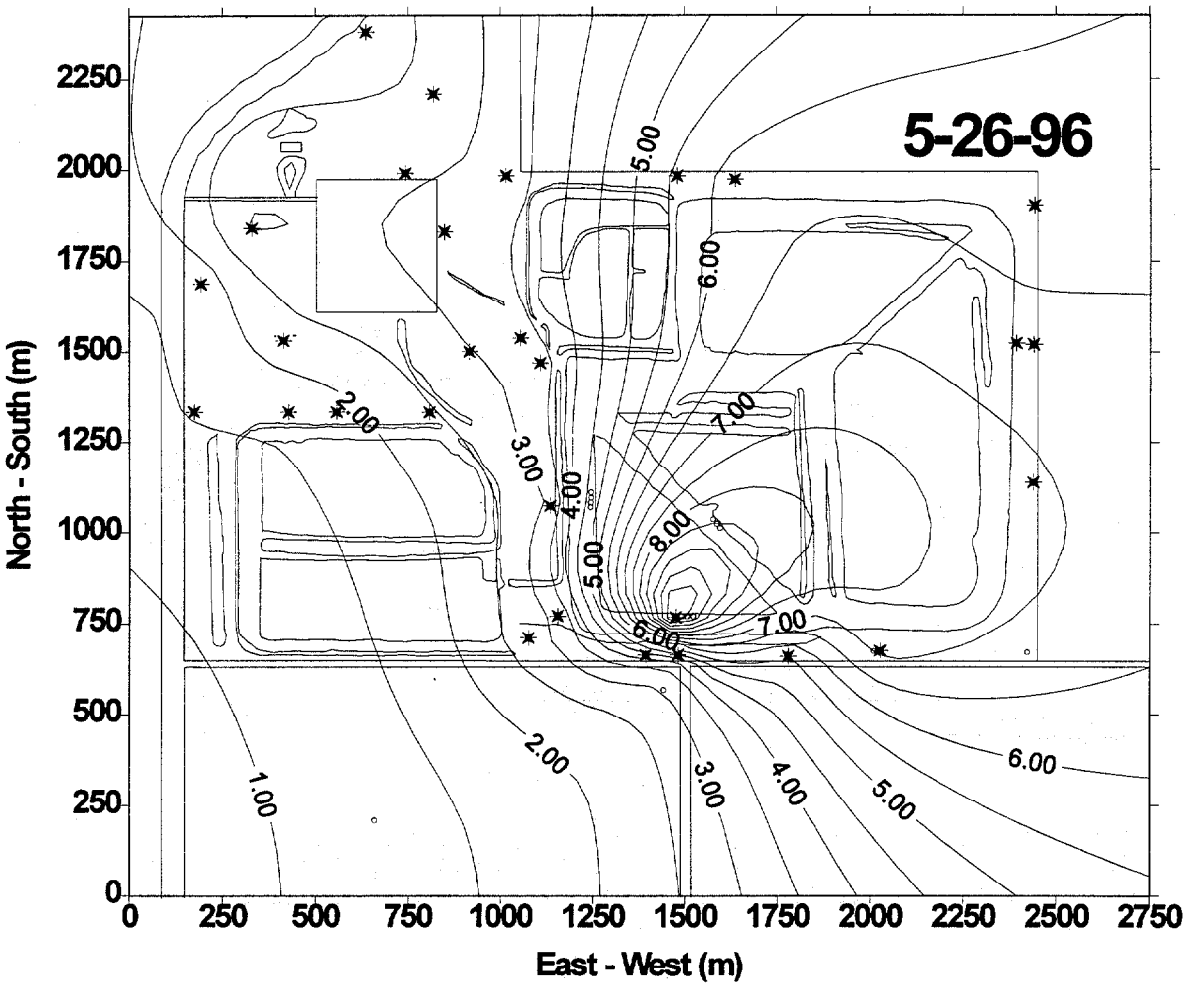

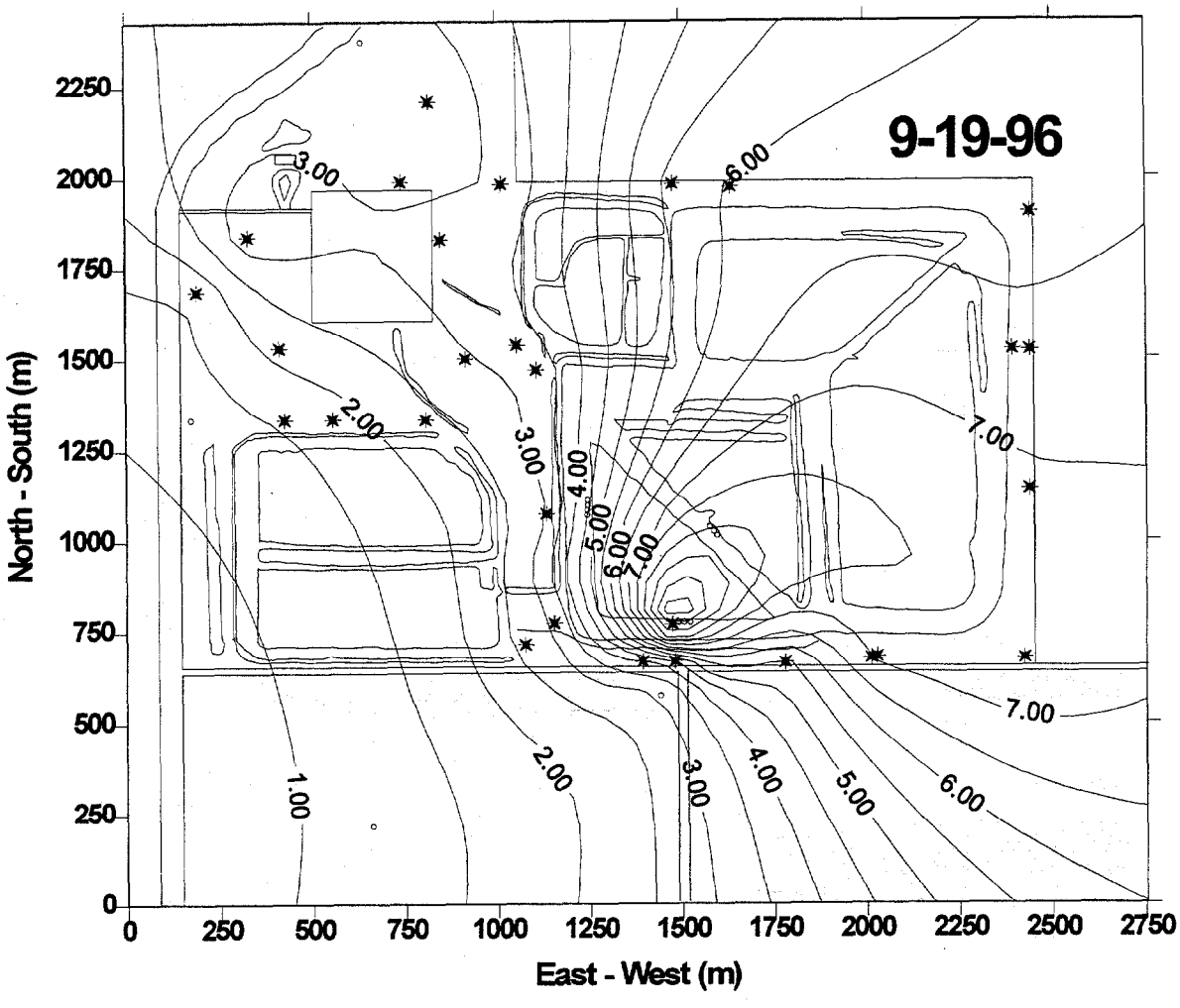
9-19-96
North - South (m)
East - West (m)
0
250
500
750
1000
1250
1500
1750
2000
2250
2500
2750
1.00
2.00
3.00
4.00
5.00
6.00
7.00

Appendix IV : Bouwer Rice Conductivity Tests

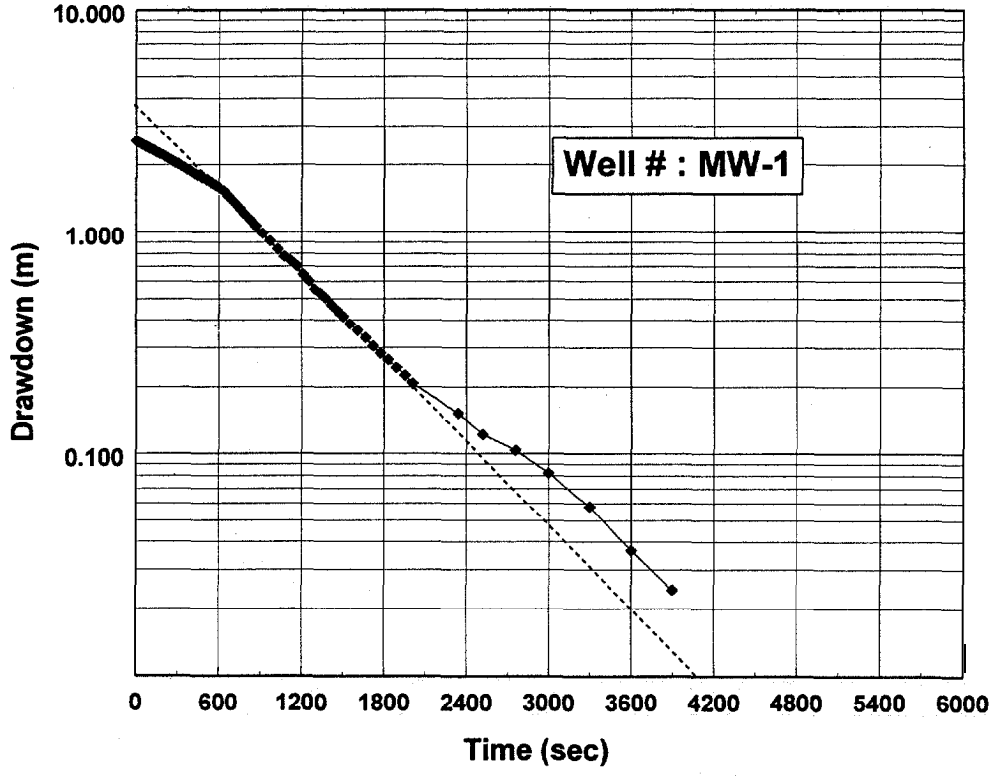

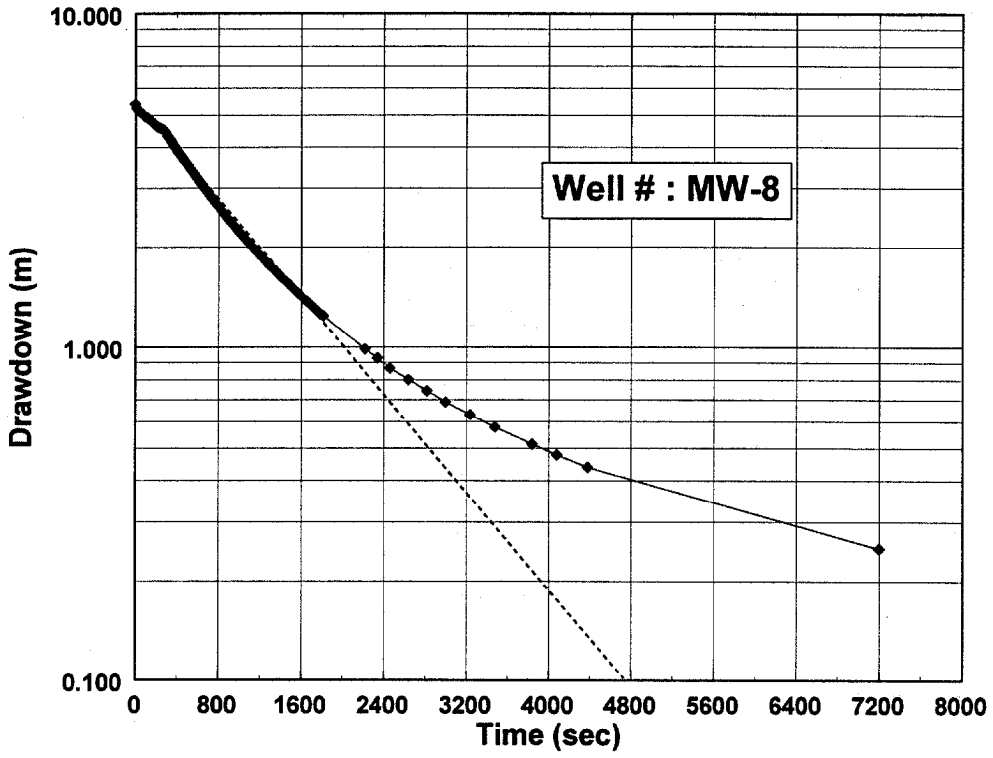
10.000
1.000
0.100
Drawdown (m)
Well # : MW-8
0
800
1600
2400
3200
4000
4800
5600
6400
7200
8000
Time (sec)

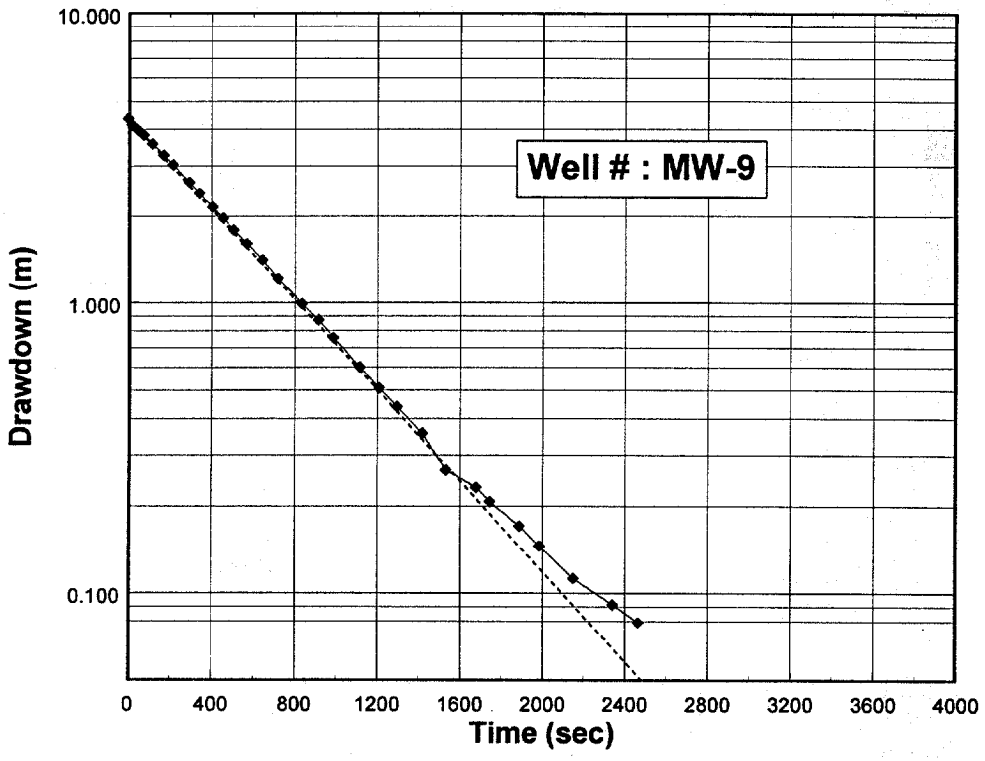
Well # : MW-9
10.000
1.000
0.100
Drawdown (m)
0
400
800
1200
1600
2000
2400
2800
3200
3600
4000
Time (sec)

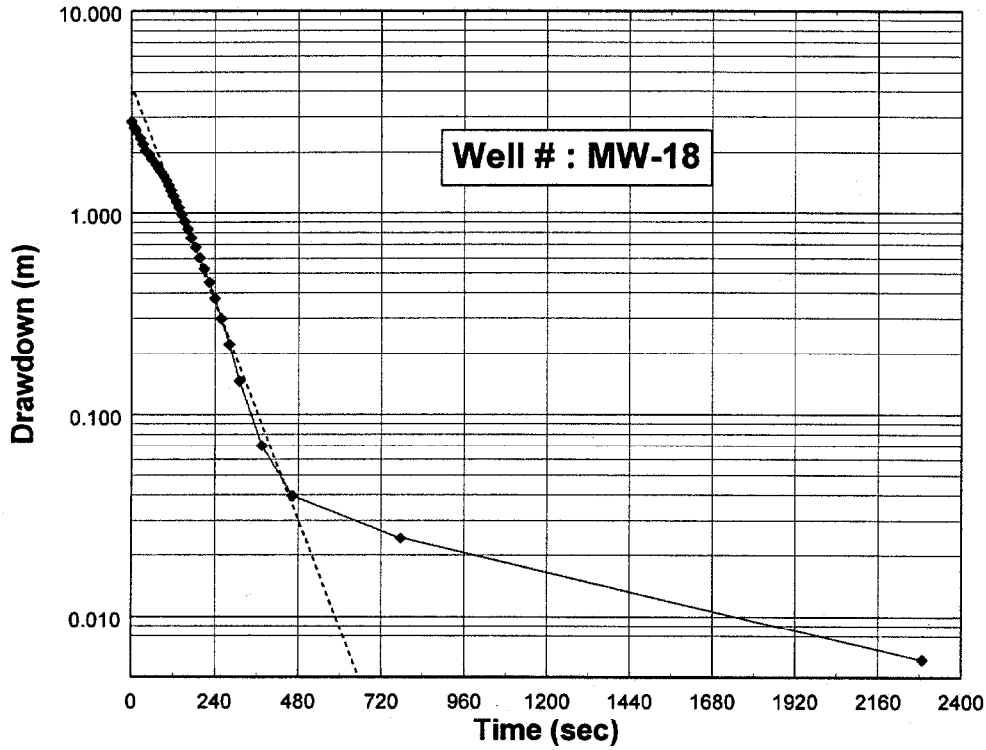
Well # : MW-18
10.000
1.000
0.100
0.010
Drawdown (m)
0
240
480
720
960
1200
1440
1680
1920
2160
2400
Time (sec)

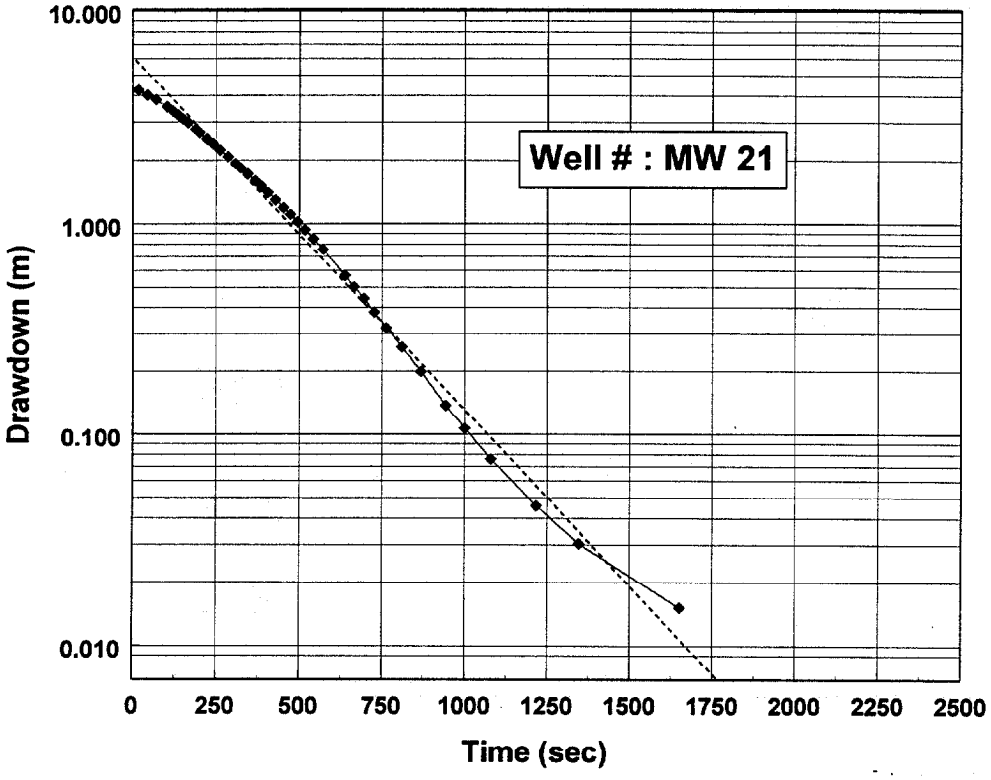
Well # : MW 21
Drawdown (m)
10.000
1.000
0.100
0.010
0
250
500
750
1000
1250
1500
1750
2000
2250
2500
Time (sec)

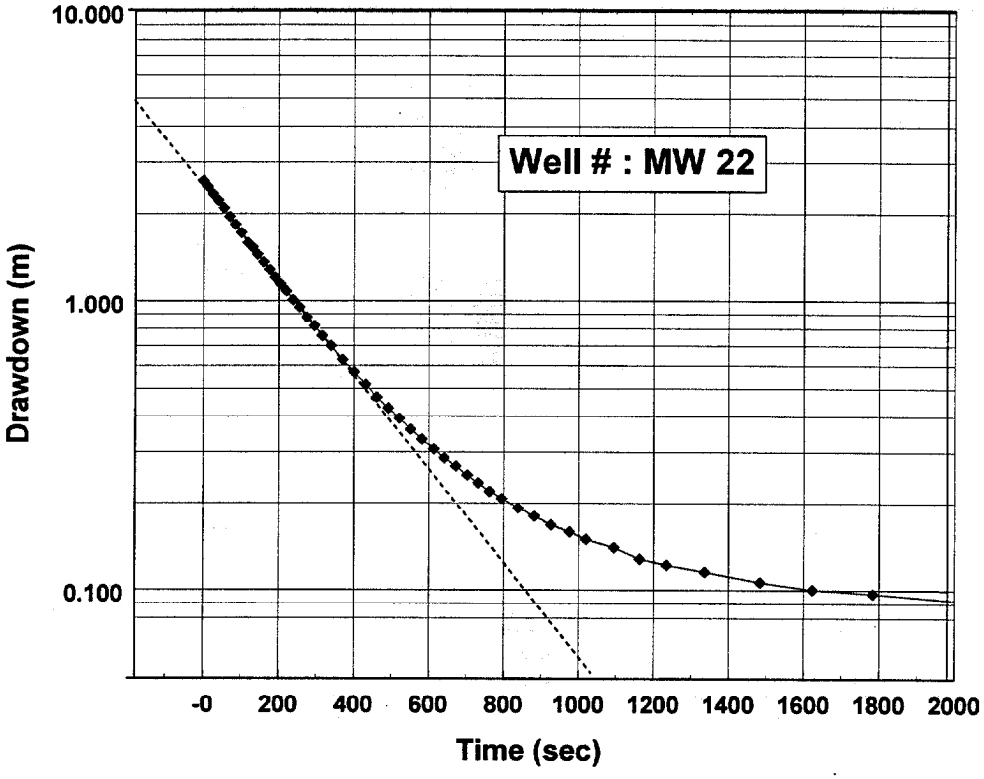
Well # : MW 22
10.000
1.000
0.100
Drawdown (m)
-0
200
400
600
800
1000
1200
1400
1600
1800
2000
Time (sec)

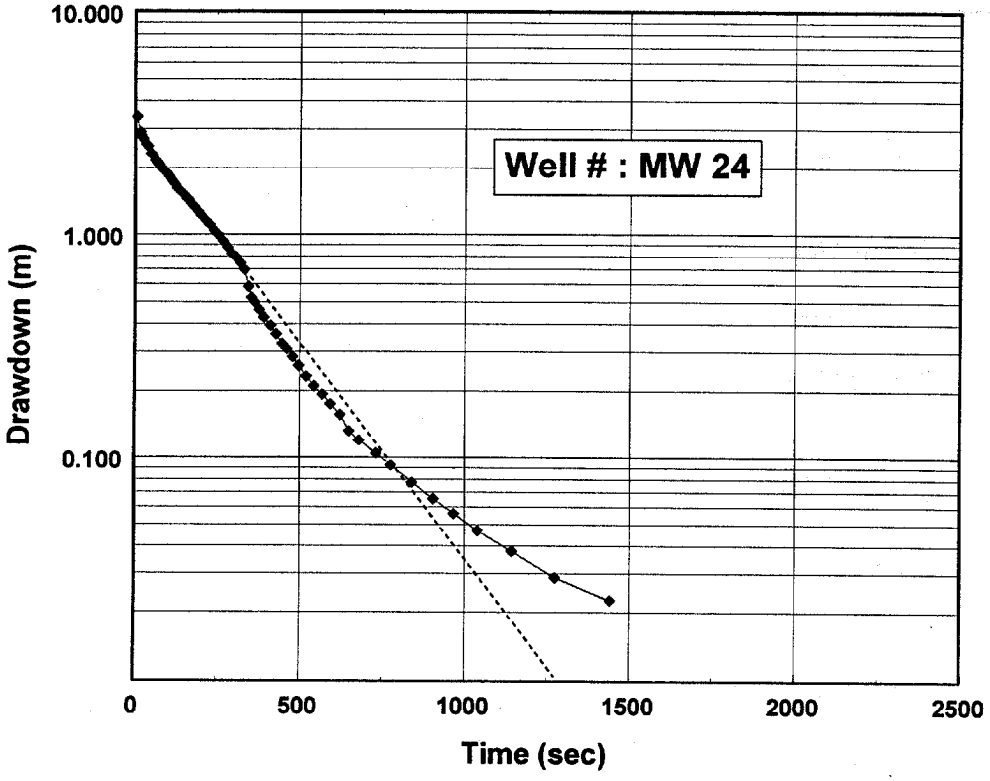
Well # : MW 24
10.000
1.000
0.100
Drawdown (m)
0
500
1000
1500
2000
2500
Time (sec)

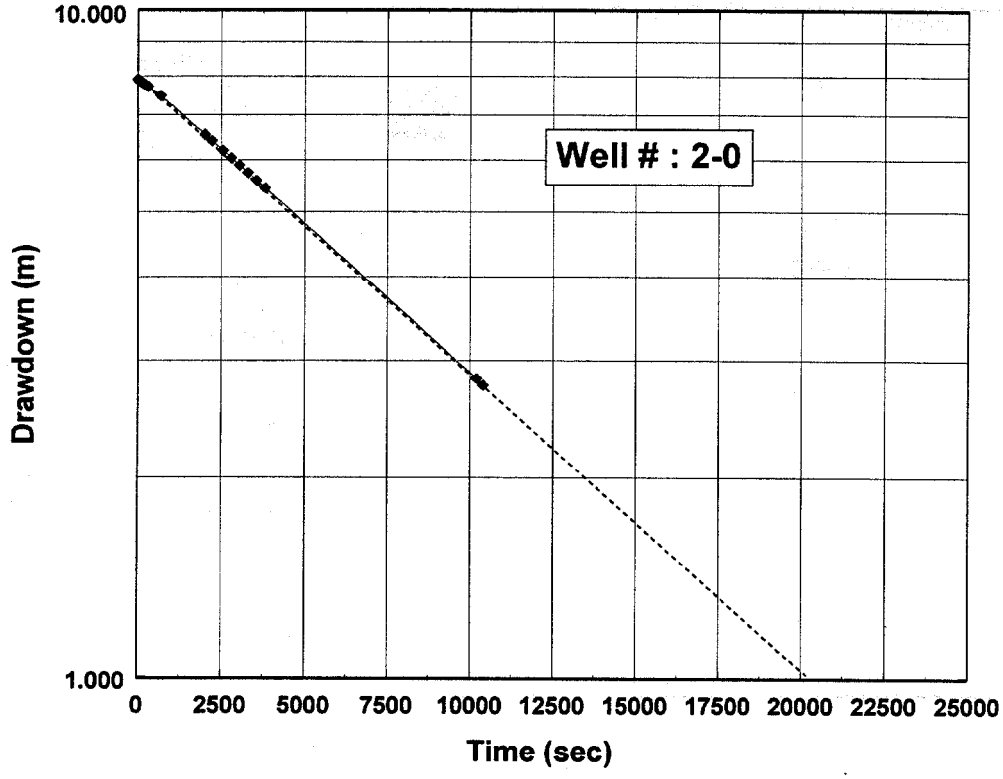
10.000
1.000
Drawdown (m)
Well # : 2-0
0
2500
5000
7500
10000
12500
15000
17500
20000
22500
25000
Time (sec)

APPENDICES

CHAPTER 2

Data Tables

Radiochemistry

Chemistry

Comparison of isotopic uranium results determined by PERALS spectrometry and alpha spectrometry for stack solutions (PP and S3), monitor wells (MW), and an EPA standard.

Uranium Perals/ Alpha

PERALS sample ID	238U dpm/l	238 +/-	234U dpm/l	234 +/-	% yield	ALPHA sample ID	238U dpm/l	238 +/-	234U dpm/l	234 +/-	% yield
PP1-1 (3)	1060.9	8.6	1090.4	8.8	103	PP1-1 (3)	1044	15.6	1066.1	13	
PP1-2 (3)	779.1	12	833.3	12.4	116	PP1-2 (3)	804.3	12	810	12.1	
PP1-3 (2)	664.5	10.9	727	11.4	97	PP1-3 (2)	670	11.5	677.6	11.7	
PP1-4 (2)	589.8	5.7	613	5.8	100	PP1-4 (2)	605.1	8	609.4	8	
PP2-1 (3)	1051.7	11.3	1159	11.9	100	PP2-1 (3)	1052.4	15.4	1065.5	15.6	
PP2-2 (3)	952.9	8.8	1002.8	9.1	97	PP2-2 (3)	953.6	14	956	14.1	
PP3-2 (3)	744.6	7.5	757.5	7.6	98	PP3-2 (3)	730.4	11.9	738.8	12.1	
PP2-1 (4)	915.8	10.9	999	11.3	100	PP2-1 (4)	905.1	14	914.6	14.1	
PP2-2 (4)	800.5	9.5	845.3	9.7	100	PP2-2 (4)	800.9	11.7	811	13	
S3	589.9	8.5	604.2	8.6	99	S3	590	8.9	593.1	9	
MW-2 (2)	0.29	0.03	0.32	0.03	106	MW-2 (2)	0.259	0.01	0.236	0.013	
MW-3 (2)	0.11	0.01	0.12	0.02	97	MW-3 (2)	0.074	0.007	0.102	0.008	
MW-5 (1)	3.36	0.09	3.98	0.01	96	MW-5 (1)	3.35	0.19	4.35	0.26	89
MW-8 (1)	0.49	0.03	0.51	0.03	74	MW-8 (1)	0.04	0.02	0.07	0.01	77
MW-10 (1)	0.95	0.05	0.89	0.05	75	MW-10 (1)	1.38	0.05	1.33	0.05	77
MW-8 (2)	0.76	0.04	0.81	0.04	90	MW-8 (2)	0.43	0.03	0.44	0.03	80
MW-24 (1)	0.21	0.02	0.23	0.02	52	MW-24 (1)	0.23	0.01	0.38	0.02	63
usepa u1	63.9	4.2	63.9	4.2	100	usepa u1	63.3	0.78	62.43	0.84	68
usepa u2	63.8	4.2	63.8	4.2	100	usepa u2	63.2	0.74	62.2	0.8	76
				average =	94.7					average =	75.7
				sd =	14.0					sd =	8.4
				n =	19					n =	7

Chemical analyses of fluids sampled from Piney Point phosphogypsum stack (PP), surrounding monitor wells (MW)/(USGS), and pond surface(S). All analyses given in ppm. ND = not detected (below detection limit); NA = not analyzed.
Also analyzed for: B, Li, Zn, As, Bi, Cd, Ce, Cr, Cu, La, Ni, Pb, Th, Ti, U, Zr, Br, Hg, Se (see appendix 1-3 for trace elements).

Fieldtrip #1, March 20-25, 1995.

Well	Na	K	Ca	Mg	Fe	Al	SiO_2	Sr	Ba	Mn	NH_4	HCO_3	Cl	F	SO_4	PO_4	TOC	Field pH
MW 1 (1)	94	5	81	40	1.1	N.D.	33	0.52	N.D.	0.03	0.53	493	88	0.5	55	0.60	8.8	6.73
MW 3 (1)	301	11	279	14	7.6	0.1	19	1.0	0.08	0.15	0.27	467	68	0.8	1138	33	18	6.55
MW 4A (1)	77	3	197	24	0.9	N.D.	25	1.4	0.03	N.D.	N.A.	507	71	0.6	178	0.67	16	6.91
MW 5 (1)	49	12	166	48	0.004	N.D.	10	5.1	0.03	N.D.	N.A.	290	116	0.6	303	N.D.	7.7	7.06
USGS 9 (1)	38	3	114	33	5.9	N.D.	19	0.24	N.D.	0.08	N.A.	145	95	1.7	214	20	7.8	6.49

Fieldtrip #2, May 3-8, 1995.

Well	Na	K	Ca	Mg	Fe	Al	SiO_2	Sr	Ba	Mn	NH_4	HCO_3	Cl	F	SO_4	PO_4	TOC	Field pH
MW 2 (1)	44	1.28	87	36	54.3	2.1	23	0.09	N.D.	0.05	1.0	N.D.	142	1.1	232	11	13	5.91
PP 1-1 (1)	1790	267	678	261	9.5	8.6	958	15.6	0.03	6.36	1234	N.D.	203	1495	5725	10580	97	2.19
PP 1-2 (1)	1638	262	657	245	6.3	3.4	930	14.4	0.03	5.73	1158	N.D.	181	1419	5379	9739	86	2.24
PP 1-3 (1)	1529	246	657	229	2.0	5.8	742	12.1	0.02	5.00	1053	N.D.	168	1120	5091	8720	81	2.38
PP 1-4 (1)	1497	233	655	230	0.95	6.8	723	11.8	0.02	4.93	1126	N.D.	171	1033	5104	8733	82	2.40
D1	1572	258	680	238	9.0	4.1	833	15.0	0.02	5.40	1212	N.D.	173	1593	5120	9871	68	2.32
S1	1563	264	673	247	21.5	19.2	749	12.4	0.04	5.03	1148	N.D.	211	1157	5544	9485	97	2.49

Fieldtrip #3, June 8-12, 1995.

Well	Na	K	Ca	Mg	Fe	Al	SiO_2	Sr	Ba	Mn	NH_4	HCO_3	Cl	F	SO_4	PO_4	TOC	Field pH
PP 2-1 (1)	1639	265	687	238	13.2	4.1	1046	17.1	N.D.	5.68	1274	N.D.	188	1712	5412	10275	90	2.35
PP 2-2 (1)	1496	233	681	222	20.8	10.6	986	14.7	0.04	5.29	1321	N.D.	208	1525	5616	9698	96	2.19
PP 3-2 (1)	1477	222	663	223	1.2	2.1	647	12.1	0.02	4.57	1135	N.D.	262	1015	5153	8496	82	2.47
PP 3-3 (1)	1542	236	671	230	1.2	4.7	665	11.4	0.03	4.77	1115	N.D.	190	998	5178	8568	86	2.54
S2	1451	213	651	209	11.2	13.2	562	11.4	0.04	4.70	1021	N.D.	165	897	4939	8389	88	2.54

Fieldtrip #4, July 17-22, 1995.

Well	Na	K	Ca	Mg	Fe	Al	SiO_2	Sr	Ba	Mn	NH_4	HCO_3	Cl	F	SO_4	PO_4	TOC	Field pH
PP 1-1 (2)	1800	265	674	256	8.5	5.3	851	15.4	0.02	5.62	1274	N.D.	175	1344	5700	10313	106	2.56
PP 1-2 (2)	1677	255	672	236	4.1	4.9	786	12.9	N.D.	5.23	1186	N.D.	172	1277	5375	9485	88	2.57
PP 2-1 (2)	1696	267	695	244	12.1	3.5	998	16.5	0.02	5.86	1292	N.D.	171	1479	5548	10398	95	2.37
PP 2-2 (2)	1703	266	664	249	10.3	5.7	945	15.9	0.03	5.67	1212	N.D.	158	1308	5350	10248	91	2.48

Fieldtrip #5, November 13-18, 1995.

Well	Na	K	Ca	Mg	Fe	Al	SiO_2	Sr	Ba	Mn	NH_4	HCO_3	Cl	F	SO_4	PO_4	TOC	Field pH
PP-1-1(3)	1598	225	671	222	7.9	3.1	673	15.0	N.D.	5.34	1210	N.D.	250	1300	5519	9278	109	2.37
PP 1-2 (3)	1403	211	656	209	3.6	4.1	587	12.6	N.D.	4.53	992	N.D.	180	930	5079	7996	90	2.47
PP 1-3 (2)	1367	203	660	206	1.7	5.9	543	11.8	N.D.	4.30	925	N.D.	149	819	4857	7589	82	2.50
PP 1-4 (2)	1243	177	662	194	1.0	6.3	443	10.4	N.D.	3.83	848	N.D.	138	595	4544	6901	76	2.57
PP 2-1 (3)	1622	235	673	221	8.5	2.8	699	14.9	N.D.	5.15	1100	N.D.	179	214	5359	9421	97	2.42
PP 2-2 (3)	1582	232	672	220	5.4	4.3	631	13.3	N.D.	4.85	1103	N.D.	164	1160	5320	8977	92	2.38
PP 3-2 (3)	1334	191	659	202	2.9	1.8	472	10.7	N.D.	3.99	929	N.D.	141	685	4980	7476	85	2.40
S3	1276	182	674	192	13.2	13.0	439	8.3	0.03	3.64	882	N.D.	143	679	4688	6887	76	2.58
MW 1 (2)	81	4.7	84	38	0.91	N.D.	34	0.40	N.D.	0.03	N.A.	467	82	0.36	41	0.88	7.3	6.60
MW 2 (2)	45	1.04	87	35	N.D.	0.11	13	0.08	N.D.	0.04	N.A.	N.D.	139	0.51	256	6.2	2.8	5.85
MW 3 (2)	381	13	386	17	8.7	N.D.	21	1.1	0.09	0.16	N.A.	502	N.D.	0.71	1300	27	18.0	6.48
MW 4A (2)	77	2.9	194	23	0.9	N.D.	23	1.4	0.03	N.D.	N.A.	615	82	0.62	169	0.58	9.9	6.84
MW 5 (2)	35	10	132	34	0.3	N.D.	10	3.7	N.D.	N.D.	N.A.	287	72	0.66	208	0.98	7.4	7.00
USGS 9 (2)	40	3.3	172	31	4.2	N.D.	21	0.31	N.D.	0.04	N.A.	142	78	2.3	350	17	6.7	6.42

No compositional samples analyzed for fieldtrip #6

Fieldtrip #7, March 17-27 , 1996.

Well	Na	K	Ca	Mg	Fe	Al	SiO_2	Sr	Ba	Mn	NH_4	HCO_3	Cl	F	SO_4	PO_4	TOC	pH
MW8(1)	40	2.8	85	46	1.4	N.D.	33	0.35	N.D.	N.D.	N.A.	365	64	1.2	40	N.D.	18.0	6.86
MW9(1)	25	1.9	221	33	12.0	N.D.	7.6	0.37	N.D.	N.D.	N.A.	96	46	0.6	548	23	8.3	6.11
MW10(1)	1226	160	219	229	3.8	N.D.	166	0.47	N.D.	N.D.	445	2622	145	0.2	3115	5555	62	6.25
MW11(1)	427	54	345	141	9.6	N.D.	107	1.2	N.D.	N.D.	121	1147	55	0.4	1855	213	17	6.34
MW12(1)	1173	156	479	312	65.8	8.2	303	6.1	N.D.	2.97	581	N.D.	N.D.	1.9	4367	2073	57	3.48
MW13(1)	1550	218	124	324	4.0	N.D.	1.7	4.4	N.D.	N.D.	865	2588	153	1.8	4279	2270	N.A.	6.30
MW14(1)	732	327	241	245	5.7	N.D.	150	1.1	N.D.	N.D.	587	2982	59	0.4	4018	262	20	6.40
MW15(1)	1447	189	224	171	0.25	N.D.	164	2.5	N.D.	N.D.	831	3121	131	0.3	3824	650	36	6.33
MW16(1)	1093	18	501	138	10.5	N.D.	46	4.3	N.D.	N.D.	39	2293	8	0.5	2992	133	39	6.21
MW17(1)	187	4.6	328	283	11.5	N.D.	18	1.3	N.D.	N.D.	2.9	524	231	0.4	666	1179	7.5	6.61
PP2-0(1)	1324	195	474	253	37.3	37.1	1091	13.5	N.D.	4.92	406	N.D.	130	1540	4744	8492	68	2.35
PP2-3(1)	1080	157	460	210	6.9	21.8	539	10.2	N.D.	4.07	277	N.D.	123	586	4744	6762	70	2.52

Fieldtrip #8 May 23-28 , 1996.

Well	Na	K	Ca	Mg	Fe	Al	SiO_2	Sr	Ba	Mn	NH_4	HCO_3	Cl	F	SO_4	PO_4	TOC	pH
PP2-0(2)	2264	232	776	227	41.7	40.4	1028	16.6	0.06	6.35	1300	N.D.	230	1622	5500	11397	122	2.25
PP2-3(2)	1391	173	688	179	4.4	7.6	440	10.5	0.03	4.29	996	N.D.	150	657	4630	6817	81	2.50
MW-18(1)	25	0.1	173	7.9	2.2	N.D.	13	0.8	0.03	N.D.	N.A.	485	46	0.5	73	0.8	N.A.	6.84
MW-19(1)	558	18	488	48	13.8	N.D.	133	2.1	0.06	0.15	N.A.	785	63	0.1	1520	315	N.A.	6.06
MW-20(1)	561	81	321	93	11.0	N.D.	79	1.5	N.D.	N.D.	29	930	62	0.3	1810	124	N.A.	6.35
MW-21(1)	89	4.6	230	10	20.2	N.D.	13	0.99	N.D.	N.D.	5.7	556	183	0.3	160	32	N.A.	6.66
MW-22(1)	83	6.3	386	19	22.4	N.D.	11	2.0	0.03	N.D.	N.A.	253	45	0.4	880	5.4	N.A.	6.60
MW-23(1)	1446	6.4	1001	95	38.9	N.D.	15	5.0	0.16	0.04	N.A.	225	4345	0.2	171	2.3	N.A.	6.57
MW-24(1)	105	2.0	258	29	13.8	N.D.	28	1.1	N.D.	0.05	N.A.	165	115	0.4	590	32	N.A.	6.27

Fieldtrip #9 September 16-20,1996

Well	Na	K	Ca	Mg	Fe	Al	SiO_2	Sr	Ba	Mn	NH_4	HCO_3	Cl	F	SO_4	PO_4	TOC	pH
MW-8(3)	50	2.8	74	35	1.2	N.D.	30	0.37	N.D.	0.08	N.A.	354	60	1.23	38	0.4	13.5	6.76
MW-9(3)	26	1.9	175	17	12.0	N.D.	7.3	0.48	N.D.	N.D.	N.A.	61	43	0.70	386	0.8	7.4	6.17
MW-11(3)	835	89	274	205	12.0	N.D.	114	1.4	N.D.	0.08	157	1567	86	0.22	2560	404	24.5	6.21
MW-13(3)	1688	212	113	380	5.0	N.D.	157	4.7	1.96	0.12	813	2538	157	1.48	4288	1668	56.9	6.31
MW-14(3)	759	327	256	247	5.9	N.D.	127	1.4	N.D.	N.D.	708	2871	44	0.26	2875	221	18.5	6.35
MW-15(2)	1580	200	233	228	0.17	N.D.	162	3.0	0.03	0.08	772	2824	145	0.29	3875	797	48.6	6.34
MW-16(2)	1070	22	852	89	7.9	N.D.	37	3.9	0.11	0.06	N.D.	2022	93	0.48	2750	6.4	54.8	6.19
MW-18(2)	26	N.D.	180	8.0	2.3	N.D.	13	0.88	0.05	N.D.	1.5	450	50	0.42	77	0.7	15.9	6.82
MW- 19(2)	542	20	502	57	11.7	N.D.	123	2.0	N.D.	0.14	88	1231	70	0.41	1525	290	58	6.10
MW-20(2)	483	82	349	96	11.0	N.D.	75	1.5	N.D.	N.D.	192	1044	64	0.22	1919	120	29.1	6.34
MW-21(2)	125	7.4	219	11	20.1	N.D.	16	1.00	N.D.	N.D.	32	556	198	0.24	180	64	60.5	6.58
MW-22(2)	75	7.0	378	19	21.9	N.D.	13	1.8	N.D.	N.D.	N.D.	249	59	0.41	861	10	40.3	6.51
MW-23(2)	2056	8.5	1115	98	39.8	N.D.	15	5.0	0.22	0.04	N.D.	206	4987	0.18	171	N.D.	N.D.	6.49
MW-24(2)	31	2.4	202	28	6.8	N.D.	28	0.77	N.D.	0.06	N.D.	179	39	0.36	400	37	31.7	6.13

Chemical analyses of fluids sampled from Piney Point phosphogypsum stack (PP), surrounding monitor wells (MW)/(USGS), and pond surface(S). All analyses given in ppm unless otherwise stated. ND = not detected (below detection limit); NA= not analyzed.

Field trip #1																	ppb	ppb		Misc.
Well	B	Li	Zn	As	Bi	Cd	Ce	Cr	Cu	La	Ni	Pb	Th	Ti	U	Zr	Br	Hg	Se	H_2S	Analysis
MW-1(1)	0.08	N.D.	N.D.	N.D.	N.D.	N.D.	0.06	N.D.	N.D.	0.04	N.D.	N.D.	N.D.	N.D.	N.D.	N.D.	N.A.	N.A.	N.A.	N.A.	
MW-3(1)	0.04	N.D.	N.D.	N.D.	N.D.	N.D.	0.12	N.D.	N.D.	0.03	N.D.	N.D.	N.D.	N.D.	N.D.	N.D.	N.D.	N.A.	N.A.	N.A.	
MW-4A(1)	0.03	N.D.	N.D.	N.D.	N.D.	0.01	N.D.	N.D.	0.02	0.03	N.D.	N.D.	N.D.	N.D.	N.D.	N.D.	N.A.	N.A.	N.A.	N.A.	
MW-5(1)	N.D.	N.D.	N.D.	N.D.	N.D.	N.D.	N.D.	N.D.	N.D.	0.05	N.D.	N.D.	N.D.	N.D.	N.D.	N.D.	N.A.	N.A.	N.A.	N.A.	
USGS-9(1)	N.D.	0.006	N.D.	N.D.	0.20	N.D.	0.12	N.D.	N.D.	0.04	0.03	0.08	N.D.	N.D.	N.D.	N.D.	2.90	N.A.	N.A.	N.A.	

Field trip #2																	ppb	ppb		Misc.
Well	B	Li	Zn	As	Bi	Cd	Ce	Cr	Cu	La	Ni	Pb	Th	Ti	U	Zr	Br	Hg	Se	H_2S	Analysis
MW-2(1)	0.01	N.D.	N.D.	N.D.	N.D.	N.D.	0.04	N.D.	N.D.	0.05	N.D.	N.D.	N.D.	0.02	N.D.	N.D.	3.50	N.A.	N.A.	N.A.	
PP 1-1(1)	1.16	1.24	1.95	0.80	N.D.	0.15	0.03	0.29	0.05	0.03	0.90	N.D.	N.D.	1.06	N.D.	N.D.	2.40	<0.5	12	N.A.	
PP 1-2(1)	1.05	1.16	1.81	0.65	N.D.	0.14	N.D.	0.25	N.D.	0.02	0.76	N.D.	N.D.	0.81	N.D.	N.D.	3.30	<0.5	8	N.A.	
PP 1-3(1)	0.97	1.07	1.50	0.80	N.D.	0.12	0.15	0.21	0.03	0.05	0.68	N.D.	N.D.	0.48	N.D.	N.D.	3.10	N.A.	N.A.	N.A.	
PP 1-4(1)	0.93	1.13	1.39	0.59	N.D.	0.12	0.15	0.21	0.04	N.D.	0.68	N.D.	N.D.	0.20	N.D.	N.D.	2.60	N.A.	N.A.	N.A.	
D1	0.94	1.03	1.66	0.52	N.D.	0.13	N.D.	0.23	N.D.	0.04	0.76	N.D.	N.D.	1.04	N.D.	N.D.	3.60	N.A.	N.A.	N.A.	
S1	0.95	1.13	1.67	0.42	N.D.	0.11	N.D.	0.22	N.D.	N.D.	0.71	N.D.	N.D.	0.41	N.D.	N.D.	2.20	N.A.	N.A.	N.A.	

Field trip #3																	ppb	ppb		Misc.
Well	B	Li	Zn	As	Bi	Cd	Ce	Cr	Cu	La	Ni	Pb	Th	Ti	U	Zr	Br	Hg	Se	H_2S	Analysis
PP 2-1(1)	1.10	1.06	1.78	0.68	N.D.	0.15	0.07	0.28	0.02	0.05	0.86	N.D.	N.D.	1.24	N.D.	N.D.	2.70	<0.5	10	N.A.	
PP 2-2(1)	1.12	0.97	1.60	0.64	N.D.	0.13	N.D.	0.28	N.D.	0.05	0.81	N.D.	N.D.	1.08	N.D.	N.D.	2.70	N.A.	N.A.	N.A.	
PP 3-2(1)	0.93	0.98	1.20	0.41	N.D.	0.10	N.D.	0.18	0.05	0.05	0.69	N.D.	N.D.	1.08	N.D.	N.D.	2.80	<0.5	11	N.A.	
PP 3-3(1)	0.94	1.00	1.48	0.43	N.D.	0.11	0.02	0.20	0.04	0.04	0.69	N.D.	N.D.	0.26	N.D.	N.D.	2.70	N.A.	N.A.	N.A.	
S2	0.92	0.89	0.56	0.43	N.D.	0.13	0.19	0.21	0.02	N.D.	0.47	N.D.	N.D.	0.15	0.6	N.D.	1.60	N.A.	20	N.A.	

Field trip #4																		ppb	ppb		Misc.
Well	B	Li	Zn	As	Bi	Cd	Ce	Cr	Cu	La	Ni	Pb	Th	Ti	U	Zr	Br	Hg	Se	H_2S	Analysis
PP 1-1(2)	1.14	1.14	1.66	0.49	N.D.	0.13	N.D.	0.25	0.04	0.03	0.77	N.D.	N.D.	0.90	N.D.	N.D.	1.60	N.A.	N.A.	N.A.	
PP 1-2(2)	1.02	1.05	1.50	0.68	N.D.	0.11	0.21	0.23	N.D.	0.05	0.73	N.D.	N.D.	0.58	N.D.	N.D.	N.A.	N.A.	N.A.	N.A.	
PP 2-1(2)	1.14	1.01	1.78	0.73	N.D.	0.14	N.D.	0.26	N.D.	0.03	0.83	N.D.	N.D.	1.11	N.D.	N.D.	N.A.	N.A.	N.A.	N.A.	
PP 2-2(2)	1.01	1.14	1.63	0.58	N.D.	0.13	0.14	0.25	0.02	0.05	0.80	N.D.	N.D.	1.24	N.D.	N.D.	N.A.	N.A.	N.A.	N.A.	
Field trip #5																		ppb	ppb		Misc.
Well	B	Li	Zn	As	Bi	Cd	Ce	Cr	Cu	La	Ni	Pb	Th	Ti	U	Zr	Br	Hg	Se	H_2S	Analysis
PP 1-1(3)	1.03	1.06	N.D.	N.D.	1.0	0.01	1.00	N.D.	N.D.	1.00	N.D.	N.D.	1.00	1.00	1.00	1.00	1.10	N.A.	N.A.	N.A.	
PP 1-2(3)	0.91	0.98	0.55	0.38	N.D.	0.14	N.D.	0.18	0.06	N.D.	0.45	N.D.	N.D.	0.50	0.76	N.D.	1.00	N.A.	N.A.	N.A.	
PP 1-3(2)	0.87	0.96	0.51	0.41	N.D.	0.12	0.07	0.17	N.D.	N.D.	0.43	N.D.	N.D.	0.44	N.D.	N.D.	1.40	N.A.	N.A.	N.A.	
PP 1-4(2)	0.79	0.91	0.54	0.59	N.D.	0.12	0.16	0.16	0.06	N.D.	0.39	N.D.	N.D.	0.20	0.8	N.D.	2.00	N.A.	N.A.	N.A.	
PP 2-1(3)	0.96	1.00	0.69	0.37	N.D.	0.17	0.13	0.26	N.D.	N.D.	0.50	N.D.	N.D.	0.78	N.D.	0.10	1.50	N.A.	20	N.D.	
PP 2-3(3)	0.96	1.00	0.65	0.61	N.D.	0.16	0.05	0.25	N.D.	N.D.	0.52	N.D.	N.D.	0.70	0.6	N.D.	1.20	N.A.	23	N.D.	
PP 3-2(3)	0.74	0.87	0.50	0.37	N.D.	0.13	0.10	0.18	0.04	N.D.	0.43	N.D.	N.D.	0.65	0.6	N.D.	N.D.	N.A.	21	N.A.	
S3	0.72	0.78	0.47	0.33	N.D.	0.11	0.11	0.18	0.02	N.D.	0.39	N.D.	N.D.	0.23	0.7	N.D.	1.50	N.A.	11	N.A.	
MW-1(2)	0.12	0.02	N.D.	N.D.	N.D.	N.D.	N.D.	N.D.	N.D.	N.D.	N.D.	N.D.	N.D.	N.D.	N.D.	N.D.	N.D.	N.A.	N.A.	0.24	NO_3 0.88
MW-2(2)	0.07	N.D.	N.D.	N.D.	N.D.	N.D.	N.D.	N.D.	N.D.	N.D.	N.D.	N.D.	N.D.	N.D.	N.D.	N.D.	N.D.	N.A.	N.A.	N.D.	NO_3 0.13
MW-3(2)	0.10	0.01	N.D.	N.D.	N.D.	N.D.	N.D.	N.D.	N.D.	N.D.	N.D.	N.D.	N.D.	N.D.	N.D.	N.D.	N.A.	N.A.	N.A.	0.008	NO_3 65.4
MW-4A(2)	0.10	0.01	N.D.	0.13	N.D.	0.01	N.D.	N.D.	N.D.	N.D.	N.D.	N.D.	N.D.	N.D.	N.D.	N.D.	N.A.	N.A.	N.A.	0.004	NO_3 0.31
MW-5(2)	0.06	N.D.	N.D.	N.D.	0.2	0.01	N.D.	N.D.	N.D.	N.D.	N.D.	N.D.	N.D.	N.D.	N.D.	N.D.	N.A.	N.D.	N.D.	N.A.	NO_3 9.90
USGS-9(2)	0.07	0.01	N.D.	N.D.	N.D.	N.D.	N.D.	N.D.	N.D.	N.D.	N.D.	N.D.	N.D.	N.D.	0.6	N.D.	N.D.	N.A.	N.A.	1.79	NO_3 8.36

Chemical compositional samples not analyzed for Fieldtrip #6

Field trip #7																				
Well	B	Li	Zn	As	Bi	Cd	Ce	Cr	Cu	La	Ni	Pb	Th	Ti	U	Zr	Br	ppb Hg	ppb Se	H_2S	Misc. Analysis
MW-8(1)	0.05	N.D.	N.D.	N.D.	N.D.	N.D.	N.D.	N.D.	N.D.	N.D.	N.D.	N.D.	N.D.	N.D.	N.D.	N.D.	2.10	N.A.	N.A.	N.A.	
MW-9(1)	N.D.	N.D.	N.D.	N.D.	N.D.	N.D.	N.D.	N.D.	N.D.	N.D.	N.D.	N.D.	N.D.	N.D.	N.D.	N.D.	3.00	N.A.	N.A.	N.A.	
MW-10(1)	0.79	0.97	N.D.	N.D.	N.D.	N.D.	N.D.	N.D.	N.D.	N.D.	N.D.	N.D.	N.D.	N.D.	N.D.	N.D.	3.00	N.A.	N.A.	N.A.	
MW-11(1)	0.34	0.28	N.D.	N.D.	N.D.	N.D.	N.D.	N.D.	N.D.	N.D.	N.D.	N.D.	N.D.	N.D.	N.D.	N.D.	2.70	N.A.	N.A.	N.A.	
MW-12(1)	1.21	0.90	0.31	N.D.	N.D.	0.07	N.D.	N.D.	N.D.	N.D.	0.33	N.D.	N.D.	0.24	N.D.	N.D.	1.70	N.A.	N.A.	N.A.	
MW-13(1)	1.09	1.04	N.D.	N.D.	N.D.	N.D.	N.D.	N.D.	N.D.	N.D.	N.D.	N.D.	N.D.	N.D.	N.D.	N.D.	3.00	N.A.	N.A.	N.A.	
MW-14(1)	N.D.	0.24	N.D.	N.D.	N.D.	N.D.	N.D.	N.D.	N.D.	N.D.	N.D.	N.D.	N.D.	N.D.	N.D.	N.D.	3.20	N.A.	N.A.	N.A.	
MW-15(1)	4.25	1.00	N.D.	N.D.	N.D.	N.D.	N.D.	N.D.	N.D.	N.D.	N.D.	N.D.	N.D.	N.D.	N.D.	N.D.	2.90	N.A.	N.A.	N.A.	
MW-16(1)	0.46	0.25	N.D.	N.D.	N.D.	N.D.	N.D.	N.D.	N.D.	N.D.	N.D.	N.D.	N.D.	N.D.	N.D.	N.D.	1.60	N.A.	N.A.	N.A.	
MW-17(1)	1.01	N.D.	N.D.	N.D.	N.D.	N.D.	N.D.	N.D.	N.D.	N.D.	N.D.	N.D.	N.D.	N.D.	N.D.	N.D.	1.60	N.A.	N.A.	N.A.	
PP 2-0(1)	0.91	0.75	0.89	N.D.	N.D.	0.24	N.D.	0.67	N.D.	N.D.	0.76	N.D.	N.D.	1.24	N.D.	N.D.	7.90	N.D.	10	N.A.	NO_3 3.50
PP 2-3(1)	0.87	0.75	0.67	N.D.	N.D.	0.20	N.D.	0.33	N.D.	N.D.	0.59	N.D.	N.D.	0.54	N.D.	N.D.	7.00	N.D.	5	N.A.	NO_3 3.60

Field trip #8																				
Well	B	Li	Zn	As	Bi	Cd	Ce	Cr	Cu	La	Ni	Pb	Th	Ti	U	Zr	Br	ppb Hg	ppb Se	H_2S	Misc. Analysis
PP 2-0(2)	1.52	1.02	1.63	N.D.	N.D.	0.18	3.79	0.43	N.D.	2.06	0.91	N.D.	N.D.	1.25	4.43	N.D.	0.50	N.D.	3.2	N.A.	
PP 2-3(2)	1.14	0.83	0.95	N.D.	N.D.	0.10	2.01	0.14	N.D.	1.06	0.59	0.18	N.D.	0.33	2.35	N.D.	1.23	N.D.	4.9	N.A.	
MW-18(1)	0.04	N.D.	N.D.	N.D.	N.D.	N.D.	0.79	N.D.	N.D.	0.36	N.D.	N.D.	N.D.	N.D.	1.04	N.D.	N.D.	N.A.	N.A.	N.A.	
MW-19(1)	0.34	0.15	N.D.	N.D.	N.D.	N.D.	0.83	N.D.	N.D.	0.47	N.D.	N.D.	N.D.	N.D.	0.96	N.D.	0.63	N.A.	N.A.	N.A.	
MW-20(1)	0.37	0.34	N.D.	N.D.	N.D.	0.01	0.85	N.D.	N.D.	0.46	N.D.	0.11	N.D.	N.D.	1.04	N.D.	0.63	N.A.	N.A.	N.A.	
MW-21(1)	0.05	N.D.	N.D.	0.17	N.D.	N.D.	N.D.	N.D.	N.D.	0.37	0.02	N.D.	N.D.	N.D.	0.98	N.D.	0.50	N.A.	N.A.	N.A.	
MW-22(1)	0.05	N.D.	N.D.	N.D.	N.D.	N.D.	0.84	N.D.	N.D.	0.41	N.D.	N.D.	N.D.	N.D.	1.03	N.D.	N.D.	N.A.	N.A.	N.A.	
MW-23(1)	N.D.	N.D.	N.D.	N.D.	N.D.	N.D.	2.22	N.D.	N.D.	1.24	N.D.	N.D.	N.D.	N.D.	2.50	N.D.	0.50	N.A.	N.A.	N.A.	
MW-24(1)	0.06	N.D.	N.D.	0.20	N.D.	N.D.	0.88	N.D.	N.D.	0.44	N.D.	N.D.	N.D.	N.D.	1.09	N.D.	N.D.	N.A.	N.A.	N.A.	

Field trip #9																				Misc.
Well	B	Li	Zn	As	Bi	Cd	Ce	Cr	Cu	La	Ni	Pb	Th	Ti	U	Zr	Br	Hg	Se	H_2S	Analysis
MW-8(3)	0.15	N.D.	N.D.	N.D.	N.D.	N.D.	0.74	N.D.	N.D.	0.36	N.D.	N.D.	N.D.	N.D.	1.00	N.D.	N.D.	N.A.	N.A.	N.A.	
MW-9(3)	0.00	N.D.	N.D.	N.D.	N.D.	N.D.	0.78	N.D.	N.D.	0.37	N.D.	N.D.	N.D.	N.D.	1.06	N.D.	N.D.	N.A.	N.A.	N.A.	
MW-11(3)	0.68	0.50	N.D.	N.D.	N.D.	N.D.	0.89	N.D.	N.D.	0.50	N.D.	N.D.	N.D.	N.D.	1.05	N.D.	0.72	N.A.	N.A.	N.A.	
MW-13(3)	1.68	1.10	N.D.	N.D.	N.D.	N.D.	1.96	N.D.	N.D.	1.04	N.D.	N.D.	N.D.	0.02	2.34	N.D.	23.6	N.A.	N.A.	N.A.	
MW-14(3)	1.21	0.23	N.D.	N.D.	N.D.	N.D.	0.99	N.D.	N.D.	0.53	0.93	N.D.	N.D.	N.D.	N.D.	N.D.	0.56	N.A.	N.A.	N.A.	
MW-15(2)	1.72	0.92	N.D.	N.D.	N.D.	N.D.	2.02	N.D.	N.D.	1.05	N.D.	N.D.	N.D.	N.D.	2.44	N.D.	1.34	N.A.	N.A.	N.A.	
MW-16(2)	0.50	0.24	N.D.	N.D.	N.D.	N.D.	1.11	N.D.	N.D.	0.61	N.D.	N.D.	N.D.	N.D.	1.25	N.D.	0.95	N.A.	N.A.	N.A.	
MW-18(2)	0.01	N.D.	N.D.	N.D.	N.D.	N.D.	0.09	N.D.	N.D.	0.01	N.D.	0.10	N.D.	N.D.	N.D.	N.D.	N.D.	N.A.	N.A.	N.A.	
MW-19(2)	0.38	0.20	N.D.	N.D.	N.D.	N.D.	0.87	N.D.	N.D.	0.49	N.D.	N.D.	N.D.	N.D.	1.06	N.D.	1.0	N.A.	N.A.	N.A.	
MW-20(2)	0.39	0.33	N.D.	N.D.	N.D.	N.D.	0.89	N.D.	N.D.	0.47	N.D.	N.D.	N.D.	N.D.	1.05	N.D.	0.78	N.A.	N.A.	N.A.	
MW-21(2)	0.06	N.D.	N.D.	N.D.	N.D.	N.D.	0.88	N.D.	N.D.	0.45	N.D.	N.D.	N.D.	N.D.	1.08	N.D.	0.72	N.A.	N.A.	N.A.	
MW-22(2)	0.08	N.D.	N.D.	N.D.	N.D.	N.D.	0.89	N.D.	N.D.	0.45	N.D.	N.D.	N.D.	N.D.	1.10	N.D.	N.D.	N.A.	N.A.	N.A.	
MW-23(2)	N.D.	N.D.	N.D.	0.32	N.D.	0.01	0.44	N.D.	N.D.	0.11	N.D.	0.22	N.D.	N.D.	0.94	N.D.	0.69	N.A.	N.A.	N.A.	
MW-24(2)	0.08	N.D.	N.D.	N.D.	N.D.	N.D.	0.80	N.D.	N.D.	0.42	N.D.	N.D.	N.D.	N.D.	0.99	N.D.	N.D.	N.A.	N.A.	N.A.	

Well and field data for wells sampled at the Piney Point Complex.

Field trip #1

Well	Total Well Depth (ft)	Screened Interval (ft)	Field pH	Lab pH	Field EC u mhos	Lab EC u mhos	Measured TDS	Calculated TDS	Date of Collection
MW-1(1)	20.0	15.0 - 20.0	6.73	7.63	1030	1050	672	642	24-Mar-95
MW-3(1)	20.0	15.0 - 20.0	6.55	7.54	2550	2680	2288	2104	23-Mar-95
MW-4A(1)	20.0	15.0 - 20.0	6.91	7.59	1310	1250	868	826	24-Mar-95
MW-5(1)	20.0	15.0 - 20.0	7.06	7.74	1280	1300	920	854	24-Mar-95
USGS-9(1)	20.0	15.0 - 20.0	6.49	7.55	970	920	626	618	22-Mar-95

Field trip #2

Well	Total Well Depth (ft)	Screened Interval (ft)	Field pH	Lab pH	Field EC u mhos	Lab EC u mhos	Measured TDS	Calculated TDS	Date of Collection
MW-2(1)	17.0	12.0 - 17.0	5.91	3.49?	970	1050	732	638	11-May-95
PP 1-1(1)	62.3	52.3 - 62.3	2.19	2.34	16500	15000	22060	23227	9-May-95
PP 1-2(1)	45.0	35.0 - 45.0	2.24	2.35	16000	14000	20340	21685	9-May-95
PP 1-3(1)	35.0	25.0 - 35.0	2.38	2.44	14500	12300	18360	19589	10-May-95
PP 1-4(1)	25.0	15.0 - 25.0	2.40	2.46	14000	13000	18350	19536	10-May-95
D1	Stack base, drain		2.32	2.31	16400	17200	19560	21595	12-May-95
S1	Pond Surface		2.49	2.47	17900	16000	19740	21106	12-May-95

Field trip #3

Well	Total Well Depth (ft)	Screened Interval (ft)	Field pH	Lab pH	Field EC u mhos	Lab EC u mhos	Measured TDS	Calculated TDS	Date of Collection
PP 2-1(1)	55.0	45.0 - 55.0	2.35	2.31	18000	15000	21520	22771	11-Jun-95
PP 2-2(1)	45.0	35.0 - 45.0	2.35	2.19	17100	16000	21570	22047	12-Jun-95
PP 3-2(1)	45.0	35.0 - 45.0	2.47	2.41	14000	14500	17520	19059	12-Jun-95
PP 3-3(1)	35.0	25.0 - 35.0	2.54	2.44	13800	15000	18140	19424	12-Jun-95
S2	Pond Surface		2.54	2.64	16900	15000	17630	18561	12-Jun-95

Field trip #4									
Well	Total Well Depth (ft)	Screened Interval (ft)	Field pH	Lab pH	Field EC u mhos	Lab EC u mhos	Measured TDS	Calculated TDS	Date of Collection
PP 1-1(2)	62.3	52.3 - 62.3	2.56	2.34	16700	17000	20810	22694	22-Jul-95
PP 1-2(2)	45.0	35.0 - 45.0	2.57	2.39	15200	16000	19060	21154	22-Jul-95
PP 2-1(2)	55.0	45.0 - 55.0	2.37	2.35	18000	17000	21110	21540	21-Jul-95
PP 2-2(2)	45.0	35.0 - 45.0	2.48	2.39	17000	17000	19640	22147	21-Jul-95
Field trip #5									
Well	Total Well Depth (ft)	Screened Interval (ft)	Field pH	Lab pH	Field EC u mhos	Lab EC u mhos	Measured TDS	Calculated TDS	Collection
PP 1-1(3)	62.3	52.3 - 62.3	2.37	2.36	15900	13800	19810	20988	17-Nov-95
PP 1-2(3)	45.0	35.0 - 45.0	2.47	2.44	14800	13000	17150	18274	17-Nov-95
PP 1-3(2)	35.0	25.0 - 35.0	2.50	2.48	14600	13000	16120	17347	17-Nov-95
PP 1-4(2)	25.0	15.0 - 25.0	2.57	2.52	14100	13000	14850	15774	17-Nov-95
PP 2-1(3)	55.0	45.0 - 55.0	2.42	2.35	16000	15500	19780	19784	14-Nov-96
PP 2-3(3)	45.0	35.0 - 45.0	2.38	2.40	15400	15880	19020	20113	15-Nov-96
PP 3-2(3)	45.0	35.0 - 45.0	2.40	2.44	14700	14200	15650	17113	18-Nov-96
S3	Pond Surface		2.58	2.87	11200	13200	15175	16106	15-Nov-96
MW-1(2)	20.0	15.0 - 20.0	6.60	7.11	1010	945	596	598	15-Nov-96
MW-2(2)	17.0	12.0 - 17.0	5.85	3.19	1040	958	672	583	17-Nov-96
MW-3(2)	20.0	15.0 - 20.0	6.48	6.98	3200	2800	2555	2539	16-Nov-96
MW-4A(2)	20.0	15.0 - 20.0	6.84	7.49	1310	1360	928	877	16-Nov-96
MW-5(2)	20.0	15.0 - 20.0	7.00	7.62	1040	950	688	657	16-Nov-96
USGS-9(2)	20.0	15.0 - 20.0	6.42	6.72	1130	1380	864	799	16-Nov-96
Field trip #6		**No chemical anlayses performed for these samples**							
Well	Total Well Depth (ft)	Screened Interval (ft)	Field pH	Lab pH	Field EC u mhos	Lab EC u mhos	Measured TDS	Calculated TDS	Collection
PP 2-1 (4)	55.0	55.0-45.0	2.40	N.A.	15200	N.A.	N.A.	N.A.	7-Feb-96
PP 2-2 (4)	45.0	35.0-45.0	2.45	N.A.	14700	N.A.	N.A.	N.A.	7-Feb-96
MW-1 (3)	20.0	15.0-20.0	6.68	N.A.	970	N.A.	N.A.	N.A.	9-Feb-96
MW-2 (3)	17.0	12.0-17.0	5.84	N.A.	970	N.A.	N.A.	N.A.	8-Feb-96
MW-3 (3)	20.0	15.0-20.0	6.47	N.A.	3000	N.A.	N.A.	N.A.	8-Feb-96
MW-4A (3)	20.0	15.0-20.0	6.79	N.A.	1300	N.A.	N.A.	N.A.	8-Feb-96
USGS -9 (3)	20.0	15.0-20.0	6.40	N.A.	970	N.A.	N.A.	N.A.	8-Feb-96

Field trip #7									
Well	Total Well Depth (ft)	Screened Interval (ft)	Field pH	Lab pH	Field EC u mhos	Lab EC u mhos	Measured TDS	Calculated TDS	Collection
MW-8(1)	22.0	12.0-22.0	6.86	7.08	720	760	560	493	22-Mar-96
MW-9(1)	21.0	11.0-21.0	6.11	6.27	1210	1120	1155	969	22-Mar-96
MW-10(1)	24.0	14.0-24.0	6.25	6.68	9000	8450	6060	12558	24-Mar-96
MW-11(1)	24.0	14.0-24.0	6.34	6.68	4800	4200	3247	3897	24-Mar-96
MW-12(1)	16.0	6.0-16.0	3.48	3.35	8800	9500	13740	9534	24-Mar-96
MW-13(1)	25.0	15.0-25.0	6.30	6.61	12100	11000	7710	11072	25-Mar-96
MW-14(1)	22.0	12.0-22.0	6.40	6.89	8200	8450	5780	8097	25-Mar-96
MW-15(1)	25.0	15.0-25.0	6.33	6.67	10500	10600	6650	9177	25-Mar-96
MW-16(1)	22.0	12.0-22.0	6.21	6.67	6200	6550	6650	6112	26-Mar-96
MW-17(1)	21.0	11.0-21.0	6.61	6.86	2400	2400	1970	3171	26-Mar-96
PP 2-0(1)	72.0	66.8-71.8	2.35	2.29	15000	14000	19320	18758	27-Mar-96
PP 2-3(1)	35.0	25.0-35.0	2.52	2.47	12700	13000	14880	14996	26-Mar-96

Field trip #8									
Well	Total Well Depth (ft)	Screened Interval (ft)	Field pH	Lab pH	Field EC u mhos	Lab EC u mhos	Measured TDS	Calculated TDS	Collection
PP 2-0(2)	72.0	67.0-72.0	2.25	2.38	15200	16000	22330	24698	23-May-96
PP 2-3(2)	35.0	25.0-35.0	2.50	2.53	12000	12000	15245	16353	23-May-96
MW-18(1)	18.0	8.0-18.0	6.84	7.90	810	855	640	583	26-May-96
MW-19(1)	23.0	13.0-23.0	6.06	7.09	3420	3450	3080	3548	25-May-96
MW-20(1)	21.5	11.5-21.5	6.35	7.19	4700	4500	3407	3635	23-May-96
MW-21(1)	21.0	11.0-21.0	6.63	7.17	1620	1700	1015	1024	24-May-96
MW-22(1)	18.0	8.0-18.0	6.60	7.29	2100	1980	1825	1597	24-May-96
MW-23(1)	18.0	8.0-18.0	6.57	7.47	10000	13000	8920	7243	24-May-96
MW-24(1)	15.0	5.0-15.0	6.27	7.42	1440	1500	1285	1259	25-May-96

Field trip #9

Well	Total Well Depth (ft)	Screened Interval (ft)	Field pH	Lab pH	Field EC u mhos	Lab EC u mhos	Measured TDS	Calculated TDS	Collection
MW-8(3)	22.0	12.0-22.0	6.76	7.15	680	738	480	469	18-Sep-96
MW-9(3)	21.0	11.0-21.0	6.17	6.47	990	790	708	702	18-Sep-96
MW-11(3)	24.0	14.0-24.0	6.21	6.63	5100	6300	5180	5512	18-Sep-96
MW-13(3)	25.0	15.0-25.0	6.31	6.58	9900	11000	7885	10767	18-Sep-96
MW-14(3)	23.0	13.0-23.0	6.35	6.79	6800	8200	5200	6989	18-Sep-96
MW-15(2)	25.0	15.0-25.0	6.34	6.80	7900	11000	7000	9393	19-Sep-96
MW-16(2)	22.0	12.0-22.0	6.19	6.58	5000	6700	6160	5931	19-Sep-96
MW-18(2)	18.0	8.0-18.0	6.82	7.15	880	832	620	581	16-Sep-96
MW-19(2)	23.0	13.0-23.0	6.10	6.50	3110	3900	3567	3841	16-Sep-96
MW-20(2)	21.5	11.5-21.5	6.34	6.73	3820	4900	3393	3910	17-Sep-96
MW-21(2)	21.0	11.0-21.0	6.58	6.71	2000	2100	1225	1150	17-Sep-96
MW-22(2)	18.0	8.0-18.0	6.51	6.61	1800	1820	1785	1571	17-Sep-96
MW-23(2)	18.0	8.0-18.0	6.49	6.40	9800	13000	10080	8601	17-Sep-96
MW-24(2)	15.0	15.0-25.0	6.13	6.53	1200	1300	1270	867	17-Sep-96

Radiochemical results for wells sampled at Piney Point during 1995-96.

All activities given in dpm/L. N.A.= Not Analyzed; N.D.= Not Detected (below detection limit);

PP=Piney Point stack wells; MW and USGS= monitor wells around the stack; S= pond surface;

D= stack base; Numbers in parentheses indicate first, second, or third sampling of same well.

Field Trip #1, March 20-25, 1995

Well	^{238}U	±	^{234}U	±	^{226}Ra	±	^{222}Rn	±	^{210}Pb	±	^{210}Po	±	($^{210}Pb/^{226}Ra$) Ratio	±	($^{210}Po/^{210}Pb$) Ratio	±	Field pH	Field EC u mhos
MW-1(1)	N.A.	N.A.	N.A.	N.A.	3.82	0.25	407	27	1.10	0.10	0.72	0.01	0.29	0.03	0.65	0.06	6.73	1030
MW-3(1)	N.A.	N.A.	N.A.	N.A.	18.35	0.72	429	30	2.80	0.10	0.050	0.002	0.15	0.01	0.018	0.001	6.55	2550
MW-4A(1)	N.A.	N.A.	N.A.	N.A.	7.16	0.24	455	14	0.58	0.02	0.060	0.003	0.081	0.004	0.10	0.01	6.91	1310
MW-5(1)	N.A.	N.A.	N.A.	N.A.	6.11	0.25	3054	33	0.45	0.04	0.74	0.03	0.07	0.01	1.64	0.16	7.06	1280
USGS-9(1)	N.A.	N.A.	N.A.	N.A.	1.99	0.31	16325	135	2.21	0.04	0.94	0.03	1.11	0.17	0.43	0.02	6.49	970

Fieldtrip #2, May 3-8, 1995.

Well	^{238}U	±	^{234}U	±	^{226}Ra	±	^{222}Rn	±	^{210}Pb	±	^{210}Po	±	($^{210}Pb/^{226}Ra$) Ratio	±	($^{210}Po/^{210}Pb$) Ratio	±	Field pH	Field EC u mhos
MW-2(1)	N.A.	N.A.	N.A.	N.A.	2.46	0.19	12967	122	4.02	0.16	2.46	0.06	1.64	0.14	0.612	0.029	5.91	970
PP 1-1(1)	N.A.	N.A.	N.A.	N.A.	6.46	0.22	34536	154	1152	12	15.8	0.2	178.37	6.42	1.4E-02	2.2E-04	2.19	16500
PP 1-2(1)	N.A.	N.A.	N.A.	N.A.	5.33	0.49	21497	271	1034	14	34.3	0.3	193.82	18.02	0.033	0.001	2.24	16000
PP 1-3(1)	N.A.	N.A.	N.A.	N.A.	6.15	0.52	19002	373	735	7	12.3	0.1	119.51	10.10	1.7E-02	2.1E-04	2.38	14500
PP 1-4(1)	N.A.	N.A.	N.A.	N.A.	16.41	1.02	27492	338	404	4	11.5	0.2	24.62	1.55	0.028	0.001	2.40	14000
D1	N.A.	N.A.	N.A.	N.A.	6.60	0.60	17440	356	1937	14	8.3	0.1	293.26	26.60	4.3E-03	6.0E-05	2.32	16400
S1	N.A.	N.A.	N.A.	N.A.	6.12	0.56	87	3	450	3	67.8	0.7	73.59	6.70	0.151	0.002	2.49	17900

Fieldtrip #3, June 8-12, 1995.

Well	^{238}U	±	^{234}U	±	^{226}Ra	±	^{222}Rn	+/-	^{210}Pb	±	^{210}Po	±	($^{210}Pb/^{226}Ra$) Ratio	±	($^{210}Po/^{210}Pb$) Ratio	±	Field pH	Field EC u mhos
PP 2-1(1)	N.A.	N.A.	N.A.	N.A.	6.10	0.32	62235	728	3867	22	325.5	6.9	634.45	33.51	0.084	0.002	2.35	18000
PP 2-2(1)	N.A.	N.A.	N.A.	N.A.	7.49	0.29	75401	1403	3531	24	59.7	0.5	471.63	18.58	0.017	0.000	2.35	17100
PP 3-2(1)	N.A.	N.A.	N.A.	N.A.	8.34	0.16	34709	634	475	7	41.6	0.4	56.91	1.34	0.088	0.001	2.47	14000
PP 3-3(1)	N.A.	N.A.	N.A.	N.A.	9.24	0.09	46666	1149	381	5	30.8	0.3	41.21	0.70	0.081	0.001	2.54	13800
S2	N.A.	N.A.	N.A.	N.A.	6.13	0.46	244	11	170	6	33.0	0.4	27.82	2.29	0.19	0.01	2.54	16900

Fieldtrip #4, July 17-22, 1995.

Well	^{238}U	±	^{234}U	±	^{226}Ra	±	^{222}Rn	±	^{210}Pb	±	^{210}Po	±	($^{210}Pb/^{226}Ra$) Ratio	±	($^{210}Po/^{210}Pb$) Ratio	±	Field pH	Field EC u mhos
PP 1-1(2)	1867	43	1999	46	5.05	0.32	34315	426	1058.8	31.8	48.4	0.8	209.5	14.6	0.046	0.002	2.56	16700
PP 1-2(2)	902	15	902	15	4.54	0.36	20455	228	1652.0	22.1	17.3	0.3	364.1	29.5	1.0E-02	2.3E-04	2.57	15200
PP 2-1(2)	N.A.	N.A.	N.A.	N.A.	4.90	0.57	61739	571	N.A.	N.A.	153.0	1.5	N.A.	N.A.	N.A.	N.A.	2.37	18000
PP 2-2(2)	1715	99	1733	100	5.74	0.16	67700	570	N.A.	N.A.	138.1	1.4	N.A.	N.A.	N.A.	N.A.	2.48	17000

Fieldtrip #5, November 13-18, 1995.

Well	^{238}U	±	^{234}U	±	^{226}Ra	±	^{222}Rn	±	^{210}Pb	±	^{210}Po	±	($^{210}Pb/^{226}Ra$) Ratio	±	($^{210}Po/^{210}Pb$) Ratio	±	Field pH	Field EC u mhos
PP 1-1(3)	1060.9	8.6	1090.4	8.8	4.60	0.30	34817	554	1073	18	8.0	0.1	233.2	15.7	7.5E-03	1.6E-04	2.37	15900
PP 1-2(3)	779.1	12.0	833.3	12.4	5.53	0.21	22949	422	1036	21	4.4	0.1	187.18	8.11	4.2E-03	9.9E-05	2.47	14800
PP 1-3(2)	664.5	10.9	727.0	11.4	7.81	0.46	20881	150	748	15	557.8	5.1	95.79	5.91	0.75	0.02	2.50	14600
PP 1-4(2)	589:8	5.7	613.0	5.8	16.34	0.25	27377	621	319	6	2.08	0.02	19.54	0.48	6.5E-03	1.4E-04	2.57	14100
PP 2-1(3)	1051.7	11.3	1159.0	11.9	5.46	0.43	69556	854	2965	35	17.7	0.2	543.6	43.5	6.0E-03	9.7E-05	2.42	16000
PP 2-3(3)	952.9	8.8	1002.8	9.1	6.55	0.45	78083	358	3154	61	2506.9	16.2	481.5	34.5	5.1E-03	1.1E-04	2.38	15400
PP 3-2(3)	744.6	7.5	757.5	7.6	7.86	0.20	39371	177	632	11	6.3	0.1	80.47	2.50	9.9E-03	2.0E-04	2.40	14700
S3	589.9	8.5	604.2	8.6	11.15	0.27	51	37	262	6	59.6	0.6	23.53	0.77	0.23	0.01	2.58	11200
MW-1(2)	0.67	0.04	0.83	0.05	4.44	0.26	9929	99	2.81	0.38	1.47	0.03	0.63	0.09	0.52	0.07	6.60	1010
MW-2(2)	0.29	0.03	0.32	0.03	2.30	0.13	14850	181	3.49	0.38	2.73	0.04	1.52	0.19	0.78	0.09	5.85	1040
MW-3(2)	0.11	0.01	0.12	0.02	26.69	1.67	3481	164	1.09	0.25	0.44	0.01	0.04	0.01	0.40	0.09	6.48	3200
MW-4A(2)	0.12	0.01	0.13	0.01	7.72	0.25	3543	106	1.35	0.39	0.44	0.02	0.17	0.05	0.33	0.10	6.84	1310
MW-5(2)	3.28	0.21	4.25	0.25	5.60	0.27	3200	100	0.64	0.19	0.65	0.01	0.11	0.03	1.02	0.30	7.00	1040
USGS-9(2)	0.05	0.01	0.05	0.01	2.61	0.40	16560	793	2.21	0.21	1.71	0.03	0.85	0.15	0.77	0.07	6.42	1130

Fieldtrip #6, Feb. 4-9, 1996.

Well	^{238}U	±	^{234}U	±	^{226}Ra	±	^{222}Rn	±	^{210}Pb	±	^{210}Po	±	($^{210}Pb/^{226}Ra$) Ratio	±	($^{210}Po/^{210}Pb$) Ratio	±	Field pH	Field EC u mhos
PP 2-1 (4)	915.8	10.9	999.0	11.3	5.53	0.50	37527	412	3136	52	13.15	0.14	567.0	51.6	4.2E-03	8.3E-05	2.40	15200
PP 2-2 (4)	800.5	9.5	845.3	9.7	6.13	0.29	75105	419	2617	21	5.00	0.10	426.9	20.3	1.9E-03	4.1E-05	2.45	14700
MW-1 (3)	0.11	0.02	0.16	0.02	2.64	0.31	7325	172	1.28	0.29	0.68	0.02	0.48	0.12	0.53	0.12	6.68	970
MW-2 (3)	0.78	0.05	0.89	0.05	1.84	0.03	14864	295	3.16	0.31	2.11	0.04	1.72	0.17	0.67	0.07	5.84	970
MW-3 (3)	0.07	0.01	0.17	0.02	21.46	1.42	3263	39	1.07	0.27	0.75	0.05	0.05	0.01	0.70	0.18	6.47	3000
MW-4A (3)	0.13	0.03	0.21	0.02	7.42	0.17	3142	66	1.21	0.22	0.33	0.02	0.16	0.03	0.27	0.05	6.79	1300
USGS -9 (3)	0.04	0.01	0.05	0.01	1.84	0.18	16916	122	1.70	0.34	1.64	0.06	0.92	0.21	0.96	0.20	6.40	970

Fieldtrip #7, March 17-27, 1996.

Well	^{238}U	±	^{234}U	±	^{226}Ra	±	^{222}Rn	±	^{210}Pb	±	^{210}Po	±	($^{210}Pb/^{226}Ra$) Ratio	±	($^{210}Po/^{210}Pb$) Ratio	±	Field pH	Field EC u mhos
MW 8 (1)	0.04	0.01	0.07	0.01	1.13	0.05	4060	20	0.62	0.20	4.06	0.08	0.55	0.18	6.55	2.12	6.86	720
MW 9 (1)	2.83	0.06	3.00	0.07	7.43	0.29	24831	296	4.63	0.28	12.64	0.15	0.62	0.04	2.73	0.17	6.11	1210
MW 10 (1)	1.38	0.05	1.33	0.05	2.51	0.29	6866	147	1.15	0.32	3.39	0.04	0.46	0.14	2.95	0.82	6.25	9000
MW 11 (1)	0.10	0.02	0.11	0.02	2.24	0.30	6869	171	0.93	0.12	0.49	0.02	0.42	0.08	0.53	0.07	6.34	4800
MW 12 (1)	303.9	7.3	305.7	7.3	3.40	0.39	4834	136	30.98	1.82	7.07	0.13	9.11	1.18	0.23	0.01	3.48	8800
MW 13 (1)	0.19	0.02	0.17	0.02	0.86	0.05	7448	306	0.91	0.30	0.97	0.08	1.06	0.35	1.07	0.36	6.30	12100
MW 14 (1)	0.09	0.01	0.09	0.01	3.89	0.13	4342	83	0.47	0.24	1.52	0.07	0.12	0.06	3.23	1.66	6.40	8200
MW 15 (1)	0.09	0.01	0.08	0.01	7.95	0.30	251	37	0.34	0.13	2.22	0.05	0.04	0.02	6.53	2.50	6.33	10500
MW 16 (1)	0.45	0.02	0.52	0.02	49.90	2.82	1101	46	1.01	0.26	0.32	0.01	0.02	0.01	0.32	0.08	6.21	6200
MW 17 (1)	0.34	0.03	0.84	0.05	31.36	1.35	2296	45	0.61	0.18	2.5E-03	4.0E-04	0.02	0.01	0.004	0.001	6.61	2400
PP 2-0 (1)	1675.8	7.8	1741.9	7.9	13.21	0.39	26046	337	1699	25	3.14	0.03	128.68	4.22	1.8E-03	3.2E-05	2.35	15000
PP 2-3 (1)	574.6	5.6	579.2	9.7	18.49	0.36	58256	665	1299	25	N.D.	N.D.	70.28	1.92	N.D.	N.D.	2.52	12700

Fieldtrip #8, May 22-30, 1996.

Well	^{238}U	±	^{234}U	±	^{226}Ra	±	^{222}Rn	±	^{210}Pb	±	^{210}Po	±	($^{210}Pb/^{226}Ra$) Ratio	±	($^{210}Po/^{210}Pb$) Ratio	±	Field pH	Field EC u mhos
PP 2-0 (2)	1756.2	9.0	1857.2	9.2	9.87	0.39	17898	240	2083.2	10.6	17.8	0.20	211.06	8.35	0.0085	0.0001	2.25	15200
PP 2-3 (2)	737.9	7.9	784.7	8.2	11.29	0.29	59014	730	1094.5	20.6	0.67	0.01	96.95	3.09	6.1E-04	1.5E-05	2.50	12000
MW 8 (2)	0.43	0.03	0.44	0.03	2.16	0.10	4165	43	0.93	0.44	3.01	0.06	0.43	0.20	3.24	1.53	6.99	700
MW 9 (2)	1.65	0.06	1.72	0.06	7.01	0.21	23359	819	5.02	1.11	9.96	0.14	0.72	0.16	1.98	0.44	6.14	880
MW 10 (2)	0.33	0.03	0.36	0.03	0.70	0.05	5543	241	0.71	0.37	4.35	0.09	1.01	0.53	6.13	3.20	6.28	7100
MW 11 (2)	0.10	0.01	0.10	0.01	5.70	0.18	7245	260	0.83	0.12	0.37	0.02	0.15	0.02	0.45	0.07	6.31	4140
MW 12 (2)	265.8	6.90	272.2	7.1	9.11	0.25	4036	118	22.89	0.85	N.A.	N.A.	2.51	0.12	N.A.	N.A.	3.19	9000
MW 13 (2)	0.08	0.01	0.11	0.02	2.09	0.10	7099	208	0.62	0.22	0.40	0.01	0.30	0.11	0.65	0.23	6.26	10100
MW 14 (2)	0.75	0.70	0.04	0.50	5.89	0.19	4441	51	0.73	0.21	3E-02	0E+00	0.12	0.04	0.04	0.01	6.42	6800
MW 18 (1)	0.22	0.02	0.21	0.02	5.45	0.17	4948	193	0.80	0.25	2E-02	0E+00	0.15	0.05	0.03	0.01	6.84	810
MW 19 (1)	0.04	0.01	0.13	0.02	18.21	0.42	3053	191	0.26	0.29	0.23	0.02	0.01	0.02	0.88	0.99	6.06	3420
MW 20 (1)	0.25	0.02	0.28	0.03	5.17	0.17	4209	33	0.40	0.72	1.26	0.03	0.08	0.14	3.15	5.67	6.35	4700
MW 21 (1)	0.17	0.01	0.40	0.02	1.32	0.07	12799	693	0.03	0.26	0.35	0.02	0.02	0.20	11.67	101.11	6.66	1620
MW 22 (1)	17.7	0.5	17.4	0.5	27.6	0.6	6452	386	0.95	0.03	5.01	0.09	0.034	0.001	5.27	0.19	6.60	2100
MW 23 (1)	0.22	0.01	0.39	0.02	148.7	2.9	8855	374	1.35	0.23	1.69	0.05	0.009	0.002	1.25	0.22	6.57	10000
MW 24 (1)	0.23	0.02	0.25	0.02	5.9	0.2	8255	202	0.94	0.17	0.73	0.03	0.16	0.03	0.78	0.14	6.27	1440

Fieldtrip #9, Sept. 16-20, 1996.

Well	^{238}U	±	^{234}U	±	^{226}Ra	±	^{222}Rn	±	^{210}Pb	±	^{210}Po	±	($^{210}Pb/^{226}Ra$) Ratio	±	($^{210}Po/^{210}Pb$) Ratio	±	Field pH	Field EC u mhos
MW 8 (3)	0.74	0.04	0.79	0.04	1.86	0.08	4071	168	1.06	0.20	4.36	0.08	0.57	0.11	4.11	0.78	6.76	6800
MW 9 (3)	1.90	0.08	1.89	0.08	6.77	0.20	23501	344	3.91	0.37	11.87	0.15	0.58	0.06	3.04	0.29	6.17	990
MW 11 (3)	0.05	0.01	0.05	0.01	2.35	0.10	7282	215	1.04	0.17	0.20	0.02	0.44	0.07	0.20	0.04	6.21	5100
MW 13 (3)	0.05	0.01	0.06	0.01	2.19	0.10	7365	277	0.74	0.15	1.49	0.05	0.34	0.07	2.01	0.41	6.31	9900
MW 14 (3)	0.08	0.02	0.06	0.02	5.76	0.18	4220	22	0.45	0.11	0.35	0.02	0.08	0.02	0.77	0.20	6.35	6800
MW 15 (2)	0.08	0.02	0.05	0.02	9.16	0.25	177	66	0.11	0.11	0.20	0.02	0.01	0.01	1.85	1.86	6.34	7900
MW 16 (2)	2.08	0.07	2.24	0.07	42.02	0.87	522	29	0.38	0.18	0.05	0.01	0.009	0.004	0.13	0.07	6.19	5000
MW 18 (2)	0.15	0.02	0.14	0.02	4.87	0.15	3707	163	0.94	0.21	N.A.	N.A.	0.19	0.04	N.A.	N.A.	6.82	880
MW 19 (2)	0.08	0.01	0.08	0.01	33.30	0.70	2822	118	0.70	0.32	0.07	0.02	0.02	0.01	0.10	0.05	6.10	3110
MW 20 (2)	0.23	0.03	0.18	0.03	10.40	0.26	4080	94	0.96	0.21	1.27	0.04	0.09	0.02	1.32	0.29	6.34	3820
MW 21 (2)	1.99	0.09	2.11	0.09	6.47	0.19	12399	332	2.37	0.25	0.38	0.02	0.37	0.04	0.16	0.02	6.58	2000
MW 22 (2)	15.30	0.41	14.86	0.40	24.96	0.54	6739	318	1.78	0.20	5.70	0.12	0.07	0.01	3.20	0.37	6.51	1800
MW 23 (2)	0.12	0.02	0.26	0.03	171.3	3.3	8525	507	1.75	0.19	0.35	0.02	0.010	0.001	0.20	0.02	6.49	9800
MW 24 (2)	0.15	0.02	0.15	0.02	7.04	0.20	6337	314	1.30	0.21	2.21	0.06	0.18	0.03	1.70	0.28	6.13	1200

PP core data 1-1		dpm/g			dpm/g			dpm/g			dpm/g								
Sample	Mean Depth	^{238}U			^{226}Ra			^{210}Pb			^{210}Po			^{210}Pb/^{226}Ra			^{210}Po/^{210}Pb		
			±			±			±			±			±			±	
Gyp-86	18.92	3.35	±	0.26	27.8	±	0.1	44.1	±	0.4	29.1	±	0.3	1.586	±	0.015	0.660	±	0.009
Gyp-85	22.76	3.16	±	0.39	23.2	±	0.2	35.4	±	0.6	25.7	±	0.4	1.528	±	0.028	0.726	±	0.017
Gyp-84	28.16	6.20	±	0.34	27.4	±	0.1	58.9	±	0.5	47.1	±	0.5	2.150	±	0.020	0.800	±	0.011
Gyp-83	31.27	3.66	±	0.28	40.3	±	0.3	59.6	±	0.8	21.0	±	0.2	1.479	±	0.023	0.352	±	0.006
Gyp-82	36.79	4.15	±	0.57	38.6	±	0.3	43.8	±	0.8	30.2	±	0.3	1.135	±	0.023	0.689	±	0.014
Gyp-81	41.30	3.55	±	0.41	31.7	±	0.3	39.2	±	0.5	31.0	±	0.3	1.237	±	0.020	0.791	±	0.013
Gyp-80	47.58	3.92	±	0.43	38.1	±	0.4	44.4	±	0.5	26.8	±	0.4	1.165	±	0.018	0.604	±	0.011
Gyp-79	54.07	5.11	±	0.62	77.1	±	0.8	57.7	±	0.7	36.3	±	0.4	0.749	±	0.012	0.629	±	0.010
Gyp-106	59.48	2.80	±	0.27	29.2	±	0.1	38.2	±	0.4	25.7	±	0.2	1.307	±	0.013	0.672	±	0.009
Gyp-107	59.69	29.72	±	0.00	1097.6	±	6.0	516.9	±	4.2	101.6	±	0.9	0.471	±	0.005	0.197	±	0.002
Gyp-108	59.86	3.96	±	0.33	37.3	±	0.2	41.3	±	0.5	27.3	±	0.3	1.108	±	0.014	0.661	±	0.011
Gyp-78	61.45	2.75	±	0.45	40.8	±	0.3	45.8	±	0.6	31.1	±	0.4	1.123	±	0.017	0.679	±	0.012
Gyp-76	62.67	137.60	±	2.57	41.4	±	0.6	176.3	±	2.4	158.8	±	1.6	4.257	±	0.085	0.901	±	0.015
Gyp-75	63.19	3.91	±	0.17	3.4	±	0.1	48.1	±	0.4	39.5	±	0.4	14.147	±	0.432	0.821	±	0.011
Gyp-77	63.50	5.74	±	0.62	98.7	±	0.5	64.7	±	0.8	54.8	±	0.6	0.655	±	0.009	0.847	±	0.014
PP core data 2-2																			
Sample	Mean Depth	^{238}U			^{226}Ra			^{210}Pb			^{210}Po			^{210}Pb/^{226}Ra			^{210}Po/^{210}Pb		
			±			±			±			±			±			±	
gyp-124	14.75	2.43	±	1.17	59.30	±	0.20	56.40	±	0.60	59.66	±	0.47	0.951	±	0.011	1.058	±	0.014
gyp-123	19.75	4.22	±	0.46	45.28	±	0.32	44.80	±	1.03	39.60	±	1.15	0.989	±	0.024	0.884	±	0.033
gyp-122	27.33	8.40	±	0.59	121.80	±	0.40	96.20	±	0.70	62.15	±	1.47	0.790	±	0.006	0.646	±	0.016
gyp-121	35.50	5.12	±	0.81	42.88	±	0.31	51.25	±	1.00	41.60	±	0.58	1.195	±	0.025	0.812	±	0.019
gyp-120	42.00	4.30	±	0.49	43.90	±	0.30	48.30	±	0.60	40.93	±	0.31	1.100	±	0.016	0.847	±	0.012
gyp-119	48.90	4.28	±	0.49	49.10	±	0.20	51.10	±	0.60	10.50	±	0.20	1.041	±	0.013	0.205	±	0.005
gyp-118	54.55	4.77	±	0.41	32.70	±	0.10	49.50	±	0.60	33.30	±	0.50	1.514	±	0.019	0.673	±	0.013
gyp-117	56.05	21.70	±	2.10	491.00	±	0.80	278.60	±	0.30	277.00	±	3.10	0.567	±	0.001	0.994	±	0.011
gyp-116	56.95	4.47	±	0.42	32.60	±	0.20	48.70	±	0.60	46.90	±	0.50	1.494	±	0.021	0.963	±	0.016
gyp-115	58.65	3.38	±	0.48	36.00	±	0.20	42.30	±	0.60	60.10	±	0.70	1.175	±	0.018	1.421	±	0.026
gyp-114	62.61	4.21	±	0.21	23.10	±	0.10	39.10	±	0.30	39.70	±	0.40	1.693	±	0.015	1.015	±	0.013
gyp-112	64.05	50.80	±	0.20	1.19	±	0.01	72.00	±	0.40	49.50	±	0.50	60.504	±	0.610	0.688	±	0.008
gyp-113	64.74	59.60	±	1.90	1.32	±	0.16	69.80	±	3.70	66.38	±	1.05	52.879	±	6.996	0.951	±	0.053
gyp-111	65.69	17.20	±	0.40	7.10	±	0.10	19.20	±	0.40	17.40	±	0.20	2.704	±	0.068	0.906	±	0.022
gyp-110	69.87	56.80	±	0.70	28.80	±	0.10	33.40	±	0.60	28.90	±	0.30	1.160	±	0.021	0.865	±	0.018
gyp-109	72.91	64.80	±	0.40	16.80	±	0.20	19.30	±	0.40	23.20	±	0.30	1.149	±	0.027	1.202	±	0.029

Sample	^{238}U dpm/g	^{226}Ra dpm/g	^{210}Pb dpm/g	^{210}Po dpm/g	^{210}Pb/^{226}Ra	^{210}Po/^{210}Pb
Southern Wall Stratigraphic Samples Collected 12 May 1995						
Gyp-88	1.75 ± 0.15	0.8 ± 0.1	2.4 ± 0.2	2.4 ± 0.1	3.00 ± 0.29	0.98 ± 0.08
Gyp-89	3.39 ± 0.34	32.7 ± 0.4	41.9 ± 0.5	29.0 ± 0.3	1.28 ± 0.02	0.69 ± 0.01
Gyp-90	3.77 ± 0.53	40.3 ± 0.2	58.0 ± 0.7	29.4 ± 0.4	1.44 ± 0.02	0.51 ± 0.01
Gyp-91	8.41 ± 0.35	35.6 ± 0.1	48.3 ± 0.5	32.7 ± 0.4	1.36 ± 0.01	0.68 ± 0.01
Gyp-92	4.65 ± 0.47	33.8 ± 0.3	46.7 ± 0.7	30.7 ± 0.4	1.38 ± 0.02	0.66 ± 0.01
Gyp-93	1.52 ± 0.47	47.2 ± 0.1	50.7 ± 0.7	34.2 ± 0.4	1.07 ± 0.02	0.67 ± 0.01
Western Wall Stratigraphic Samples Collected 13 March 1995						
Gyp-71	4.26 ± 0.26	34.3 ± 0.4	70.9 ± 0.4	52.2 ± 0.7	2.067 ± 0.027	0.736 ± 0.011
Gyp-72	4.06 ± 0.43	35.1 ± 0.1	38.8 ± 0.5	29.8 ± 0.4	1.106 ± 0.016	0.769 ± 0.015
Gyp-73	3.27 ± 0.28	28.1 ± 0.1	35.5 ± 0.5	27.0 ± 0.3	1.262 ± 0.018	0.761 ± 0.014
Gyp-74	4.01 ± 0.41	29.0 ± 0.1	41.9 ± 0.6	31.4 ± 0.3	1.446 ± 0.021	0.749 ± 0.013

Sediment cuttings from monitor wells

WELL	SAMPLE DEPTH	^{238}U dpm/g	^{226}Ra dpm/g	^{210}Pb dpm/g	^{210}Po dpm/g	^{210}Pb/^{226}Ra	^{210}Po/^{210}Pb	^{232}Th dpm/g	^{40}K dpm/g
MW-8	19.0	19.46 ± 2.40	13.34 ± 0.15	15.79 ± 0.51	14.17 ± 0.13	1.18 ± 0.04	0.90 ± 0.03	0.79 ± 0.18	4.81 ± 0.37
MW-9	21.0	18.48 ± 2.34	13.18 ± 0.15	16.67 ± 0.62	13.54 ± 0.25	1.26 ± 0.05	0.81 ± 0.03	0.47 ± 0.16	0.35 ± mda
MW-9	16.0-17.0	18.12 ± 2.31	13.46 ± 0.15	16.36 ± 0.55	14.39 ± 0.15	1.22 ± 0.04	0.88 ± 0.03	1.08 ± 0.17	11.70 ± 0.56
MW-10	16.0	35.76 ± 4.34	25.10 ± 0.25	28.60 ± 0.80	26.14 ± 0.21	1.14 ± 0.03	0.91 ± 0.03	0.79 ± 0.27	4.98 ± 0.51
MW-10	19.0-20.0	16.98 ± 2.04	11.80 ± 0.10	14.21 ± 0.35	12.21 ± 0.26	1.20 ± 0.03	0.86 ± 0.03	1.17 ± 0.08	15.32 ± 0.33
MW-11	22.0-23.0	21.48 ± 2.70	13.82 ± 0.40	17.84 ± 0.57	14.89 ± 0.27	1.29 ± 0.06	0.83 ± 0.03	0.49 ± 0.20	6.11 ± 0.42
MW-12	12.0	18.98 ± 2.10	6.35 ± 0.06	10.68 ± 0.27	9.19 ± 0.11	1.68 ± 0.05	0.86 ± 0.02	0.37 ± 0.07	1.70 ± 0.15
MW-13	15.0	18.02 ± 2.26	13.61 ± 0.15	15.01 ± 0.57	14.83 ± 0.27	1.10 ± 0.04	0.99 ± 0.04	0.78 ± 0.18	2.84 ± 0.39
MW-13	23.0-24.0	15.07 ± 1.87	11.65 ± 0.16	13.82 ± 0.59	11.99 ± 0.29	1.19 ± 0.05	0.87 ± 0.04	0.56 ± 0.17	8.53 ± 0.47
MW-14	21.0	15.99 ± 2.01	15.31 ± 0.27	16.31 ± 0.53	14.90 ± 0.26	1.07 ± 0.04	0.91 ± 0.03	0.66 ± 0.13	5.84 ± 0.55
MW-15	24.0	10.03 ± 1.24	7.10 ± 0.10	7.83 ± 0.41	6.06 ± 0.19	1.10 ± 0.06	0.77 ± 0.05	0.33 ± 0.12	1.31 ± 0.25
MW-16	19.0-20.0	8.69 ± 1.12	6.43 ± 0.11	7.21 ± 0.35	7.18 ± 0.14	1.12 ± 0.06	1.00 ± 0.05	0.27 ± 0.11	2.14 ± 0.30
MW-17	19.0	21.40 ± 2.73	15.74 ± 0.32	17.77 ± 0.70	15.89 ± 0.14	1.13 ± 0.05	0.89 ± 0.04	1.37 ± 0.19	13.37 ± 0.74
MW-17	Phosphate Pebb.2	54.10 ± 2.75	37.73 ± 0.32	38.74 ± 1.04	38.70 ± 0.48	1.03 ± 0.03	1.00 ± 0.03	1.01 ± 0.24	3.22 ± 0.57
MW-17	Phosphate Pebb.	54.92 ± 6.60	37.48 ± 0.63	36.87 ± 0.84	38.77 ± 0.48	0.98 ± 0.03	1.05 ± 0.03	0.75 ± 0.15	4.43 ± 0.38
MW-18	18.0	32.54 ± 3.92	20.31 ± 0.40	21.29 ± 0.63	18.86 ± 0.29	1.05 ± 0.04	0.89 ± 0.03	0.54 ± 0.18	2.19 ± 0.52
MW-19	23.0	9.09 ± 1.51	9.21 ± 0.12	10.45 ± 0.42	8.86 ± 0.23	1.13 ± 0.05	0.85 ± 0.04	0.64 ± 0.12	1.11 ± 0.33
MW-19	16.0-18.0	13.83 ± 1.84	10.89 ± 0.14	10.47 ± 0.46	11.18 ± 0.22	0.96 ± 0.04	1.07 ± 0.05	0.56 ± 0.16	1.65 ± 0.41
MW-20	20.0	18.31 ± 2.38	13.40 ± 0.12	15.30 ± 0.40	13.33 ± 0.34	1.14 ± 0.03	0.87 ± 0.03	0.90 ± 0.10	9.96 ± 0.35
MW-20	21.5	12.94 ± 1.79	26.19 ± 0.25	34.51 ± 0.89	34.84 ± 0.23	1.32 ± 0.04	1.01 ± 0.03	0.90 ± 0.22	1.46 ± 0.49
MW-21	20.0-21.0	41.56 ± 5.16	31.34 ± 0.27	34.93 ± 0.90	33.45 ± 0.45	1.11 ± 0.03	0.96 ± 0.03	0.56 ± 0.23	4.09 ± 0.55
MW-22	18.0	22.54 ± 2.73	16.36 ± 0.17	20.04 ± 0.59	17.67 ± 0.39	1.22 ± 0.04	0.88 ± 0.03	0.31 ± 0.17	2.16 ± 0.38
MW-23	18.0	23.13 ± 2.89	17.86 ± 0.22	20.84 ± 0.62	18.78 ± 0.13	1.17 ± 0.04	0.90 ± 0.03	0.49 ± 0.18	1.80 ± 0.49
MW-23	16.0	28.07 ± 3.50	20.97 ± 0.38	23.75 ± 0.66	24.05 ± 0.40	1.13 ± 0.04	1.01 ± 0.03	0.84 ± 0.18	3.89 ± 0.49
MW-24	9.0-10.0	28.86 ± 3.52	22.72 ± 0.18	25.37 ± 0.51	23.21 ± 0.19	1.12 ± 0.02	0.91 ± 0.02	0.73 ± 0.10	2.86 ± 0.22

APPENDICES

CHAPTER 3

Output Summary from MINTEQA2

MAJOR COMPONENTS - BACKGROUND WELL
(model MW 1, Trip 1)

Temperature (Celsius): 25.00
Units of concentration: PPM
Ionic strength to be computed.
If specified, carbonate concentration represents total inorganic carbon.
Do not automatically terminate if charge imbalance exceeds 30%
Precipitation is allowed for all solids in the thermodynamic database and
the print option for solids is set to: 1
The maximum number of iterations is: 40
The method used to compute activity coefficients is: Davies equation
Intermediate output file

INPUT DATA BEFORE TYPE MODIFICATIONS

ID	NAME	ACTIVITY GUESS	LOG GUESS	ANAL TOTAL
330	H+1	1.862E-07	-6.730	0.000E-01
500	Na+1	4.074E-03	-2.390	9.400E+01
410	K+1	1.288E-04	-3.890	5.000E+00
150	Ca+2	2.042E-03	-2.690	8.100E+01
460	Mg+2	1.660E-03	-2.780	4.000E+01
140	CO3-2	8.128E-03	-2.090	4.850E+02
180	Cl-1	2.455E-03	-2.610	8.800E+01
732	SO4-2	5.754E-04	-3.240	5.500E+01
2	H2O	1.000E+00	0.000	0.000E-01

PERCENTAGE DISTRIBUTION OF COMPONENTS AMONG
TYPE I and TYPE II (dissolved and adsorbed) species

SO4-2

79.2 PERCENT BOUND IN SPECIES # 732 SO4-2

11.5 PERCENT BOUND IN SPECIES #1507320 CaSO4 AQ

8.2 PERCENT BOUND IN SPECIES #4607320 MgSO4 AQ

Na+l

99.6 PERCENT BOUND IN SPECIES # 500 Na+l

K+l

99.8 PERCENT BOUND IN SPECIES # 410 K+l

Ca+2

93.2 PERCENT BOUND IN SPECIES # 150 Ca+2

3.5 PERCENT BOUND IN SPECIES #1501400 CaHCO3 +

3.3 PERCENT BOUND IN SPECIES #1507320 CaSO4 AQ

Mg+2

93.2 PERCENT BOUND IN SPECIES # 460 Mg+2

3.9 PERCENT BOUND IN SPECIES #4601401 MgHCO3 +

2.9 PERCENT BOUND IN SPECIES #4607320 MgSO4 AQ

CO3-2

71.7 PERCENT BOUND IN SPECIES #3301400 HCO3 -

26.5 PERCENT BOUND IN SPECIES #3301401 H2CO3 AQ

Cl-1

100.0 PERCENT BOUND IN SPECIES # 180 Cl-1

H2O

84.4 PERCENT BOUND IN SPECIES #3300020 OH-

2.5 PERCENT BOUND IN SPECIES #1503300 CaOH +

13.1 PERCENT BOUND IN SPECIES #4603300 MgOH +

H+1

56.7 PERCENT BOUND IN SPECIES #3301400 HCO3 -

41.9 PERCENT BOUND IN SPECIES #3301401 H2CO3 AQ

---------- EQUILIBRATED MASS DISTRIBUTION ----------

IDX	NAME	DISSOLVED		SORBED		PRECIPITATED	
		MOL/KG	PERCENT	MOL/KG	PERCENT	MOL/KG	PERCENT
732	SO4-2	5.730E-04	100.0	0.000E-01	0.0	0.000E-01	0.0
500	Na+1	4.092E-03	100.0	0.000E-01	0.0	0.000E-01	0.0
410	K+1	1.280E-04	100.0	0.000E-01	0.0	0.000E-01	0.0
150	Ca+2	2.023E-03	100.0	0.000E-01	0.0	0.000E-01	0.0
460	Mg+2	1.647E-03	100.0	0.000E-01	0.0	0.000E-01	0.0
140	CO3-2	8.089E-03	100.0	0.000E-01	0.0	0.000E-01	0.0
180	Cl-1	2.484E-03	100.0	0.000E-01	0.0	0.000E-01	0.0
2	H2O	7.206E-08	100.0	0.000E-01	0.0	0.000E-01	0.0
330	H+1	1.023E-02	100.0	0.000E-01	0.0	0.000E-01	0.0

MINOR PLUS MAJOR COMPONENTS - UNCONTAMINATED
(model is MW 1, plus ~< detection limit when no data)

Temperature (Celsius): 25.00
Units of concentration: PPM
Ionic strength to be computed.
If specified, carbonate concentration represents total inorganic carbon.
Do not automatically terminate if charge imbalance exceeds 30%
Precipitation is allowed for all solids in the thermodynamic database and
the print option for solids is set to: 1
The maximum number of iterations is: 200
The method used to compute activity coefficients is: Davies equation
Intermediate output file
INPUT DATA BEFORE TYPE MODIFICATIONS

ID	NAME	ACTIVITY GUESS	LOG GUESS	ANAL TOTAL
330	H+1	1.862E-07	-6.730	0.000E-01
500	Na+1	4.074E-03	-2.390	9.400E+01
410	K+1	1.288E-04	-3.890	5.000E+00
150	Ca+2	2.042E-03	-2.690	8.100E+01
460	Mg+2	1.660E-03	-2.780	4.000E+01
140	CO3-2	8.128E-03	-2.090	4.850E+02
180	Cl-1	2.455E-03	-2.610	8.800E+01
732	SO4-2	5.754E-04	-3.240	5.500E+01
281	Fe+3	1.950E-05	-4.710	1.100E+00
30	Al+3	1.862E-05	-4.730	5.000E-01
800	Sr+2	5.888E-06	-5.230	5.200E-01
100	Ba+2	1.445E-07	-6.840	2.000E-02
470	Mn+2	5.495E-07	-6.260	3.000E-02
490	NH4+1	2.951E-05	-4.530	5.300E-01
270	F-1	2.630E-05	-4.580	5.000E-01
580	PO4-3	6.310E-06	-5.200	6.000E-01
600	Pb+2	2.399E-07	-6.620	5.000E-02
893	UO2+2	1.862E-06	-5.730	5.000E-01
650	Ra+2	4.467E-12	-11.350	1.000E-06
130	Br-1	6.310E-06	-5.200	5.000E-01
2	H2O	1.000E+00	0.000	0.000E-01

Type IV - FINITE SOLIDS (present at equilibrium)

ID	NAME	CALC MOL	LOG MOL	NEW LOGK	DH
3028100	HEMATITE	9.857E-06	-5.006	4.008	30.845
7089307	UP2O7:20H2O	1.574E-06	-5.803	53.268	0.000
2003002	DIASPORE	1.855E-05	-4.732	-6.873	24.630
7015002	FCO3APATITE	6.537E-07	-6.185	114.400	-39.390

PERCENTAGE DISTRIBUTION OF COMPONENTS AMONG
TYPE I and TYPE II (dissolved and adsorbed) species

Br-1

100.0 PERCENT BOUND IN SPECIES # 130 Br-1

Na+l

99.6 PERCENT BOUND IN SPECIES # 500 Na+l

K+1

99.8 PERCENT BOUND IN SPECIES # 410 K+1

Ca+2

93.2 PERCENT BOUND IN SPECIES # 150 Ca+2

3.5 PERCENT BOUND IN SPECIES #1501400 CaHCO3 +

3.3 PERCENT BOUND IN SPECIES #1507320 CaSO4 AQ

Mg+2

93.1 PERCENT BOUND IN SPECIES # 460 Mg+2

3.9 PERCENT BOUND IN SPECIES #4601401 MgHCO3 +

2.8 PERCENT BOUND IN SPECIES #4607320 MgSO4 AQ

CO3-2

71.7 PERCENT BOUND IN SPECIES #3301400 HCO3 -

26.5 PERCENT BOUND IN SPECIES #3301401 H2CO3 AQ

Cl-1

100.0 PERCENT BOUND IN SPECIES # 180 Cl-1

SO4-2

79.2 PERCENT BOUND IN SPECIES # 732 SO4-2

11.5 PERCENT BOUND IN SPECIES #1507320 CaSO4 AQ

8.2 PERCENT BOUND IN SPECIES #4607320 MgSO4 AQ

Ra+2

100.0 PERCENT BOUND IN SPECIES # 650 Ra+2

Pb+2

5.6 PERCENT BOUND IN SPECIES # 600 Pb+2

77.7 PERCENT BOUND IN SPECIES #6001401 PbCO3 AQ

14.9 PERCENT BOUND IN SPECIES #6001402 PbHCO3 +

Sr+2

96.5 PERCENT BOUND IN SPECIES # 800 Sr+2

3.3 PERCENT BOUND IN SPECIES #8007320 SrSO4(aq)

Ba+2

100.0 PERCENT BOUND IN SPECIES # 100 Ba+2

Mn+2

90.6 PERCENT BOUND IN SPECIES # 470 Mn+2

6.0 PERCENT BOUND IN SPECIES #4701400 MnHCO3 +

2.8 PERCENT BOUND IN SPECIES #4707320 MnSO4 AQ

NH4+1

99.4 PERCENT BOUND IN SPECIES # 490 NH4+1

UO2+2

4.7 PERCENT BOUND IN SPECIES #8931400 UO2CO3 AQ

78.4 PERCENT BOUND IN SPECIES #8931401 UO2CO3)2-2

16.5 PERCENT BOUND IN SPECIES #8931402 UO2CO3)3-4

H2O

76.4 PERCENT BOUND IN SPECIES #3300020 OH-

2.8 PERCENT BOUND IN SPECIES # 303302 Al(OH)3 AQ

2.3 PERCENT BOUND IN SPECIES # 303303 Al(OH)4 -

2.2 PERCENT BOUND IN SPECIES #1503300 CaOH +

11.8 PERCENT BOUND IN SPECIES #4603300 MgOH +

1.2 PERCENT BOUND IN SPECIES #6003300 PbOH +

2.8 PERCENT BOUND IN SPECIES #8933301 UO2(OH)2

Al+3

1.1 PERCENT BOUND IN SPECIES # 302700 AlF +2

8.4 PERCENT BOUND IN SPECIES # 302701 AlF2 +

2.8 PERCENT BOUND IN SPECIES # 302702 AlF3 AQ

8.2 PERCENT BOUND IN SPECIES # 303301 Al(OH)2 +

49.2 PERCENT BOUND IN SPECIES # 303302 Al(OH)3 AQ

29.9 PERCENT BOUND IN SPECIES # 303303 Al(OH)4 -

Fe+3

94.3 PERCENT BOUND IN SPECIES #2813301 FeOH2 +

5.3 PERCENT BOUND IN SPECIES #2813302 FeOH3 AQ

F-1

93.2 PERCENT BOUND IN SPECIES # 270 F-1

5.8 PERCENT BOUND IN SPECIES #4602700 MgF +

H+1

56.7 PERCENT BOUND IN SPECIES #3301400 HCO3 -

41.9 PERCENT BOUND IN SPECIES #3301401 H2CO3 AQ

PO4-3

9.6 PERCENT BOUND IN SPECIES #1505800 CaHPO4 AQ

1.5 PERCENT BOUND IN SPECIES #1505802 CaH2PO4 +

24.6 PERCENT BOUND IN SPECIES #3305800 HPO4 -2

51.4 PERCENT BOUND IN SPECIES #3305801 H2PO4 -

1.6 PERCENT BOUND IN SPECIES #4605801 MgH2PO4 +

10.7 PERCENT BOUND IN SPECIES #4605802 MgHPO4 AQ

---- EQUILIBRATED MASS DISTRIBUTION ------

IDX	NAME	DISSOLVED		SORBED		PRECIPITATED	
		MOL/KG	PERCENT	MOL/KG	PERCENT	MOL/KG	PERCENT
130	Br-1	6.263E-06	100.0	0.000E-01	0.0	0.000E-01	0.0
500	Na+1	4.092E-03	100.0	0.000E-01	0.0	2.353E-07	0.0
410	K+1	1.280E-04	100.0	0.000E-01	0.0	0.000E-01	0.0
150	Ca+2	2.016E-03	99.7	0.000E-01	0.0	6.208E-06	0.3
460	Mg+2	1.647E-03	100.0	0.000E-01	0.0	9.413E-08	0.0
140	CO3-2	8.088E-03	100.0	0.000E-01	0.0	7.845E-07	0.0
180	Cl-1	2.484E-03	100.0	0.000E-01	0.0	0.000E-01	0.0
732	SO4-2	5.730E-04	100.0	0.000E-01	0.0	0.000E-01	0.0
650	Ra+2	4.428E-12	100.0	0.000E-01	0.0	0.000E-01	0.0
600	Pb+2	2.415E-07	100.0	0.000E-01	0.0	0.000E-01	0.0
800	Sr+2	5.940E-06	100.0	0.000E-01	0.0	0.000E-01	0.0
100	Ba+2	1.457E-07	100.0	0.000E-01	0.0	0.000E-01	0.0
470	Mn+2	5.465E-07	100.0	0.000E-01	0.0	0.000E-01	0.0
490	NH4+1	2.941E-05	100.0	0.000E-01	0.0	0.000E-01	0.0
893	UO2+2	2.788E-07	15.1	0.000E-01	0.0	1.574E-06	84.9
2	H2O	7.970E-08	100.0	0.000E-01	0.0	0.000E-01	0.0
30	Al+3	1.512E-09	0.0	0.000E-01	0.0	1.855E-05	100.0
281	Fe+3	4.717E-15	0.0	0.000E-01	0.0	1.971E-05	100.0
270	F-1	2.472E-05	93.8	0.000E-01	0.0	1.621E-06	6.2
330	H+1	1.022E-02	100.0	0.000E-01	0.0	0.000E-01	0.0
580	PO4-3	3.791E-08	0.6	0.000E-01	0.0	6.285E-06	99.4

pE/MINOR+MAJOR - UNCONTAMINATED
(model = MW 1, plus -<detection limit when no data, set Eh to 770 mv)

Temperature (Celsius): 25.00
Units of concentration: PPM
Ionic strength to be computed.
If specified, carbonate concentration represents total inorganic carbon.
Do not automatically terminate if charge imbalance exceeds 30%
Precipitation is allowed for all solids in the thermodynamic database and
the print option for solids is set to: 1
The maximum number of iterations is: 200
The method used to compute activity coeficients is: Davies equation
Intermediate output tile

INPUT DATA BEFORE TYPE MODIFICATIONS

ID	NAME	ACTIVITY GUESS	LOG GUESS	ANAL TOTAL
330	H+1	1.862E-07	-6.730	0.000E-01
500	Na+1	4.074E-03	-2.390	9.400E+01
410	K+1	1.288E-04	-3.890	5.000E+00
150	Ca+2	2.042E-03	-2.690	8.100E+01
460	Mg+2	1.660E-03	-2.780	4.000E+01
140	CO3-2	8.128E-03	-2.090	4.850E+02
180	Cl-1	2.455E-03	-2.610	8.800E+01
732	SO4-2	5.754E-04	-3.240	5.500E+01
281	Fe+3	1.950E-05	-4.710	1.100E+00
30	Al+3	1.862E-05	-4.730	5.000E-01
800	Sr+2	5.888E-06	-5.230	5.200E-01
100	Ba+2	1.445E-07	-6.840	2.000E-02
470	Mn+2	5.495E-07	-6.260	3.000E-02
490	NH4+1	2.951E-05	-4.530	5.300E-01
270	F-1	2.630E-05	-4.580	5.000E-01
580	PO4-3	6.310E-06	-5.200	6.000E-01
600	Pb+2	2.399E-07	-6.620	5.000E-02
893	UO2+2	1.862E-06	-5.730	5.000E-01
650	Ra+2	4.467E-12	-11.350	1.000E-06
130	Br-1	6.310E-06	-5.200	5.000E-01
1	E-1	9.550E-14	-13.020	0.000E-01
2	H2O	1.000E+00	0.000	0.000E-01

Type IV - FINITE SOLIDS (present at equilibrium)

ID	NAME	CALC MOL	LOG MOL	NEW LOGK	DH
3028100	HEMATITE	9.857E-06	-5.006	4.008	30.845
7089307	UP2O7:20H2O	1.574E-06	-5.803	53.268	0.000
2003002	DIASPORE	1.855E-05	-4.732	-6.873	24.630
7015002	FCO3APATITE	6.537E-07	-6.185	114.400	-39.390

PERCENTAGE DISTRIBUTION OF COMPONENTS AMONG
TYPE I and TYPE II (dissolved and adsorbed) species

Br-1

100.0 PERCENT BOUND IN SPECIES # 130 Br-1

Na+ 1

99.6 PERCENT BOUND IN SPECIES # 500 Na+l

K+1

99.8 PERCENT BOUND IN SPECIES # 410 K+1

Ca+2

93.2 PERCENT BOUND IN SPECIES # 150 Ca+2

3.5 PERCENT BOUND IN SPECIES #1501400 CaHCO3 +

3.3 PERCENT BOUND IN SPECIES #1507320 CaSO4 AQ

Mg+2

93.1 PERCENT BOUND IN SPECIES # 460 Mg+2

3.9 PERCENT BOUND IN SPECIES #4601401 MgHCO3 +

2.8 PERCENT BOUND IN SPECIES #4607320 MgSO4 AQ

CO3-2

71.7 PERCENT BOUND IN SPECIES #3301400 HCO3 -

26.5 PERCENT BOUND IN SPECIES #3301401 H2CO3 AQ

Cl-1

100.0 PERCENT BOUND IN SPECIES # 180 Cl-1

SO4-2

79.2 PERCENT BOUND IN SPECIES # 732 SO4-2

11.5 PERCENT BOUND IN SPECIES #1507320 CaSO4 AQ

8.2 PERCENT BOUND IN SPECIES #4607320 MgSO4 AQ

Ra+2

100.0 PERCENT BOUND IN SPECIES # 650 Ra+2

Pb+2

5.6 PERCENT BOUND IN SPECIES # 600 Pb+2

77.7 PERCENT BOUND IN SPECIES #6001401 PbCO3 AQ

14.9 PERCENT BOUND IN SPECIES #6001402 PbHCO3 +

Sr+2

96.5 PERCENT BOUND IN SPECIES # 800 Sr+2

3.3 PERCENT BOUND IN SPECIES #8007320 SrSO4(aq)

Ba+2

100.0 PERCENT BOUND IN SPECIES # 100 Ba+2

Mn+2

90.6 PERCENT BOUND IN SPECIES # 470 Mn+2

6.0 PERCENT BOUND IN SPECIES #4701400 MnHCO3 +

2.8 PERCENT BOUND IN SPECIES #4707320 MnSO4 AQ

NH4+1

99.4 PERCENT BOUND IN SPECIES # 490 NH4+1

UO2+2

4.7 PERCENT BOUND IN SPECIES #8931400 UO2CO3 AQ

78.4 PERCENT BOUND IN SPECIES #8931401 UO2CO3)2-2

16.5 PERCENT BOUND IN SPECIES #8931402 UO2CO3)3-4

H2O

76.4 PERCENT BOUND IN SPECIES #3300020 OH-

2.8 PERCENT BOUND IN SPECIES # 303302 Al(OH)3 AQ

2.3 PERCENT BOUND IN SPECIES # 303303 Al(OH)4 -

2.2 PERCENT BOUND IN SPECIES #1503300 CaOH +

11.8 PERCENT BOUND IN SPECIES #4603300 MgOH +

1.2 PERCENT BOUND IN SPECIES #6003300 PbOH +

2.8 PERCENT BOUND IN SPECIES #8933301 UO2(OH)2

Al+3

1.1 PERCENT BOUND IN SPECIES # 302700 AlF +2

8.4 PERCENT BOUND IN SPECIES # 302701 AlF2 +

2.8 PERCENT BOUND IN SPECIES # 302702 AlF3 AQ

8.2 PERCENT BOUND IN SPECIES # 303301 Al(OH)2 +

49.2 PERCENT BOUND IN SPECIES # 303302 Al(OH)3 AQ

29.9 PERCENT BOUND IN SPECIES # 303303 Al(OH)4 -

E-1

100.0 PERCENT BOUND IN SPECIES #4700020 MnO4 -

Fe+3

94.3 PERCENT BOUND IN SPECIES #2813301 FeOH2 +

5.3 PERCENT BOUND IN SPECIES #2813302 FeOH3 AQ

F-1

93.2 PERCENT BOUND IN SPECIES # 270 F-1

5.8 PERCENT BOUND IN SPECIES #4602700 MgF +

H+1

56.7 PERCENT BOUND IN SPECIES #3301400 HCO3 -

41.9 PERCENT BOUND IN SPECIES #3301401 H2CO3 AQ

PO4-3

9.6 PERCENT BOUND IN SPECIES #1505800 CaHPO4 AQ

1.5 PERCENT BOUND IN SPECIES #1505802 CaH2PO4 +

24.6 PERCENT BOUND IN SPECIES #3305800 HPO4 -2

51.4 PERCENT BOUND IN SPECIES #3305801 H2PO4 -

1.6 PERCENT BOUND IN SPECIES #4605801 MgH2PO4 +

10.7 PERCENT BOUND IN SPECIES #4605802 MgHPO4 AQ

---------- EQUILIBRATED MASS DISTRIBUTION ----------

IDX	NAME	DISSOLVED		SORBED		PRECIPITATED	
		MOL/KG	PERCENT	MOL/KG	PERCENT	MOL/KG	PERCENT
130	Br-1	6.263E-06	100.0	0.000E-01	0.0	0.000E-01	0.0
500	Na+1	4.092E-03	100.0	0.000E-01	0.0	2.353E-07	0.0
410	K+1	1.280E-04	100.0	0.000E-01	0.0	0.000E-01	0.0
150	Ca+2	2.016E-03	99.7	0.000E-01	0.0	6.208E-06	0.3
460	Mg+2	1.647E-03	100.0	0.000E-01	0.0	9.413E-08	0.0
140	CO3-2	8.088E-03	100.0	0.000E-01	0.0	7.845E-07	0.0
180	Cl-1	2.484E-03	100.0	0.000E-01	0.0	0.000E-01	0.0
732	SO4-2	5.730E-04	100.0	0.000E-01	0.0	0.000E-01	0.0
650	Ra+2	4.428E-12	100.0	0.000E-01	0.0	0.000E-01	0.0
600	Pb+2	2.415E-07	100.0	0.000E-01	0.0	0.000E-01	0.0
800	Sr+2	5.940E-06	100.0	0.000E-01	0.0	0.000E-01	0.0
100	Ba+2	1.457E-07	100.0	0.000E-01	0.0	0.000E-01	0.0
470	Mn+2	5.465E-07	100.0	0.000E-01	0.0	0.000E-01	0.0
490	NH4+1	2.941E-05	100.0	0.000E-01	0.0	0.000E-01	0.0
893	UO2+2	2.788E-07	15.1	0.000E-01	0.0	1.574E-06	84.9
2	H2O	7.970E-08	100.0	0.000E-01	0.0	0.000E-01	0.0
30	Al+3	1.512E-09	0.0	0.000E-01	0.0	1.855E-05	100.0
1	E-1	-2.156E-15	100.0	0.000E-01	0.0	0.000E-01	0.0
281	Fe+3	4.717E-15	0.0	0.000E-01	0.0	1.971E-05	100.0
270	F-1	2.472E-05	93.8	0.000E-01	0.0	1.621E-06	6.2
330	H+1	1.022E-02	100.0	0.000E-01	0.0	0.000E-01	0.0
580	PO4-3	3.791E-08	0.6	0.000E-01	0.0	6.285E-06	99.4

MAJOR COMPONENTS PLUS 53 MG/L H4SIO4 - UNCONTAMINATED
(model MW I, Trip 1)

Temperature (Celsius): 25.00
Units of concentration: PPM
Ionic strength to be computed.
If specified, carbonate concentration represents total inorganic carbon.
Do not automatically terminate if charge imbalance exceeds 30%
Precipitation is allowed for all solids in the thermodynamic database and
the print option for solids is set to: 1
The maximum number of iterations is: 40
The method used to compute activity coefficients is: Davies equation
Intermediate output file

INPUT DATA BEFORE TYPE MODIFICATIONS

ID	NAME	ACTIVITY GUESS	LOG GUESS	ANAL TOTAL
330	H+1	1.862E-07	-6.730	0.000E-01
500	Na+1	4.074E-03	-2.390	9.400E+01
410	K+1	1.288E-04	-3.890	5.000E+00
150	Ca+2	2.042E-03	-2.690	8.100E+01
460	Mg+2	1.660E-03	-2.780	4.000E+01
140	CO3-2	8.128E-03	-2.090	4.850E+02
180	Cl-1	2.455E-03	-2.610	8.800E+01
732	SO4-2	5.754E-04	-3.240	5.500E+01
770	H4SiO4	5.495E-04	-3.260	5.300E+01
2	H2O	1.000E+00	0.000	0.000E-01

Type IV - FINITE SOLIDS (present at equilibrium)

ID	NAME	CALC MOL	LOG MOL	NEW LOGK	DH
2077002	QUARTZ	4.536E-04	-3.343	4.006	-6.220

PERCENTAGE DISTRIBUTION OF COMPONENTS AMONG
TYPE I and TYPE II (dissolved and adsorbed) species

SO4-2

79.2 PERCENT BOUND IN SPECIES # 732 SO4-2

11.5 PERCENT BOUND IN SPECIES #1507320 CaSO4 AQ

8.2 PERCENT BOUND IN SPECIES #4607320 MgSO4 AQ

Na+1

99.6 PERCENT BOUND IN SPECIES # 500 Na+1

K+1

99.8 PERCENT BOUND IN SPECIES # 410 K+1

Ca+2

93.2 PERCENT BOUND IN SPECIES # 150 Ca+2

3.5 PERCENT BOUND IN SPECIES #1501400 CaHCO3 +

3.3 PERCENT BOUND IN SPECIES #1507320 CaSO4 AQ

Mg+2

93.2 PERCENT BOUND IN SPECIES # 460 Mg+2

3.9 PERCENT BOUND IN SPECIES #4601401 MgHCO3 +

2.9 PERCENT BOUND IN SPECIES #4607320 MgSO4 AQ

CO3-2

71.7 PERCENT BOUND IN SPECIES #3301400 HCO3 -

26.5 PERCENT BOUND IN SPECIES #3301401 H2CO3 AQ

Cl-1

100.0 PERCENT BOUND IN SPECIES # 180 Cl-1

H4SiO4

99.9 PERCENT BOUND IN SPECIES # 770 H4SiO4

H+1

56.7 PERCENT BOUND IN SPECIES #3301400 HCO3 -

41.9 PERCENT BOUND IN SPECIES #3301401 H2CO3 AQ

H2O

84.4 PERCENT BOUND IN SPECIES #3300020 OH-

2.5 PERCENT BOUND IN SPECIES #1503300 CaOH +

13.1 PERCENT BOUND IN SPECIES #4603300 MgOH +

---------- EQUILIBRATED MASS DISTRIBUTION ----------

IDX	NAME	DISSOLVED		SORBED		PRECIPITATED	
		MOL/KG	PERCENT	MOL/KG	PERCENT	MOL/KG	PERCENT
732	SO4-2	5.731E-04	100.0	0.000E-01	0.0	0.000E-01	0.0
500	Na+1	4.092E-03	100.0	0.000E-01	0.0	0.000E-01	0.0
410	K+1	1.280E-04	100.0	0.000E-01	0.0	0.000E-01	0.0
150	Ca+2	2.023E-03	100.0	0.000E-01	0.0	0.000E-01	0.0
460	Mg+2	1.647E-03	100.0	0.000E-01	0.0	0.000E-01	0.0
140	CO3-2	8.089E-03	100.0	0.000E-01	0.0	0.000E-01	0.0
180	Cl-1	2.484E-03	100.0	0.000E-01	0.0	0.000E-01	0.0
770	H4SiO4	9.831E-05	17.8	0.000E-01	0.0	4.536E-04	82.2
330	H+1	1.023E-02	100.0	0.000E-01	0.0	0.000E-01	0.0
2	H2O	7.206E-08	100.0	0.000E-01	0.0	0.000E-01	0.0

MAJOR PLUS SOME MINOR PLUS SI - UNCONTAMINATED
(model MW 1, Trip 1)

Temperature (Celsius): 25.00
Units of concentration: PPM
Ionic strength to be computed.
If specified, carbonate concentration represents total inorganic carbon.
Do not automatically terminate if charge imbalance exceeds 30%
Precipitation is allowed for all solids in the thermodynamic database and
the print option for solids is set to: 1
The maximum number of iterations is: 200
The method used to compute activity coefficients is: Davies equation
Intermediate output tile

INPUT DATA BEFORE TYPE MODIFICATIONS

ID	NAME	ACTIVITY GUESS	LOG GUESS	ANAL TOTAL
330	H+1	1.862E-07	-6.730	0.000E-01
500	Na+1	4.074E-03	-2.390	9.400E+01
410	K+1	1.288E-04	-3.890	5.000E+00
150	Ca+2	2.042E-03	-2.690	8.100E+01
460	Mg+2	1.660E-03	-2.780	4.000E+01
140	CO3-2	8.128E-03	-2.090	4.850E+02
180	Cl-1	2.455E-03	-2.610	8.800E+01
732	SO4-2	5.754E-04	-3.240	5.500E+01
770	H4SiO4	5.495E-04	-3.260	5.300E+01
30	Al+3	1.862E-05	-4.730	5.000E-01
800	Sr+2	5.888E-06	-5.230	5.200E-01
100	Ba+2	1.445E-07	-6.840	2.000E-02
470	Mn+2	5.495E-07	-6.260	3.000E-02
270	F-1	2.630E-05	-4.580	5.000E-01
580	PO4-3	6.310E-06	-5.200	6.000E-01
600	Pb+2	2.399E-07	-6.620	5.000E-02
130	Br-1	6.310E-06	-5.200	5.000E-01
893	UO2+2	1.862E-06	-5.730	5.000E-01
2	H2O	1.000E+00	0.000	0.000E-01

Type IV - FINITE SOLIDS (present at equilibrium)

ID	NAME	CALC MOL	LOG MOL	NEW LOGK	DH
7089307	UP2O7:20H2O	1.576E-06	-5.802	53.268	0.000
2003002	DIASPORE	1.342E-05	-4.872	-6.873	24.630
2077002	QUARTZ	4.434E-04	-3.353	4.006	-6.220
7015002	FCO3APATITE	6.528E-07	-6.185	114.400	-39.390
8415000	LEONHARDITE	1.280E-06	-5.893	-16.490	85.360

PERCENTAGE DISTRIBUTION OF COMPONENTS AMONG
TYPE I and TYPE II (dissolved and adsorbed) species

UO2+2

4.7 PERCENT BOUND IN SPECIES #8931400 UO2CO3 AQ

78.4 PERCENT BOUND IN SPECIES #8931401 UO2CO3)2-2

16.5 PERCENT BOUND IN SPECIES #8931402 UO2CO3)3-4

Na+1

99.6 PERCENT BOUND IN SPECIES # 500 Na+1

K+1

99.8 PERCENT BOUND IN SPECIES # 410 K+1

Pb+2

5.6 PERCENT BOUND IN SPECIES # 600 Pb+2

77.7 PERCENT BOUND IN SPECIES #6001401 PbCO3 AQ

14.9 PERCENT BOUND IN SPECIES #6001402 PbHCO3 +

Mg+2

93.1 PERCENT BOUND IN SPECIES # 460 Mg+2

3.9 PERCENT BOUND IN SPECIES #4601401 MgHCO3 +

2.9 PERCENT BOUND IN SPECIES #4607320 MgSO4 AQ

CO3-2

71.7 PERCENT BOUND IN SPECIES #3301400 HCO3 -

26.5 PERCENT BOUND IN SPECIES #3301401 H2CO3 AQ

Cl-1

100.0 PERCENT BOUND IN SPECIES # 180 Cl-1

SO4-2

79.2 PERCENT BOUND IN SPECIES # 732 SO4-2

11.5 PERCENT BOUND IN SPECIES #1507320 CaSO4 AQ

8.2 PERCENT BOUND IN SPECIES #4607320 MgSO4 AQ

Br-1

100.0 PERCENT BOUND IN SPECIES # 130 Br-1

Mn+2

90.5 PERCENT BOUND IN SPECIES # 470 Mn+2

6.0 PERCENT BOUND IN SPECIES #4701400 MnHCO3 +

2.8 PERCENT BOUND IN SPECIES #4707320 MnSO4 AQ

Sr+2

96.5 PERCENT BOUND IN SPECIES # 800 Sr+2

3.3 PERCENT BOUND IN SPECIES #8007320 SrSO4(aq)

Ba+2

100.0 PERCENT BOUND IN SPECIES # 100 Ba+2

Ca+2

93.2 PERCENT BOUND IN SPECIES # 150 Ca+2

3.5 PERCENT BOUND IN SPECIES #1501400 CaHCO3 +

3.3 PERCENT BOUND IN SPECIES #1507320 CaSO4 AQ

F-1

93.2 PERCENT BOUND IN SPECIES # 270 F-1

5.8 PERCENT BOUND IN SPECIES #4602700 MgF +

H2O

76.4 PERCENT BOUND IN SPECIES #3300020 OH-

2.8 PERCENT BOUND IN SPECIES # 303302 Al(OH)3 AQ

2.3 PERCENT BOUND IN SPECIES # 303303 Al(OH)4 -

2.2 PERCENT BOUND IN SPECIES #1503300 CaOH +

11.8 PERCENT BOUND IN SPECIES #4603300 MgOH +

1.2 PERCENT BOUND IN SPECIES #6003300 PbOH +

2.8 PERCENT BOUND IN SPECIES #8933301 UO2(OH)2

H+1

56.7 PERCENT BOUND IN SPECIES #3301400 HCO3 -

41.9 PERCENT BOUND IN SPECIES #3301401 H2CO3 AQ

Al+3

1.1 PERCENT BOUND IN SPECIES # 302700 AlF +2

8.4 PERCENT BOUND IN SPECIES # 302701 AlF2 +

2.8 PERCENT BOUND IN SPECIES # 302702 AlF3 AQ

8.2 PERCENT BOUND IN SPECIES # 303301 Al(OH)2 +

49.2 PERCENT BOUND IN SPECIES # 303302 Al(OH)3 AQ

29.9 PERCENT BOUND IN SPECIES # 303303 Al(OH)4 -

PO4-3

9.6 PERCENT BOUND IN SPECIES #1505800 CaHPO4 AQ

1.5 PERCENT BOUND IN SPECIES #1505802 CaH2PO4 +

24.6 PERCENT BOUND IN SPECIES #3305800 HPO4 -2

51.4 PERCENT BOUND IN SPECIES #3305801 H2PO4 -

1.6 PERCENT BOUND IN SPECIES #4605801 MgH2PO4 +

10.7 PERCENT BOUND IN SPECIES #4605802 MgHPO4 AQ

H4SiO4

99.9 PERCENT BOUND IN SPECIES # 770 H4SiO4

---------- EQUILIBRATED MASS DISTRIBUTION ----------

IDX	NAME	DISSOLVED		SORBED		PRECIPITATED	
		MOL/KG	PERCENT	MOL/KG	PERCENT	MOL/KG	PERCENT
893	UO2+2	2.778E-07	15.0	0.000E-01	0.0	1.576E-06	85.0
500	Na+1	4.092E-03	100.0	0.000E-01	0.0	2.350E-07	0.0
410	K+1	1.280E-04	100.0	0.000E-01	0.0	0.000E-01	0.0
600	Pb+2	2.415E-07	100.0	0.000E-01	0.0	0.000E-01	0.0
460	Mg+2	1.647E-03	100.0	0.000E-01	0.0	9.400E-08	0.0
140	CO3-2	8.089E-03	100.0	0.000E-01	0.0	7.834E-07	0.0
180	Cl-1	2.484E-03	100.0	0.000E-01	0.0	0.000E-01	0.0
732	SO4-2	5.731E-04	100.0	0.000E-01	0.0	0.000E-01	0.0
130	Br-1	6.263E-06	100.0	0.000E-01	0.0	0.000E-01	0.0
470	Mn+2	5.466E-07	100.0	0.000E-01	0.0	0.000E-01	0.0
800	Sr+2	5.941E-06	100.0	0.000E-01	0.0	0.000E-01	0.0
100	Ba+2	1.458E-07	100.0	0.000E-01	0.0	0.000E-01	0.0
150	Ca+2	2.014E-03	99.6	0.000E-01	0.0	8.760E-06	0.4
270	F-1	2.472E-05	93.9	0.000E-01	0.0	1.619E-06	6.1
2	H2O	7.968E-08	100.0	0.000E-01	0.0	0.000E-01	0.0
330	H+1	1.022E-02	100.0	0.000E-01	0.0	0.000E-01	0.0
30	Al+3	1.512E-09	0.0	0.000E-01	0.0	1.855E-05	100.0
580	PO4-3	3.797E-08	0.6	0.000E-01	0.0	6.285E-06	99.4
770	H4SiO4	9.831E-05	17.8	0.000E-01	0.0	4.536E-04	82.2

MAJOR COMPONENTS - CONTAMINATED WELL
(model PP 1-3 Trip 2)

Temperature (Celsius): 25.00
Units of concentration: PPM
Ionic strength to be computed.
If specified, carbonate concentration represents total inorganic carbon.
Do not automatically terminate if charge imbalance exceeds 30%
Precipitation is allowed for all solids in the thermodynamic database and
the print option for solids is set to: 1
The maximum number of iterations is: 40
The method used to compute activity coeficients is: Davies equation
Intermediate output tile

INPUT DATA BEFORE TYPE MODIFICATIONS

ID	NAME	ACTIVITY GUESS	LOG GUESS	ANAL TOTAL
330	H+1	4.169E-03	-2.380	0.000E-01
500	Na+1	4.074E-03	-2.390	1.529E+03
410	K+1	1.288E-04	-3.890	2.460E+02
150	Ca+2	2.042E-03	-2.690	6.570E+02
460	Mg+2	1.660E-03	-2.780	2.290E+02
140	CO3-2	8.128E-03	-2.090	6.000E-01
180	Cl-1	2.455E-03	-2.610	1.680E+02
732	SO4-2	5.754E-04	-3.240	5.091E+03
2	H2O	1.000E+00	0.000	0.000E-01

Type IV - FINITE SOLIDS (present at equilibrium)

ID	NAME	CALC MOL	LOG MOL	NEW LOGK	DH
6015001	GYPSUM	9.404E-03	-2.027	4.848	-0.261

PERCENTAGE DISTRIBUTION OF COMPONENTS AMONG
TYPE I and TYPE II (dissolved and adsorbed) species

SO4-2

65.8 PERCENT BOUND IN SPECIES # 732 SO4-2

7.1 PERCENT BOUND IN SPECIES #5007320 NaSO4 -

6.4 PERCENT BOUND IN SPECIES #1507320 CaSO4 AQ

11.8 PERCENT BOUND IN SPECIES #3307320 HSO4 -

7.9 PERCENT BOUND IN SPECIES #4607320 MgSO4 AQ

Na+1

95.3 PERCENT BOUND IN SPECIES # 500 Na+1

4.7 PERCENT BOUND IN SPECIES #5007320 NaSO4 -

K+1

93.5 PERCENT BOUND IN SPECIES # 410 K+1

6.5 PERCENT BOUND IN SPECIES #4107320 KSO4 -

Cl-1

100.0 PERCENT BOUND IN SPECIES # 180 Cl-1

Mg+2

63.5 PERCENT BOUND IN SPECIES # 460 Mg+2

36.5 PERCENT BOUND IN SPECIES #4607320 MgSO4 AQ

CO3-2

100.0 PERCENT BOUND IN SPECIES #3301401 H2CO3 AQ

Ca+2

60.3 PERCENT BOUND IN SPECIES # 150 Ca+2

39.7 PERCENT BOUND IN SPECIES #1507320 CaSO4 AQ

H+1

51.1 PERCENT BOUND IN SPECIES # 330 H+1

48.7 PERCENT BOUND IN SPECIES #3307320 HSO4 -

H2O

73.0 PERCENT BOUND IN SPECIES #3300020 OH-

2.7 PERCENT BOUND IN SPECIES #1503300 CaOH +

24.4 PERCENT BOUND IN SPECIES #4603300 MgOH +

--- EQUILIBRATED MASS DISTRIBUTION ---

IDX	NAME	DISSOLVED		SORBED		PRECIPITATED	
		MOL/KG	PERCENT	MOL/KG	PERCENT	MOL/KG	PERCENT
732	SO4-2	4.402E-02	82.4	0.000E-01	0.0	9.404E-03	17.6
500	Na+1	6.704E-02	100.0	0.000E-01	0.0	0.000E-01	0.0
410	K+1	6.342E-03	100.0	0.000E-01	0.0	0.000E-01	0.0
180	Cl-1	4.777E-03	100.0	0.000E-01	0.0	0.000E-01	0.0
460	Mg+2	9.495E-03	100.0	0.000E-01	0.0	0.000E-01	0.0
140	CO3-2	1.008E-05	100.0	0.000E-01	0.0	0.000E-01	0.0
150	Ca+2	7.119E-03	43.1	0.000E-01	0.0	9.404E-03	56.9
330	H+1	1.069E-02	100.0	0.000E-01	0.0	0.000E-01	0.0
2	H2O	4.318E-12	100.0	0.000E-01	0.0	0.000E-01	0.0

MINOR PLUS MAJOR COMPONENTS - CONTAMINATED
(model PP 1-3, minor plus major components, U as U+4)

Temperature (Celsius): 25.00
Units of concentration: PPM
Ionic strength to be computed.
If specified, carbonate concentration represents total inorganic carbon.
Do not automatically terminate if charge imbalance exceeds 30%
Precipitation is allowed for all solids in the thermodynamic database and
the print option for solids is set to: 1
The maximum number of iterations is: 40
The method used to compute activity coefficients is: Davies equation
Intermediate output file

INPUT DATA BEFORE TYPE MODIFICATIONS

ID	NAME	ACTIVITY GUESS	LOG GUESS	ANAL TOTAL
330	H+1	4.169E-03	-2.380	0.000E-01
500	Na+1	4.074E-03	-2.390	1.529E+03
410	K+1	1.288E-04	-3.890	2.460E+02
150	Ca+2	2.042E-03	-2.690	6.570E+02
460	Mg+2	1.660E-03	-2.780	2.290E+02
140	CO3-2	8.128E-03	-2.090	6.000E-01
180	Cl-1	2.455E-03	-2.610	1.680E+02
732	SO4-2	5.754E-04	-3.240	5.091E+03
281	Fe+3	3.548E-05	-4.450	2.000E+00
30	Al+3	2.138E-04	-3.670	5.800E+00
800	Sr+2	1.380E-04	-3.860	1.210E+01
100	Ba+2	1.445E-07	-6.840	2.000E-02
470	Mn+2	9.120E-05	-4.040	5.000E+00
490	NH4+1	5.888E-02	-1.230	1.053E+03
270	F-1	5.888E-02	-1.230	1.120E+03
580	PO4-3	9.120E-02	-1.040	8.720E+03
600	Pb+2	2.399E-07	-6.620	5.000E-02
891	U+4	2.089E-06	-5.680	5.000E-01
650	Ra+2	4.467E-12	-11.350	1.000E-06
130	Br-1	3.890E-05	-4.410	3.100E+00
2	H2O	1.000E+00	0.000	0.000E-01

Type IV - FINITE SOLIDS (present at equilibrium)

ID	NAME	CALC MOL	LOG MOL	NEW LOGK	DH
4215000	FLUORITE	1.670E-02	-1.777	10.949	-4.710
7047001	MNHPO4(C)	9.211E-05	-4.036	25.400	0.000
4289101	UF4.2.5H2O	2.129E-06	-5.672	33.380	-5.947
6010000	BARITE	1.143E-07	-6.942	9.976	-6.280

PERCENTAGE DISTRIBUTION OF COMPONENTS AMONG
TYPE I and TYPE II (dissolved and adsorbed) species

Br-1

100.0 PERCENT BOUND IN SPECIES # 130 Br-1

Na+1

95.0 PERCENT BOUND IN SPECIES # 500 Na+1

5.0 PERCENT BOUND IN SPECIES #5007320 NaSO4 -

K+1

93.2 PERCENT BOUND IN SPECIES # 410 K+1

6.8 PERCENT BOUND IN SPECIES #4107320 KSO4 -

Ca+2

47.6 PERCENT BOUND IN SPECIES # 150 Ca+2

23.2 PERCENT BOUND IN SPECIES #1505802 CaH2PO4 +

28.7 PERCENT BOUND IN SPECIES #1507320 CaSO4 AQ

Mg+2

44.8 PERCENT BOUND IN SPECIES # 460 Mg+2

3.8 PERCENT BOUND IN SPECIES #4602700 MgF +

27.8 PERCENT BOUND IN SPECIES #4605801 MgH2PO4 +

23.6 PERCENT BOUND IN SPECIES #4607320 MgSO4 AQ

CO3-2

100.0 PERCENT BOUND IN SPECIES #3301401 H2CO3 AQ

Cl-1

100.0 PERCENT BOUND IN SPECIES # 180 Cl-1

SO4-2

65.0 PERCENT BOUND IN SPECIES # 732 SO4-2

10.6 PERCENT BOUND IN SPECIES #3307320 HSO4 -

4.2 PERCENT BOUND IN SPECIES #4607320 MgSO4 AQ

13.1 PERCENT BOUND IN SPECIES #4907320 NH4SO4 -

6.2 PERCENT BOUND IN SPECIES #5007320 NaSO4 -

Fe+3

21.7 PERCENT BOUND IN SPECIES #2812701 FeF2 +

76.7 PERCENT BOUND IN SPECIES #2812702 FeF3 AQ

1.1 PERCENT BOUND IN SPECIES #2815801 FeH2PO4 +2

Al+3

30.7 PERCENT BOUND IN SPECIES # 302702 AlF3 AQ

68.6 PERCENT BOUND IN SPECIES # 302703 AlF4 -

Sr+2

58.9 PERCENT BOUND IN SPECIES # 800 Sr+2

6.0 PERCENT BOUND IN SPECIES #8005802 SrH2PO4+

34.9 PERCENT BOUND IN SPECIES #8007320 SrSO4(aq)

PO4-3

68.7 PERCENT BOUND IN SPECIES #3305801 H2PO4 -

28.4 PERCENT BOUND IN SPECIES #3305802 H3PO4

2.9 PERCENT BOUND IN SPECIES #4605801 MgH2PO4 +

Pb+2

32.6 PERCENT BOUND IN SPECIES # 600 Pb+2

1.9 PERCENT BOUND IN SPECIES #6001800 PbCl +

54.3 PERCENT BOUND IN SPECIES #6007320 PbSO4 AQ

10.5 PERCENT BOUND IN SPECIES #6007321 Pb(SO4)2-2

NH4+1

88.2 PERCENT BOUND IN SPECIES # 490 NH4+1

11.8 PERCENT BOUND IN SPECIES #4907320 NH4SO4 -

Ra+2

100.0 PERCENT BOUND IN SPECIES # 650 Ra+2

U+4

4.8 PERCENT BOUND IN SPECIES #8912702 UF3 +1

76.7 PERCENT BOUND IN SPECIES #8912703 UF4 AQ

10.1 PERCENT BOUND IN SPECIES #8912704 UF5 -1

8.5 PERCENT BOUND IN SPECIES #8912705 UF6 -2

Mn+2

64.3 PERCENT BOUND IN SPECIES # 470 Mn+2

34.7 PERCENT BOUND IN SPECIES #4707320 MnSO4 AQ

F-1

16.0 PERCENT BOUND IN SPECIES # 270 F-1

2.3 PERCENT BOUND IN SPECIES # 302703 AlF4 -

69.6 PERCENT BOUND IN SPECIES #3302700 HF AQ

2.4 PERCENT BOUND IN SPECIES #3302701 HF2 -

7.3 PERCENT BOUND IN SPECIES #3302702 H2F2 AQ

1.3 PERCENT BOUND IN SPECIES #4602700 MgF +

H+1

2.3 PERCENT BOUND IN SPECIES # 330 H+1

7.6 PERCENT BOUND IN SPECIES #3302700 HF AQ

52.3 PERCENT BOUND IN SPECIES #3305801 H2PO4 -

32.4 PERCENT BOUND IN SPECIES #3305802 H3PO4

2.3 PERCENT BOUND IN SPECIES #3307320 HSO4 -

2.2 PERCENT BOUND IN SPECIES #4605801 MgH2PO4 +

H2O

5.8 PERCENT BOUND IN SPECIES #3300020 OH-

87.1 PERCENT BOUND IN SPECIES #2813300 FeOH +2

5.5 PERCENT BOUND IN SPECIES #2813301 FeOH2 +

1.2 PERCENT BOUND IN SPECIES #4603300 MgOH +

Ba+2

100.0 PERCENT BOUND IN SPECIES # 100 Ba+2

---------- EQUILIBRATED MASS DISTRIBUTION ----------

IDX	NAME	DISSOLVED MOL/KG	PERCENT	SORBED MOL/KG	PERCENT	PRECIPITATED MOL/KG	PERCENT
130	Br-1	3.954E-05	100.0	0.000E-01	0.0	0.000E-01	0.0
500	Na+1	6.778E-02	100.0	0.000E-01	0.0	0.000E-01	0.0
410	K+1	6.412E-03	100.0	0.000E-01	0.0	0.000E-01	0.0
150	Ca+2	8.020E-06	0.0	0.000E-01	0.0	1.670E-02	100.0
460	Mg+2	9.600E-03	100.0	0.000E-01	0.0	0.000E-01	0.0
140	CO3-2	1.019E-05	100.0	0.000E-01	0.0	0.000E-01	0.0
180	Cl-1	4.830E-03	100.0	0.000E-01	0.0	0.000E-01	0.0
732	SO4-2	5.401E-02	100.0	0.000E-01	0.0	1.143E-07	0.0
281	Fe+3	3.650E-05	100.0	0.000E-01	0.0	0.000E-01	0.0
30	Al+3	2.191E-04	100.0	0.000E-01	0.0	0.000E-01	0.0
800	Sr+2	1.407E-04	100.0	0.000E-01	0.0	0.000E-01	0.0
580	PO4-3	9.349E-02	99.9	0.000E-01	0.0	9.211E-05	0.1
600	Pb+2	2.460E-07	100.0	0.000E-01	0.0	0.000E-01	0.0
490	NH4+1	5.950E-02	100.0	0.000E-01	0.0	0.000E-01	0.0
650	Ra+2	4.509E-12	100.0	0.000E-01	0.0	0.000E-01	0.0
891	U+4	1.161E-08	0.5	0.000E-01	0.0	2.129E-06	99.5
470	Mn+2	6.541E-07	0.7	0.000E-01	0.0	9.211E-05	99.3
270	F-1	2.668E-02	44.4	0.000E-01	0.0	3.341E-02	55.6
330	H+1	2.457E-01	100.0	0.000E-01	0.0	0.000E-01	0.0
2	H2O	5.559E-11	100.0	0.000E-01	0.0	0.000E-01	0.0
100	Ba+2	3.409E-08	23.0	0.000E-01	0.0	1.143E-07	77.0

MAJOR PLUS 1187 MG/L H4SIO4 - CONTAMINATED
(model PP 1-3 Trip 2)

Temperature (Celsius): 25.00
Units of concentration: PPM
Ionic strength to be computed.
If specified, carbonate concentration represents total inorganic carbon.
Do not automatically terminate if charge imbalance exceeds 30%
Precipitation is allowed for all solids in the thermodynamic database and
the print option for solids is set to: 1
The maximum number of iterations is: 40
The method used to compute activity coefficients is: Davies equation
Intermediate output file

INPUT DATA BEFORE TYPE MODIFICATIONS

ID	NAME	ACTIVITY GUESS	LOG GUESS	ANAL TOTAL
330	H+1	4.169E-03	-2.380	0.000E-01
500	Na+1	4.074E-03	-2.390	1.529E+03
410	K+1	1.288E-04	-3.890	2.460E+02
150	Ca+2	2.042E-03	-2.690	6.570E+02
460	Mg+2	1.660E-03	-2.780	2.290E+02
140	CO3-2	8.128E-03	-2.090	6.000E-01
180	Cl-1	2.455E-03	-2.610	1.680E+02
732	SO4-2	5.754E-04	-3.240	5.091E+03
770	H4SiO4	1.230E-02	-1.910	1.187E+03
2	H2O	1.000E+00	0.000	0.000E-01

Type IV - FINITE SOLIDS (present at equilibrium)

ID	NAME	CALC MOL	LOG MOL	NEW LOGK	DH
2077002	QUARTZ	1.237E-02	-1.908	4.006	-6.220
6015001	GYPSUM	9.422E-03	-2.026	4.848	-0.261

PERCENTAGE DISTRIBUTION OF COMPONENTS AMONG
TYPE I and TYPE II (dissolved and adsorbed) species

SO4-2

65.8 PERCENT BOUND IN SPECIES # 732 SO4-2

7.1 PERCENT BOUND IN SPECIES #5007320 NaSO4 -

6.4 PERCENT BOUND IN SPECIES #1507320 CaSO4 AQ

11.8 PERCENT BOUND IN SPECIES #3307320 HSO4 -

7.9 PERCENT BOUND IN SPECIES #4607320 MgSO4 AQ

Na+1

95.3 PERCENT BOUND IN SPECIES # 500 Na+1

4.7 PERCENT BOUND IN SPECIES #5007320 NaSO4 -

K+1

93.5 PERCENT BOUND IN SPECIES # 410 K+1

6.5 PERCENT BOUND IN SPECIES #4107320 KSO4 -

Cl-1

100.0 PERCENT BOUND IN SPECIES # 180 Cl-1

Mg+2

63.5 PERCENT BOUND IN SPECIES # 460 Mg+2

36.5 PERCENT BOUND IN SPECIES #4607320 MgSO4 AQ

CO3-2

100.0 PERCENT BOUND IN SPECIES #3301401 H2CO3 AQ

Ca+2

60.3 PERCENT BOUND IN SPECIES # 150 Ca+2

39.7 PERCENT BOUND IN SPECIES #1507320 CaSO4 AQ

H+1

51.1 PERCENT BOUND IN SPECIES # 330 H+1

48.7 PERCENT BOUND IN SPECIES #3307320 HSO4 -

H4SiO4

100.0 PERCENT BOUND IN SPECIES # 770 H4SiO4

H2O

72.9 PERCENT BOUND IN SPECIES #3300020 OH-

2.7 PERCENT BOUND IN SPECIES #1503300 CaOH +

24.4 PERCENT BOUND IN SPECIES #4603300 MgOH +

---------- EQUILIBRATED MASS DISTRIBUTION ----------

IDX	NAME	DISSOLVED		SORBED		PRECIPITATED	
		MOL/KG	PERCENT	MOL/KG	PERCENT	MOL/KG	PERCENT
732	SO4-2	4.407E-02	82.4	0.000E-01	0.0	9.422E-03	17.6
500	Na+1	6.712E-02	100.0	0.000E-01	0.0	0.000E-01	0.0
410	K+1	6.349E-03	100.0	0.000E-01	0.0	0.000E-01	0.0
180	Cl-1	4.782E-03	100.0	0.000E-01	0.0	0.000E-01	0.0
460	Mg+2	9.507E-03	100.0	0.000E-01	0.0	0.000E-01	0.0
140	CO3-2	1.009E-05	100.0	0.000E-01	0.0	0.000E-01	0.0
150	Ca+2	7.121E-03	43.0	0.000E-01	0.0	9.422E-03	57.0
330	H+1	1.069E-02	100.0	0.000E-01	0.0	0.000E-01	0.0
770	H4SiO4	9.530E-05	0.8	0.000E-01	0.0	1.237E-02	99.2
2	H2O	4.319E-12	100.0	0.000E-01	0.0	0.000E-01	0.0

MAJOR PLUS MINOR PLUS 1187 MG/L H4SO4 - CONTAMINATED
(model PP 1-3, plus minor components, U as UO2+2)

Temperature (Celsius): 25.00
Units of concentration: PPM
Ionic strength to be computed.
If specified, carbonate concentration represents total inorganic carbon.
Do not automatically terminate if charge imbalance exceeds 30%
Precipitation is allowed for all solids in the thermodynamic database and
the print option for solids is set to: 1
The maximum number of iterations is: 200
The method used to compute activity coefficients is: Davies equation
Intermediate output file

INPUT DATA BEFORE TYPE MODIFICATIONS

ID	NAME	ACTIVITY GUESS	LOG GUESS	ANAL TOTAL
330	H+1	4.169E-03	-2.380	0.000E-01
500	Na+1	4.074E-03	-2.390	1.529E+03
410	K+1	1.288E-04	-3.890	2.460E+02
150	Ca+2	2.042E-03	-2.690	6.570E+02
460	Mg+2	1.660E-03	-2.780	2.290E+02
140	CO3-2	8.128E-03	-2.090	6.000E-01
180	Cl-1	2.455E-03	-2.610	1.680E+02
732	SO4-2	5.754E-04	-3.240	5.091E+03
281	Fe+3	3.548E-05	-4.450	2.000E+00
30	Al+3	2.138E-04	-3.670	5.800E+00
800	Sr+2	1.380E-04	-3.860	1.210E+01
100	Ba+2	1.445E-07	-6.840	2.000E-02
470	Mn+2	9.120E-05	-4.040	5.000E+00
490	NH4+1	5.888E-02	-1.230	1.053E+03
270	F-1	5.888E-02	-1.230	1.120E+03
580	PO4-3	9.120E-02	-1.040	8.720E+03
600	Pb+2	2.399E-07	-6.620	5.000E-02
650	Ra+2	4.467E-12	-11.350	1.000E-06
130	Br-1	3.890E-05	-4.410	3.100E+00
893	UO2+2	1.862E-06	-5.730	5.000E-01
770	H4SiO4	1.230E-02	-1.910	1.187E+03
2	H2O	1.000E+00	0.000	0.000E-01

Type IV - FINITE SOLIDS (present at equilibrium)

ID	NAME	CALC MOL	LOG MOL	NEW LOGK	DH
2077002	QUARTZ	8.756E-03	-2.058	4.006	-6.220
7089307	UP2O7:20H2O	2.021E-06	-5.694	53.268	0.000
7047001	MNHPO4(C)	9.222E-05	-4.035	25.400	0.000
4215000	FLUORITE	1.645E-02	-1.784	10.949	-4.710
7028100	STRENGITE	3.201E-05	-4.495	26.400	2.030
6010000	BARITE	1.139E-07	-6.943	9.976	-6.280

PERCENTAGE DISTRIBUTION OF COMPONENTS AMONG
TYPE I and TYPE II (dissolved and adsorbed) species

UO2+2

2.4 PERCENT BOUND IN SPECIES #8935801 UO2H2PO4+1

93.0 PERCENT BOUND IN SPECIES #8935802 UO2H2PO4)2

3.6 PERCENT BOUND IN SPECIES #8935803 UO2H2PH3P +1

Na+1

95.1 PERCENT BOUND IN SPECIES # 500 Na+1

4.9 PERCENT BOUND IN SPECIES #5007320 NaSO4 -

K+1

93.2 PERCENT BOUND IN SPECIES # 410 K+1

6.8 PERCENT BOUND IN SPECIES #4107320 KSO4 -

Ca+2

48.1 PERCENT BOUND IN SPECIES # 150 Ca+2

23.2 PERCENT BOUND IN SPECIES #1505802 CaH2PO4 +

28.5 PERCENT BOUND IN SPECIES #1507320 CaSO4 AQ

Mg+2

46.5 PERCENT BOUND IN SPECIES # 460 Mg+2

28.7 PERCENT BOUND IN SPECIES #4605801 MgH2PO4 +

24.1 PERCENT BOUND IN SPECIES #4607320 MgSO4 AQ

CO3-2

100.0 PERCENT BOUND IN SPECIES #3301401 H2CO3 AQ

Cl-1

100.0 PERCENT BOUND IN SPECIES # 180 Cl-1

SO4-2

65.0 PERCENT BOUND IN SPECIES # 732 SO4-2

10.5 PERCENT BOUND IN SPECIES #3307320 HSO4 -

4.3 PERCENT BOUND IN SPECIES #4607320 MgSO4 AQ

13.0 PERCENT BOUND IN SPECIES #4907320 NH4SO4 -

6.2 PERCENT BOUND IN SPECIES #5007320 NaSO4 -

Br-1

100.0 PERCENT BOUND IN SPECIES # 130 Br-1

Al+3

9.3 PERCENT BOUND IN SPECIES # 302701 AlF2 +

65.5 PERCENT BOUND IN SPECIES # 302702 AlF3 AQ

25.1 PERCENT BOUND IN SPECIES # 302703 AlF4 -

Sr+2

59.4 PERCENT BOUND IN SPECIES # 800 Sr+2

6.0 PERCENT BOUND IN SPECIES #8005802 SrH2PO4+

34.5 PERCENT BOUND IN SPECIES #8007320 SrSO4(aq)

Pb+2

33.2 PERCENT BOUND IN SPECIES # 600 Pb+2

1.9 PERCENT BOUND IN SPECIES #6001800 PbCl +

54.3 PERCENT BOUND IN SPECIES #6007320 PbSO4 AQ

10.5 PERCENT BOUND IN SPECIES #6007321 Pb(SO4)2-2

Ra+2

100.0 PERCENT BOUND IN SPECIES # 650 Ra+2

NH4+1

88.2 PERCENT BOUND IN SPECIES # 490 NH4+1

11.8 PERCENT BOUND IN SPECIES #4907320 NH4SO4 -

PO4-3

68.7 PERCENT BOUND IN SPECIES #3305801 H2PO4 -

28.3 PERCENT BOUND IN SPECIES #3305802 H3PO4

2.9 PERCENT BOUND IN SPECIES #4605801 MgH2PO4 +

Fe+3

3.4 PERCENT BOUND IN SPECIES #2812700 FeF +2

28.9 PERCENT BOUND IN SPECIES #2812701 FeF2 +

17.3 PERCENT BOUND IN SPECIES #2812702 FeF3 AQ

50.2 PERCENT BOUND IN SPECIES #2815801 FeH2PO4 +2

H4SiO4

2.4 PERCENT BOUND IN SPECIES # 770 H4SiO4

97.6 PERCENT BOUND IN SPECIES #7702700 SiF6 -2

Mn+2

65.0 PERCENT BOUND IN SPECIES # 470 Mn+2

34.5 PERCENT BOUND IN SPECIES #4707320 MnSO4 AQ

H+1

2.3 PERCENT BOUND IN SPECIES # 330 H+1

1.3 PERCENT BOUND IN SPECIES #3302700 HF AQ

52.9 PERCENT BOUND IN SPECIES #3305801 H2PO4 -

32.6 PERCENT BOUND IN SPECIES #3305802 H3PO4

2.3 PERCENT BOUND IN SPECIES #3307320 HSO4 -

2.3 PERCENT BOUND IN SPECIES #4605801 MgH2PO4 +

6.2 PERCENT BOUND IN SPECIES #7702700 SiF6 -2

F-1

2.7 PERCENT BOUND IN SPECIES # 270 F-1

1.6 PERCENT BOUND IN SPECIES # 302702 AlF3 AQ

11.6 PERCENT BOUND IN SPECIES #3302700 HF AQ

82.6 PERCENT BOUND IN SPECIES #7702700 SiF6 -2

H2O

100.0 PERCENT BOUND IN SPECIES #7702700 SiF6 -2

Ba+2

100.0 PERCENT BOUND IN SPECIES # 100 Ba+2

---------- EQUILIBRATED MASS DISTRIBUTION ----------

IDX	NAME	DISSOLVED		SORBED		PRECIPITATED	
		MOL/KG	PERCENT	MOL/KG	PERCENT	MOL/KG	PERCENT
893	UO2+2	4.515E-12	0.0	0.000E-01	0.0	2.021E-06	100.0
500	Na+1	6.787E-02	100.0	0.000E-01	0.0	0.000E-01	0.0
410	K+1	6.420E-03	100.0	0.000E-01	0.0	0.000E-01	0.0
150	Ca+2	2.746E-04	1.6	0.000E-01	0.0	1.645E-02	98.4
460	Mg+2	9.612E-03	100.0	0.000E-01	0.0	0.000E-01	0.0
140	CO3-2	1.020E-05	100.0	0.000E-01	0.0	0.000E-01	0.0
180	Cl-1	4.835E-03	100.0	0.000E-01	0.0	0.000E-01	0.0
732	SO4-2	5.408E-02	100.0	0.000E-01	0.0	1.139E-07	0.0
130	Br-1	3.959E-05	100.0	0.000E-01	0.0	0.000E-01	0.0
30	Al+3	2.194E-04	100.0	0.000E-01	0.0	0.000E-01	0.0
800	Sr+2	1.409E-04	100.0	0.000E-01	0.0	0.000E-01	0.0
600	Pb+2	2.463E-07	100.0	0.000E-01	0.0	0.000E-01	0.0
650	Ra+2	4.515E-12	100.0	0.000E-01	0.0	0.000E-01	0.0
490	NH4+1	5.957E-02	100.0	0.000E-01	0.0	0.000E-01	0.0
580	PO4-3	9.357E-02	99.9	0.000E-01	0.0	1.283E-04	0.1
281	Fe+3	4.534E-06	12.4	0.000E-01	0.0	3.201E-05	87.6
770	H4SiO4	3.846E-03	30.5	0.000E-01	0.0	8.756E-03	69.5
470	Mn+2	6.540E-07	0.7	0.000E-01	0.0	9.222E-05	99.3
330	H+1	2.432E-01	100.0	0.000E-01	0.0	0.000E-01	0.0
270	F-1	2.725E-02	45.3	0.000E-01	0.0	3.291E-02	54.7
2	H2O	-1.501E-02	100.0	0.000E-01	0.0	0.000E-01	0.0
100	Ba+2	3.468E-08	23.3	0.000E-01	0.0	1.139E-07	76.7

MINOR + MAJOR + SILICON -CONTAMINATED U AS UO2+2
(model PP 1-3, plus minor components, U as UO2+2)

Temperature (Celsius): 25.00
Units of concentration: PPM
Ionic strength to be computed.
If specified, carbonate concentration represents total inorganic carbon.
Do not automatically terminate if charge imbalance exceeds 30%
Precipitation is allowed for all solids in the thermodynamic database and
the print option for solids is set to: 1
The maximum number of iterations is: 200
The method used to compute activity coefficients is: Davies equation
Intermediate output file

INPUT DATA BEFORE TYPE MODIFICATIONS

ID	NAME	ACTIVITY GUESS	LOG GUESS	ANAL TOTAL
330	H+1	4.169E-03	-2.380	0.000E-01
500	Na+1	4.074E-03	-2.390	1.529E+03
410	K+1	1.288E-04	-3.890	2.460E+02
150	Ca+2	2.042E-03	-2.690	6.570E+02
460	Mg+2	1.660E-03	-2.780	2.290E+02
140	CO3-2	8.128E-03	-2.090	6.000E-01
180	Cl-1	2.455E-03	-2.610	1.680E+02
732	SO4-2	5.754E-04	-3.240	5.091E+03
281	Fe+3	3.548E-05	-4.450	2.000E+00
30	Al+3	2.138E-04	-3.670	5.800E+00
800	Sr+2	1.380E-04	-3.860	1.210E+01
100	Ba+2	1.445E-07	-6.840	2.000E-02
470	Mn+2	9.120E-05	-4.040	5.000E+00
490	NH4+1	5.888E-02	-1.230	1.053E+03
270	F-1	5.888E-02	-1.230	1.120E+03
580	PO4-3	9.120E-02	-1.040	8.720E+03
600	Pb+2	2.399E-07	-6.620	5.000E-02
650	Ra+2	4.467E-12	-11.350	1.000E-06
130	Br-1	3.890E-05	-4.410	3.100E+00
893	UO2+2	1.862E-06	-5.730	5.000E-01
770	H4SiO4	7.762E-03	-2.110	7.420E+02
2	H2O	1.000E+00	0.000	0.000E-01

Type IV - FINITE SOLIDS (present at equilibrium)

ID	NAME	CALC MOL	LOG MOL	NEW LOGK	DH
7089307	UP2O7:20H2O	1.889E-06	-5.724	53.268	0.000
4215000	FLUORITE	1.645E-02	-1.784	10.949	-4.710
2077002	QUARTZ	4.030E-03	-2.395	4.006	-6.220
7047001	MNHPO4(C)	9.218E-05	-4.035	25.400	0.000
7028100	STRENGITE	3.226E-05	-4.491	26.400	2.030
6010000	BARITE	1.138E-07	-6.944	9.976	-6.280

PERCENTAGE DISTRIBUTION OF COMPONENTS AMONG
TYPE I and TYPE II (dissolved and adsorbed) species

Ra+2

100.0 PERCENT BOUND IN SPECIES # 650 Ra+2

Na+1

95.1 PERCENT BOUND IN SPECIES # 500 Na+1

4.9 PERCENT BOUND IN SPECIES #5007320 NaSO4 -

K+1

93.2 PERCENT BOUND IN SPECIES # 410 K+1

6.8 PERCENT BOUND IN SPECIES #4107320 KSO4 -

Ca+2

48.1 PERCENT BOUND IN SPECIES # 150 Ca+2

23.2 PERCENT BOUND IN SPECIES #1505802 CaH2PO4 +

28.5 PERCENT BOUND IN SPECIES #1507320 CaSO4 AQ

Mg+2

46.5 PERCENT BOUND IN SPECIES # 460 Mg+2

28.7 PERCENT BOUND IN SPECIES #4605801 MgH2PO4 +

24.1 PERCENT BOUND IN SPECIES #4607320 MgSO4 AQ

CO3-2

100.0 PERCENT BOUND IN SPECIES #3301401 H2CO3 AQ

Cl-1

100.0 PERCENT BOUND IN SPECIES # 180 Cl-1

SO4-2

65.0 PERCENT BOUND IN SPECIES # 732 SO4-2

10.5 PERCENT BOUND IN SPECIES #3307320 HSO4 -

4.3 PERCENT BOUND IN SPECIES #4607320 MgSO4 AQ

13.0 PERCENT BOUND IN SPECIES #4907320 NH4SO4 -

6.2 PERCENT BOUND IN SPECIES #5007320 NaSO4 -

Fe+3

3.4 PERCENT BOUND IN SPECIES #2812700 FeF +2

28.9 PERCENT BOUND IN SPECIES #2812701 FeF2 +

17.4 PERCENT BOUND IN SPECIES #2812702 FeF3 AQ

50.2 PERCENT BOUND IN SPECIES #2815801 FeH2PO4 +2

Al+3

9.3 PERCENT BOUND IN SPECIES # 302701 AlF2 +

65.5 PERCENT BOUND IN SPECIES # 302702 AlF3 AQ

25.1 PERCENT BOUND IN SPECIES # 302703 AlF4 -

Sr+2

59.4 PERCENT BOUND IN SPECIES # 800 Sr+2

6.0 PERCENT BOUND IN SPECIES #8005802 SrH2PO4+

34.5 PERCENT BOUND IN SPECIES #8007320 SrSO4(aq)

Pb+2

33.2 PERCENT BOUND IN SPECIES # 600 Pb+2

1.9 PERCENT BOUND IN SPECIES #6001800 PbCl +

54.3 PERCENT BOUND IN SPECIES #6007320 PbSO4 AQ

10.5 PERCENT BOUND IN SPECIES #6007321 Pb(SO4)2-2

Br-1

100.0 PERCENT BOUND IN SPECIES # 130 Br-1

NH4+1

88.2 PERCENT BOUND IN SPECIES # 490 NH4+1

11.8 PERCENT BOUND IN SPECIES #4907320 NH4SO4 -

H2O

100.0 PERCENT BOUND IN SPECIES #7702700 SiF6 -2

Mn+2

65.1 PERCENT BOUND IN SPECIES # 470 Mn+2

34.5 PERCENT BOUND IN SPECIES #4707320 MnSO4 AQ

UO2+2

2.4 PERCENT BOUND IN SPECIES #8935801 UO2H2PO4+1

93.0 PERCENT BOUND IN SPECIES #8935802 UO2H2PO4)2

3.6 PERCENT BOUND IN SPECIES #8935803 UO2H2PH3P +1

F-1

2.7 PERCENT BOUND IN SPECIES # 270 F-1

1.6 PERCENT BOUND IN SPECIES # 302702 AlF3 AQ

11.6 PERCENT BOUND IN SPECIES #3302700 HF AQ

82.6 PERCENT BOUND IN SPECIES #7702700 SiF6 -2

H4SiO4

2.4 PERCENT BOUND IN SPECIES # 770 H4SiO4

97.6 PERCENT BOUND IN SPECIES #7702700 SiF6 -2

H+1

2.3 PERCENT BOUND IN SPECIES # 330 H+1

1.3 PERCENT BOUND IN SPECIES #3302700 HF AQ

52.9 PERCENT BOUND IN SPECIES #3305801 H2PO4 -

32.6 PERCENT BOUND IN SPECIES #3305802 H3PO4

2.3 PERCENT BOUND IN SPECIES #3307320 HSO4 -

2.3 PERCENT BOUND IN SPECIES #4605801 MgH2PO4 +

6.2 PERCENT BOUND IN SPECIES #7702700 SiF6 -2

PO4-3

68.7 PERCENT BOUND IN SPECIES #3305801 H2PO4 -

28.3 PERCENT BOUND IN SPECIES #3305802 H3PO4

2.9 PERCENT BOUND IN SPECIES #4605801 MgH2PO4 +

Ba+2

100.0 PERCENT BOUND IN SPECIES # 100 Ba+2

---------- EQUILIBRATED MASS DISTRIBUTION ----------

IDX	NAME	DISSOLVED MOL/KG	DISSOLVED PERCENT	SORBED MOL/KG	SORBED PERCENT	PRECIPITATED MOL/KG	PRECIPITATED PERCENT
650	Ra+2	4.513E-12	100.0	0.000E-01	0.0	0.000E-01	0.0
500	Na+1	6.784E-02	100.0	0.000E-01	0.0	0.000E-01	0.0
410	K+1	6.417E-03	100.0	0.000E-01	0.0	0.000E-01	0.0
150	Ca+2	2.746E-04	1.6	0.000E-01	0.0	1.645E-02	98.4
460	Mg+2	9.607E-03	100.0	0.000E-01	0.0	0.000E-01	0.0
140	CO3-2	1.020E-05	100.0	0.000E-01	0.0	0.000E-01	0.0
180	Cl-1	4.833E-03	100.0	0.000E-01	0.0	0.000E-01	0.0
732	SO4-2	5.405E-02	100.0	0.000E-01	0.0	1.138E-07	0.0
281	Fe+3	4.533E-06	12.3	0.000E-01	0.0	3.226E-05	87.7
30	Al+3	2.193E-04	100.0	0.000E-01	0.0	0.000E-01	0.0
800	Sr+2	1.409E-04	100.0	0.000E-01	0.0	0.000E-01	0.0
600	Pb+2	2.461E-07	100.0	0.000E-01	0.0	0.000E-01	0.0
130	Br-1	3.957E-05	100.0	0.000E-01	0.0	0.000E-01	0.0
490	NH4+1	5.954E-02	100.0	0.000E-01	0.0	0.000E-01	0.0
2	H2O	-1.501E-02	100.0	0.000E-01	0.0	0.000E-01	0.0
470	Mn+2	6.542E-07	0.7	0.000E-01	0.0	9.218E-05	99.3
893	UO2+2	4.508E-12	0.0	0.000E-01	0.0	1.889E-06	100.0
270	F-1	2.724E-02	45.3	0.000E-01	0.0	3.289E-02	54.7
770	H4SiO4	3.844E-03	48.8	0.000E-01	0.0	4.030E-03	51.2
330	H+1	2.431E-01	100.0	0.000E-01	0.0	0.000E-01	0.0
580	PO4-3	9.352E-02	99.9	0.000E-01	0.0	1.282E-04	0.1
100	Ba+2	3.469E-08	23.4	0.000E-01	0.0	1.138E-07	76.6

MAJOR PLUS MINOR PLUS 1187 MG/L H4SIO4 - CONTAMINATED - U AS U+4
(model PP 1-3, minor plus major components, U as U+4)

Temperature (Celsius): 25.00
Units of concentration: PPM
Ionic strength to be computed.
If specified, carbonate concentration represents total inorganic carbon.
Do not automatically terminate if charge imbalance exceeds 30%
Precipitation is allowed for all solids in the thermodynamic database and
the print option for solids is set to: 1
The maximum number of iterations is: 200
The method used to compute activity coefficients is: Davies equation
Intermediate output file

INPUT DATA BEFORE TYPE MODIFICATIONS

ID	NAME	ACTIVITY GUESS	LOG GUESS	ANAL TOTAL
330	H+1	4.169E-03	-2.380	0.000E-01
500	Na+1	4.064E-03	-2.390	1.529E+03
410	K+1	1.288E-04	-3.890	2.460E+02
150	Ca+2	2.042E-03	-2.690	6.570E+02
460	Mg+2	1.660E-03	-2.780	2.290E+02
140	CO3-2	8.128E-03	-2.090	6.000E-01
180	Cl-1	2.455E-03	-2.610	1.680E+02
732	SO4-2	5.754E-04	-3.240	5.091E+03
281	Fe+3	3.548E-05	-4.450	2.000E+00
30	Al+3	2.138E-04	-3.670	5.800E+00
800	Sr+2	1.380E-04	-3.860	1.210E+01
100	Ba+2	1.445E-07	-6.840	2.000E-02
470	Mn+2	9.120E-05	-4.040	5.000E+00
490	NH4+1	5.888E-02	-1.230	1.053E+03
270	F-1	5.888E-02	-1.230	1.120E+03
580	PO4-3	9.120E-02	-1.040	8.720E+03
600	Pb+2	2.399E-07	-6.620	5.000E-02
891	U+4	2.089E-06	-5.680	5.000E-01
650	Ra+2	4.467E-12	-11.350	1.000E-06
130	Br-1	3.890E-05	-4.410	3.100E+00
770	H4SiO4	1.230E-02	-1.910	1.187E+03
2	H2O	1.000E+00	0.000	0.000E-01

Type IV - FINITE SOLIDS (present at equilibrium)

ID	NAME	CALC MOL	LOG MOL	NEW LOGK	DH
2077002	QUARTZ	8.756E-03	-2.058	4.006	-6.220
7047001	MNHPO4(C)	9.222E-05	-4.035	25.400	0.000
4215000	FLUORITE	1.645E-02	-1.784	10.949	-4.710
7089100	UHPO4)2,4H2O	2.136E-06	-5.670	57.510	-10.882
7028100	STRENGITE	3.227E-05	-4.491	26.400	2.030
6010000	BARITE	1.139E-07	-6.943	9.976	-6.280

PERCENTAGE DISTRIBUTION OF COMPONENTS AMONG
TYPE I and TYPE II (dissolved and adsorbed) species

Br-1

100.0 PERCENT BOUND IN SPECIES # 130 Br-1

Na+1

95.1 PERCENT BOUND IN SPECIES # 500 Na+1

4.9 PERCENT BOUND IN SPECIES #5007320 NaSO4 -

K+1

93.2 PERCENT BOUND IN SPECIES # 410 K+1

6.8 PERCENT BOUND IN SPECIES #4107320 KSO4 -

Ca+2

48.1 PERCENT BOUND IN SPECIES # 150 Ca+2

23.2 PERCENT BOUND IN SPECIES #1505802 CaH2PO4 +

28.5 PERCENT BOUND IN SPECIES #1507320 CaSO4 AQ

Mg+2

46.5 PERCENT BOUND IN SPECIES # 460 Mg+2

28.7 PERCENT BOUND IN SPECIES #4605801 MgH2PO4 +

24.1 PERCENT BOUND IN SPECIES #4607320 MgSO4 AQ

CO3-2

100.0 PERCENT BOUND IN SPECIES #3301401 H2CO3 AQ

Cl-1

100.0 PERCENT BOUND IN SPECIES # 180 Cl-1

SO4-2

65.0 PERCENT BOUND IN SPECIES # 732 SO4-2

10.5 PERCENT BOUND IN SPECIES #3307320 HSO4 -

4.3 PERCENT BOUND IN SPECIES #4607320 MgSO4 AQ

13.0 PERCENT BOUND IN SPECIES #4907320 NH4SO4 -

6.2 PERCENT BOUND IN SPECIES #5007320 NaSO4 -

Fe+3

3.4 PERCENT BOUND IN SPECIES #2812700 FeF +2

28.9 PERCENT BOUND IN SPECIES #2812701 FeF2 +

17.3 PERCENT BOUND IN SPECIES #2812702 FeF3 AQ

50.2 PERCENT BOUND IN SPECIES #2815801 FeH2PO4 +2

Al+3

9.3 PERCENT BOUND IN SPECIES # 302701 AlF2 +

65.5 PERCENT BOUND IN SPECIES # 302702 AlF3 AQ

25.1 PERCENT BOUND IN SPECIES # 302703 AlF4 -

Sr+2

59.4 PERCENT BOUND IN SPECIES # 800 Sr+2

6.0 PERCENT BOUND IN SPECIES #8005802 SrH2PO4+

34.5 PERCENT BOUND IN SPECIES #8007320 SrSO4(aq)

Pb+2

33.2 PERCENT BOUND IN SPECIES # 600 Pb+2

1.9 PERCENT BOUND IN SPECIES #6001800 PbCl +

54.3 PERCENT BOUND IN SPECIES #6007320 PbSO4 AQ

10.5 PERCENT BOUND IN SPECIES #6007321 Pb(SO4)2-2

Ra+2

100.0 PERCENT BOUND IN SPECIES # 650 Ra+2

NH4+1

88.2 PERCENT BOUND IN SPECIES # 490 NH4+1

11.8 PERCENT BOUND IN SPECIES #4907320 NH4SO4 -

PO4-3

68.7 PERCENT BOUND IN SPECIES #3305801 H2PO4 -

28.3 PERCENT BOUND IN SPECIES #3305802 H3PO4

2.9 PERCENT BOUND IN SPECIES #4605801 MgH2PO4 +

Mn+2

65.0 PERCENT BOUND IN SPECIES # 470 Mn+2

34.5 PERCENT BOUND IN SPECIES #4707320 MnSO4 AQ

H4SiO4

2.4 PERCENT BOUND IN SPECIES # 770 H4SiO4

97.6 PERCENT BOUND IN SPECIES #7702700 SiF6 -2

U+4

26.1 PERCENT BOUND IN SPECIES #8912702 UF3 +1

71.5 PERCENT BOUND IN SPECIES #8912703 UF4 AQ

1.6 PERCENT BOUND IN SPECIES #8912704 UF5 -1

F-1

2.7 PERCENT BOUND IN SPECIES # 270 F-1

1.6 PERCENT BOUND IN SPECIES # 302702 AlF3 AQ

11.6 PERCENT BOUND IN SPECIES #3302700 HF AQ

82.6 PERCENT BOUND IN SPECIES #7702700 SiF6 -2

H+1

2.3 PERCENT BOUND IN SPECIES # 330 H+1

1.3 PERCENT BOUND IN SPECIES #3302700 HF AQ

52.9 PERCENT BOUND IN SPECIES #3305801 H2PO4 -

32.6 PERCENT BOUND IN SPECIES #3305802 H3PO4

2.3 PERCENT BOUND IN SPECIES #3307320 HSO4 -

2.3 PERCENT BOUND IN SPECIES #4605801 MgH2PO4 +

6.2 PERCENT BOUND IN SPECIES #7702700 SiF6 -2

H2O

100.0 PERCENT BOUND IN SPECIES #7702700 SiF6 -2

Ba+2

100.0 PERCENT BOUND IN SPECIES # 100 Ba+2

---------- EQUILIBRATED MASS DISTRIBUTION ----------

IDX	NAME	DISSOLVED		SORBED		PRECIPITATED	
		MOL/KG	PERCENT	MOL/KG	PERCENT	MOL/KG	PERCENT
130	Br-1	3.959E-05	100.0	0.000E-01	0.0	0.000E-01	0.0
500	Na+1	6.787E-02	100.0	0.000E-01	0.0	0.000E-01	0.0
410	K+1	6.420E-03	100.0	0.000E-01	0.0	0.000E-01	0.0
150	Ca+2	2.746E-04	1.6	0.000E-01	0.0	1.645E-02	98.4
460	Mg+2	9.612E-03	100.0	0.000E-01	0.0	0.000E-01	0.0
140	CO3-2	1.020E-05	100.0	0.000E-01	0.0	0.000E-01	0.0
180	Cl-1	4.835E-03	100.0	0.000E-01	0.0	0.000E-01	0.0
732	SO4-2	5.408E-02	100.0	0.000E-01	0.0	1.139E-07	0.0
281	Fe+3	4.534E-06	12.3	0.000E-01	0.0	3.227E-05	87.7
30	Al+3	2.194E-04	100.0	0.000E-01	0.0	0.000E-01	0.0
800	Sr+2	1.409E-04	100.0	0.000E-01	0.0	0.000E-01	0.0
600	Pb+2	2.463E-07	100.0	0.000E-01	0.0	0.000E-01	0.0
650	Ra+2	4.515E-12	100.0	0.000E-01	0.0	0.000E-01	0.0
490	NH4+1	5.957E-02	100.0	0.000E-01	0.0	0.000E-01	0.0
580	PO4-3	9.356E-02	99.9	0.000E-01	0.0	1.288E-04	0.1
470	Mn+2	6.540E-07	0.7	0.000E-01	0.0	9.222E-05	99.3
770	H4SiO4	3.846E-03	30.5	0.000E-01	0.0	8.756E-03	69.5
891	U+4	7.706E-09	0.4	0.000E-01	0.0	2.136E-06	99.6
270	F-1	2.725E-02	45.3	0.000E-01	0.0	3.291E-02	54.7
330	H+1	2.432E-01	100.0	0.000E-01	0.0	0.000E-01	0.0
2	H2O	-1.501E-02	100.0	0.000E-01	0.0	0.000E-01	0.0
100	Ba+2	3.468E-08	23.3	0.000E-01	0.0	1.139E-07	76.7